APPENDIX A

THE EFFECT OF TEST STIFFNESS ON THE UNLOADING BEHAVIOUR OF CONCENTRICALLY LOADED SHORT MEMBERS

As illustrated in Figs. 3.2 and 3.4, concrete has the ability to "unload" or reduce its stress capacity with increasing strains after the maximum stress has been reached. This unloading can only be achieved if the load can be transferred from the concrete to other parts of the member, to the rest of the structure and to the testing machine or system that is applying the load. This transfer of load will depend on the redundancy and therefore the stiffness of the other parts of the member, the rest of the structure and the testing machine, the overall stiffness being defined as the "test stiffness".

Consider the model of a testing machine in Fig. A.1 which is applying load concentrically to a short composite column which forms part of a simple redundant frame. The column is assumed to be short enough to prevent lateral buckling and the beam in the frame is assumed to remain elastic.

Let L_m = length of the vertical legs of the testing machine,
A_m = total crossectional area of the legs,
E_m = elastic modulus of the material in the legs,
L_b = length of the beam in the frame,
I_b = second moment of area of the beam,
E_b = elastic modulus of the material in the beam,
P_m = load in the machine legs,
P_b = load carried by the beam,
P_c = load carried by the column,

Δ_c = total compression of the column,
Δ_m = extension of the machine legs,
Δ_r = total movement of the screwjack relative to the horizontal loading beam
L_c = length of the column,
A_c = crossectional area of the concrete in the column,
A_s = crossectional area of the steel in the column,
E_s = elastic modulus of the steel in the column,
ε_c = axial strain in the column and
σ_c = concrete stress in the column at this strain.

For compatibility,

$$\Delta_r = \Delta_m + \Delta_c \qquad \text{——————(A.1)}$$

and for equilibrium,

$$P_m = P_b + P_c \qquad \text{——————(A.2)}$$

Now $$\Delta_c = \frac{P_b L_b^{\,3}}{48 E_b I_b}$$

The structural redundant stiffness, k_b, can be expressed as

$$k_b = \frac{48 E_b I_b}{L_b^{\,3}}$$

hence $$\Delta_c = \frac{P_b}{k_b}$$

Also $$\Delta_c = \varepsilon_c L_c \qquad \text{——————(A.3)}$$

therefore

$$P_b = k_b \varepsilon_c L_c \qquad \text{——————(A.4)}$$

Now $$\Delta_m = \frac{P_m L_m}{E_m A_m}$$

The testing machine stiffness, k_m, can be expressed as

$$k_m = \frac{E_m A_m}{L_m} \qquad \text{(A.5)}$$

Therefore

$$\Delta_m = \frac{P_m}{k_m} \qquad \text{(A.6)}$$

Combining equations (A.4) and (A.2) then

$$P_m = P_c + k_b \varepsilon_c L_c$$

and substitution into equation (A.6) yields

$$\Delta_m = \frac{1}{k_m} \cdot (P_c + k_b \varepsilon_c L_c) \qquad \text{(A.7)}$$

Now $$\Delta_r = \Delta_m + \Delta_c$$

then from equation (A.7) and (A.3)

$$\Delta_r = \frac{1}{k_m} \cdot (P_c + k_b \varepsilon_c L_c) + \varepsilon_c L_c$$

Differentiating with respect to ε_c, then

$$\frac{d\Delta_r}{d\varepsilon_c} = \frac{1}{k_m} \cdot \frac{dP_c}{d\varepsilon_c} + \frac{k_b L_c}{k_m} + L_c \qquad \text{(A.8)}$$

Now $$P_c = \sigma_c A_c + E_s A_s \varepsilon_c$$

The member redundant stiffness, k_c, can be expressed as

$$k_c = \frac{E_s A_s}{L_c}$$

Therefore

$$P_c = \sigma_c A_c + k_c \varepsilon_c L_c$$

and $$\frac{dP_c}{d\varepsilon_c} = A_c \frac{d\sigma_c}{d\varepsilon_c} + k_c L_c \qquad \text{——————(A.9)}$$

Substitution into equation (A.8) yields

$$\frac{d\Delta_r}{d\varepsilon_c} = \frac{1}{k_m} \left(A_c \frac{d\sigma_c}{d\varepsilon_c} + k_c L_c\right) + \frac{k_b L_c}{k_m} + L_c \qquad \text{———(A.10)}$$

Instability occurs when a very small increment of screwjack movement, Δ_r, produces a very large increment of column strain. Therefore, the criterion for instability is

$$\frac{d\Delta_r}{d\varepsilon_c} = 0 \qquad \text{——————(A.11)}$$

and from equation (A.10), when

$$\frac{1}{k_m} \left(A_c \frac{d\sigma_c}{d\varepsilon_c} + k_c L_c\right) + \frac{k_b L_c}{k_m} + L_c = 0$$

Rearranging, then

$$\frac{d\sigma_c}{d\varepsilon_c} = -(k_b + k_m + k_c) \frac{L_c}{A_c}$$

$$= E_t \qquad \text{——————(A.12)}$$

where E_t is defined as the test instability modulus and is a function of the test stiffness, k_t, where

$$k_t = k_b + k_m + k_c \qquad \text{——————(A.13)}$$

Therefore

$$E_t = -k_t \frac{L_c}{A_c} \qquad \text{——————(A.14)}$$

Column instability will therefore occur when the slope of the descending portion of the stress-strain curve for the concrete reaches a critical value of the test instability modulus, E_t, given by equation (A.12). This behaviour is illustrated in Fig. A.2.

Listed below are expressions for E_t for some particular cases discussed in other Sections.

(a) Standard Compression Test on a Plain Concrete Cylinder or Prism.

The instability modulus, E_t, is a function of the testing machine stiffness, k_m, alone where

$$E_t = -k_m \frac{L_c}{A_c} \qquad \text{——————(A.15)}$$

This is referred to in Section 3.2.1. The value of E_t can be increased to give a greater coverage of strain in the test by increasing $\frac{L_c}{A_c}$. However, lateral instability effects are an obvious limitation to practical dimensions of the specimen.

(b) Composite Columns - Steel Yielded

This is the case for columns containing a low yield stress steel where the steel yields before instability takes place and is referred to in Section 4.1.3.

Thus, the member redundancy stiffness, k_c, is zero. Hence,

$$E_t = -(k_b + k_m) \frac{L_c}{A_c} \qquad \text{——————(A.16)}$$

For a pin-ended composite column in a testing machine, there is no structural redundancy and hence

$$E_t = -k_m \frac{L_c}{A_c} \qquad \text{——————(A.17)}$$

For a dead load test on a pin-ended composite column, the machine stiffness is zero, hence

$$E_t = 0 \qquad \text{——————(A.18)}$$

Therefore, instability occurs when the maximum load, P_{sh}, for the column is reached, at which point the concrete has also attained its maximum stress, f''_c.

(c) Composite Columns - Steel Elastic

This is the case for columns containing a high yield stress steel where instability takes place while the steel is still elastic and is also referred to in Section 4.1.3. Hence

$$E_t = -(k_b + k_m + k_c) \frac{L_c}{A_c} \qquad \text{——————(A.19)}$$

For a pin-ended composite column in a testing machine, there is no structural redundancy and hence

$$E_t = -(k_m + k_c) \frac{L_c}{A_c} \qquad \text{——————(A.20)}$$

For a dead load test on a pin-ended composite column, the machine stiffness is zero, hence

$$E_t = - k_c \frac{L_c}{A_c} \qquad \text{——————(A.21)}$$

Note: If the test stiffness is high such that the value of E_t is greater than the maximum slope of the descending portion of the concrete stress-strain curve, instability will not occur.

APPENDIX B

THE INFLUENCE OF STRAIN GRADIENT ON EQUILIBRIUM AND THE APPARENT ULTIMATE STRAIN OF CONCRETE

Consider the concrete prism shown in Fig. B.1

Let P_c = axial force on the prism,
M_c = moment about the centre of the prism,
b = width of the prism,
d = depth of the prism,
ε_H = maximum concrete strain,
ε_L = minimum concrete strain,
ε_c = intermediate concrete strain,
σ_H = stress corresponding to ε_H,
σ_L = stress corresponding to ε_L,
x = distance from the centroid to the intermediate concrete strain, ε_c,
σ_c = stress corresponding to ε_c and
ρ = curvature or strain gradient.

The following assumptions are made.

(i) Plane sections remain plane, i.e. the strain distribution is linear across the section,

(ii) The compressive concrete stress is a function of strain alone

i.e. $\sigma_c = F(\varepsilon_c)$ ——————(B.1)

(iii) and the tensile strength of the concrete is assumed to be zero.

Now $$\rho = \frac{\varepsilon_H - \varepsilon_L}{d} \qquad \text{——————(B.2)}$$

$$x = \frac{d}{2} - \frac{\varepsilon_H - \varepsilon_c}{\rho} \qquad \text{——————(B.3)}$$

and $$dx = \frac{d\varepsilon_c}{\rho} \qquad \text{——————(B.4)}$$

For vertical equilibrium,

$$P_c = \int_{-\frac{d}{2}}^{+\frac{d}{2}} \sigma_c b dx$$

Changing the variable to ε_c from equations (B.1) and (B.4)

$$P_c = \frac{b}{\rho} \int_{\varepsilon_L}^{\varepsilon_H} F(\varepsilon_c) d\varepsilon_c \qquad \text{——————(B.5)}$$

For moment equilibrium,

$$M_c = \int_{-\frac{d}{2}}^{+\frac{d}{2}} \sigma_c \, b \, x \, dx$$

Changing the variable to ε_c from equations (B.1) (B.3) and (B.4) and rearranging

$$M_c = P_c\left(\frac{d}{2} - \frac{\varepsilon_H}{\rho}\right) + \frac{b}{\rho^2} \int_{\varepsilon_L}^{\varepsilon_H} F(\varepsilon_c) \varepsilon_c d\varepsilon_c$$

$$= -\frac{P_c}{\rho}\left(\frac{\varepsilon_H + \varepsilon_L}{2}\right) + \frac{b}{\rho^2}\int_{\varepsilon_L}^{\varepsilon_H} F(\varepsilon_c)\,d\varepsilon_c \qquad \text{——(B.6)}$$

Case I: $\varepsilon_L = 0$

This is the case used by Hognestad et al.(41) Karsan and Jirsa(96) and Smith(97). From equation (B.2) then

$$\rho = \frac{\varepsilon_H}{d} \qquad \text{——————(B.7)}$$

(a) Considering the load, P_c, and substituting equation (B.7) into equation (B.5) then

$$P_c = \frac{bd}{\varepsilon_H}\int_{o}^{\varepsilon_H} F(\varepsilon_c)\,d\varepsilon_c \qquad \text{——————(B.8)}$$

Differentiating with respect to ε_H

$$\frac{dP_c}{d\varepsilon_H} = -\frac{bd}{\varepsilon_H^2}\int_{o}^{\varepsilon_H} F(\varepsilon_c)\,d\varepsilon_c + \frac{bd}{\varepsilon_H} F(\varepsilon_H) \qquad \text{————(B.9)}$$

and substituting equations (B.1) and (B.8) into equation (B.9) then

$$\frac{dP_c}{d\varepsilon_H} = \frac{1}{\varepsilon_H}(\sigma_H bd - P_c) \qquad \text{——————(B.10)}$$

For a maximum load

$$\frac{dP_c}{d\varepsilon_H} = 0$$

and $$\sigma_H = \frac{P_c}{bd} \qquad \text{(B.11)}$$

This condition is shown graphically in Fig. B.2. If the testing machine lacks stiffness, then failure occurs at the maximum load and equation (B.11) defines the stress and therefore the maximum strain, ε_{HU}, at failure. Substituting equations (B.1) and (B.8) into equation (B.11)

$$F(\varepsilon_{HU}) = \frac{1}{\varepsilon_{HU}} \int_0^{\varepsilon_{HU}} F(\varepsilon_c)\, d\varepsilon_c \qquad \text{(B.12)}$$

To give a simple quantitative example of the above result, it is assumed that the stress-strain relationship is the parabolic shape shown in Fig. 3.4 where

$$\sigma_c = F(\varepsilon_c) = f''_c\left[2\left(\frac{\varepsilon_c}{\varepsilon_o}\right) - \left(\frac{\varepsilon_c}{\varepsilon_o}\right)^2\right] \qquad \text{(B.13)}$$

Substituting equation (B.13) into (B.12) then

$$\varepsilon_{HU} = \frac{3}{2}\,\varepsilon_o \qquad \text{(B.14)}$$

where ε_o is the strain at the maximum stress of the concrete stress-strain curve. It can be seen from Fig. 3.6(a) that values of maximum strain predicted by equation (B.14) are of the same order as those given by the termination points of the stress-strain curves shown in the Figure. If the testing machine has reasonable stiffness then strains in excess of those predicted by equation (B.14) can be achieved as was the case for tests by Karsan and Jirsa(96) and shown in Fig. 3.19.

(b) Considering the moment, M_c, it can be similarly shown that

$$\frac{dM_c}{d\varepsilon_H} = \frac{1}{2\varepsilon_H}(\sigma_H bd^2 - P_c d - 4M_c) \qquad \text{——————(B.15)}$$

and for maximum moment,

$$\frac{dM_c}{d\varepsilon_H} = 0$$

and $$\sigma_H = \frac{Pc}{bd} + \frac{4M_c}{bd^2} \qquad \text{——————(B.16)}$$

This expression is not amenable to any graphical interpretation as was equation (B.11). However, using the simple parabolic stress-strain curve of equation (B.13) together with equations (B.5) and (B.6) and substituting into equation (B.16) and re-arranging

$$\varepsilon_H = \varepsilon_o$$

which defines the condition for maximum moment. If the loading system applying this moment cannot unload, as in a dead weight system, instability or failure occurs at a strain, ε_{HU}, where

$$\varepsilon_{HU} = \varepsilon_o \qquad \text{——————(B.17)}$$

From equations (B.17) and (B.14) it can be seen that the moment reaches its maximum value before the load with increasing strains.

Case II: ρ = Constant

This is the case used by Clark et al.(85). If the depth, d, of the section is constant, then from equation (B.2)

$$\varepsilon_H - \varepsilon_L = \rho d = \text{Constant}$$

(a) Considering the load, P_c, from equation (B.5) and differentiating with respect to ε_H, then

$$\frac{dP_c}{d\varepsilon_H} = \frac{b}{\rho} (\sigma_H - \sigma_L) \qquad \text{——————(B.18)}$$

For a maximum load

$$\frac{dP_c}{d\varepsilon_H} = 0$$

and $$\sigma_H = \sigma_L \qquad \text{——————(B.19)}$$

This condition is shown graphically in Fig. B.3. It the testing machine lacks stiffness, instability or failure occurs at the maximum load and equation (B.19) defines the stress and therefore the maximum strain, ε_{HU} at failure. Using the simple parabolic stress-strain curve of equation (B.13), equations (B.1) and (B.2) and substituting into equation (B.19)

$$\varepsilon_{HU} = \varepsilon_o + \tfrac{1}{2} \rho d \qquad \text{——————(B.20)}$$

Values of maximum strain predicted by equation (B.20) are of the same order as those shown in Fig. 3.18. Higher values of strain can be attained if the testing machine stiffness is increased.

(b) Considering the moment, M_c, it can be similarly shown that

$$\frac{dM_c}{d\varepsilon_H} = \frac{1}{\rho} \left(\sigma_H \, bd - P_c - \frac{\rho d}{2} \cdot \frac{dP_c}{d\varepsilon_H}\right) \qquad \text{——————(B.21)}$$

and for maximum moment

$$\frac{dM_c}{d\varepsilon_H} = 0$$

and $$\frac{P_c}{bd} = \tfrac{1}{2}(\sigma_H + \sigma_L) \qquad \text{——————(B.22)}$$

This condition is shown graphically in Fig. (B.4) where for a normal shape of stress-strain curve for concrete, the maximum moment occurs when the lower strain, ε_L, is tensile. For the tests by Clark et al.(85) the strains were always compressive and the maximum possible moment under this condition occurs when the minimum strain, ε_L, is zero. With increasing strains from this point, the moment continually decreases. From Figs. B.4 and B.3, it can be seen that the moment reaches its maximum before the load for increasing strains.

APPENDIX C

EVALUATION OF THE STRESS-STRAIN CURVE OF CONCRETE USING THE METHOD OF LEAST SQUARES

Consider the same prism shown in Fig.B.1 and use the same notation as Appendix B. For a particular loading stage, the measured and known values are the edge strains, ε_H and ε_L, the dimensions, b and d, the axial load, P_c, and the moment, M_c, about the centroidal axis. The stress-strain curve can be derived from these values. The curvature or strain gradient, ρ, is known as

$$\rho = \frac{\varepsilon_H - \varepsilon_L}{d} \qquad \text{——————(C.1)}$$

Using the expression for the load, P_c, from equation (B.5) of Appendix B,

$$\int_{\varepsilon_L}^{\varepsilon_H} F(\varepsilon_c)\,d\varepsilon_c = \frac{\rho\, P_c}{b} \qquad \text{——————(C.2)}$$

and using the expression for moment, M_c, from equation (B.6) of Appendix B,

$$\int_{\varepsilon_L}^{\varepsilon_H} F(\varepsilon_c)\,\varepsilon_c\,d\varepsilon_c = \left(\frac{\varepsilon_H + \varepsilon_L}{2}\right)\rho\,\frac{P_c}{b} + \rho^2\,\frac{M_c}{b} \qquad \text{———(C.3)}$$

Let the concrete stress-strain curve be represented by a polynomial expression where

$$\sigma_c = F(\varepsilon_c) = a_1\varepsilon_c + a_2\varepsilon_c^2 + a_3\varepsilon_c^3 \ldots . a_n\varepsilon_c^n \qquad \text{——————(C.4)}$$

and $a_1, a_2, a_3 \ldots . a_n$ are the constants to be determined by the method of least squares. Substituting equation (C.4) into equation (C.2)

$$\int_{\varepsilon_L}^{\varepsilon_H} (a_1\varepsilon_c + a_2\varepsilon_c^2 + a_3\varepsilon_c^3 \ldots . a_n\varepsilon_c^n) d\varepsilon_c = \frac{\rho P_c}{b}$$

Therefore

$$\left[\frac{(\varepsilon_H^2 - \varepsilon_L^2)}{2} . a_1 + \frac{(\varepsilon_H^3 - \varepsilon_L^3)}{3} . a_2 + \ldots . + \frac{(\varepsilon_H^{n+1} - \varepsilon_L^{n+1})}{(n+1)} . a_n\right]$$

$$= \frac{\rho P_c}{b} \qquad \text{——————(C.5)}$$

Substituting equation (C.4) into equation (C.3)

$$\int_{\varepsilon_L}^{\varepsilon_H} (a_1\varepsilon_c^2 + a_2\varepsilon_c^3 + a_3\varepsilon_c^4 + \ldots . + a_n\varepsilon_c^{n+1}) d\varepsilon_c$$

$$= \left(\frac{\varepsilon_H + \varepsilon_L}{2}\right) \frac{\rho P_c}{b} + \frac{\rho^2 M_c}{b}$$

Therefore

$$\left[\frac{(\varepsilon_H^3 - \varepsilon_L^3)}{3} a_1 + \frac{(\varepsilon_H^4 - \varepsilon_L^4)}{4} a_2 + \ldots . + \frac{(\varepsilon_H^{n+2} - \varepsilon_L^{n+2})}{(n+2)} a_n\right]$$

$$= \left(\frac{\varepsilon_H + \varepsilon_L}{2}\right) \frac{\rho P_c}{b} + \frac{\rho^2 M_c}{b} \qquad \text{——————(C.6)}$$

Therefore, for each loading stage, two equations, (C.5) and (C.6), can be written for the unknown constants $(a_1, a_2, a_3 \ldots . a_n)$. Hence, if there are q loading

stages, where P_c, M_c, ε_H and ε_L are known for each stage, then there are $2q$ equations for the n unknown constants a. Pennington(125) recommends that the number of coefficients should not be greater than one half of the number of experimental points to eliminate fluctuations of the higher degree polynomials.

The system of $2q$ equations given by both equations (C.5) and (C.6) for q loading stages may be written in general as follows

$$\begin{aligned}
&\alpha_{1,1}a_1 + \alpha_{1,2}a_2 + \ldots + \alpha_{1,n}a_n = \beta_1\\
&\alpha_{2,1}a_1 + \alpha_{2,2}a_2 + \ldots + \alpha_{2,n}a_n = \beta_2\\
&\quad\vdots \qquad\quad \vdots \qquad\qquad\quad \vdots \qquad\quad \vdots\\
&\alpha_{r,1}a_1 + \alpha_{r,2}a_2 + \ldots + \alpha_{r,n}a_n = \beta_r\\
&\quad\vdots \qquad\quad \vdots \qquad\qquad\quad \vdots \qquad\quad \vdots\\
&\alpha_{2q-1,1}a_1 + \alpha_{2q-1,2}a_2 + \ldots + \alpha_{2q-1,n}a_n = \beta_{2q-1}\\
&\alpha_{2q,1}a_1 + \alpha_{2q,2}a_2 + \ldots + \alpha_{2q,n}a_n = \beta_{2q}
\end{aligned}$$

where

$$\left.\begin{aligned}
\alpha_{2i-1,j} &= \frac{\varepsilon_{Hi}^{j+1} - \varepsilon_{Li}^{j+1}}{j+1}\\
\alpha_{2i,j} &= \alpha_{2i-1,j+1}\\
\beta_{2i-1} &= \frac{\rho_i P_{ci}}{D}\\
\beta_{2i} &= \left(\frac{\varepsilon_{Hi} + \varepsilon_{Li}}{2}\right)\frac{\rho_i P_{ci}}{b} + \frac{\rho_i^2 M_{ci}}{b}
\end{aligned}\right\} \text{for } i = 1 \text{ to } q,\ j = 1 \text{ to } n$$

Let δ_r be the residual for the equation in row r

$$\therefore \delta_r = w_r[\beta_r - (\alpha_{r,1}a_1 + \alpha_{r,2}a_2 + \ldots + \alpha_{r,j}a_j + \ldots + \alpha_{r,n}a_n)]$$

——————(C.7)

where w_r is a weighting depending on the relative importance of the experimental data used to obtain the values of α_r and β_r. For example, in a test on a concrete prism to failure, strain data up to the strain at maximum stress might be numerous whereas strain data beyond this point might be scanty. By giving additional weighting to the residuals of the equations containing this latter data will ensure that the descending portion of the stress-strain curve of "best fit" will be more influenced by this data than the more numerous data for the rising portion of the curve.

For the "best" values of a, the sum of the squares of the residuals should be a minimum, hence

$$\sum_{r=1}^{r=2q} \delta_r^2$$

should be minimum.

i.e. $$\frac{\partial}{\partial a_j} \sum_{r=1}^{r=2q} \delta_r^2 = 0 \qquad \text{for } j = 1 \text{ to } n$$

$$\therefore \sum_{r=1}^{2q} \delta_r \frac{\partial(\delta_r)}{\partial a_j} = 0 \qquad \text{——————(C.8)}$$

Now from equation (C.7)

$$\frac{\partial(\delta_r)}{\partial a_j} = - w_r \alpha_{r,j}$$

Hence equation (C.8) becomes

$$\sum_{r=1}^{2q} [-w_r^2 \alpha_{r,j} \beta_r + w_r^2 \alpha_{r,j} (\alpha_{r,1} a_1 + \alpha_{r,2} a_2 + \ldots + \alpha_{r,j} a_j + \ldots + \alpha_{r,n} a_n)]$$

$$= 0 \qquad \text{——————(C.9)}$$

for $j = 1$ to n.

Expanding equation (C.9) and re-arranging

$$\left(\sum_{r=1}^{2q} w_r^2 \alpha_{r,j} \alpha_{r,1}\right) a_1 + \left(\sum_{r=1}^{2q} w_r^2 \alpha_{r,j} \alpha_{r,2}\right) a_2 + \ldots\ldots$$

$$\ldots\ldots + \left(\sum_{r=1}^{2q} w_r^2 \alpha_{r,j}^2\right) a_j + \ldots\ldots + \left(\sum_{r=1}^{2q} w_r^2 \alpha_{r,j} \alpha_{r,n}\right) a_n$$

$$= \sum_{r=1}^{2q} w_r^2 \alpha_{r,j} \beta_r \qquad \text{——————(C.10)}$$

for $j = 1$ to n.

Equation (C.10) may be re-arranged in matrix form for $j = 1$ to n as follows

$$\begin{bmatrix} \sum_{r=1}^{2q} w_r^2\alpha_{r,1}^2 & \sum_{r=1}^{2q} w_r^2\alpha_{r,1}\alpha_{r,2} & \cdots & \sum_{r=1}^{2q} w_r^2\alpha_{r,1}\alpha_{r,n} \\ \sum_{r=1}^{2q} w_r^2\alpha_{r,2}\alpha_{r,1} & \sum_{r=1}^{2q} w_r^2\alpha_{r,2}^2 & \cdots & \sum_{r=1}^{2q} w_r^2\alpha_{r,2}\alpha_{r,n} \\ \vdots & \vdots & & \vdots \\ \sum_{r=1}^{2q} w_r^2\alpha_{r,i}\alpha_{r,1} & \sum_{r=1}^{2q} w_r^2\alpha_{r,i}\alpha_{r,2} & \cdots & \sum_{r=1}^{2q} w_r^2\alpha_{r,i}\alpha_{r,n} \\ \vdots & \vdots & & \vdots \\ \sum_{r=1}^{2q} w_r^2\alpha_{r,n}\alpha_{r,1} & \sum_{r=1}^{2q} w_r^2\alpha_{r,n}\alpha_{r,2} & \cdots & \sum_{r=1}^{2q} w_r^2\alpha_{r,n}^2 \end{bmatrix} \cdot \begin{bmatrix} a_1 \\ a_2 \\ \\ a_i \\ \\ a_n \end{bmatrix} = \begin{bmatrix} \sum_{r=1}^{2q} w_r^2\alpha_{r,1}\beta_r \\ \sum_{r=1}^{2q} w_r^2\alpha_{r,2}\beta_r \\ \vdots \\ \sum_{r=1}^{2q} w_r^2\alpha_{r,i}\beta_r \\ \vdots \\ \sum_{r=1}^{2q} w_r^2\alpha_{r,n}\beta_r \end{bmatrix}$$

Symmetric matrix ——————(C.11)

Using the following algorithms where

$d_{i,j}$ = element in row i, column j,

then $$d_{i,j} = \sum_{r=1}^{2q} \alpha_{r,i}\alpha_{r,j}w_r^2 \qquad \text{——————(C.12)}$$

and $$b_i = \sum_{r=1}^{2q} \alpha_{r,i}\beta_r w_r^2 \qquad \text{——————(C.13)}$$

The matrix equation (C.11) now becomes

$$[d]_{nxn} \cdot [a]_{nx1} = [b]_{nx1} \qquad \text{——————(C.14)}$$

The solution of equation (C.14) yields the values of the coefficients a_1 to a_n which when substituted into equation (C.4) gives the polynomial expression for the stress-strain curve of best-fit to the experimental data. A reliable measure of the number of terms, n, in equation (C.4) to provide a sufficiently high standard of correlation with the number of experimental points, q, is provided by comparing the standard error, S, given by

$$S = \sqrt{\frac{\sum_{r=1}^{2q} \left(\frac{\delta_r}{w_r}\right)^2}{q}} \qquad \text{——————(C.15)}$$

for different values of n. The residuals, δ_r, can be calculated from equation (C.7) for the computed values of the coefficients, a, from equation (C.14).

Note: If tensile strains exist in the crossection and the normal theoretical assumption, that the tensile strength of concrete can be neglected, is used, equations (C.2) and (C.3) become

$$\int_0^{\varepsilon_H} F(\varepsilon_c)\, d\varepsilon_c = \frac{\phi P_c}{b} \qquad \text{——————(C.16)}$$

$$\int_0^{\varepsilon_H} F(\varepsilon_c)\, \varepsilon_c\, d\varepsilon_c = \left(\frac{\varepsilon_H + \varepsilon_L}{2}\right) \frac{\phi P_c}{b} + \frac{\phi^2 M_c}{b} \qquad \text{———————(C.17)}$$

and $$\alpha_{2i-1,j} = \frac{\varepsilon_{Hi}^{\,j+1}}{j+1} \qquad \text{——————(C.18)}$$

NOTATION

Unless otherwise defined, the symbols used in this thesis have the following significance

a_1, a_2, a_3, a_n	Coefficients of a polynomial
$A_{cci}, A_{ccj}, A_{cti}, A_{ctk}, A_{sci}, A_{sti}$	Area of i,j and kth elements of steel and concrete as defined in Fig. 4.7, Fig. 4.8
A_{cc}, A_{sc}	Concrete and steel areas as defined in Fig.4.9
A_c	Crossectional area of concrete
A_s, A_t	Crossectional area of steel sections
A_g	Gross crossectional area
A_T	Crossectional area transformed to concrete
A(n,i,j)	Area of n,i,jth element
b,B	Minimum dimension, width of crossection
c_{Ox}, c_{OX}, c_{OY}	Initial deflection at midheight in the Ox, OX and OY directions
C_m	Column conversion factor (ACI 318-71(190))
d,D	Depth of crossection
d_X, d_Y	Distances as defined in Fig. 4.6
e	Eccentricity
e_x, e_y, e_X, e_Y	Eccentricity in Ox, Oy, OX and OY directions
e_1, e_{n+1}	Eccentricity at bottom and top of column
E, E_c, E_s	Moduli of elasticity, concrete, steel
E_{tc}, E_{ts}	Tangent moduli, concrete, steel
E_{ta}	Effective elastic modulus for axial load
E_{tb}	Effective elastic modulus in flexure
E_{ti}	Effective modulus in flexure for inelastic range
f_c, f_{bc}	Respectively calculated axial and bending stresses (BS 449(188))

f_{ct}	Tensile strength of concrete
f'_c	Compressive strength of concrete cylinder
f''_c	Compressive strength of concrete in a column
f_{sy}	Lower yield stress of steel
f_{uy}	Upper yield stress of steel
$F(\ )$	Functions
$F_c(\ ), F_s(\ )$	
h	Length of a column element
I	Second moment of area
I_c	Second moment of area of concrete section about the centroidal axis of whole crossection
I_s, I_t	Second moment of area of steel section about the centroidal axis of whole crossection
I_g	Second moment of area of whole crossection about its centroidal axis
I_{cx}, I_{cy} I_{cX}, I_{cY} I_{sx}, I_{sy} I_{sX}, I_{sY}	Second moment of concrete, steel areas about the Ox, Oy, OX (minor) and OY (major) axes respectively
I_{cxy}, I_{sxy}	Product moment of concrete, steel areas for the xOy axis system
I_{Txy}	Product moment of area, transformed to concrete, for the xOy axis system
I_{Tx}, I_{Ty} I_{TX}, I_{TY}	Second moment of area, transformed to concrete, about the Ox, Oy, OX and OY axes respectively
I_{cci}, I_{ccj}, I_{cti}, I_{ctk}, I_{sci}, I_{sti} I_{cc}, I_{sc}	Second moments of the corresponding areas A_{cci} to A_{sc} about their own centroidal axes parallel to the centroidal axis of whole crossection
k_b, k_c, k_m, k_t	Structural redundant, member redundant, testing machine and overall test stiffness as defined in Appendix A.
kl_u	Effective length of column (ACI 318-71)

K	Concrete age with origin at time of manufacture of the concrete
K_d, K_o, K_f	Concrete age at commencement of drying, first loading and cessation of loading respectively
$K_c(t), K_c(T)$	Creep coefficient rate at time, t,T (Fig.8.1)
$K_s(t), K_s(T)$	Shrinkage rate at time, t,T (Fig. 8.1)
l	Effective length of column
L, L_c	Actual length of column
L_{ci}, L_{si}	Length of ith strip of concrete, steel
M	Applied moment
M_c	Magnified ultimate moment (ACI 318-71)
M_c, M_s	Moment resisted by concrete, steel section
M_i, M_r	Bending moment at ith, rth section
M_o	Moment capacity as a beam (zero axial load)
M_p	Plastic moment of steel sections
M_x, M_y	Moment applied about the Ox, Oy axes
M_u	Ultimate moment capacity with axial load P_u applied
M_{cci}, M_{ccj} M_{cti}, M_{ctk} M_{sci}, M_{sti}	Elemental moments corresponding to areas A_{cci} to A_{sti} as defined in Fig. 4.7
M_1	Smaller end moment of column (ACI 318-71)
M_2	Larger end moment of column (ACI 318-71)
nc,ns	Number of strips or segments into which concrete, steel area is divided
N_c, N_s	Constants for hyperbolic creep, shrinkage function
NX'(n),NY'(n)	Number of strips into which the nth segment of area is divided in the OX', OY' direction as defined in Fig. 4.10
p_{bc}, p_c	Respectively permissible bending and axial stresses (BS 449)

P	Applied load
P_c, P_s	Load carried by concrete, steel
P_{cr}	Elastic critical buckling load
P_{max}	Maximum load
P_o	Axial load capacity
P_{sh}	Axial load capacity as a short column
P_{sy}	Load at yield of steel
P_{tc}, P_{ts}	Tangent modulus buckling load for concrete, steel section
P_u	Ultimate load capacity with moment M_u applied
P_{cci}, P_{ccj} P_{cti}, P_{ctk} P_{sci}, P_{sti}	Elemental forces for corresponding areas A_{cci} to A_{sti} as defined in Fig. 4.7
r	Radius of gyration of crossectional area transformed to concrete
r_X, r_Y	Radii of gyration of steel section about OX, OY axes
S	Plastic section modulus for steel section
t	Time with origin at first loading of concrete
T	Time with origin at commencement of drying of the concrete
T_{nc}, T_{ns}	Thickness of elemental strips of concrete, steel
u_i, u_i'	Column deflection at ith section
u_{oi}	Initial column deflection at ith section
v_r	Column deflection measured from tangent at midheight
v/s	Volume to surface area ratio
WX'(n), WY'(n)	Width of the nth segment in the OX', OY' directions as defined in Fig. 4.10

x_{cci}, x_{ccj} x_{cti}, x_{ctk} x_{sci}, x_{sti}	Distances from the centroidal axis to the nearest edge of the corresponding areas A_{cci} to A_{sti} as defined in Fig. 4.7
$\bar{x}_{cci}, \bar{x}_{ccj}$ $\bar{x}_{cti}, \bar{x}_{ctk}$ $\bar{x}_{sci}, \bar{x}_{sti}$	Distances of the centroids of the corresponding areas A_{cci} to A_{sti} from the centroidal axis for the whole crossection as defined in Fig.4.7
$x(n,i,j)$	Distance from the centroid of the n,i,jth element to the centroidal axis as defined in Fig. 4.10
$\bar{x}_{ci}, \bar{x}_{si}$	Distance from the ith strip of concrete, steel to the centroidal axis
$X'(n,i,j)$ $Y'(n,i,j)$	Coordinates of the centroid of the n,i,jth element for the Y'OX' axes system
y	Column deflection at distance z from an end
y_o	Sum of central deflection and end eccentricity $\delta_o + e$
y_r	Column deflection at the rth section
z, z_i	Distance along column from an end, ith section
Z	Elastic section modulus for steel section
α	Angle between the major principal axis and the direction of the plane of the applied end moments
β	Angle between the neutral axis and the major principal axis
β_d	Ratio of maximum design dead load to maximum design total load (ACI 318-71)
γ	A constant, taken as 0.00075
δ	Moment magnification factor (ACI 318-71)
δ_o	Central deflection
Δ	Deflection
$\Delta t_k, \Delta T_j$	Interval of time commencing at time t_k, T_j
$\Delta\varepsilon_c, \Delta\varepsilon_{cc}$ $\Delta\varepsilon_{cs}, \Delta\varepsilon_s$	Increment in applied concrete, creep, shrinkage and applied steel strain respectively

ε	Strain, in general
ε_a	Centroidal axis strain
$\varepsilon_{ao}, \varepsilon_{ar}$	Centroidal axis strain at midheight, rth section
$\varepsilon_{ac}, \varepsilon_{aci}$	Applied centroidal axis strain to the concrete, ith section
$\varepsilon_{as}, \varepsilon_{asi}$	Applied centroidal axis strain to the steel, ith section
$\varepsilon_c, \varepsilon_s$	Applied strain to the concrete, steel
$\varepsilon_c(t)$	Strain applied to the concrete at time t
$\varepsilon_{cc}(t)$	Creep strain of the concrete at time t
$\varepsilon_{cs}(t)$	Concrete shrinkage strain at time t
$\varepsilon_{cci}, \varepsilon_{ccj}$ $\varepsilon_{cti}, \varepsilon_{ctk}$ $\varepsilon_{sci}, \varepsilon_{sti}$	Strain at the nearest edge of corresponding areas, A_{cci} to A_{sti}, to the centroidal axis for the whole crossection
ε_o	Strain corresponding to compressive strength of concrete f''_c
ε_{ps}	Strain corresponding to short column load P_{sh}
ε_{sy}	Yield strain for steel
ε_t	Strain at instability of an axially loaded column
$\varepsilon_{r1}(n)$ $\varepsilon_{r2}(n)$ $\varepsilon_{r3}(n)$	Residual strains at three corners of the nth segment of area
$\varepsilon_r(n,i,j)$	Residual strain at the centroid of the n,i,jth element
$\varepsilon(n,i,j)$	Applied strain at the centroid of the n,i,jth element
$\varepsilon_H, \varepsilon_L$	Maximum, minimum strain at a section
θ_1, θ'_1	Slope at end of column
ν_{cc}, ν_{ct} ν_{sc}, ν_{st}	Coefficients which define the slope of the stress-strain curves as in Fig. 4.6

ρ_c, ρ_{ci}	Curvature applied to concrete, ith section
ρ_s, ρ_{si}	Curvature applied to steel, ith section
ρ_o	Curvature at central section
ρ_x	Curvature in the Ox direction
σ_c, σ_s	Stress in concrete, steel
σ_{sl}, σ_{st}	Steel stress in longitudinal, tangential direction
$\sigma_{r1}, \sigma_{r2}, \sigma_{r3}$	Steel residual stresses
σ_H, σ_L	Stress corresponding to strain $\varepsilon_H, \varepsilon_L$
ϕ	Capacity reduction factor (ACI 318-71)
$\phi_c(t), \phi_c(T)$	Creep coefficient at time t, T

REFERENCES

1. EMPERGER,F. 'Handbuch fur Eisenbetonbau, Dritte, Neubearbeitete Auflage', vol.I, 1921, pp. 391-395, 434-436, 442-444, 447-448.

2. EMPERGER,F. 'Composite Columns', Int.Ass.Bridge Struct. Engng, 1st Congress, 1932, pp. 595-618.

3. BURR,W.H. 'Composite Columns of Concrete and Steel', Proc.Inst.civ.Engrs, Lond., vol.CLXXXVIII, 1912, pp. 115-210.

4. MENSCH,L.J. 'Composite Columns', J. Am. Concr. Inst., Proc. vol. XXVII, 1930, pp. 263-280.

5. TUCKER,J. 'Reinforced Concrete Columns', Trans. Am. Soc. civ. Engrs, vol. LXXXVI, 1923, pp. 1074-1236.

6. BOUÉ,P. 'Concrete-Filled Steel Stanchions', Acier, Brux., No.9, Sept., 1957, pp. 351-356.

7. STANG, A.H, WHITTEMORE, H.L. and PARSONS,D.E. 'Some Tests of Steel Columns Incased in Concrete', U.S. Nat. Bur. Stand., J. Res., vol. XVI, 1936, pp. 265-287.

8. BONDALE, D.S. 'Column Theory with Special Reference to Composite Columns', Consult.Engr., vol.XXX, no.7, 1966, pp. 72-77; no.8, pp. 43-48; no.9, pp. 68-70.

9. PUDDY,H.M. 'Welding and the Mopin System', Welded Steel Structures, Inst. of Welding, London.

10. BELFORD,D. 'Composite Steel-Concrete Building Frame', Civ. Engng. A.S.C.E., vol. XLII, no. 7, 1972, pp. 61-65.

11. 'Construction's Man of the Year: Fazlur Khan', Engng News Rec., vol.CLXXXVIII, no.6, 1972, pp. 20-25.

12. RODERICK,J.W. 'Further Studies of Composite Steel and Concrete Structures', Congr. int. Ass. Bridge Struct. Engng, no. IX, Amsterdam, 1972, pp. 157-164.

13. RODERICK,J.W. and ROGERS,D.F. 'Load Carrying Capacity of Simple Composite Columns', Proc. Am. Soc. civ. Engrs, J. struct. Div., vol. XCV, no. ST2, 1969, pp. 209-228.

14. LOKE,Y.O. 'The Behaviour of Composite Steel-Concrete Columns', Thesis submitted to the University of Sydney for the degree of Ph.D., 1968, 203 pp.

15. FABER,O. 'Savings to be Effected by the More Rational Design of Cased Stanchions as a Result of Recent Full Size Tests', Struct. Engr, vol. XXXIV, no. 3, 1956, pp. 88-109.

16. SWAIN,F.W. and HOLMES,A.F. 'An Investigation of the Strength and Elastic Properties of Concrete-Filled Pipe Columns', Proc. Am. Soc. Test. Mater., vol. XV, pt. II, 1915, pp. 230.

17. KLOPELL,K. and GODER,W. 'Collapse Load Tests on Concrete Filled Tubes and Establishment of a Design Formula', Der Stahlbau, vol. XXVI, no.1, 1957.

18. SALANI,H.J. and SIMS,J.R. 'Behaviour of Mortar Filled Steel Tubes in Compression', J. Am. Concr. Inst., Proc. vol. LXI, no.10, 1964, pp. 1271-1283.

19. GARDNER,N.J. and JACOBSON,E.R. 'Structural Behaviour of Concrete Filled Steel Tubes', J. Am. Concr. Inst., Proc. vol. LXIV, no.7, 1967, pp. 404-413.

20. RODERICK,J.W. 'Studies in Composite Construction', Proc. 1965 Summer Conference on Plastic Design of Multi-storey Frames, Uni. Lehigh, Bethlehem, Penn.

21. FURLONG, R.W. 'Strength of Steel-Encased Concrete Beam-Columns', Proc. Am. Soc. civ. Engrs, J. struct. Div., vol. XCIII, no.ST5, 1967, pp. 113-124.

22. FURLONG,R.W. 'Design of Steel-Encased Concrete Beam Columns', Proc. Am. Soc. civ. Engrs, J. struct. Div., vol. XCIV, no. ST1, 1968, pp. 267-281.

23. KNOWLES,R.B. and PARK,R. 'Strength of Concrete Filled Steel Tubular Columns', Proc. Am. Soc. civ. Engrs, J. struct. Div., vol. XCV, no. ST12, 1969, pp. 2565-2585.

24. KNOWLES,R.B. and PARK,R. 'Axial Load Design for Concrete Filled Steel Tubes', Proc. Am. Soc. civ. Engrs, J. struct. Div., vol. XCVI, no. ST10, 1970, pp. 2125-2153.

25. NEOGI,P.K., SEN,H.K. and CHAPMAN,J.C. 'Concrete Filled Tubular Steel Columns under Eccentric Loading', Struct. Engr, vol. XLVII, no.5, 1969, pp. 187-195.

26. STANG,A.H. and WHITTEMORE,H.L. 'Tests of Steel Tower Columns for the George Washington Bridge', U.S. Nat. Bur. Stand., J. Res., vol. XV, 1935, pp. 317-339.

27. SALIGER,R. 'Versuche an Betonumschnurten Stahlsaulen', Der Bauingenieur, vol. XII, no. 15, 1931, pp. 255-258; no. 16, 1931, pp. 282-286.

28. TALBOT, A.N. and LORD,A.R. 'Tests of Columns. An Investigation of the Value of Concrete as Reinforcement for Structural Steel Sections', Uni. Ill. Engng. Exp. Stn Bull., no. 56, 1912.

29. ANDREWS,E.S. 'Structural Steelwork Reinforced with Concrete', Concr. Construct. Engng, vol. XVIII, 1923, pp. 505-508.

30. MENSCH,L.J. 'Tests of Concrete Columns with Cast-Iron Reinforcement', Proc. Am. Concr. Inst., vol. XIII, 1917, pp. 22.

31. HOGNESTAD,E. 'A Study of Combined Bending and Axial Load in Reinforced Concrete Members', Bull. Ill. Univ. Engng. Exp. Stn., no. 399, 1951, 128 pp.

32. WARREN,W.H. 'Engineering Construction. Part II: In Masonry and Concrete', London, 1921, 494 pp.

33. RITTER,W. 'Die Banweise Hennebique', Schweizerische Bauzeitung, vol. XXXIII, nos. 5, 6 and 7, 1899, pp. 41-43, 49-52 and 59-61.

34. MEMMLER,K., BIERETT,G. and GRÜNING,G. 'Tragfahigkeit von Stahlstutzen mit Betonkern bei mittigem Kraftangriff', Der Stahlbau, vol. VII, no.7, 1934, pp. 49-53; no.8, 1934, pp. 61-64.

35. v. KARMAN,T. 'Untersuchungen über Knickfestigkeit', Mitteilungen über Forschungsarbeiten auf dem Gebiete des Ingenieurwesens, no. 81, Berlin, 1910.

36. WESTERGAARD,H.M. and OSGOOD,W.R. 'Strength of Steel Columns', Trans. Am. Soc. mech. Engrs, vol. L, 1928, pp. 65-80.

37. ERNST,G.C., HROMADIK,J.J. and RIVELAND,A.R. 'Inelastic Buckling of Plain and Reinforced Concrete Columns, Plates and Shells', Univ.Nebraska. Engng Exp. Stn. Bull., no. 3, 1953.

38. BROMS,B. and VIEST,I.M. 'Long Reinforced Concrete Columns - A Symposium', Trans. Am. Soc. civ. Engrs, vol. CXXVI, pt. II, 1961, pp. 308-401.

39. AMERICAN INSTITUTE OF STEEL CONSTRUCTION, 'Specification for the Design, Fabrication and Erection of Structural Steel for Buildings', New York, 1969, 117 pp.

40. LOHR,W.S. 'Concrete Encased in Steel Shells Proposed', Eng. News. Rec., vol. CXIII, 1934, pp. 760-762.

41. HOGNESTAD,E., HANSON,N.W. and McHENRY,D. 'Concrete Stress Distribution in Ultimate Strength Design', J. Am. Concr. Inst., vol. XXVII, no.4, 1955, pp. 455-479.

42. JOHNSON,J.B., BRYAN,C.W. and TURNEAURE,F.E. 'Theory and Practice of Modern Framed Structures', New York, 1899.

43. JOHNSTON,B.G. (Edit.) 'The Column Research Council Guide to Design Criteria for Metal Compression Members', 2nd edn.; New York, 1966, 217 pp.

44. GURFINKEL,G. and ROBINSON,A. 'Determination of Strain Distribution in a Reinforced Concrete Section Subjected to Bending Moment and Longitudinal Load', J. Am. Concr. Inst., Proc. vol. LXIV, no.7, 1967, pp. 398-402.

45. KATO,B. and KANATANI,H. 'Experimental Studies on Concrete Filled Tubular Columns', Steel Struct. Lab. Rep., Dept. Arch, Univ. Tokio, 1966.

46. COIGNET,E. and TEDESCO,N.de. 'Du Calcul des Ouvrages, en Ciment avec Ossature Metallique', Memoires de la Société des Ingénieurs Civils de France, pt.1, 1894, pp. 282-363.

47. McMILLAN,F.R. 'A Study of Column Test Data', Proc. Am. Concr. Inst., vol. XVII, 1921, pp. 150-171.

48. SLATER,W.A. and LYSE,I. 'Reports on Column Tests Made at Lehigh University', J. Am. Concr. Inst., Proc. vol. XXVII, 1931, pp. 677-730. J. Am. Concr. Inst., Proc. vol. XXVII, 1931, pp. 791-835. J. Am. Concr. Inst., Proc. vol. XXVIII, 1931, pp. 159-166.

49. LYSE,I. and KREIDLER,C.L. 'Fourth Progress Report on Column Tests at Lehigh University, J. Am. Concr. Inst., Proc. vol. XXVIII, 1932, pp. 317-346.

50. LYSE,I. 'Fifth Report on Column Tests at Lehigh University', J. Am. Concr. Inst., Proc. vol. XXIX, 1933, pp. 433-442.

51. RICHART,F.E. and STAEHLE,G.C. 'Reports on Column Tests made at the University of Illinois', J. Am. Concr. Inst., Proc. vol. XXVII, 1931, pp. 731-790. J. Am. Concr. Inst., Proc. vol. XXVIII, 1931, pp. 167-175. J. Am. Concr. Inst., Proc. vol. XXVIII, 1932, pp. 279-315.

52. RICHART,F.E. 'Reinforced Concrete Column Investigation. Tentative Final Report of Committee 105', J. Am. Concr. Inst., Proc. vol. XXIX, 1933, pp. 275-284.

53. STANDARDS ASSOCIATION OF AUSTRALIA 'SAA Code for Concrete in Building, AS CA2-1963', Sydney, 1963.

54. HOGNESTAD,E. 'Inelastic Behaviour in Tests of Eccentrically Loaded Short Reinforced Concrete Columns', J. Am. Concr. Inst., vol. XXIV, no.2, 1952, pp. 117-139.

55. BROMS,B. and VIEST,I.M. 'Long Reinforced Concrete Columns - A Symposium', Trans. Am. Soc. civ. Engrs, vol. CXXVI, pt. II, 1961, pp. 309-400.

56. PFRANG,E.O., SIESS,C.P. and SOZEN,M.A. 'Load-Moment-Curvature Characteristics of Reinforced Concrete Cross Sections', J. Am. Concr. Inst., Proc. vol. LXI, no.7, 1964, pp. 763-778.

57. PIOBERT,G., MORIN and DIDION, Mém de l'Artillerie, vol. V, 1842, pp. 525.

58. LUDERS,W., J. Dinglers Polytech., vol. CLV, 1860, pp. 18.

59. HARTMANN, 'Distribution des Deformations dans les Métaux soumis aux Efforts', Paris, 1896.

60. BAKER,J.F., HORNE,M.R. and HEYMAN,J. 'The Steel Skeleton, Volume II, Plastic Behaviour and Design', London, 1956, 403 pp.

61. WICKSTEED, J.H. 'Description of an Autographic Test-recording Apparatus', Proc. Instn. mech. Engrs, Lond., 1886.

62. KENNEDY,A.B.W. 'Experiments on the Yield Point of Steel under Transverse Tests', Engineering, Lond., vol. CXV, 1923.

63. ROBERTSON,A. and COOK,G. 'Transition from the Elastic to the Plastic State in Mild Steel', Proc. Roy. Soc. A, vol. LXXXVIII, 1913.

64. LOVE,A.E.H. 'A Treatise on the Mathematical Theory of Elasticity', Lond., 1892.

65. EWING,J.A. 'The Strength of Materials', Lond., 1899.

66. BLEICH,F. 'Stahlhochbauten, ihre Theorie, Berechnung und bauliche Gestaltung', Berlin, 1936.

67. MAIER-LEIBNITZ,H. 'Test Results, their Interpretation and Application', Int. Ass. Bridge Struct. Engng., Prelim. Publ., 2nd Congr., Berlin, 1936.

68. HORNE,M.R. 'The Effect of Strain-Hardening on the Equalization of Moments in the Simple Plastic Theory, Br. Weld. Res. Ass. FE.1, Committee on the Load Carrying Capacity of Frame Structures, 1949.

69. LAY,M.G. and SMITH,P.D. 'Role of Strain-Hardening in Plastic Design', Proc. Am. Soc. civ. Engrs, J. struct. Div., vol. XCI, no. ST3, 1965.

70. WHITE,M.W. 'The Lateral-Torsional Buckling of Yielded Structural Steel Members', Thesis submitted to Lehigh University for the degree of Ph.D., 1956.

71. BAKER,J.F. and HORNE,M.R. 'Effect of Internal Stresses on the Behaviour of Members in the Plastic Range', Engineering, Lond., vol. CLXXI, 1951.

72. OSGOOD,W.R. 'The Effect of Residual Stress on Column Strength', Proc. First U.S. Natl. Congr. App. Mech., 1951, pp. 415.

73. YANG,C.H., BEEDLE,L.S. and JOHNSTON,B.G. 'Residual Stress and the Yield strength of Steel Beams', Weld. J., Easton, Res. Supp., vol. XXXI, 1952, pp. 224.

74. HUBER,A.W. and BEEDLE,L.S. 'Residual Stress and the Compressive Strength of Steel', Weld. J., Easton, Res. Supp., vol. XXXIII, 1954, pp. 589.

75. GLANVILLE,W.H. 'Studies in Reinforced Concrete III' Tech. Pap. Bldg. Res. D.S.I.R., no.12, 1930.

76. RUSCH,H. 'Researches Toward a General Flexural Theory for Structural Concrete', J. Am. Concr. Inst., vol. XXXII, no.1, 1960, pp. 1-28.

77. SIGVALDASON,O.T. 'The Influence of Testing Machine Characteristics upon the Cube and Cylinder Strength of Concrete', Mag. Concr. Res., vol. XVIII, no. 57, 1966, pp. 197-206.

78. WHITNEY,C.S., Discussion of a paper by JENSEN,V.P. 'The Plasticity Ratio of Concrete and its Effect on the Ultimate Strength of Beams', J. Am. Concr. Inst., Proc. vol. XXXIX, 1943, Supplement pp. 584-2 to 584-6.

79. RAMALEY,D. and McHENRY,D. 'Stress-Strain Curves for Concrete Strained Beyond the Ultimate Load', Lab. Rep. U.S. Bur. Rec., no. SP-12, 1947, 22 pp.

80. BARNARD,P.R. 'Researches into the Complete Stress-Strain Curve for Concrete', Mag. Concr. Res, vol. XVI, no. 49, 1964, pp. 203-210.

81. HUGHES,B.P. and CHAPMAN,G.P. 'The Complete Stress-Strain Curve for Concrete in Direct Tension', RILEM Bull., no. 30, 1966, pp. 95-97.

82. EVANS,R.H. and MARATHE,M.S. 'Stress Concentration in Prestressed Concrete', Instn. civ. Engrs, Conference on Prestressed Concrete Pressure Vessels, Pap. no.47, 1968.

83. HOLFORD,J.G. 'Stress and Deformation in Columns of Steel and Concrete', Instn Engrs Aust., Concrete Conference: Problems in Composite Structures, 1971.

84. RASCH,C. 'Stress-Strain Diagrams of Concrete Obtained by Constant Rates of Strain', RILEM Symposium - The Influence of Time on the Strength and Deformation of Concrete, Munich, 1958.

85. CLARK,L.E., GERSTLE,K.H. and TULIN,L.G. 'Effect of Strain Gradient on the Stress-Strain Curve for Mortar and Concrete', J. Am. Concr. Inst., Proc. vol. LXIV, no.9, 1967, pp. 580-586.

86. BLANKS,R.F. and McNAMARA,C.C. 'Mass Concrete Tests on Large Cylinders', J. Am. Concr. Inst., Proc. vol. XXXI, 1935, pp. 280-303.

87. ENDERSBEE,L.A. 'Brittle Failure in Concrete and Rocks', Civ. Eng. Trans. Instn Engrs Aust., vol. CEIX, no.2, 1967, pp. 217-234.

88. RICHART,F.E. and BROWN,R.L. 'An Investigation of Reinforced Concrete Columns', Bull. Ill. Univ. Engng. Exp. Stn, no. 267, 1934, 91 pp.

89. SHAH,S.P. and VIJAY RANGAN,B. 'Effects of Reinforcements on Ductility of Concrete', Proc. Am. Soc. civ. Engrs, J. struct. Div., vol. XCVI, no. ST6, 1970, pp. 1176-1183.

90. SOLIMAN,M.T.M. and YU,C.W. 'The Flexural Stress-Strain Relationship of Concrete Confined by Rectangular Transverse REinforcement', Mag. Concr. Res., vol. XIX, no.61, 1967, pp. 223-238.

91. PARK,R. and SAMPSON,R.A. 'Ductility of Concrete Column Sections in Seismic Design', J. Am. Concr. Inst., Proc. vol. LXIX, no. 9, 1972, pp. 543-550.

92. VARGHESE,P.C. 'Strength of Axially Loaded Steel Columns Encased in Concrete', J. India Rds. Congr., vol. XXV-2, 1960, pp. 193-201.

93. HUDSON,F.M. 'Reinforced Concrete Columns: Effects of Lateral Tie Spacing on Ultimate Strength', Am. Concr. Inst. Spec. Publ., no. 13, 1966, pp. 235-244.

94. KARSAN,I.D. and JIRSA,J.O. 'Behaviour of Concrete under Compressive Loadings', Proc. Am. Soc. civ. Engrs, J. struct. Div., vol. XCV, no. ST12, 1969, pp. 2543-2563.

95. SINHA,B.P., GERSTLE,K.H. and TULIN,L.G. 'Stress-Strain Relations for Concrete under Cyclic Loading', J. Am. Concr. Inst., Proc. vol. LX1, no.2, 1964, pp. 195-211.

96[1] KARSAN,I.D. and JIRSA,J.O. 'Behaviour of Concrete under Varying Strain Gradients', Proc. Am. Soc. civ. Engrs, J. struct. Div., vol. XCVI, no. ST8, 1970, pp. 1675-1696.

96[2] STURMAN,G.M., SHAH,S.P. and WINTER,G. 'Effect of Flexural Strain Gradients on Microcracking and Stress-Strain Behaviour of Concrete', J. Am. Concr. Inst., Proc. vol. LXII, no.7, 1965, pp. 805-822.

97. SMITH,R.G. 'The Determination of the Compressive Stress-Strain Properties of Concrete in Flexure', Mag. Concr. Res., vol. XII, no.36, 1960, pp. 165-170.

98. SMITH,R.G. 'The Determination of the Stress-Strain Properties of Concrete in Flexure', Mag. Concr. Res., vol. XII, no.36, 1960, pp. 165-170.

99. PRENTIS,J.M. 'Analysis of Inelastic Bending Strength in Concrete Beams, J. Am. Concr. Inst., Proc. vol. LIII, no.3, 1956, pp. 309-318.

100. SMITH,R.G. and ORANGUN,C.O. 'Evaluation of the Stress-Strain Curve of Concrete in Flexure Using Method of Least Squares', J. Am. Concr. Inst., Proc. vol. LXVI, no.7, 1969, pp. 553-559.

101. WARNER,R.F. and HULSBOS,C.L. 'Probable Fatigue Life of Prestressed Concrete Flexural Members', Lehigh Univ. Fritz Lab. Rep., no. 223.24A, 1962.

102. STANDARDS ASSOCIATION OF AUSTRALIA 'Mild Steel for General Structural Purposes, AS 149, Sydney.

103. LOW,J.R. and GENSAMER,M. Trans. Am. Inst. Min. Metal. Petr. Engrs, vol. CLVIII, 1944, pp. 207. (Trans. AIME)

104. COTTRELL,A.H. and BILBY,B.A., Proc.Phys. Soc. vol. ALXII, 1949, pp. 49.

105. JOHNSTON,W.G. and GILMAN,J.J. 'Dislocation Velocities, Dislocation Densities and Plastic Flow', J. Appl. Phys., vol. XXX, 1959, pp. 129-144.

106. JOHNSTON,W.G., J. Appl. Phys., vol. XXIII, 1962, pp.2716.

107. HAHN,G.T., Acta Met., vol. X, 1962, pp. 727.

108. HALL,E.O. 'Yield Point Phenomena in Metals and Alloys', London, 1970.

109. COOK, G. 'Some Factors Affecting the Yield Point in Mild Steel' Trans. Instn. Engrs Shipb. Scot., vol. LXXXI, 1938.

110. STEIDEL,R.F. and MAKEROV,C.E. 'Yield Strength, Elongation and Reduction in Area as a Function of Strain Rate', Bull. Am. Soc. Test. Mater., no.247, 1960, pp. 57.

111. RODERICK,J.W. and PHILLIPS,I.H. 'Carrying Capacity of Simply Supported Mild Steel Beams', Res.' Engng Struct. Suppl., 1949.

112. FORSCHER,F. 'A Theory of the Yield Point and Transition Temperature of Mild Steel', J. Appl. Mech., vol. XXIII, no.2, 1956, pp. 219.

113. BEEDLE,L.S. and TALL,L. 'Basic Column Strength', Proc. Am. Soc. Civ. Engrs, J. struct. Div., vol. LXXXVI, no. ST7, 1960.

114. GOZUM,A.T. and HUBER,A.W. 'Material Properties, Residual Stresses and Column Strength', Lehigh Univ., Fritz Lab. Rep., no. 220A. 33, 1958.

115. WELTER,G. Metallurgia, vol. XVIII, no. 8, 1945, pp. 143.

116. RODERICK,J.W. 'Load-deflection Relationship for a Partially Plastic Rolled - Steel Joist', Brit. Weld. J., vol. I, 1954.

117. RODERICK,J.W. and HEYMAN,J. 'Extension of the Simple Plastic Theory to Take Account of the Strain-hardening Range', Instn. Mech. Engrs, War Emergency Publication, no.67, 1951.

118. DALBY, 'The Mechanical Properties of Steel', Proc. Instn. civ. Engrs., vol. CCXXI, 1925-6, pp. 21.

119. MORRISON,J.L.M. 'The Yield Point of Mild Steel with Particular Reference to the Effect of Size of Specimen', Proc. Instn. Mech. Engrs, vol. CXLII, 1939.

120. PONOMAREV,S.D. a kol. 'Raschet na prochnost v mashinostroienii I', Moscow, 1956.

121. O'CONNOR,C. 'Residual Stresses and Their Influence on Structural Design', J. Instn.Engrs.Aust., vol. XXVII, 1955, pp. 313-321.

122. BEEDLE,L.S. and TALL,L. 'Basic Column Strength', Trans. Am. Soc. civ. Engrs, vol. CXXVII, pt.II, 1962.

123. STANDARDS ASSOCIATION OF AUSTRALIA 'Methods for Tensile Testing of Metals, A 23-1960'.

124. ADAMS,P.F. and GALAMBOS,T.V. 'Material Considerations in Plastic Design' Publ. int. Ass. Bridge Struct. Engng, vol. XXIX, 1969.

125. PENNINGTON,R.H. 'Introductory Computer Methods and Numerical Analysis' London, 1966, pp. 361-372.

126. BRETTLE,H.J. 'Ultimate Strength Design of Universal Steel Section Struts Encased in Concrete and Subjected to Biaxial Bending', Civ. Engng Trans. Instn Engrs Aust., vol. CE XIV, no.1, 1972, pp. 1-12.

127. BASU,A.K. 'Computation of Failure Loads of Composite Columns', Proc. Instn civ. Engrs, vol. XXXVI, 1967, pp. 557-578.

128. WARNER,R.F. 'Biaxial Moment Thrust Curvature Relations', Proc. Am. Soc. civ. Engrs, J. Struct. Div., vol. CXV, no. ST5, 1969, pp. 923-940.

129. VIRDI,K.S. and DOWLING,P.J. 'The Ultimate Strength of Composite Columns in Biaxial Bending', Proc. Instn civ. Engrs, vol. LV, pt. 2, 1973, pp. 251-272.

130. CHEN,W.F. and SANTATHADAPORN,S. 'Review of Column Behaviour under Biaxial Load', Proc. Am. Soc. civ. Engrs, J. struct. Div., vol. CXIV, no. ST12, 1968, pp. 2999-3020.

131. PROCTER,A.N. 'Lateral-Torsional Stability of Composite Members', Consult. Engr, Lond., vol. XXVII, no. 2, 1965, pp. 171-174.

132. SHERMAN,D.R. and LUKAS,D.E. 'Torsionally Stiff Columns under Eccentric Load', Proc. Am. Soc. civ. Engrs, J. struct. Div., vol. XCVI, no.ST2, 1970, pp. 335-351.

133. WARNER,R.F. 'Long Reinforced Columns in Biaxial Bending', Rep. R. Univ. N.S.W. Sch. civ. Engng., no. R-33, 1968, 34pp.

134. AYRTON and PERRY 'On Struts', Engineer, Lond., Dec.10, 1886, pp. 464.

135. TIMOSHENKO,S.P. and GERE,J.M. 'Theory of Elastic Stability', 2nd edn, New York, 1961, pp. 13-33.

136. NEWMARK,N.M. 'Numerical Procedures for Computing Deflections, Moments and Buckling Loads', Proc. Am. Soc. civ. Engrs, vol. LXVIII, no. 5, pt. 1, 1942, pp. 691-718.

137. BASU,A.K. and HILL,W.F. 'A More Exact Computation of Failure Loads of Composite Columns', Proc. Instn. civ. Engrs, vol. XL, 1968, pp. 37-60.

138. GALAMBOS,T.V. 'Structural Members and Frames', New Jersey, 1968, 373 pp.

139. HATT,W.K. 'Notes on the Effect of Time Element in Loading Reinforced Concrete Beams', Proc. Am. Soc. Test, vol. VII, 1907, pp. 421-433.

140. DAVIS,R.E. and DAVIS,H.E. 'Flow of Concrete under the Action of Sustained Loads', J. Am. Concr. Inst., Proc. vol. XXVII, 1931, pp.837-901.

141. NEVILLE,A.M. 'Creep of Concrete: Plain, Reinforced and Prestressed, Amsterdam, 1970, 622pp.

142. ACI COMMITTEE 209. 'Annotated Bibliography on Shrinkage and Creep in Concrete. 1905-1964', Detroit, 1967, 102 pp.

143. LORMAN,W.R. 'List of Additional References to Creep and Volume Changes of Concrete. 1901-1964', Detroit, 1967, 58pp.

144. RILEM 'Physical and Chemical Causes of Creep and Shrinkage of Concrete', Materiaux et Constructions, vol. II, no.8, 1969, pp. 153-162.

145. CAMPBELL-ALLEN,D. 'Creep and Shrinkage in Concrete as Influenced by Concrete Practice and Environment', Constrl. Rev., vol. XXXVI, no. 12, 1963, pp. 1-6.

146. ALEXANDER,K.M. 'Factors Affecting the Drying Shrinkage of Concrete', Constrl. Rev., vol. XXXVII, no. 3, 1964, pp. 3-10.

147. PATTEN,B.J.F. and WELCH,G.B. 'A Critical Review of Creep and Drying Shrinkage', Cem. Concr. Ass. Aust., Research Report, 1968.

148. NEVILLE,A.M. 'Role of Cement in the Creep of Mortar', J. Am. Concr. Inst., Proc. vol. LV, no.9, 1955, pp. 963-984.

149. NEVILLE,A.M. 'The Relation between Creep of Concrete and the Stress-Strength Ratio', Appl. Sci. Res., vol. IX, sect. A., 1960, pp. 285-292.

150. FREUDENTHAL,A.M. and ROLL,F. 'Creep and Creep Recovery of Concrete under High Stress', J. Am. Concr. Inst., Proc. vol. LIV, 1958, pp. 1111-1142.

151. MAMILLAN,M. 'Etude sur le Fluage du Beton', Ann. Inst. Technique Batiment et des Travaux Publics, Paris, 1959, pp.221-233.

152. GVOZDEV,A.A. 'Creep of Concrete', Mekhanika Tverdogo Tela, Moscow, 1966, pp. 137-152.

153. RUSCH,H. 'Versuche zur Festigkeit der Biegerdruckzone', Deutscher Ausschuss fur Stahlbeton, no.120.

154. GOYAL,B.B. and JACKSON,N. 'Slender Concrete Columns under Sustained Load', Proc. Am. Soc. civ. Engrs, J. struct. Div., vol. XCVII, no. ST11, 1971, pp. 2729-2750.

155. GLUKLICH, J. 'The Complete Rheological Law for Lightweight and Normal-weight Mortars', Technion Department of Mechanics, Haifa, Report no.68-5, 1968, 78 pp.

156. L'HERMITE,R. 'What do We Know about the Plastic Deformation and Creep of Concrete', RILEM Bulletin, no. 1, 1959, pp. 21-51.

157. ILLSTON,J.M. 'The Creep of Concrete under Uniaxial Tension', Mag. Concr. Res., vol. XXVII, no. 51, 1965, pp. 77-84.

158. HANSEN,T.C. and MATTOCK,A.H. 'Influence of Size and Shape of Member on the Shrinkage and Creep of Concrete', J. Am. Concr. Inst., Proc. vol. LXIII, no.2, 1966, pp. 267-289.

159. ROSS,A.D. 'Concrete Creep Data', Struct.Engr, vol.XV, no.8, 1937, pp. 314-326.

160. LORMAN,W.R. 'The Theory of Concrete Creep', Proc. Am. Soc. Test. Mater., vol. XL, 1940, pp. 1082-1102.

161. TROXELL,G.E., RAPHAEL,J.M. and DAVIS,R.E. 'Long-time Creep Tests of Plain and Reinforced Concrete', Proc. Am. Soc. Test. Mater., vol. LXVIII, 1958, pp. 1101-1120.

162. WIERIG,H.J. 'Einflusse auf das Biegekriechen von Zementmortel' Schweizerische Bauzeitung, vol. LXXXII, no. 29, 1964, pp. 512-515.

163. DUTRON,R. 'Creep in Concretes', RILEM Bulletin, no. 34, 1957, pp. 11-33.

164. HANSEN,T.C. 'Creep and Stress Relaxation of Concrete', Proc. Swedish Cem. Concr. Res. Inst., vol. XXXI, 1960, 112 pp.

165. ROPER,H. 'Dimensional Change as a Factor in Selection of Rock Types for Use in Concrete Aggregates', Constrl Rev., vol. XXXIX, no.7, 1966, pp. 22-23.

166. ROPER,H. 'Shrinking Aggregates in Concrete', CSIRO Spec. Tech. Rep. No.502, Nat. Bldg. Res. Inst., South Africa.

167. ROPER,H. 'The Properties of Concrete Manufactured with Coarse Aggregates of the Sydney Region', Res. Rep. Univ. Sydney civ.Engng Sch., no. R204, 1973.

168. HUMMEL,A., WESCHE,K. and BRAND,W. 'Einfluss der Zementart, des Wasser - Zement - Verhaltnisses und des Belastungsalters auf das Kriechen von Beton', Deutscher Auschuss fur Stahlbeton, no. 146, 1962, 133pp.

169. GLANVILLE,W.H. 'Creep on Concrete under Load', Struct. Engr, vol. XI, no.2, 1933, pp. 54-73.

170. McHENRY,D. 'A New Aspect of Creep in Concrete and its Application to Design', Proc. Am. Soc. Test. Mater., vol. XLIII, 1943, pp. 1069-1084.

171. ROSS,A.D. 'Creep of Concrete under Variable Stress', J. Am. Concr. Inst., Proc. vol. LIV, no. 9, 1958. pp. 739-758.

172. ISHAI, O. 'The Influence of Sand Concentration on Deformation of Mortar Beams under Low Stresses', J. Am. Concr. Inst., Proc.vol. LVIII, 1962, pp. 611-622.

173. THOMAS,F.G. 'A Conception of Creep of Unreinforced Concrete, and an Estimation of the Limiting Values', Struct. Engr, vol. XI, no. 2, 1933.

174. JONES,T.R., HIRSCH,T.J. and STEPHENSON,H.K. 'The Physical Properties of Structural Quality Lightweight Aggregate Concrete', Texas Transportation Inst., Texas A. and M., College Station, 1959.

175. WAGNER,O. 'Das Kriechen unbewehrten Betons', Deutscher Auschuss fur Stahlbeton, Bull. no.31, 1958.

176. COMITE EUROPEAN DU BETON-FEDERATION INTERNATIONALE DE LA PRECONTRAINTE 'International Recommendations for the Design and Construction of Concrete Structures', 1970.

177. ACI COMMITTEE 209 'Prediction of Creep, Shrinkage and Temperature Effects in Concrete Structure', Am. Concr. Inst, Spec. Publ., no. SP-27, 1972, pp. 51-93.

178. CAMPBELL-ALLEN,D. 'The Prediction of Shrinkage for Australian Concrete', Res. Rep. Univ. Sydney civ. Engng, no. R180, 1970.

179. HELLESLAND,J. and GREEN,R. 'Sustained and Cyclic Loading of Concrete Columns', Proc. Am. Soc. civ. Engrs, J. struct. Div., vol. XCVII, no. ST4, 1971, pp. 1113-1128.

180. HELLESLAND,J. and GREEN,R. 'Sustained and Cyclic Loading of Concrete Columns' Solid Mech. Div., Univ. Waterloo Rep., no. 62, 1970, 34 pp.

181. DAVIS,H.E. 'Autogenous Volume Changes in Concrete', Proc. Am. Soc. Test. Mater., vol. XL, 1940.

182. CAMPBELL-ALLEN,D. and HOLFORD,J.G. 'Stress and Cracking in Concrete Due to Shrinkage', Trans. Instn. Engrs, Aust., vol. CEXXII, no.1, 1970, pp. 33-39.

183. HARRISON,H.B. 'Computer Methods in Structural Analysis', New Jersey, 1973, 332 pp.

184. PFRANG,E.O. and SIESS,C.P. 'Behaviour of Restrained Reinforced Concrete Columns' Proc. Am. Soc. civ. Engrs, J. struct. Div., vol. XC, no. ST5, 1964, pp. 113-135.

185. MANUEL,R.F. and MACGREGOR,J.G. 'Analysis of Restrained Reinforced Concrete Columns under Sustained Load', J. Am. Concr. Inst., Proc. vol. LXIV, no. 1, 1967, pp. 12-24.

186. WINTER,G. 'Compression Members in Trusses and Frames', Col. Res. Ccl., Proc. 4th Tech. Session, The Philosophy of Column Design, 1954.

187. MACGREGOR,J.G., BREEN,J.E. and PFRANG,E.O. 'Design of Slender Concrete Columns', J. Am. Concr. Inst., Proc. vol. LXVII, no. 1, 1970, pp. 6-28.

188. BRITISH STANDARDS INSTITUTION 'Specification for the Use of Structural Steel in Building BS 449: Part I: 1971' London, 1971, 120pp.

189. STANDARDS ASSOCIATION OF AUSTRALIA 'SAA Steel Structures Code AS CA1-1968' Sydney, 1968, 114 pp.

190. AMERICAN CONCRETE INSTITUTE 'Building Code Requirements for Reinforced Concrete (ACI 318-71)', Detroit, 1972, 78 pp.

191. ACI Committee 318, 'Commentary on Building Code Requirements for, Reinforced Concrete (ACI 318-71), Detroit, 1972, 96 pp.

192. MALHOTRA,H.L. and STEVENS,R.S. 'Fire Resistance of Encased Stanchions', Proc. Instn. civ. Engrs, vol. XXVII, 1964, pp. 77-98.

193. AUSTIN,W.J. 'Strength and Design of Metal Beam-Columns', Proc. Am. Soc. civ. Engrs, J. Struct. Div., vol. LXXXVII, no. ST4, 1961, pp. 1-32.

194. CAMPUS,C. and MASONNET,C. 'Recherches sur de Flambement de Colonnes en Acier A37, a Profil en Double Te, Sollicitees Obliquement', Comptes Rendes de Recherches, IRSIA, IWONL, April, 1956.

195. MASONNET,C. 'Stability Considerations in the Design of Steel Columns', Proc. Am. Soc. civ. Engrs, J. struct. Div., vol. LXXXV, no. ST7, 1959.

196. HORNE,M.R. 'The Stanchion Problem in Frame Structures Designed According to Ultimate Carrying Capacity', Proc. Instn. civ. Engrs, Struct. Paper no. 46, pt. 3, 1956, pp. 105.

197. GILKEY,H.J. 'The Moist Curing of Concrete', Engng. News Rec., vol. CXIX, 1937, pp. 630-633.

198. TROXELL, G.E., DAVIS,H.E. and KELLY,J.W. 'Composition and Properties of Concrete, New York, 1968, pp. 254-255.

199. BUTCHER,W.S. 'The Effect of Air Drying before Tests: 28 day Strength of Concrete', Constrl Rev., vol. XXXI, no. 12, 1958, pp. 31-32.

200. GRIEB,W.E. and WERNER,G. 'Comparison of Splitting Tensile Strength with Flexural and Compressive Strengths', Proc. Am. Soc. Test Mater., vol. LXII, pp. 972-990.

201. ROPER, H. 'Deformation of Concrete in the Sydney Area', Thesis submitted to the University of Sydney for the degree of M.Eng. Sc., 1971, 130 pp.

202. ROPER,H., COX,J.E. and ERLIN,B. 'Petrographic Studies on Concrete Containing Shrinking Aggregate', Res. Dev. Lab. Port. Cem. Ass., Bull. no. 172, 1964, 18 pp.

203. ANSOURIAN, P. 'Connections in Composite Framed Structures', Conc. Conf. - Problems in Composite Structures, Instn. Engrs. Aust., Sept. 1971.

204. ANSOURIAN, P. 'Rigid-Frame Connections to Concrete-filled Tubular Columns', Centre Rech. Scient. Tech. de l'Ind. Fab. Metal., no. MT 86, 1974, 50pp.

TABLE 2.1

TESTS BY MENSCH (4) ON SOLID CIRCULAR METAL CORES ENCASED IN SPIRALLY REINFORCED CONCRETE

Outside Diameter (in.)	Spiral Diameter (in.)	Length (ft.)	Solid Metal Core Diameter (in.)	Type of Material	Max.Load for Spiralled Concrete alone (kips) (1)	Max.Load for Metal Core alone (kips) (2)	Max. Test Load for Composite Column (kips)	Sum of Individual Strengths (kips) (1) + (2)
			Tests at Armour Institute of Technology in 1918					
7½	7	6	2	Cast-Iron	177.3	59.1	345.7	236.4
7½	7	6	2	Steel	177.3	63.9	353.9	241.2
			Tests at University of Illinois in 1930					
7½	6½	5	4	Cast-Iron	126	444	611	570
7½	6½	5	4	Cast-Iron Spliced Centre	126	444	636	570
7½	6½	5	4	Steel	126	434	590	560
7½	6½	7	4	Cast-Iron	126	295	545	421
7½	6½	7	4	Steel	126	403	559	529
7½	6½	5	5	Cast-Iron	96	867	989	963

TABLE 2.2

TESTS BY SALIGER (27) ON STEEL CHANNELS ENCASED IN REINFORCED CONCRETE (FIG.2.4)

Column Type	Type of Binder	Concrete Area A_c (sq.in.)	Structural Steel Area A_s (sq.in.)	Steel Yield Stress f_{sy} (kips/ sq.in.)	Concrete Strength f''_c (kips/ sq.in.)	Max. Test Load (kips) (1)	Theoretical Max. Load $f''_c A_c + f_{sy} A_s$ (kips) (2)	Addit. Strength Provided by Binders	
								(kips) (1)-(2)	(percent) $\frac{(1)-(2)}{(2)}$
1	Spiral	153.0	4.18	34.1	2.07	518	460	58	12.6
2	Spiral	147.5	9.64	37.7	2.07	735	668	67	10.0
3	Spiral	147.5	9.64	37.7	2.07	756	668	88	13.2
4	Rectangular	111.0	10.33	37.7	2.07	631	620	11	1.8
5	Spiral	196.0	9.32	43.2	2.07	866	809	57	7.1

TABLE 2.3

TESTS BY TALBOT AND LORD (28) ON BUILT-UP STEEL SECTION WITH A CONCRETE CORE (FIG.2.5(b))

Column Length (ft.) (1)	Max. Load for Bare Steel Section (kips) (2)	Concrete Mix Cement:Sand:Agg. (3)	Concrete Strength from Prism Tests (lb./sq.in.) (4)	Max. Load for Composite columns (kips) (5)	Theoretical Concrete Stress at Failure for Composite Columns $[\frac{(5)-(2)}{A_c}]$ (lb./sq.in.) (6)	Ratio of Max.Load for Composite to Bare Steel Columns. $[\frac{(5)}{(2)}]$ (7)
2.33	488	1 : 2 : 4				
4.67	445	1 : 2 : 4	1420	586	1320	1.32
10.00	415	1 : 2 : 4	1420	543	1200	1.31
15.33	372	1 : 2 : 4	1200	497	1170	1.34
19.33	360	1 : 2 : 4	1060	489	1210	1.36
10.00	415	1 : 1 : 2	2470	641	2120	1.54
10.00	415	1 : 3 : 6	680	519	970	1.25

TABLE 2.4

TESTS BY BURR (3) ON BATTENED AND LACED STEEL MEMBERS FILLED WITH CONCRETE (FIGS. 2.9, 2.10)

Column No. (1)	Column Type (2)	Steel Area A_s (sq.in.) (3)	Concrete Area A_c (sq.in.) (4)	Steel Yield Stress f_{sy} (kips/sq.in.) (5)	Load P (kips) (6)	Maximum Load (kips) (7)	Steel Stress σ_s (kips/sq.in.) (8)	Concrete Stress σ_c (lb./sq.in.) (9)	Concrete Secant Modulus E_c (lb./sq.in.x10^6) (10)
1	Angles. Fig. 2.9	4.00	-	40.8		148	37.05	-	-
2	"	"	-	"		152	38.00	-	-
3 & 4	"	"	38.25	"	120		16.99	1360	2.32
"	"	"	"	"	160		24.85	1580	1.85
"	"	"	"	"	180		29.85	1580	1.54
"	"	"	"	"		224	40.80	1620	1.16+
5	Channels. Fig. 2.10	4.76	-	"		155	32.60	-	-
6	"	"	-	"		153	32.14	-	-
8*	"	"	45.00	"	120		15.75	1000	1.84
"	"	"	"	"	160		21.55	1280	1.72
"	"	"	"	"	200		26.10	1480	1.65
"	"	"	"	"		252	40.80	1300	0.92+

* Column No.7 omitted because of premature failure. + Half of initial value.

TABLE 2.5

LOAD SHARING FOR STEEL AND CONCRETE IN COMPOSITE COLUMNS AT FAILURE (WARREN FIG. 2.5(c))

Column No.	Type	Steel Area	Concrete Area	Concrete Elastic Modulus	Maximum Load	Steel Yield Criterion		Concrete Crush Criterion	
						Steel Stress (kips/ sq.in.)	Concrete Stress (lb./sq. in.)	Steel Stress (kips/ sq.in.)	Concrete Stress (lb./sq. in.)
		(sq.in.)	(sq.in.)	(lb./sq. in.x10^6)	(kips)				
(1)	(2)	(3)	(4)	(5)	(6)	(7)	(8)	(9)	(10)
1	Bare Steel	8.44	-	-	363	43.0	-	43.0	-
2	Concrete Core	8.44	147.8	3.60	678	43.0	2130	38.5	2390
3	Fireproofed	8.44	187.5	4.56	765	43.0	2140	33.0	2590

TABLE 2.6

CONCENTRIC LOAD TESTS ON BARE STEEL AND COMPOSITE COLUMNS (FIG.2.11) BY MEMMLER ET AL. (34)

Column Type (1)	Mark (2)	Number of Tests (3)	Channel Spacing (in) (4)	Steel Area (sq.in) (5)	Concrete Area (sq.in) (6)	Maximum Column Load (kips) (7)	Load Carried by Steel (kips) (8)	Maximum Steel Stress (kips/sq.in) (9)	Steel Yield Stress (kips/sq.in) (10)	Load Carried by Conc. (kips) (11)	Maximum Concrete Stress (lb/sq.in) (12)	Concrete Prism Strength (lb/sq.in) (13)	Ratio of Max. Concrete Stress to Prism Strength (14)
II	1	3	2.95	5.85	-	228	228	39.1	39.1	-	-	-	-
II	4	2	7.10	6.13	-	245	245	40.0	41.3	-	-	-	-
V	1	2	2.95	5.89	-	245	245	41.6	41.1	-	-	-	-
V	4	1	7.10	6.06	-	246	246	40.6	40.6	-	-	-	-
II	1	3	2.95	5.90	18.1	268	248	42.0	42.0	20	1110	3830	0.29
II	2	3	4.72	5.86	29.0	325	239	40.8	40.8	86	2970	3750	0.75
II	3	3	5.91	5.97	36.3	350	239	40.0	40.0	111	2790	3520	0.84
II	4	4	7.10	5.87	43.6	362	234	39.9	39.9	128	2940	4110	0.72
V	1	3	2.95	5.91	38.3	340	239	40.5	40.5	101	2640	3850	0.69
V	2	3	4.72	5.81	49.3	358	230	39.6	39.6	128	2600	3940	0.66
V	3	3	5.91	5.82	56.5	373	231	39.8	39.8	142	2520	3840	0.66
V	4	3	7.10	5.77	63.7	435	238	41.3	41.3	197	3100	4540	0.68

TABLE 2.7

SUMMARY OF ECCENTRIC LOAD TESTS BY BONDALE

(8) ON ENCASED JOISTS AND BUILT-UP SECTIONS

Column Reference	Nominal Length (in.)	Ecc. (in.)	Axis of Bending	Test Max. Load P_{test} (Tons)	Theoret. Max.Load P_{theory} (Tons)	$\frac{P_{test}}{P_{theory}}$
(a) 4" x $1\frac{3}{4}$" @ 5lb. RSJ with four 0.21" dia. steel long. bars with $\frac{1}{8}$" dia. binders at 2" centres encased in concrete to 6" x $3\frac{3}{4}$" overall size with 1" concrete cover all round.						
RW 120.0	120	0	Minor	23.6	24.6	0.96
RW 100.1	100	1	"	9.3	9.1	1.02
RW 80.2	80	2	"	9.7	7.8	1.24
RW 60.3	60	3	"	8.0	6.9	1.16
RS 120.0	120	0	Major	47.8	65.9	0.73
RS 100.1	100	1	"	41.2	33.5	1.23
RS 80.2	80	2	"	31.3	25.8	1.21
RS 60.3	60	3	"	24.9	21.7	1.15
(b) Four 1" x 1" x $\frac{3}{16}$" angles connected with $\frac{3}{16}$" dia. single lattice to form a 4" x $2\frac{3}{4}$" section and encased in concrete to 5¼" x 4¼" overall size with $\frac{3}{4}$" concrete cover all round						
LW 120.0	120	0	Minor	34.8	37.2	0.93
LW 100.1	100	1	"	18.5	18.4	1.01
LW 80.2	80	2	"	15.2	15.2	1.00
LW 60.3	60	3	"	13.5	12.8	1.05
LS 120.0	120	0	Major	44.1	59.9	0.74
LS 100.1	100	1	"	34.8	31.5	1.10
LS 80.2	80	2	"	24.9	24.0	1.04
LS 60.3	60	3	"	21.9	20.5	1.07

TABLE 2.8

COMPARISON OF THREE METHODS FOR CALCULATING TANGENT MODULUS LOAD FOR TUBES USING KNOWLES AND PARK'S (24) RESULTS

Steel Tube Properties (1)	Eff. Length (in) (2)	Concrete Strength (psi) (3)	Individual Tangent Modulus					Combined Tangent Modulus				Max. Tangent Modulus			P_{short} (kips) (16)
			P_{test} (kips) (4)	P_{ts} (kips) (5)	P_{tc} (kips) (6)	P_o (kips) (7)	$\frac{P_{test}}{P_o}$ (8)	P_s (kips) (9)	P_c (kips) (10)	P_o (kips) (11)	$\frac{P_{test}}{P_o}$ (12)	P_{ts} (kips) (13)	P_c (kips) (14)	P_o (kips) (15)	
Shape-Circular	68	5805	138.2	114.7	24.9	139.6	0.99	110.7	35.4	146.1	0.95	114.7	36.5	151.2	176.9
Out.dia.=3.5 in.	56	5745	160.0	121.9	30.1	152.0	1.05	119.4	37.6	157.0	1.02	121.9	38.4	160.3	176.4
Thickness	44	5650	160.8	127.7	35.0	162.7	0.99	126.2	39.2	165.4	0.97	127.7	39.6	167.3	175.7
= 0.23 in.	32	6060	206.5	132.1	41.6	173.7	1.19	131.3	43.3*	174.6	1.18	132.1	43.6*	175.7	179.0
f_{sy} = 58 ksi	20	5925	223.0	135.1	42.6	177.7	1.26	135.1	42.7*	177.8	1.25	135.1	42.7*	177.8	177.9
$E_s = 31 \times 10^6$ psi.															
Shape-Circular	68	5995	50.5+	30.6	28.2	58.8	0.86	25.4	37.0	62.4	0.81	30.6	42.1	72.7	83.3
Out.dia.=3.25 in.	56	5365	66.2	33.2	31.2	64.4	1.03	29.7	37.9	67.6	0.98	33.2	43.5	76.7	82.0
Thickness	44	5925	80.0	35.3	39.6	74.9	1.07	33.1	43.9	77.0	1.04	35.3	45.5	80.8	83.2
= 0.055 in.	32	5925	90.0	36.9	43.7	80.6	1.12	35.4	45.6*	81.0	1.11	36.9	45.7*	82.6	83.2
f_{sy} = 70 ksi	20	5925	110.0	38.0	45.5	83.5	1.32	37.1	45.5*	82.6	1.33	38.0	42.8*	80.8	83.2
$E_s = 31 \times 10^6$ psi	10	5925	119.2	38.4	45.7	84.1	1.42	38.2	45.0*	83.2	1.43	38.4	40.3*	78.7	83.2
Shape-Square	68	5200	80.0	59.5	24.5	84.0	0.95	56.5	31.4	87.9	0.91	59.5	31.5	91.0	104.8
3 in. x 3 in.	56	4935	86.6	62.5	28.5	91.0	0.95	62.0	32.3	94.3	0.92	62.5	33.6	96.1	105.6
Thickness	44	6780	95.0	64.8	42.9	107.7	0.88	63.7	44.4	108.1	0.88	64.8	43.7	108.5	118.6
= 0.131 to 0.133 in.	32	6535	104.0	66.5	46.7	113.2	0.92	67.3	46.2	113.5	0.92	66.5	47.9	114.4	118.1
f_{sy} = 47 ksi	20	5925	113.2	67.7	43.0	110.7	1.03	68.3	44.3	112.6	1.00	67.7	44.9	112.6	113.8
$E_s = 31 \times 10^6$ psi	10	5925	115.0	68.4	43.8	112.2	1.03	68.4	44.9	113.3	1.02	68.4	44.9	113.3	113.8

* Negative concrete tangent modulus. + Some eccentricity of loading.

TABLE 2.9

DETAILS OF ECCENTRIC LOAD TESTS ON CONCRETE FILLED TUBES BY KNOWLES AND PARK (23)

Tube	Length in.	Exper. Max. Load P_u (kips)	Axial Load Capacity P_o (kips)	$\frac{P_u}{P_o}$	Initial Eccentricity e (in.)	Central Deflection at Max. Load δ (in.)	Maximum Moment $M_u = P_u(e+\delta)$ (kip.ins.)	Ultimate Moment Capacity M_o (kip. ins.)	$\frac{M_u}{M_o}$	$\frac{P_u}{P_o} + \frac{M_u}{M_o}$
(1)	(2)	(3)	(4)	(5)	(6)	(7)	(8)	(9)	(10)	(11)
3.5 in. OD	32	124.6	206.5	0.604	0.3	0.46	94.7	144.3	0.656	1.260
	56	105.5	160.0	0.660	0.3	0.36	69.6	144.3	0.482	1.142
	32	43.8	206.5	0.212	1.0	0.30	57.0	144.3	0.395	0.607
	44	43.0	160.8	0.268	1.0	0.20	51.6	144.3	0.357	0.625
3.25 in. OD	32	67.8	90.0	0.753	0.3	0.47	52.2	55.0	0.950	1.703
	32	20.0	90.0	0.222	1.0	0.15	23.0	55.0	0.418	0.640
3.00 in. square	32	77.8	104.0	0.747	0.3	0.19	37.7	98.8	0.382	1.129
	56	63.2	86.6	0.730	0.3	0.41	44.9	98.8	0.455	1.185
	32	48.7	104.0	0.468	1.0	0.32	64.2	98.8	0.650	1.118
	56	35.2	86.6	0.406	1.0	0.45	51.0	98.8	0.516	0.922

TABLE 2.10

DETAILS OF ECCENTRIC LOAD TESTS ON CONCRETE ALLED TUBES

Specimen Number	Ratio of Length to Diameter $\frac{l}{d}$	Ratio of Eccentricity to Diameter $\frac{e}{d}$	Ratio of Wall Thickness to Diameter $\frac{t}{d}$	Experimental Maximum Load P (kips)	Load Ratios	
					$\frac{P}{P_{exact}}$	$\frac{P}{P_{cos}}$
(1)	(2)	(3)	(4)	(5)	(6)	(7)
TESTS AT IMPERIAL COLLEGE BY NEOGI (25)						
M1	19.64	0.281	0.030	140	1.027	1.048
M2	19.67	0.225	0.031	158	1.033	1.060
M3	19.67	0.262	0.034	135	1.030	1.056
M4	19.76	0.283	0.039	141	1.015	1.041
M5	19.67	0.282	0.042	147	1.000	1.023
M6	19.67	0.225	0.043	166	1.010	1.033
M7	19.54	0.282	0.052	170	0.984	1.009
M8	23.73	0.226	0.068	123	0.993	1.036
M9	23.73	0.226	0.070	123	1.014	1.051
M10	23.60	0.225	0.036	94	1.021	1.055
C5	11.08	0.050	0.014	217	1.230	1.243
C6	11.10	0.050	0.022	235	1.160	1.200
C7	13.50	0.050	0.014	191	1.300	1.314
C8	13.50	0.050	0.024	181	0.989	1.016
C9	15.97	0.125	0.014	80	0.923	0.946
C10	16.00	0.125	0.026	118	1.015	1.036
C11	16.00	0.175	0.013	77	1.051	1.085
C12	16.00	0.175	0.026	113	1.068	1.091
TESTS AT TOKIO UNIVERSITY BY KATO AND KANATANI (45)						
AC7	17.3	0.220	0.022	471	0.932	0.975
AC10	17.3	0.314	0.022	386	0.926	0.967
AC20	18.8	0.628	0.022	244	0.983	1.030
AB20	18.8	0.628	0.022	244	1.024	1.073
BC7	8.9	0.220	0.022	637	0.983	1.003
BC10	8.8	0.314	0.022	516	0.963	0.989
BC20	8.8	0.628	0.022	303	1.000	1.027
BB20	10.4	0.628	0.022	312	1.061	1.095

TABLE 5.1 SUMMARY OF SHORT TERM TESTS ON BUILT-UP COMPOSITE COLUMNS

Column Designation (1)	Type (2)	Length (ft.) (3)	Axis of Loading (4)	Eccen. of Loading (in.) (5)	Observed Max.Load (kips) (6)	Theoret. Maximum Load (kips) (7)	Obs. Max.Load / Theor.Max.Load (8)	Short Column Load (kips) (9)
CC1	No battens, composite	7	Minor	1.5	117.0	109.4	1.07	296.8
CC2	No battens, composite	7	Major	0.8	195.5	201.2	0.97	315.3
CC3	No battens, composite	7	Major	1.5	159.0	150.6	1.05	321.0
CC4	No battens, composite	7	Major	0.0	270.0	272.9	0.99	292.4
CC5	No battens, composite	7	49° to Major	0.8	158.2	150.2	1.05	293.5
CC11	No battens, composite	7	Major	2.0*	158.8	154.2	1.03	326.9
CC13	No battens, bare steel	10	Major	0.8	21.3	20.0	1.06	106.4
CC13R	No battens, composite	10	Major	0.8	147.1	146.6	1.00	276.2
CC14	Battens, bare steel	10	Major	0.8	53.3	51.4	1.04	107.1
CC15	Battens, composite	10	Major	0.8	150.5	142.9	1.05	262.5
CC16	No battens, composite	10	Major	1.5	110.2	105.0	1.05	266.9

* Eccentricity at ends in opposing directions.

TABLE 5.2 INITIAL DEFORMATION IN CHANNEL LENGTHS (Ref. Fig. 5.2)

Column No.	Channel	Face	Initial Deflection (in.)			Max. Def. Length
			¼ Point	Centre	¾ Point	
CC1	A	1	-0.012	-0.040	-0.036	1/2100
		2	0.000	0.006	0.000	1/14000
		3	-0.004	-0.010	-0.012	1/7000
	B	1	-0.024	-0.026	-0.021	1/3230
		2	-0.004	-0.004	0.000	1/21000
		3	0.004	0.000	0.000	1/21000
CC2	A	1	-0.084	-0.076	-0.060	1/1000
		2	0.038	0.020	0.010	1/2210
		3	-0.014	-0.016	-0.018	1/4660
	B	1	-0.034	-0.040	-0.034	1/2100
		2	0.020	0.040	0.028	1/2100
		3	-0.016	-0.042	-0.040	1/2000
CC3	A	1	-0.088	-0.098	-0.056	1/860
		2	-0.004	-0.012	-0.012	1/7000
		3	-0.026	0.000	-0.002	1/3230
	B	1	-0.104	-0.110	-0.072	1/760
		2	-0.030	-0.048	-0.026	1/1750
		3	-0.044	-0.002	0.034	1/1910
CC4	A	1	0.012	0.038	0.026	1/2210
		2	-0.008	0.018	0.016	1/4670
		3	-0.026	-0.025	-0.014	1/3230
	B	1	-0.056	-0.046	-0.042	1/1500
		2	-0.006	0.024	0.002	1/3500
		3	-0.010	0.000	0.002	1/8400
CC5	A	1	0.124	0.174	0.120	1/480
		2	-0.036	-0.070	-0.033	1/1200
		3	0.038	0.060	0.030	1/1400
	B	1	0.080	0.100	0.064	1/840
		2	-0.008	-0.034	-0.024	1/2470
		3	0.008	0.024	0.012	1/3500

TABLE 5.2 (Cont.) INITIAL DEFORMATION

CHANNEL LENGTHS

Column No.	Channel	Face	Initial Deformation (in.)			Max.Def. Length
			¼ Point	Centre	¾ Point	
CC11	A	1	-0.064	-0.120	-0.116	1/700
		2	0.028	0.032	0.028	1/2620
		3	-0.020	0.000	0.008	1/4200
	B	1	-0.120	-0.180	-0.140	1/470
		2	-0.012	-0.020	-0.028	1/3000
		3	0.036	0.040	0.044	1/1900
CC13 CC13R	A	1	0.038	0.044	0.006	1/2730
		2	-0.032	-0.044	0.032	1/2730
		3	-0.060	-0.008	0.012	1/2000
	B	1	0.056	0.080	0.008	1/1500
		2	-0.080	0.044	0.060	1/1500
		3	-0.072	-0.052	-0.028	1/1670
CC14	A	1	0.036	0.068	0.000	1/1770
		2	-0.032	-0.012	-0.004	1/3750
		3	-0.012	-0.076	-0.100	1/1580
	B	1	0.036	0.016	-0.044	1/2730
		2	-0.004	0.052	0.088	1/1360
		3	-0.032	-0.028	-0.016	1/3750
CC15	A	1	-0.004	0.004	0.000	1/30000
		2	0.004	0.036	0.048	1/2500
		3	-0.028	0.012	0.064	1/1880
	B	1	-0.036	0.032	-0.024	1/3300
		2	-0.036	0.016	0.064	1/1880
		3	0.004	0.020	0.032	1/3750
CC16	A	1	0.032	0.072	0.048	1/1670
		2	0.052	0.072	0.052	1/1670
		3	0.028	0.020	0.032	1/3750
	B	1	0.020	0.044	0.072	1/1670
		2	0.000	-0.056	0.028	1/2140
		3	0.056	0.080	0.056	1/1500

TABLE 5.3 CROSSECTIONAL DETAILS OF CHANNELS (Ref. Fig. 5.2)

Column No.	Dimension (in.)				Computed Crossectional Area of Two Channels (sq.in.)
	Web		Flange		
	Width	Thickness	Width	Thickness	
CC1	2.975	0.205	1.512	0.278	2.673
CC2	2.978	0.208	1.508	0.264	2.612*
CC3	2.975	0.202	1.512	0.272	2.627
CC4	3.008	0.209	1.484	0.274	2.655
CC5	3.026	0.216	1.505	0.273	2.715
CC11	3.022	0.203	1.489	0.284	2.688
CC13(R)	2.953	0.207	1.520	0.264	2.609*
CC14	2.952	0.206	1.520	0.263	2.599*
CC15	2.952	0.206	1.520	0.263	2.599*
CC16	2.953	0.205	1.520	0.263	2.594*
AS A1 -1965	3.000	0.200	1.500	0.267	2.640

* Checked by immersion weighing.

TABLE 5.4 PROPERTIES OF MATERIALS

Column No.	STEEL				CONCRETE				
	Yield Stress (kip/sq.in.)			Modulus of Elasticity	Standard 28 day Compressive Strength	Properties at Age of Column Tests			
	Stub Column Comp.	Coupon Tension	Hounsfield Tension	(lb/sq.in. x10^6)	(lb/sq.in.)	Age at Testing (days)	Compressive Strength (lb/sq.in.)	Tensile Splitting Strength (lb/sq.in)	Modulus of Elasticity (lb/sq.in. x10^6)
	(1)	(2)	(3)	(4)	(5)	(6)	(7)	(8)	(9)
CC1	42.9	42.7	-	30.1	3980	43	3960	410	3.19
CC2	40.3	40.3	-	30.6	4370	31	4530	430	3.28
CC3	44.2	43.0	-	30.5	4230	41	4450	480	3.23
CC4	40.3	40.9	-	30.5	4220	34	4020	450	3.03
CC5	40.6	40.4	38.7	30.1	3710	23	4050	440	2.95
CC11	45.3	44.5	42.5	30.0	-	33	4440	510	3.38
CC13(R)	40.8	42.1	40.2	29.0	4710	18	3680	300	2.72
CC14	41.2	42.1	41.4	30.2	n.a.	n.a.	n.a.	n.a.	n.a.
CC15	41.0	42.4	40.7	29.3	4710	29	3430	330	2.83
CC16	40.7	41.5	40.0	30.0	4250	26	3560	350	2.89

n.a. not applicable - bare steel column

TABLE 5.5 CHEMICAL ANALYSIS OF CEMENT

Analysis	Percent
Silicon Dioxide (SiO_2)	20.06
Ferric Oxide ($Fe\ O_3$)	3.16
Aluminium Oxide ($Al_2\ O_3$)	6.22
Calcium Oxide (Ca O)	65.00
Magnesium Oxide (Mg O)	0.98
Sulphuric Anhydride (SO_3)	2.19
Loss on Ignition	1.80
Insoluble Residue	0.92
Alkalies as $Na_2\ O$	0.56
Hypothetical Compound Composition	**Percent**
Tricalcium Aluminate (C_3A)	11
Tetracalcium Alumino Ferrite (C_4AF)	10
Tricalcium Silicate (C_3S)	59
Dicalcium Silicate (C_2S)	13

Fineness Index 3650 sq.cms per gram

TABLE 6.1 GEOMETRICAL PROPERTIES FOR CONCRETE FILLED TUBE TESTS

Column No.	Nom. Size (in.)	Width B (in.)	Depth D (in.)	Wall Thick. TW (in.)	Max. Init. Deform. (in.)	Length L (ft)	Ecc. e (in.)	Loading Axis Inclin. β	$\frac{D}{TW}$	$\frac{L}{D}$	$\frac{e}{D}$
(1)	(2)	(3)	(4)	(5)	(6)	(7)	(8)	(9)	(10)	(11)	(12)
SHC-1	8x8x$\frac{3}{8}$	8.021	8.028	0.392	0.047	7	1.5	0°	20.5	10.5	0.187
SHC-2	"	8.032	8.003	0.394	0.055	10	0	0°	20.3	15	0
SHC-3	"	8.005	7.984	0.395	0.031	7	1.5	30°	20.2	10.5	0.187
SHC-4	"	7.984	8.010	0.389	0.022	7	1.5	45°	20.6	10.5	0.187
SHC-5	"	7.976	8.000	0.394	0.011	10	1.5	30°	20.3	15	0.187
SHC-6	"	8.000	7.955	0.385	0.044	10	2.5	45°	20.7	15	0.313
SHC-7	6x6x¼	6.003	5.997	0.255	0.020	10	1.5	0°	23.5	20	0.250
SHC-8	"	6.003	5.997	0.255	0.040	10	2.5	0°	23.5	20	0.417

TABLE 6.2 MATERIAL PROPERTIES FOR CONCRETE FILLED TUBE TEST COLUMNS

Column No.	Steel Yield Stress	Concrete Properties				
		28 Day Compressive Strength	Concrete Properties at Age of Testing			
			Age at Testing	Compressive Strength	Split Tensile Strength	Elastic Modulus
	(lb./sq.in.)	(lb./sq.in.)	(days)	(lb./sq.in.)	(lb./sq.in.)	(lb./sq.in.x10^6)
(1)	(2)	(3)	(4)	(5)	(6)	(7)
SHC-1	42200	4380	31	4340	430	3.38
SHC-2	42100	4440	40	4510	420	3.44
SHC-3	45400	5010	105	5390	590	3.83
SHC-4	46000	4800	119	5690	590	4.04
SHC-5	46300	5480	128	6420	640	4.11
SHC-6	46000	4660	133	5240	560	3.93
SHC-7	36890	5080	21	4510	480	3.49
SHC-8	36890	5080	22	4510	480	3.49

TABLE 6.3 LOAD CAPACITIES FOR CONCRETE FILLED TUBES

Column No. (1)	Tube Size (in.) (2)	Length (ft.) (3)	Load. Axis Incl. (deg.) (4)	Ecc. (in.) (5)	Short Column Load (kips) (6)	First Yield Load (kips) (7)	Obs. Max. Load (kips) (8)	$\frac{P_{sy}}{P_{max}}$ (9)	Theor. Max. Load (kips) (10)	$\frac{P_{max}}{P_{theor}}$ (11)
SHC-1	8x8x$\frac{3}{8}$	7	0	1.5	698.2	390	439.7	0.89	436.3	1.01
SHC-2	"	10	0	0	706.9	645	645.0	1.00	632.3	1.02
SHC-3	"	7	30	1.5	783.1	430	490.0	0.88	491.9	1.00
SHC-4	"	7	45	1.5	796.3	400	486.0	0.82	501.2	0.97
SHC-5	"	10	30	1.5	837.4	400	458.0	0.87	476.4	0.96
SHC-6	"	10	45	2.5	768.7	280	365.0	0.77	360.3	1.01
SHC-7	6x6x¼	10	0	1.5	333.8	135	152.8	0.88	153.9	0.99
SHC-8	"	10	0	2.5	333.8	100	115.3	0.87	123.1	0.94

TABLE 9.1

PROPERTIES OF STEEL SECTIONS FOR RESTRAINED SHRINKAGE TESTS

Column No.	Steel Section	Flange Dimensions		Web Dimensions		Max. Initial Central Deflection (in.)	Yield Stress			Elastic Modulus
		Width (in.)	Thickness (in.)	Width (in.)	Thickness (in.)		Squat Comp. (kips/sq.in.)	Coupon Tension (kips/sq.in.)	Hounsfield Tension (kips/sq.in.)	(lb./sq.in.x10^6)
CC6	2 Channels 3"x1½"x4.61b.	1.508	0.274	3.024	0.217	0.022	42.13	42.19	39.55	30.4
CC6-M12	2 Angles 1"x1"x3/16"	1.015	0.193	1.008	0.190	-	-	43.85	43.12	29.2
CC6-M34	2 Angles 1½"x1½"x¼"	1.503	0.252	1.508	0.250	-	-	40.18	38.33	30.1
CC12	2 Channels 3"x1½"x4.61b.	1.497	0.279	3.024	0.204	0.070	46.67	45.77	47.30	29.9

TABLE 9.2

CONCRETE PROPERTIES OF RESTRAINED SHRINKAGE SPECIMEN WITH SHORT TERM LOADING

Column No. (1)	Age at Start of Drying (days) (2)	Age at Column Loading (days) (3)	Age at Measurement of Properties (days) (4)	Cylinder Compressive Strength (lb./sq.in.) (5)	Cylinder Split Tensile Strength (lb./sq. in.) (6)	Cylinder Direct Tensile Strength (lb./sq. in.) (7)	Elastic Modulus in Compression (lb./sq.in. x10^6) (8)	Elastic Modulus in Tension (lb./sq.in. x10^6) (9)
CC6	36	75	36	4710	480	-	-	-
CC6-M12			69	5890	640	-	2.82	-
CC6-M34			75	6110	660	-	2.83	-
			75			390[a]		2.45[a]
			75			460[b]		2.66[b]
CC12	28	84	28	5520	506	-	3.22	-
			33	-	567	437	-	-
			70	5490	560	-	2.96	-
			84	5630	570	410	2.82	2.89
			84			420[a]		2.50[a]
			84			440[b]		2.31[b]

a Constant sustained stress of 100 lb./sq.in. during drying.
b Constant sustained stress of 150 lb./sq.in. during drying.

TABLE 9.3 COMPARISON OF LOAD CAPACITIES FOR INITIALLY CRACKED AND UNCRACKED COLUMNS

Column No.	Loading Axis	Length L (ft.)	Ecc. e (in.)	Agg.	Concrete Cylinder Strength f'_c (lb./sq.in.)	Steel Yield Stress f_{sy} (lb./sq.in.)	Short Column Load P_{sh} (kips)	Max. Load P_{max} (kips)	$\frac{P_{max}}{P_{sh}}$
CC3	Major	7	1.5	Basalt	4450	44200	321.0	159.0	0.495
CC12	Major	7	1.5	Breccia	5630	46670	380.3	154.8	0.407
CC1	Minor	7	1.5	Basalt	3960	42900	296.8	117.0	0.394
CC6	Minor	7	1.5	Breccia	6110	42130	388.9	147.0	0.378

TABLE 10.1 SPECIFICATION FOR SPRINGS

Item	Unit	Creep Rig	
		CC7	CC8, CC9, CC10
Free Length	in.	12.25	20.00
Solid Length	in.	9.00	14.15
Outside Diameter	in.	6.50	7.00
Inside Diameter	in.	3.50	4.25
Wire Diameter	in.	1.50	1.38
Active Coils		5.50	9.30
Total Coils		7.00	10.80
Spring Rate	lb./in.	10600	3340
Maximum Load	lb.	34400	19500
Safe Load	lb.	19000	14000

TABLE 10.2 DIMENSIONS AND PROPERTIES OF STEEL CHANNEL USED IN CREEP COLUMNS

Column No.	Length (in.)	Web		Flange		Maximum Initial Deflect. (in.)	Yield Stress			Eccent. (in.)
		Width (in.)	Thickness (in.)	Width (in.)	Thickness (in.)		Stub Column (kips/sq.in.)	Coupon Tension (kips/sq.in.)	Hounsfield Tension (kips/sq. in.)	
CC7	84	3.027	0.218	1.499	0.273	0.106	41.70	41.25	38.70	1.6
CC8	68	3.022	0.201	1.496	0.277	0.095	44.21	45.06	41.93	0.0
CC9	68	3.020	0.200	1.496	0.278	0.122	45.08	45.38	42.32	0.8
CC10	68	3.019	0.202	1.493	0.277	0.114	44.63	45.50	42.18	2.0*

* Eccentricity at ends in opposing directions.

TABLE 10.3 SHORT TERM LOADING PROPERTIES OF CONCRETE FOR CREEP COLUMNS

Column No.	Age at Start of Drying (days)	Age at Loading (days)	Cylinder Testing Age (days)	Cylinder Compressive Strength (lb./sq.in.)	Cylinder Split Tensile Strength (lb./sq. in.)	Modulus of Elasticity (lb./sq.in. x10^6)
(1)	(2)	(3)	(4)	(5)	(6)	(7)
CC7	74	74	74 78 1438	- 5560 4350	- 530 380	4.09* 3.65 2.80
CC8	56	65	65 69 1012	- 5910 5460	- 570 520	4.08* 3.62 3.34
CC9	49	58	58 62 1005	- 6100 5710	- 600 520	4.01* 3.57 3.49
CC10	42	51	51 55 998	- 6130 5970	- 600 520	4.01* 3.65 3.61

* Measured from loading of creep block

TABLE 11.1

OBSERVED AND ACI MAXIMUM LOADS FOR TEST COLUMNS

Column No.	Length (ft.)	Eccent. (in.)	Short Column Load (kips)	Obs. Max. Load (kips)	ACI Max. Load (kips)	Obs / ACI
(a) Two 3" x 1½" x 4.6lb. channels encased to 8" x 7"						
CC4	7	0	292.4	270.0	224.6	1.20
CC2	7	0.8	315.3	195.5	195.0	1.00
CC3	7	1.5	321.0	159.0	147.7	1.07
CC13R	10	0.8	276.2	147.1	135.3	1.09
CC16	10	1.5	266.9	110.2	103.0	1.07
CC11	7	2.0*	326.9	158.8	151.6	1.05
(b) 8" x 8" x $\frac{3}{8}$" Concrete Filled Tubes						
SHC-1	7	1.5	698.2	439.7	442.1	0.99
SHC-2	10	0	706.9	645.0	601.3	1.07
SHC-3	7	1.5	783.1	490.0	520.8	0.94
SHC-4	7	1.5	796.3	486.0	530.4	0.92
SHC-5	10	1.5	837.4	458.0	526.2	0.87
SHC-6	10	2.5	768.7	365.0	402.7	0.91
(c) 6" x 6" x ¼" Concrete Filled Tubes						
SHC-7	10	1.5	333.8	152.8	170.5	0.90
SHC-8	10	2.5	333.8	115.3	131.0	0.88

* Double Curvature

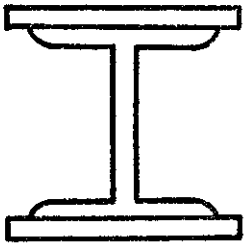

Plated RSJ

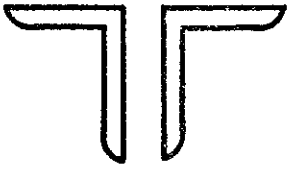

Roof Truss

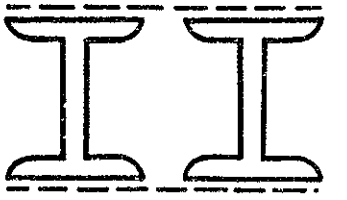

Mill Building

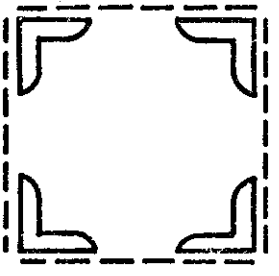

Crane Boom

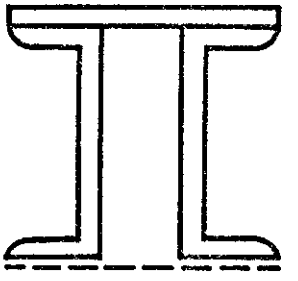

Truss Top Chord

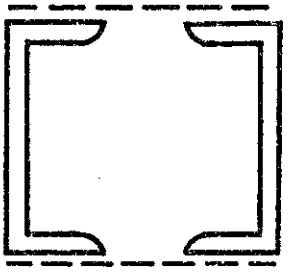

Building Column

FIG. 1·1 TYPICAL BUILT-UP SECTIONS

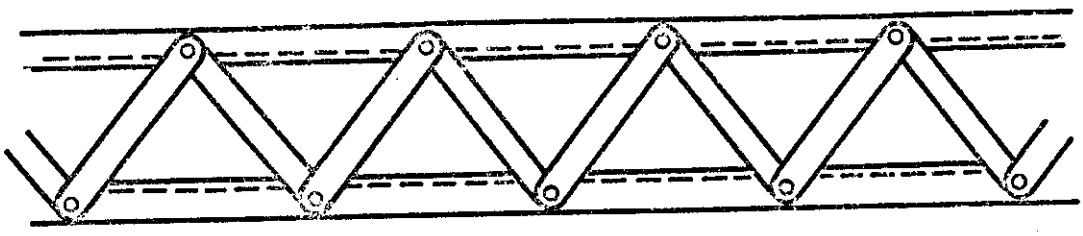

Single Lacing

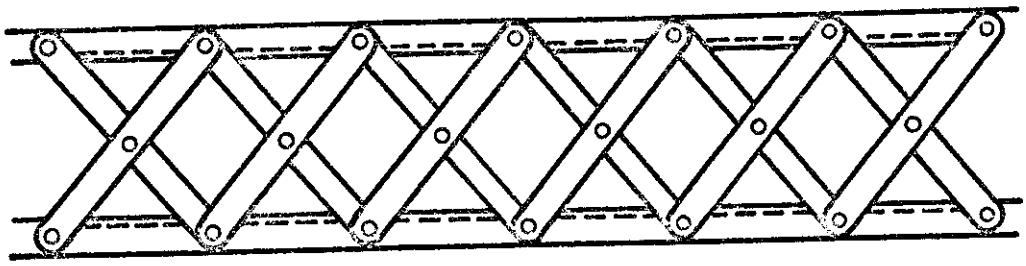

Double Lacing

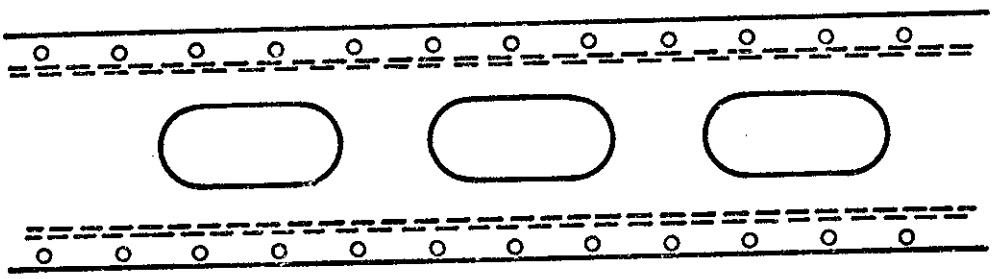

Perforated Plate

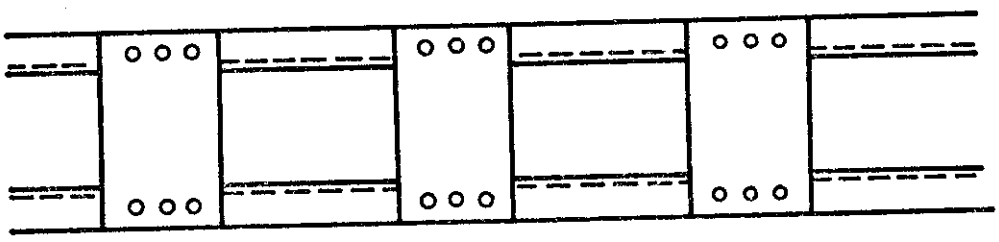

Batten Plates

FIG. 1·2 TYPES OF CONNECTIONS

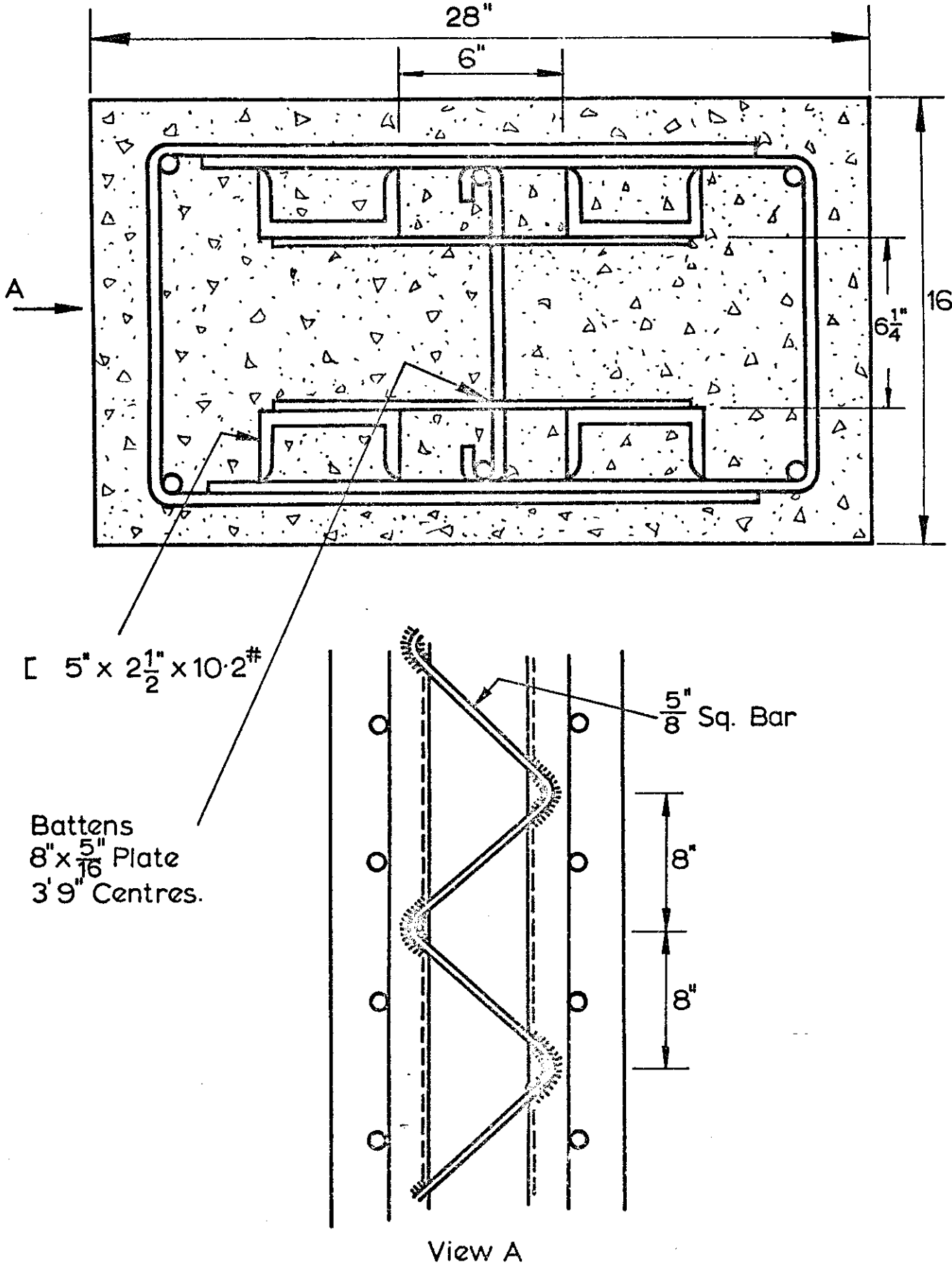

FIG. 1·3 STATE OFFICE BLOCK COLUMN.

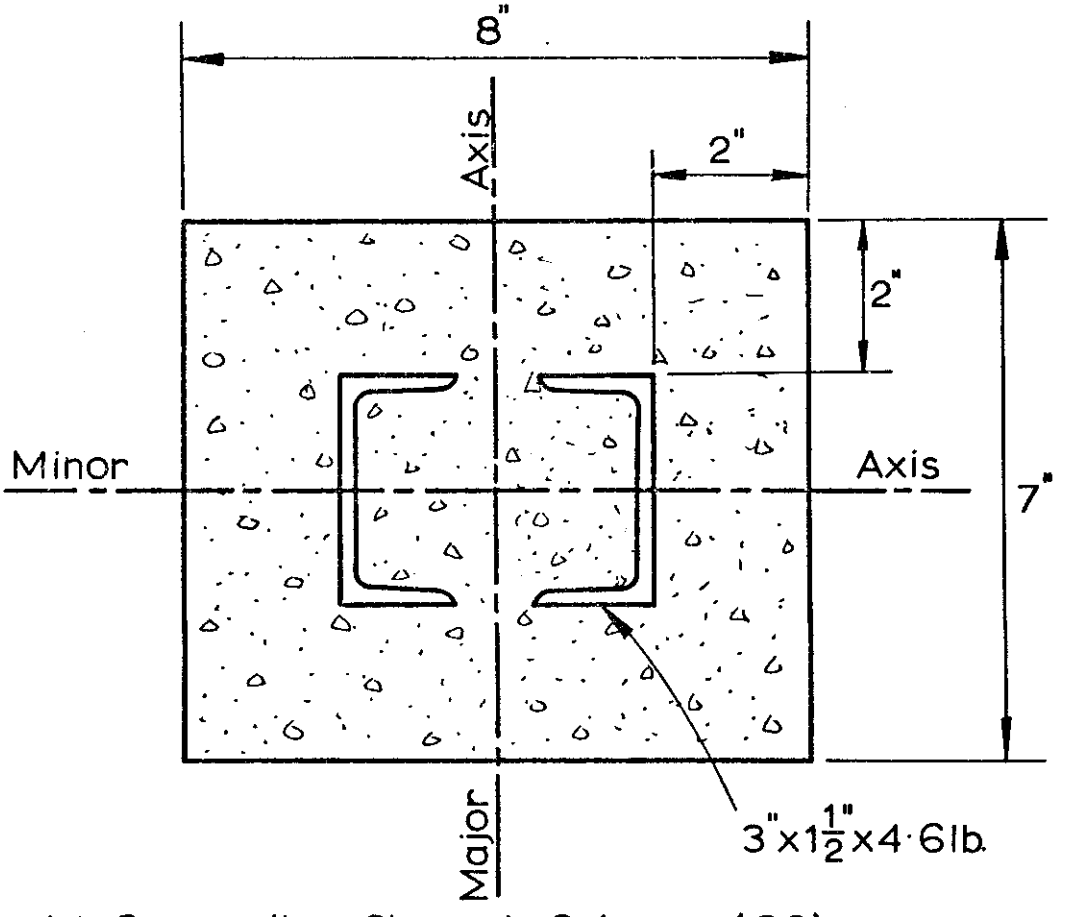

(a) Composite Channel Column (CC)

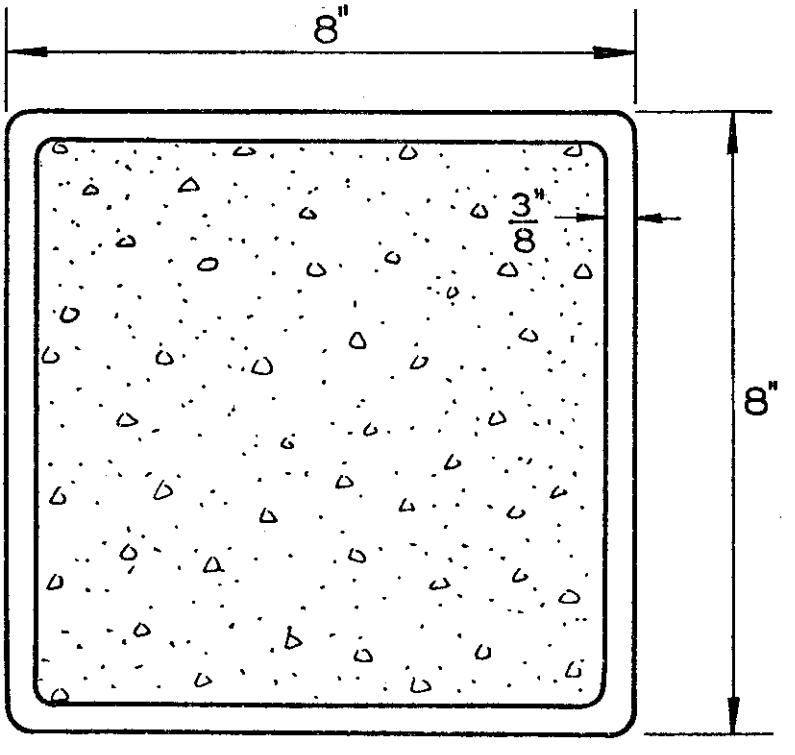

(b) Concrete-Filled Square Tube (SHC)

FIG 1·4 CROSS SECTIONS OF TEST COLUMNS.

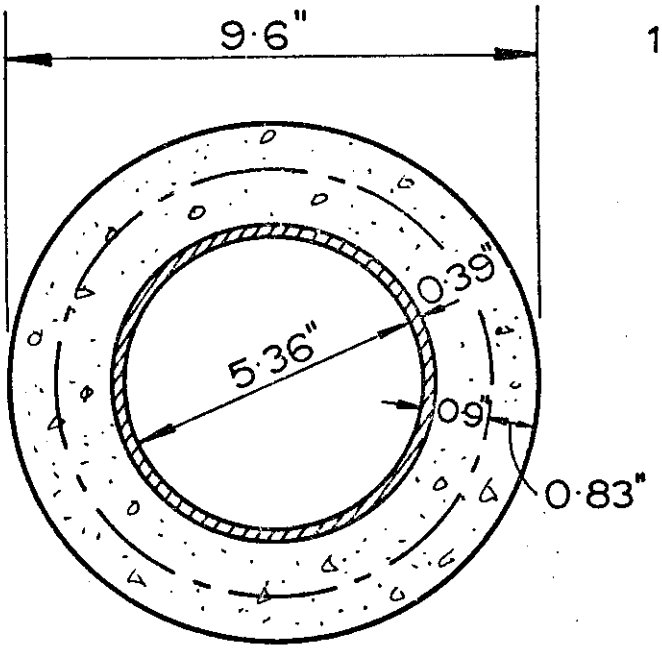

(a) C.I. Hollow Cylinder

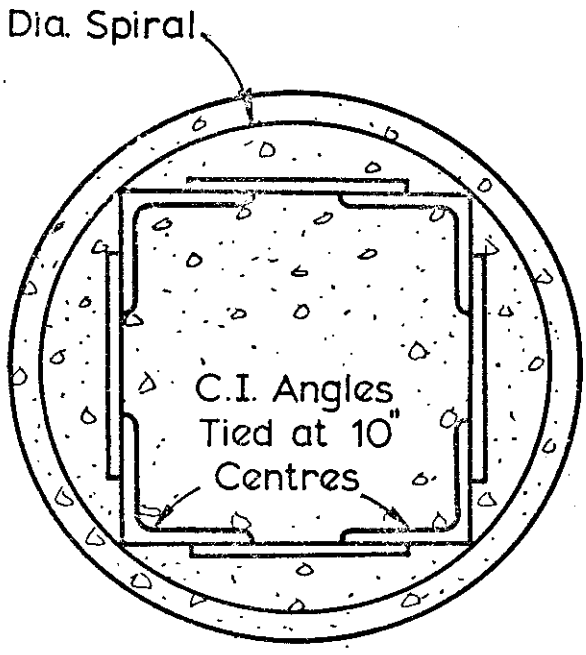

(b) 4 L 3·14" x 3·14" x 3·9"

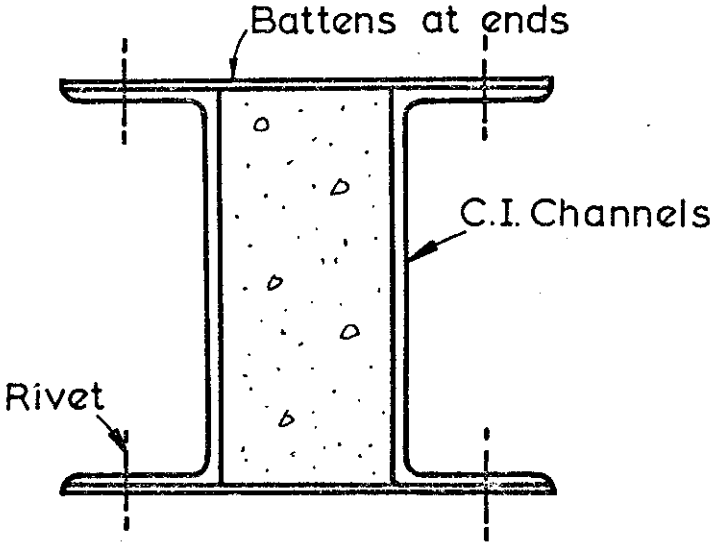

(c) 2 Channels

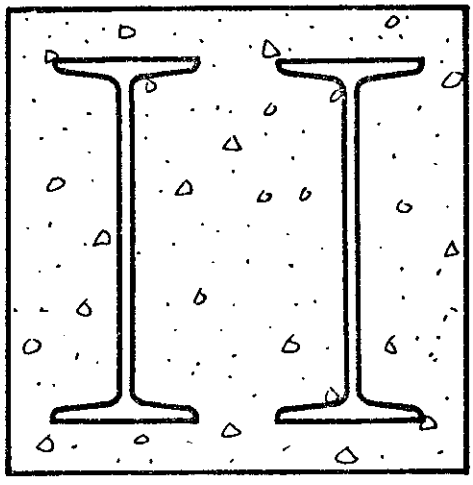

(d) 2 I-Sections

FIG. 2·1 COMPOSITE COLUMNS (EMPERGER)

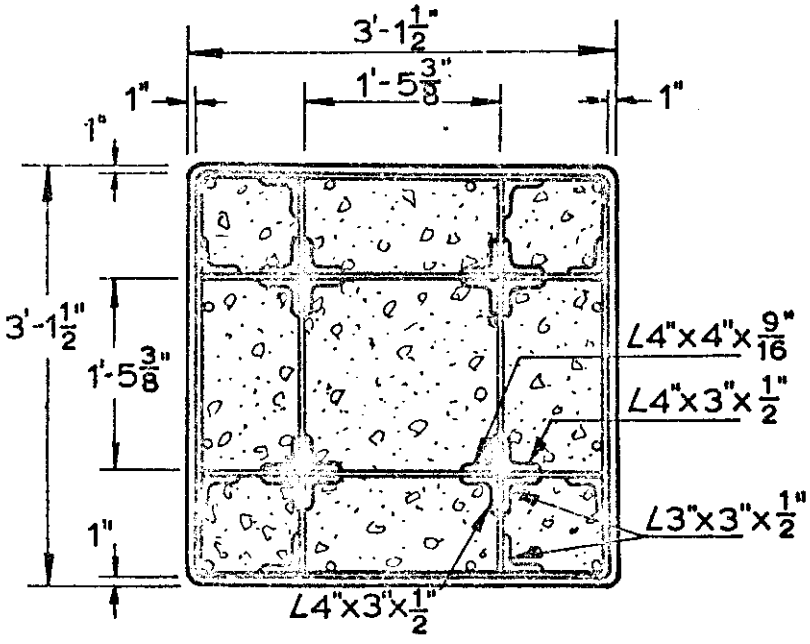

(a) Stang, Whittemore and Parsons.

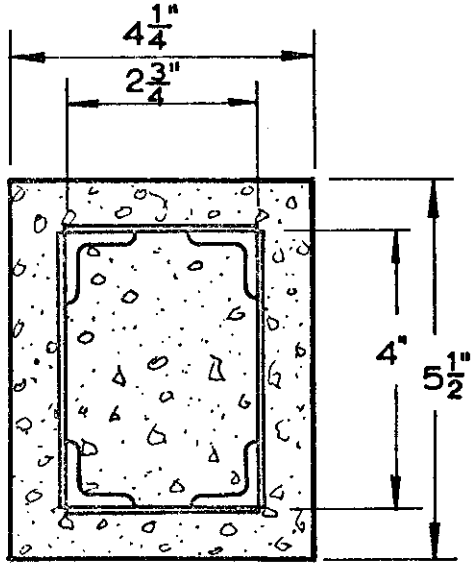

4 L1"x1"x 3/16" connected by 3/16" dia. single lacing at 5 1/2" pitch.
All welded construction.

(b) Bondale.

FIG. 2·2 CROSS-SECTIONS OF BUILT-UP COMPOSITE COLUMNS.

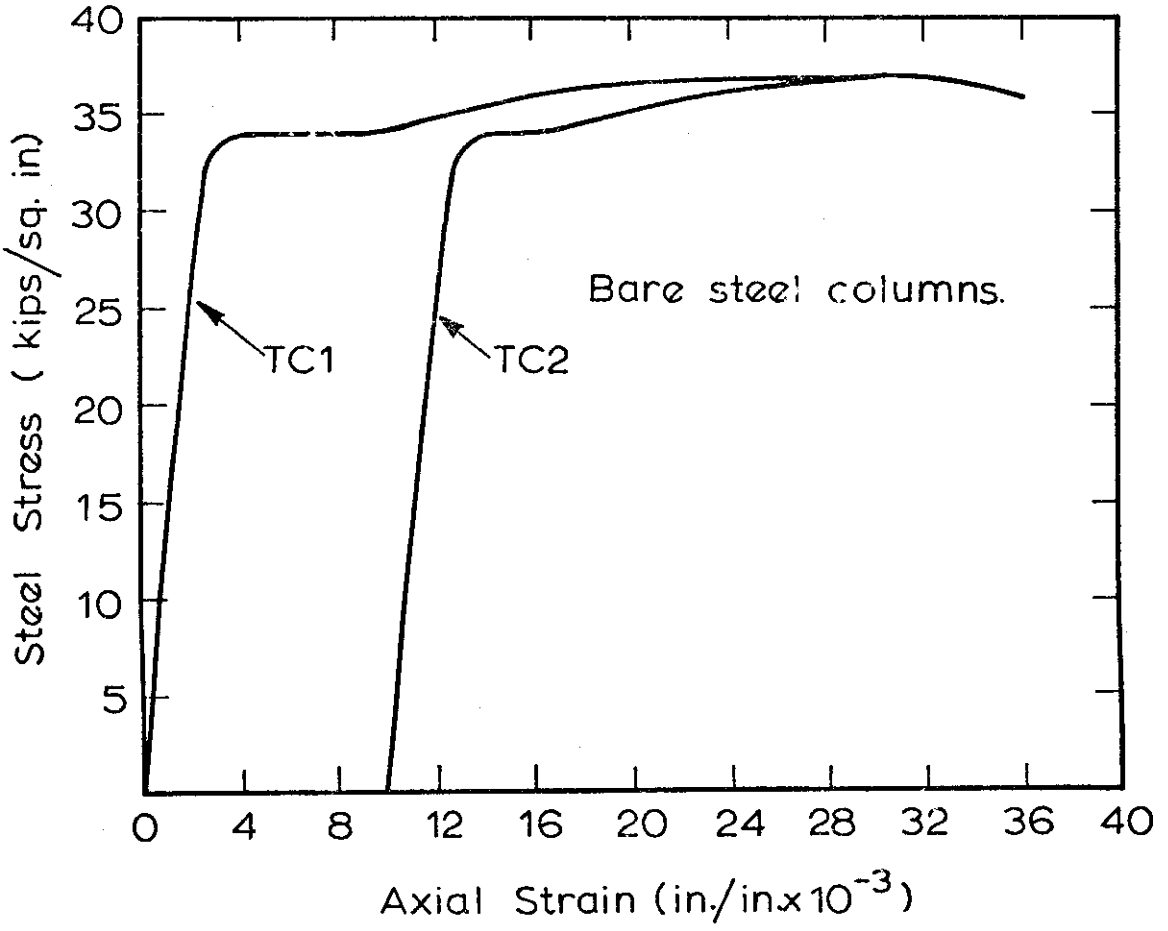

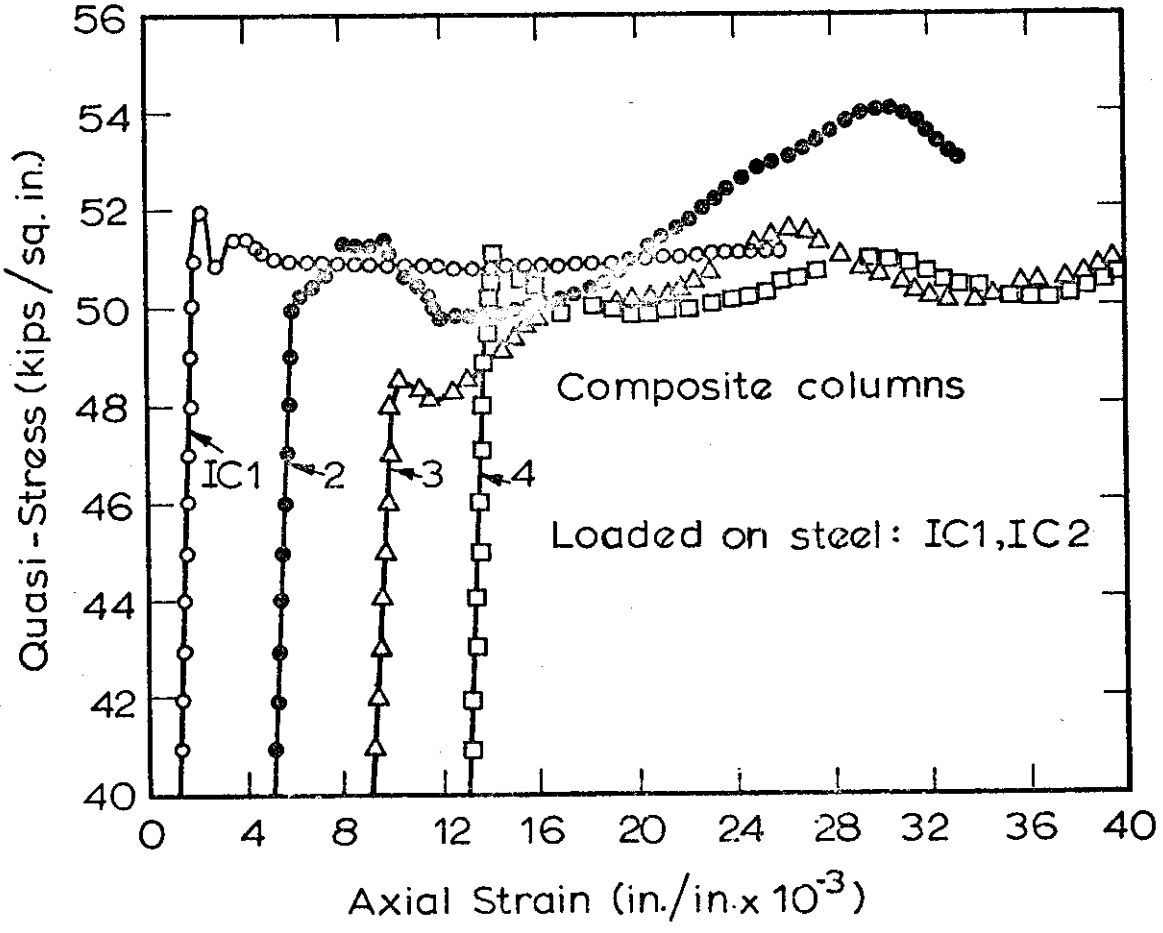

FIG. 2.3 CONCENTRIC LOAD TESTS ON BARE STEEL AND COMPOSITE COLUMNS (Stang Et Al. Fig. 2·2(a))

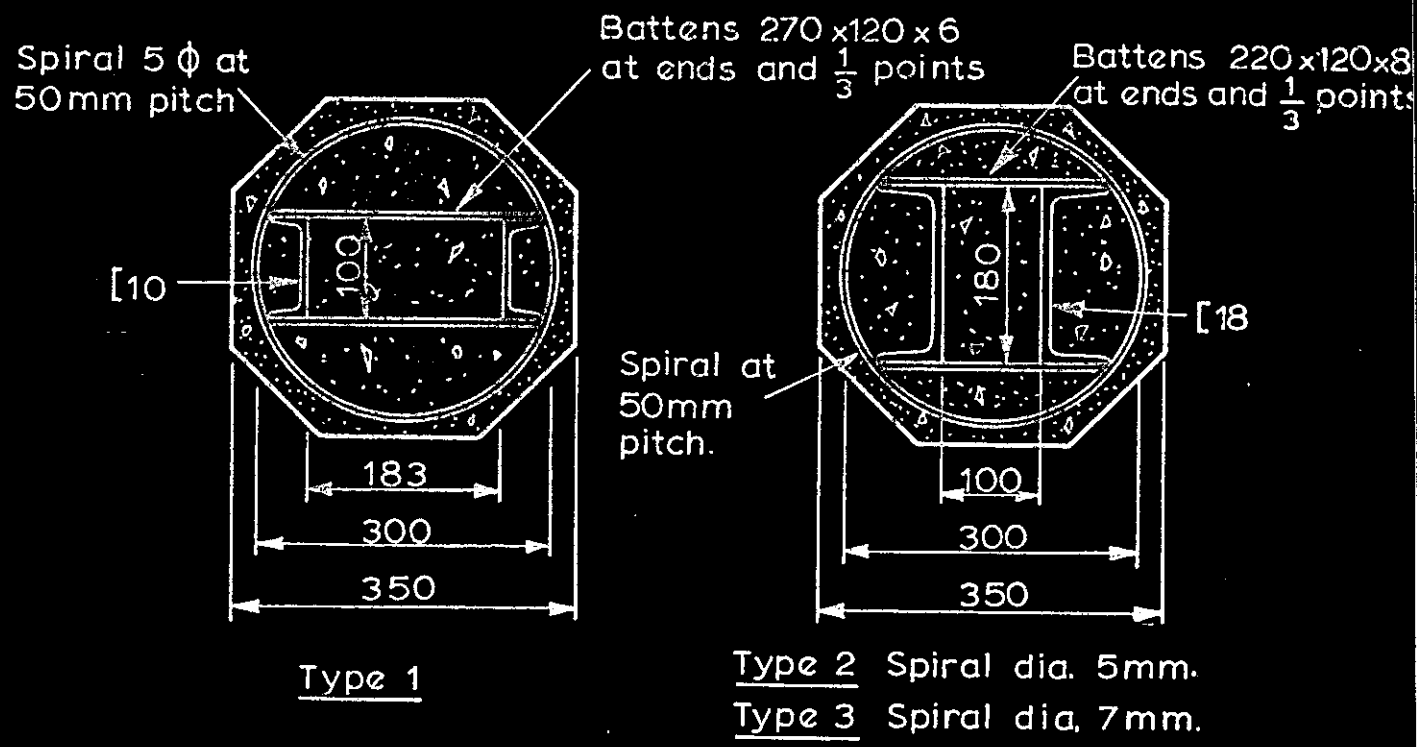

Column Length = 3000mm

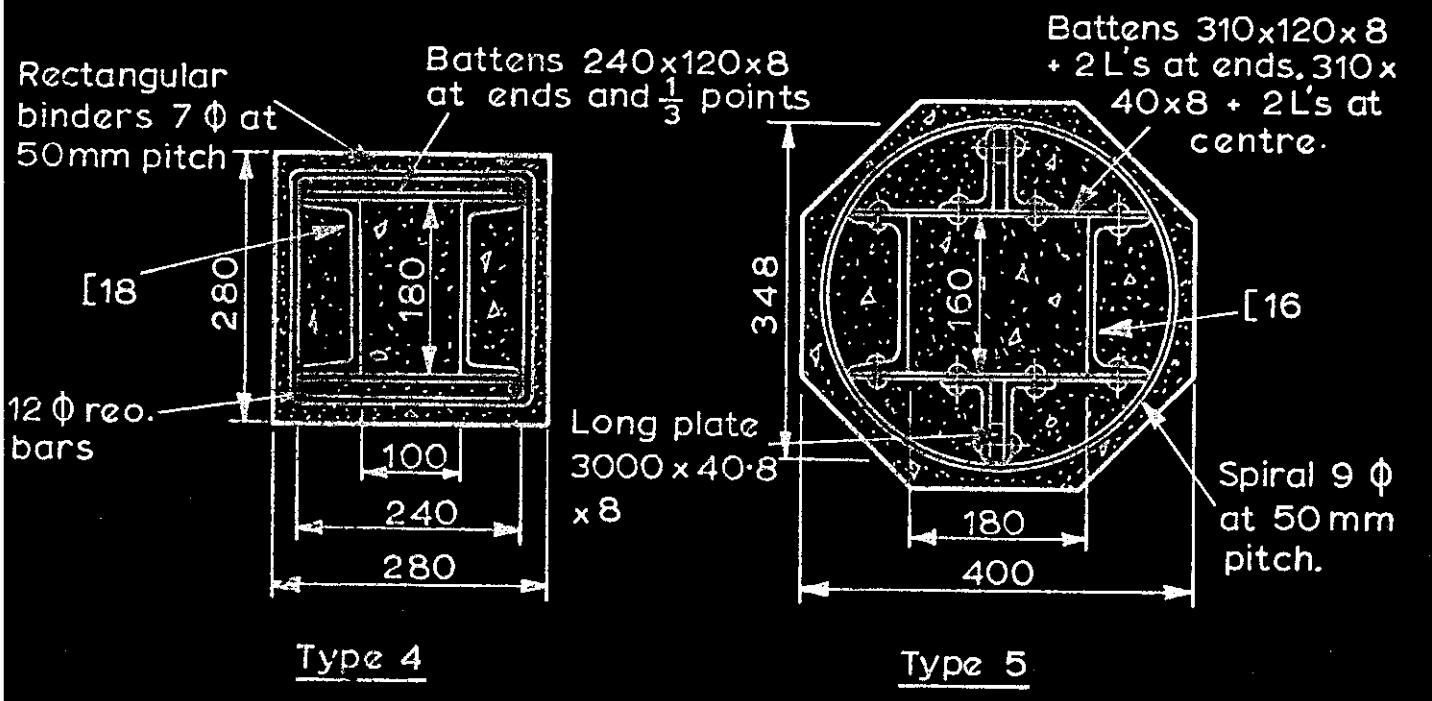

All dimensions in mm.

FIG. 2·4 COMPOSITE COLUMNS (Saliger).

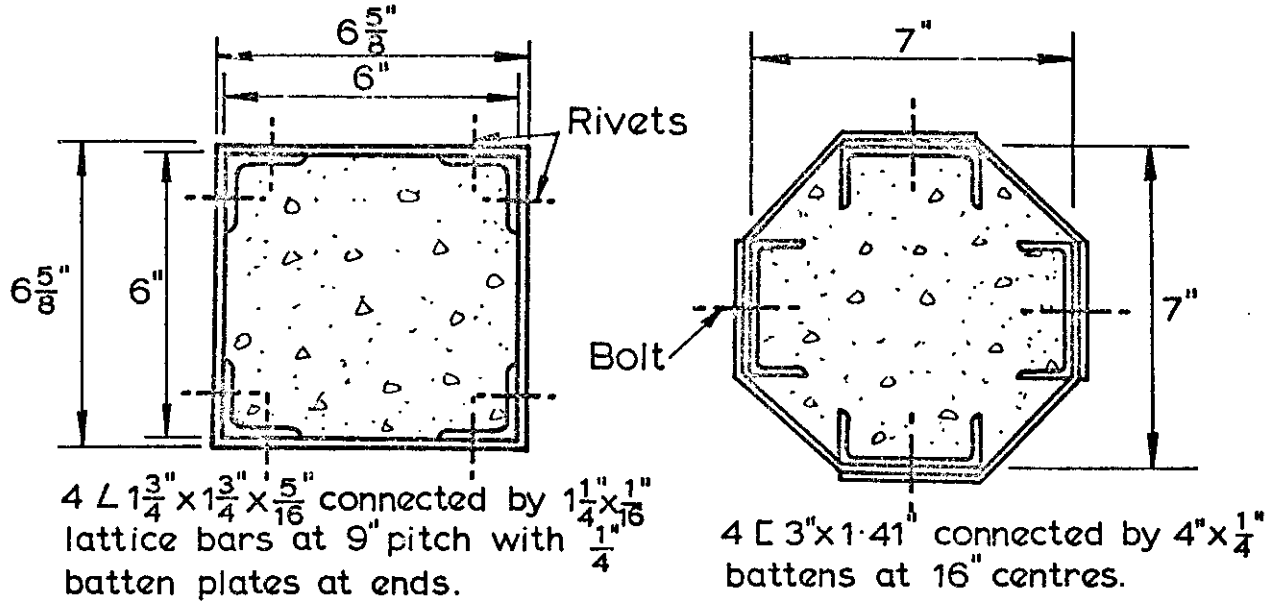

4 L 1¾" x 1¾" x 5/16" connected by 1¼" x 1/16" lattice bars at 9" pitch with 1/4" batten plates at ends.

4 [3" x 1·41" connected by 4" x 1/4" battens at 16" centres.

(a) Burr

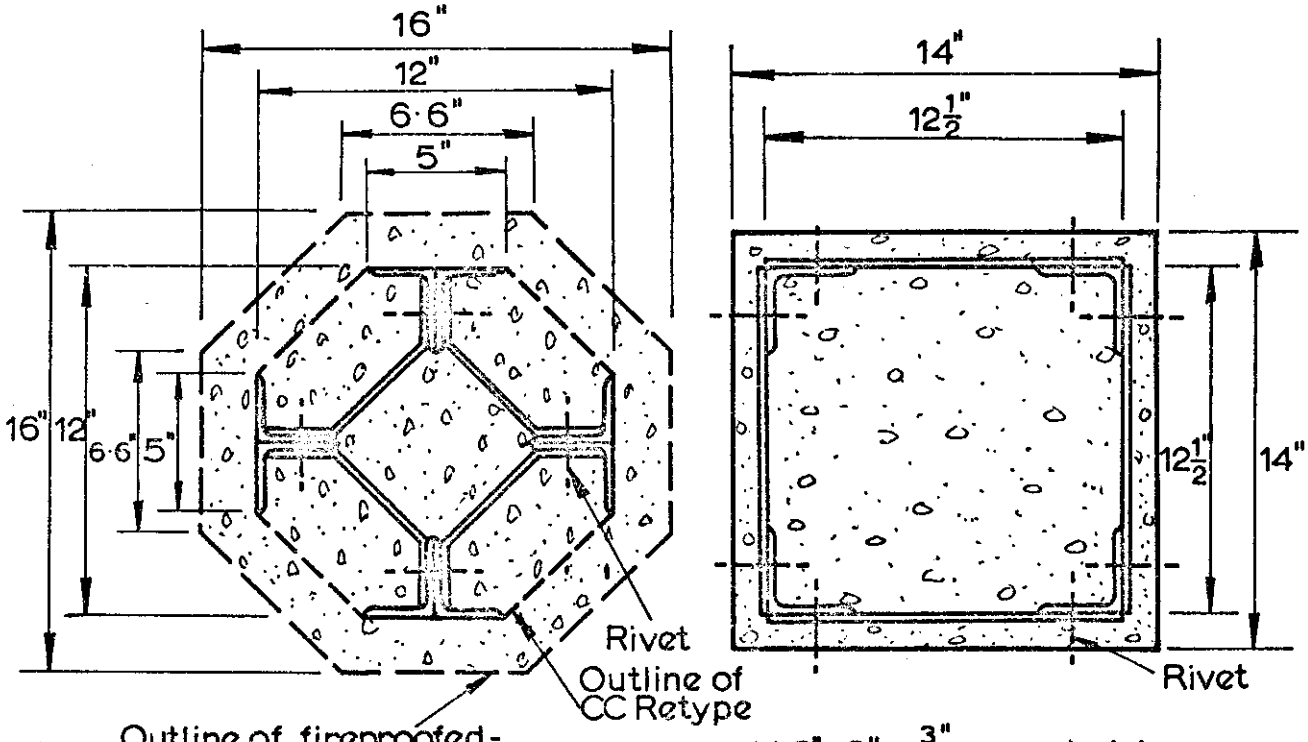

8 L 3" x 2½" x 5/16" connected by 5½" x ¼" x 8½" ties at 16" centres.

4 L 3" x 3" x 3/8" connected by 2½" x ⅜" diagonal latticing at 45°

(b) Talbot and Lord

(c) Warren

FIG. 2·5 CROSS SECTIONS OF BUILT-UP COMPOSITE COLUMNS.

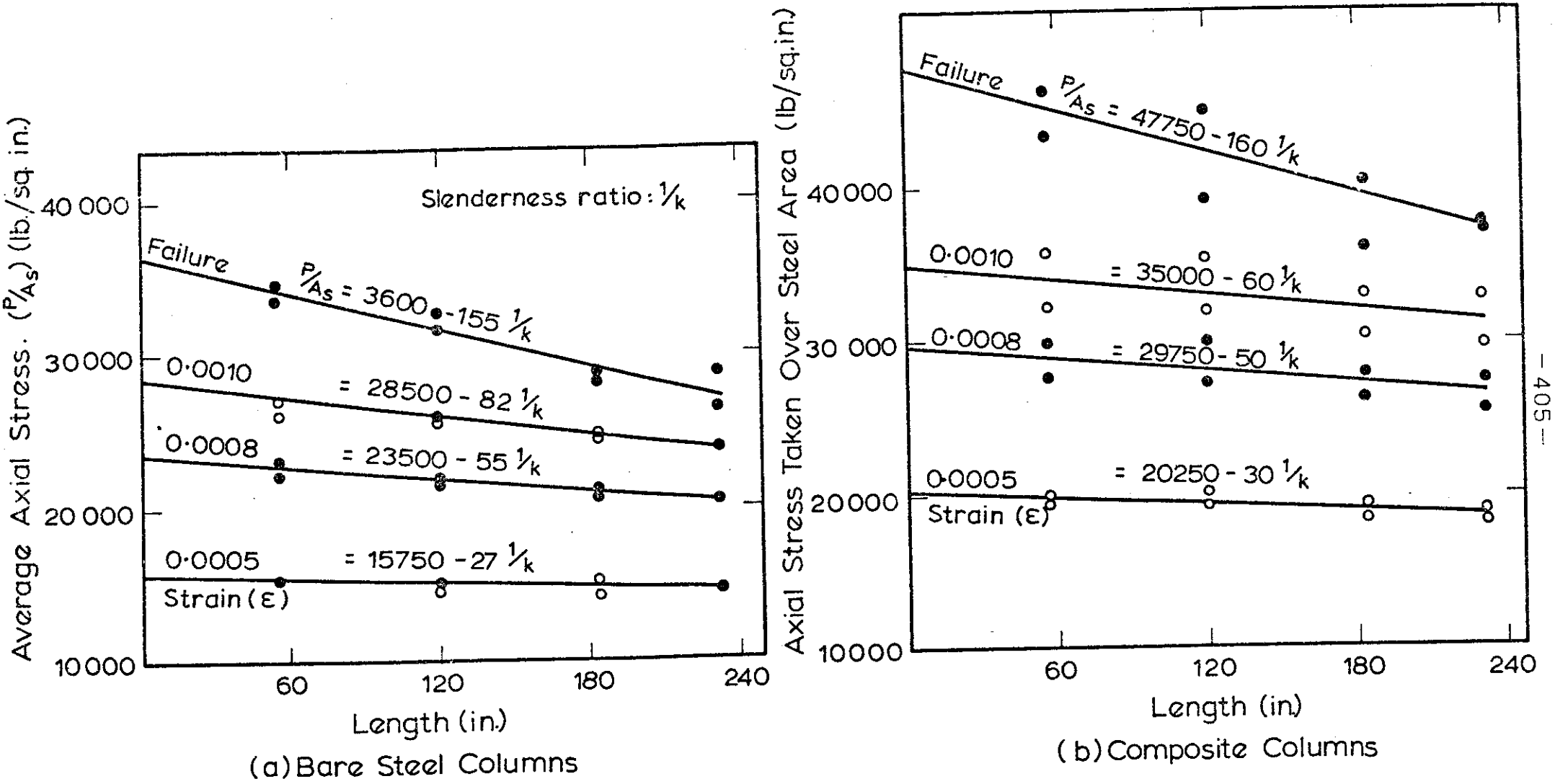

FIG. 2·6 TESTS BY TALBOT AND LORD ON AXIALLY LOADED BUILT UP BARE STEEL AND CORE TYPE COMPOSITE COLUMNS. (Fig. 2·5(b).)

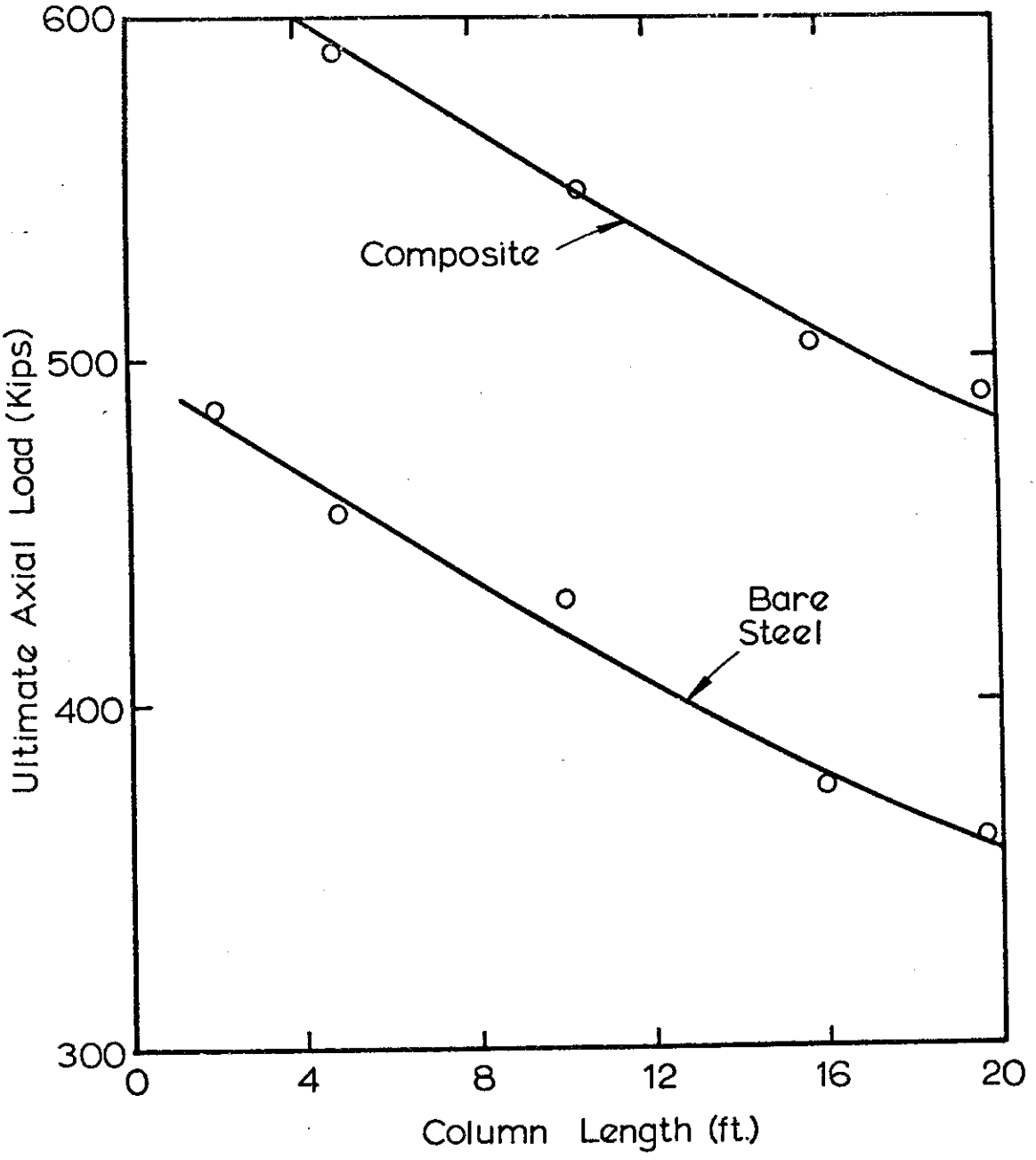

FIG.2·7 TEST RESULTS FOR TALBOT AND LORD'S BUILT-UP COMPOSITE COLUMNS (ANDREWS)

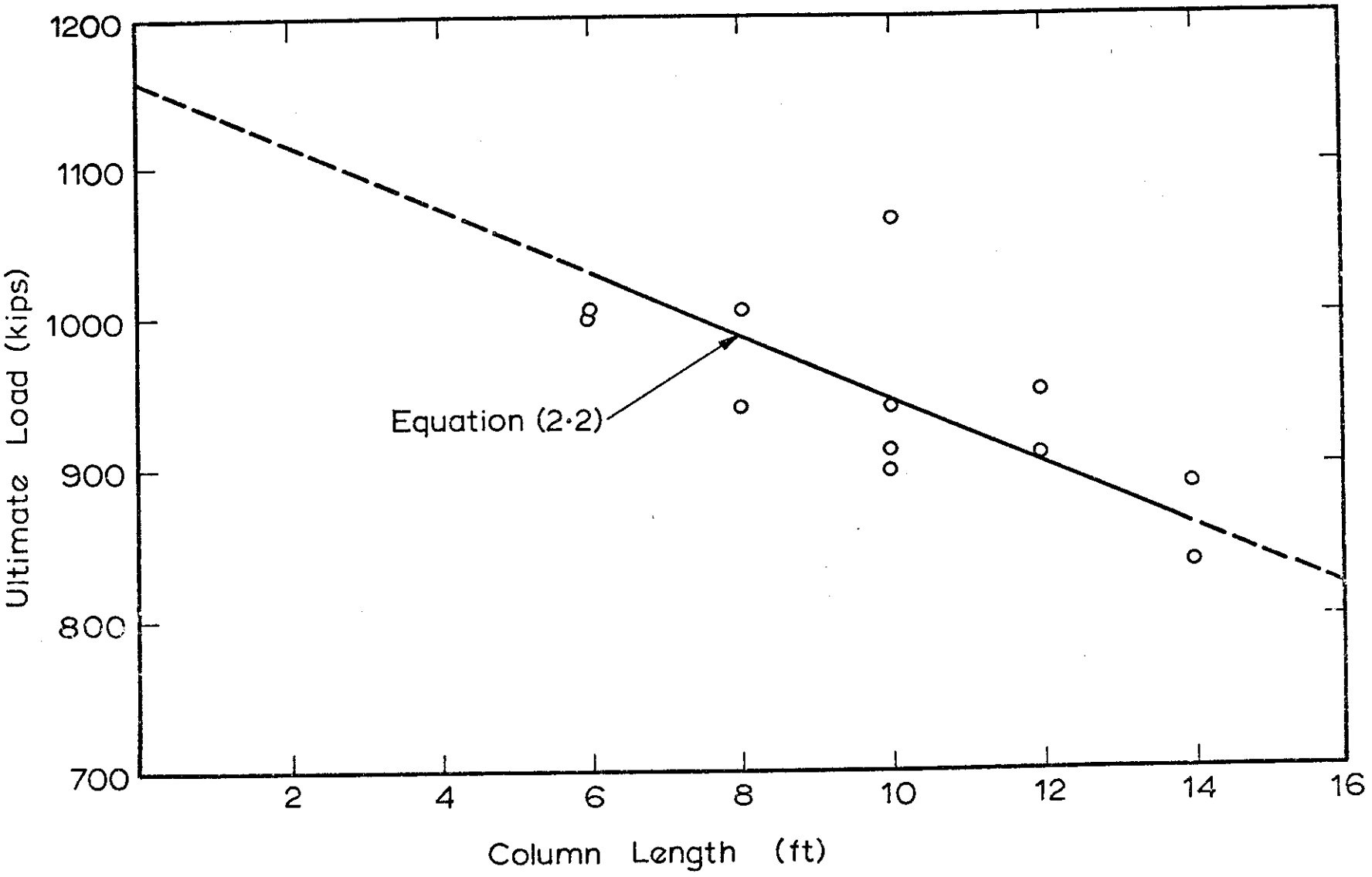

FIG. 2·8 CONCENTRIC LOAD TESTS BY MENSCH (30) ON 6 IN. CAST IRON TUBES IN THICK ENCASED IN SPIRAL CONCRETE TO 12 IN. DIA.

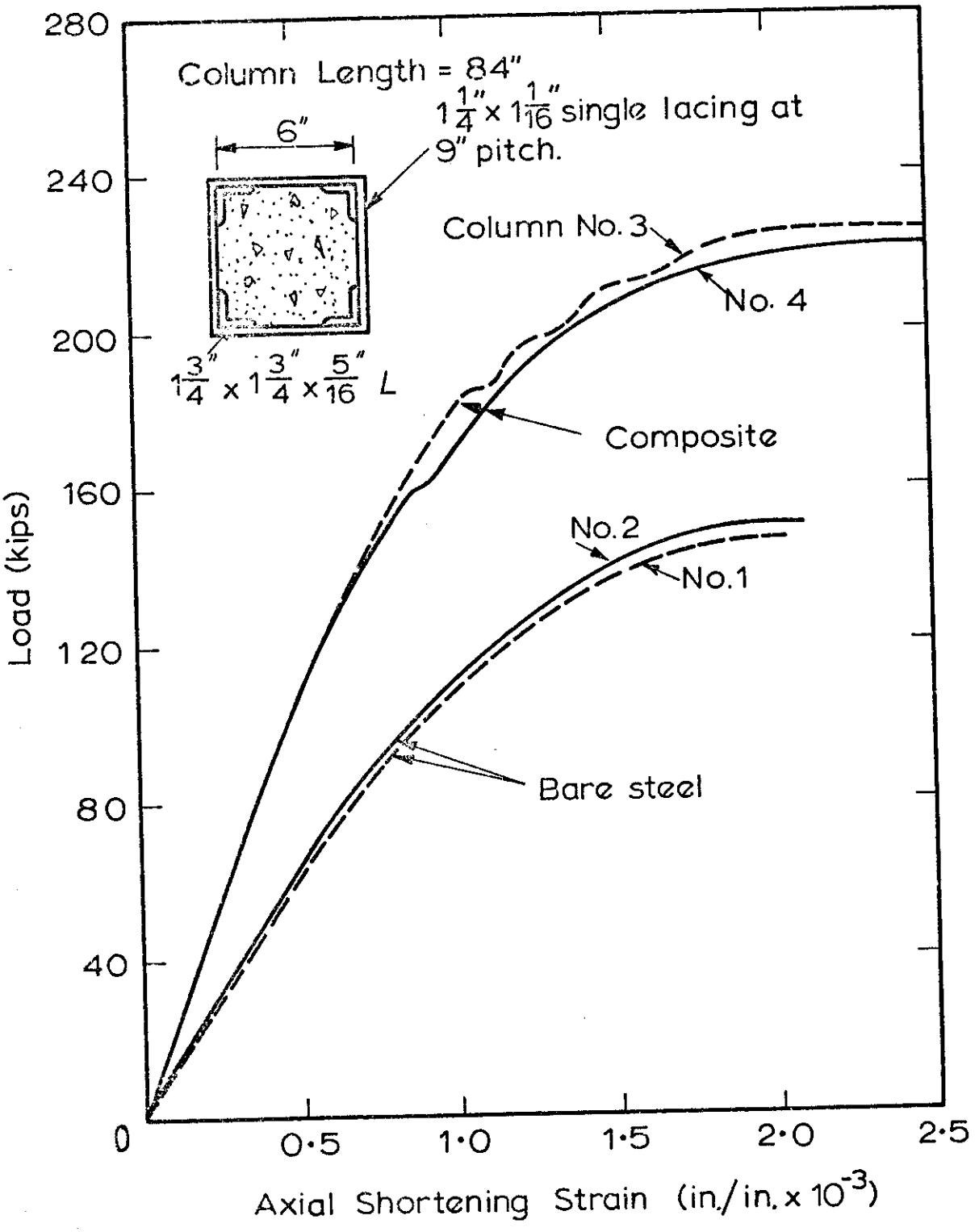

FIG. 2·9 CONCENTRIC LOAD TESTS ON BARE STEEL AND COMPOSITE COLUMNS BUILT UP FROM ANGLES (Burr)

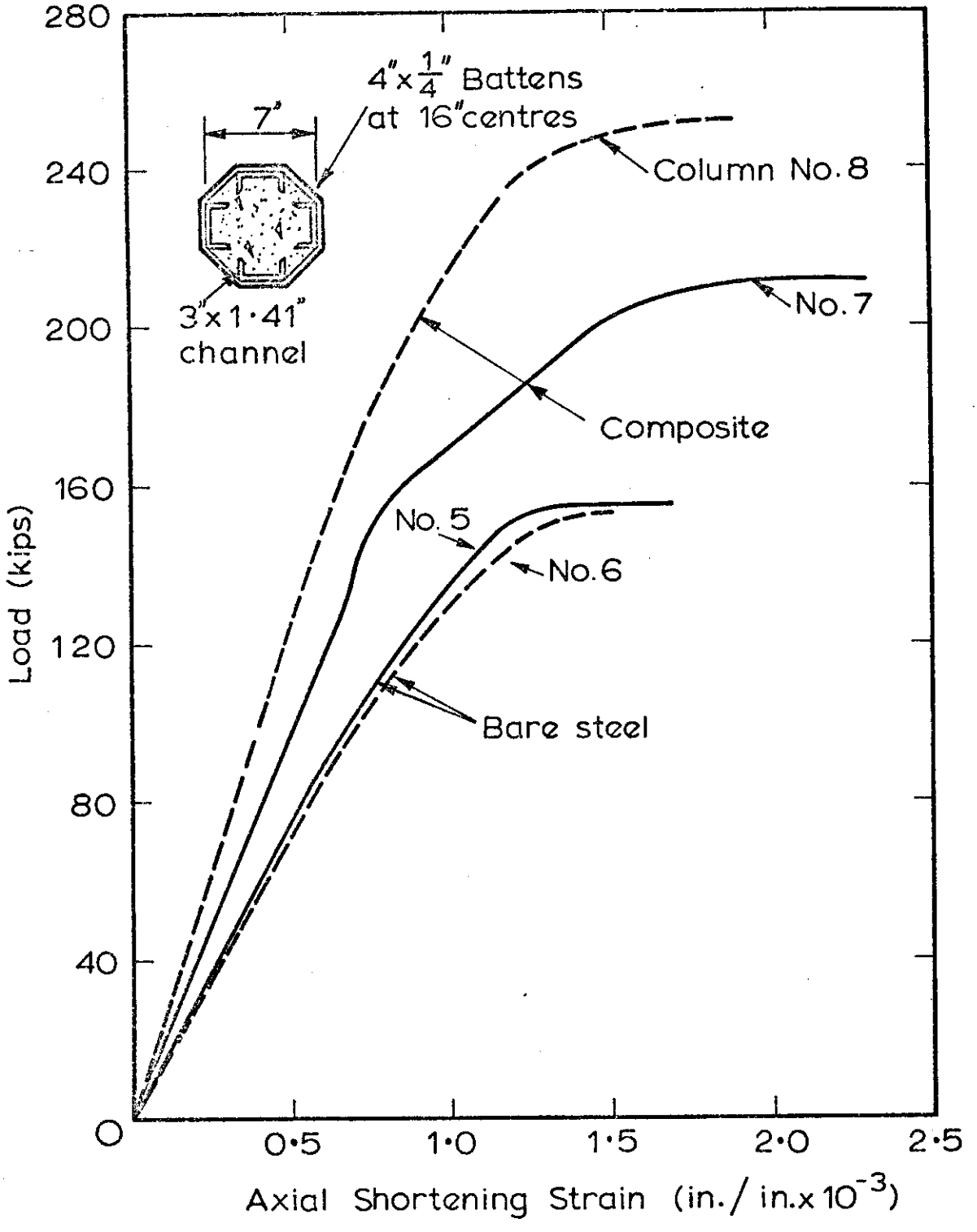

FIG. 2·10 CONCENTRIC LOAD TESTS ON BARE STEEL AND COMPOSITE COLUMNS BUILT UP FROM CHANNELS. (Burr)

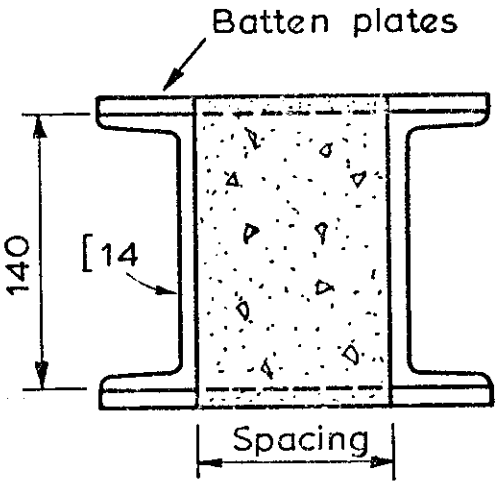

Type II

Mark	Spacing (mm)
1	75
2	120
3	150
4	180

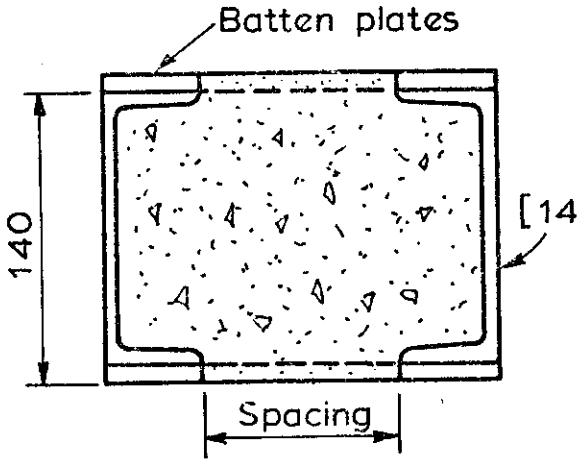

Type V

Mark	Spacing (mm)
1	75
2	120
3	150
4	180

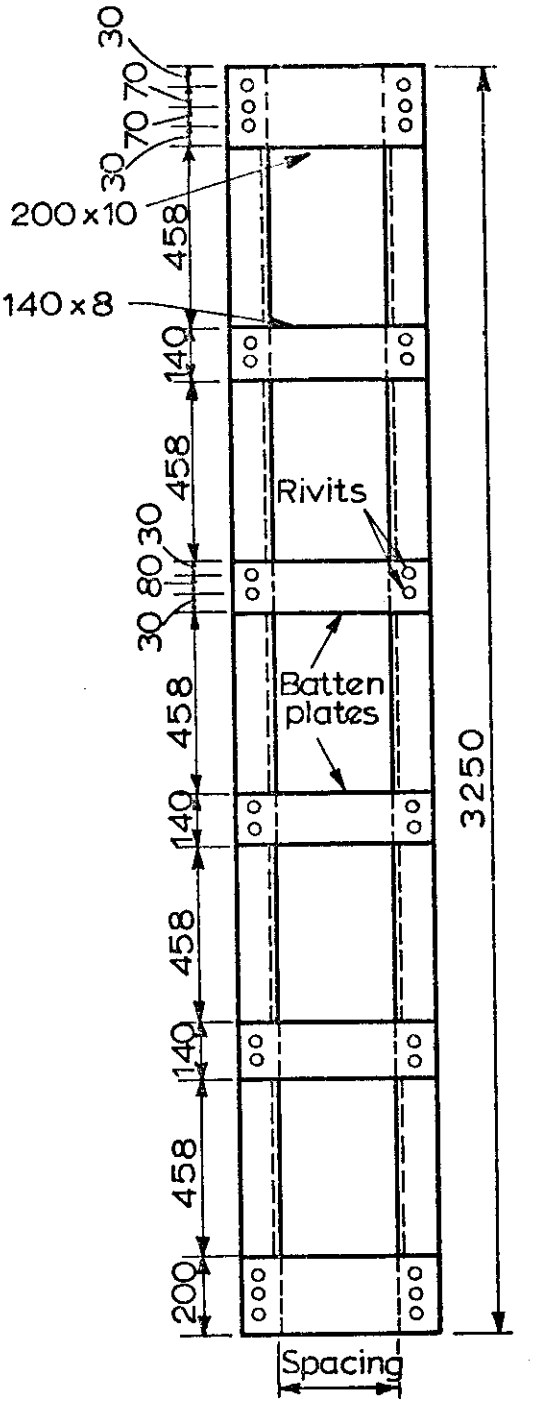

All dimensions in mm
25·4mm = 1″

FIG. 2·11 BUILT-UP COMPOSITE COLUMNS. (Memmler, Bierett and Gruning)

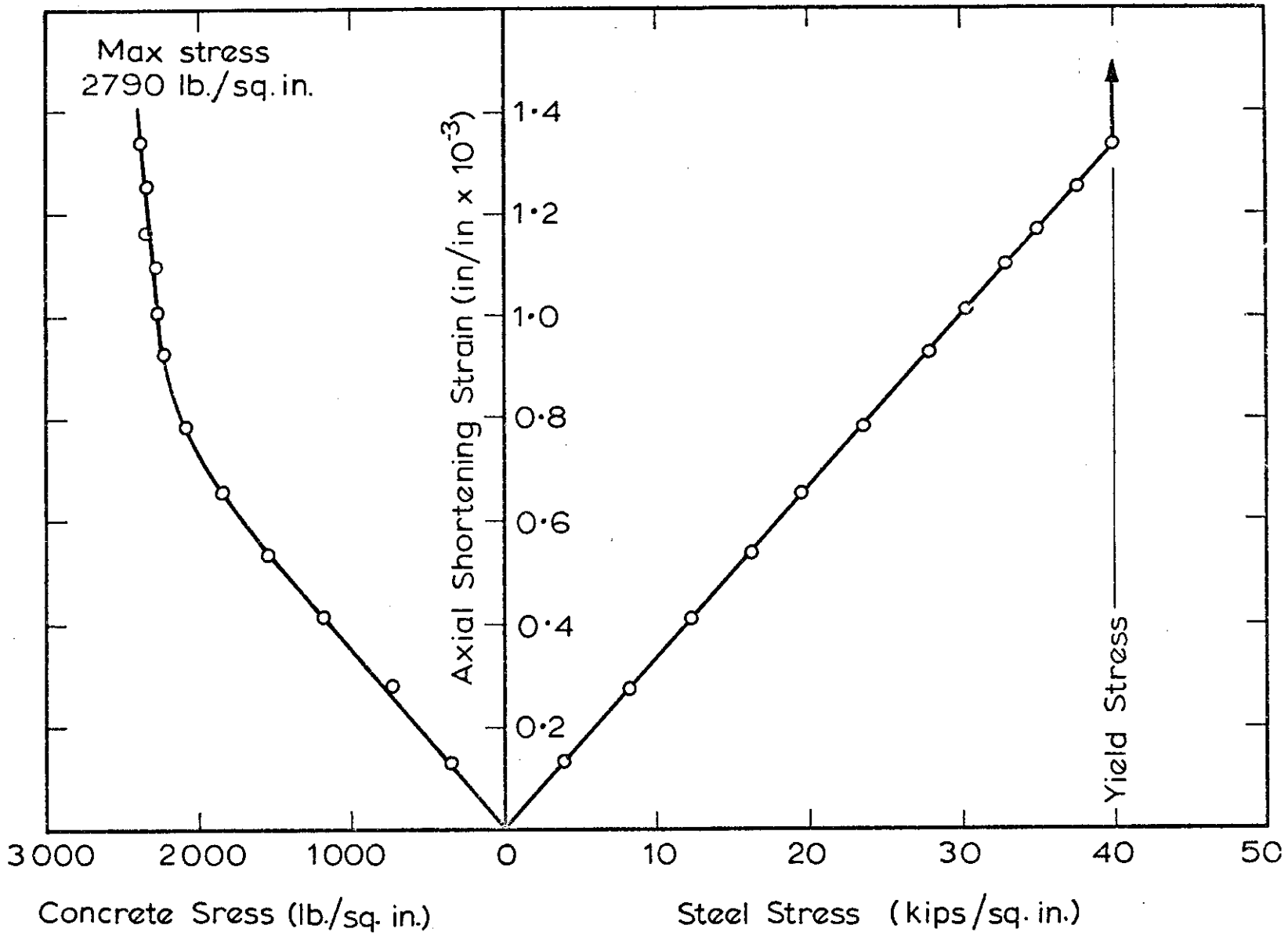

FIG. 2·12 CALCULATED STRESSES IN STEEL AND CONCRETE FOR COMPOSITE COLUMN TYPE II Mk 3 TESTED BY MEMMLER ET. AL. (FIG. 2·11)

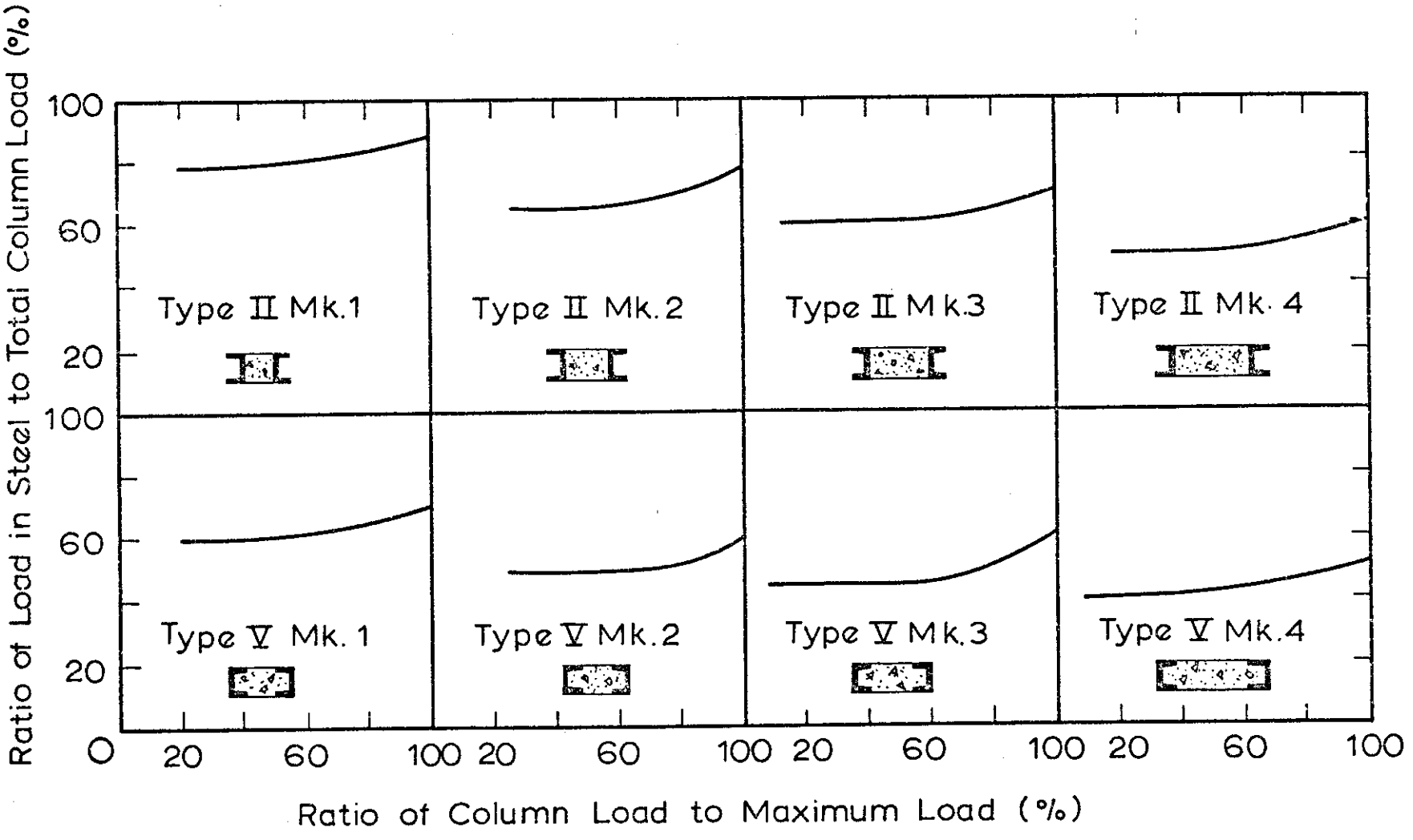

FIG. 2·13 LOAD SHARING BETWEEN STEEL CHANNELS AND CONCRETE CORE FOR COMPOSITE COLUMNS TESTED BY MEMMLER ET AL. (FIG. 2·11)

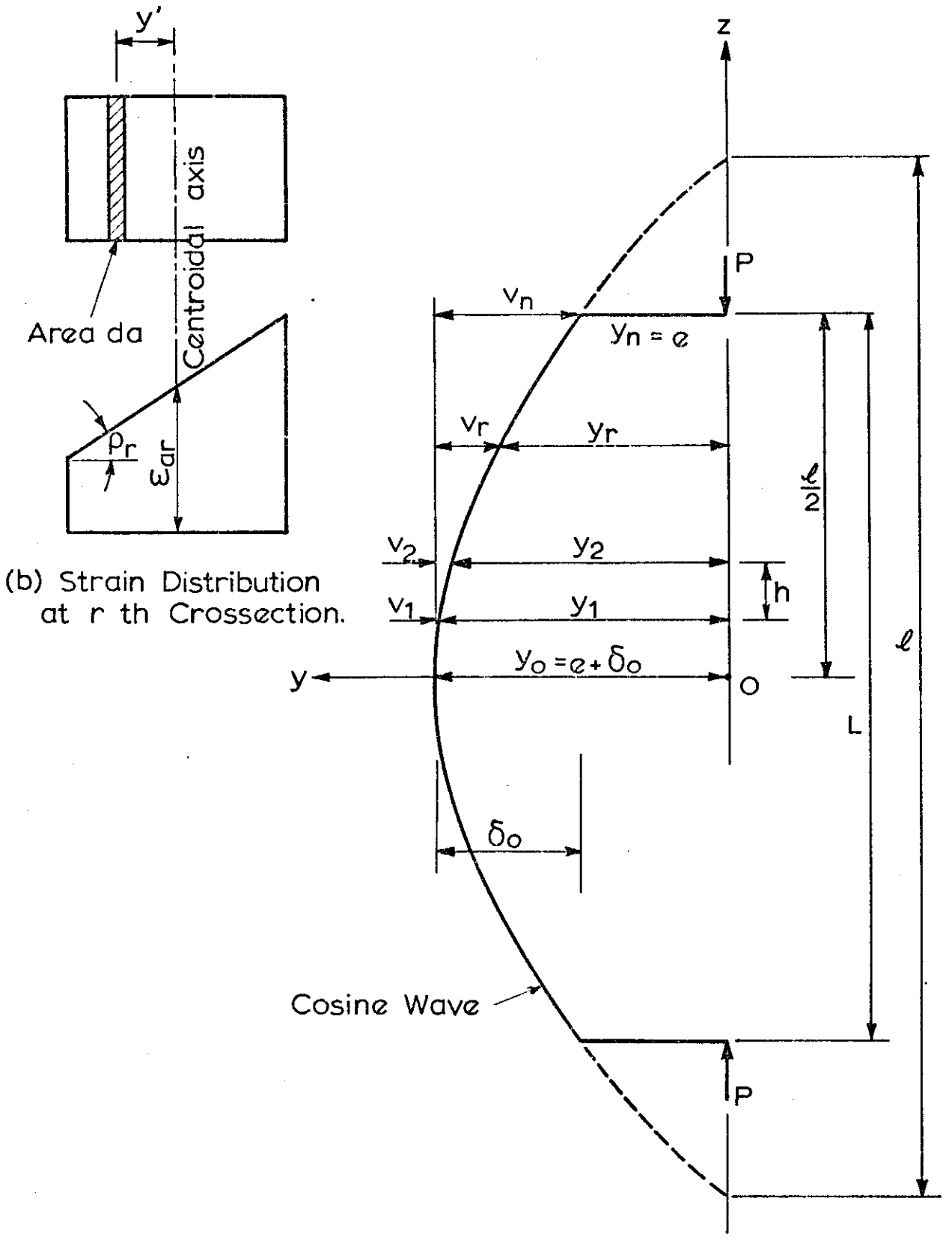

FIG. 2·14 DEFLECTED SHAPE AND STRAIN DISTRIBUTION FOR ECCENTRICALLY LOADED COLUMN.

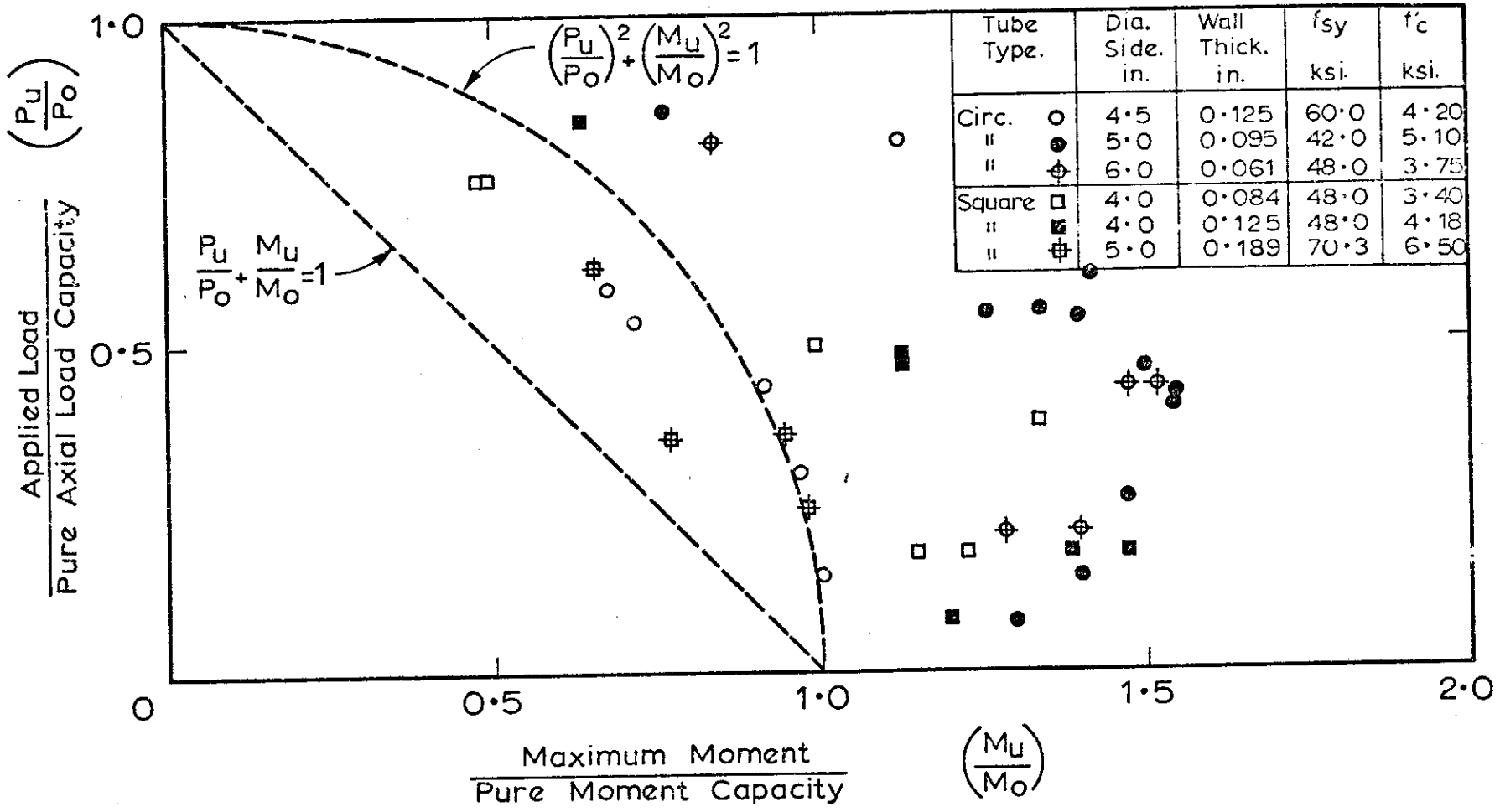

FIG. 2·15 BEAM COLUMN CAPACITY OF CONCRETE FILLED TUBES FROM TESTS BY FURLONG. (21)

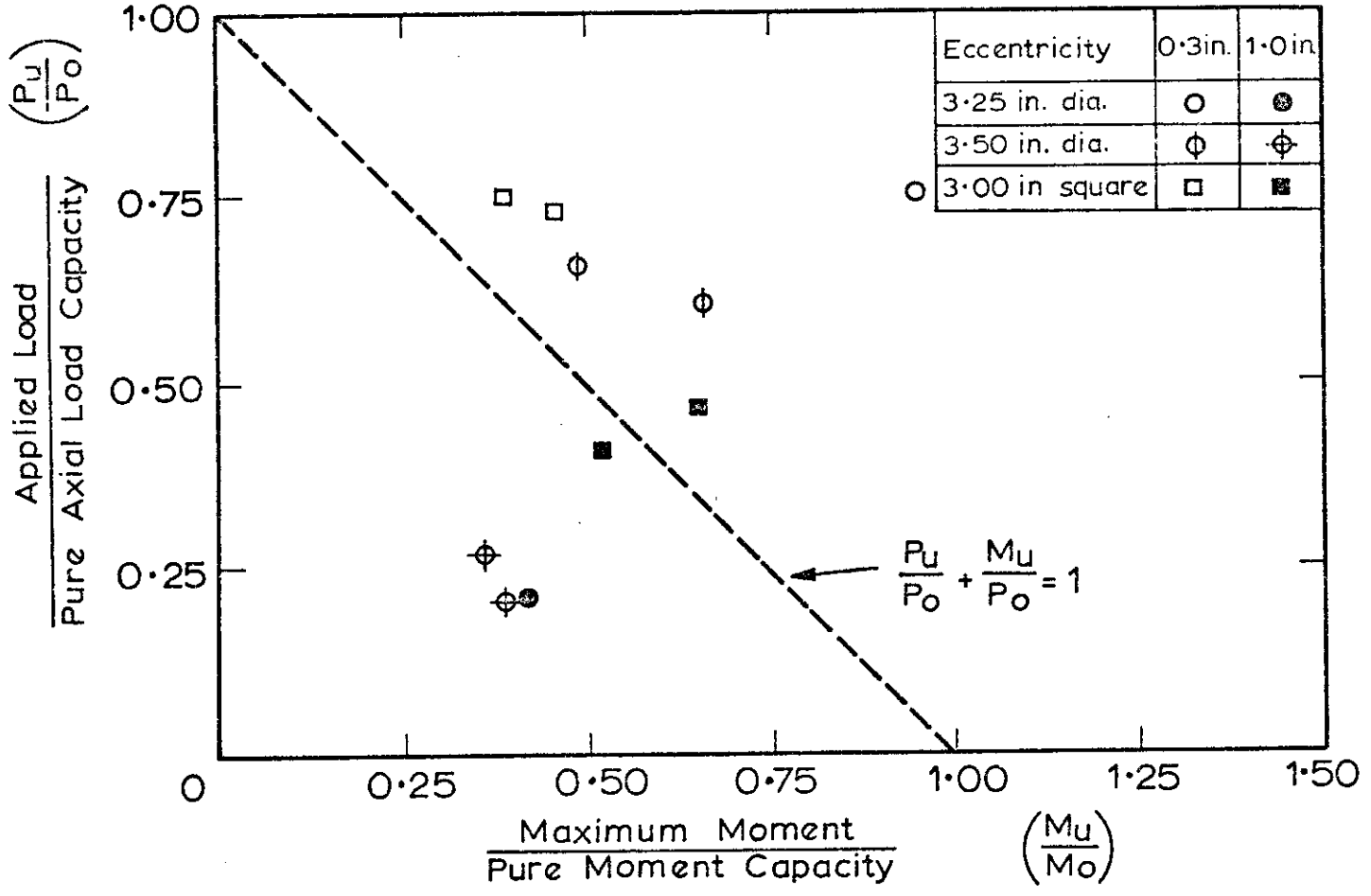

FIG·2·16 BEAM-COLUMN CAPACITY OF CONCRETE FILLED TUBES FROM TESTS BY KNOWLES AND PARK. (23)

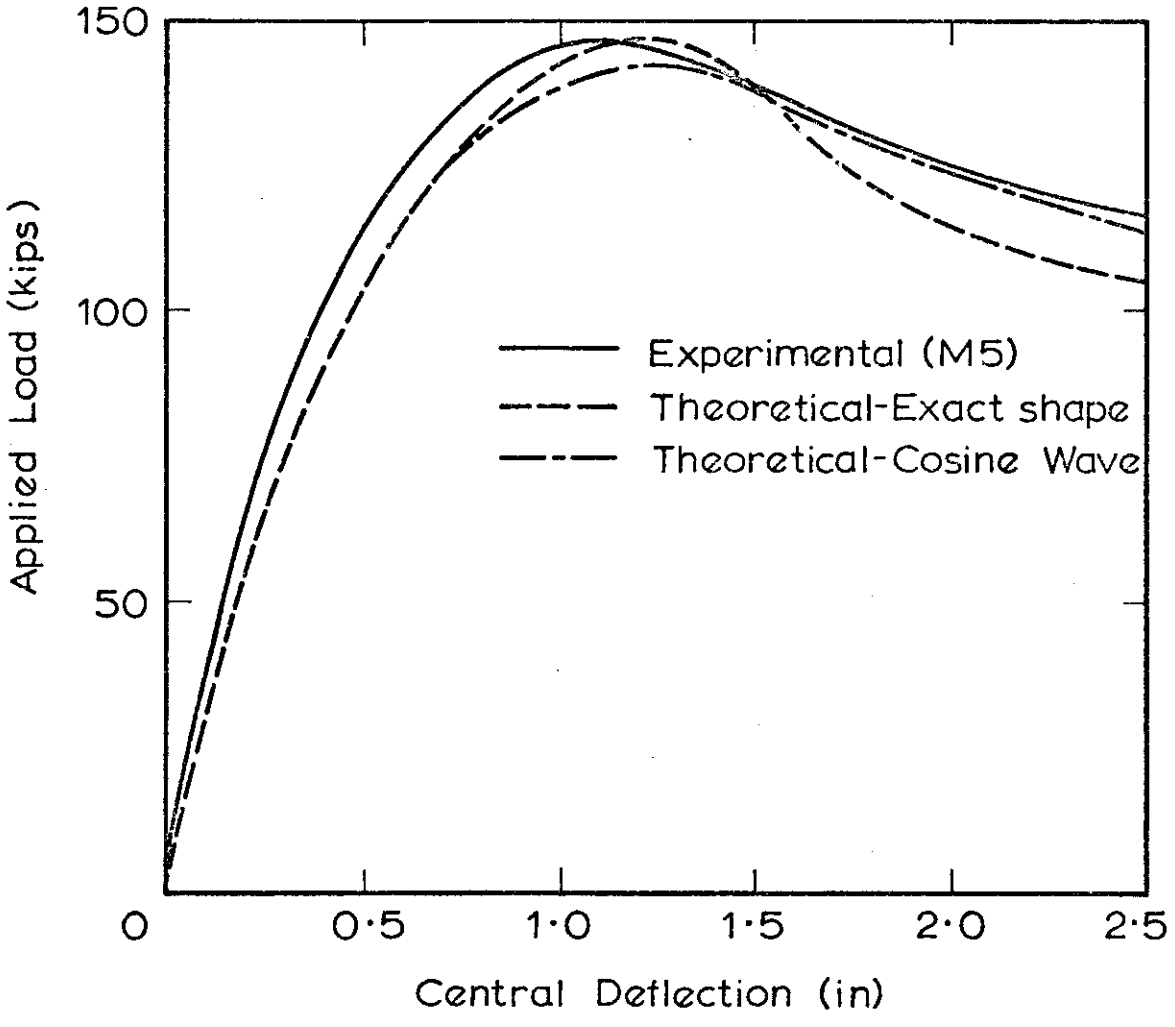

FIG. 2·17 LOAD-CENTRAL DEFLECTION CURVE FOR ECCEN--TRICALLY LOADED CONCRETE FILLED TUBE.(Neogi Et. Al.)

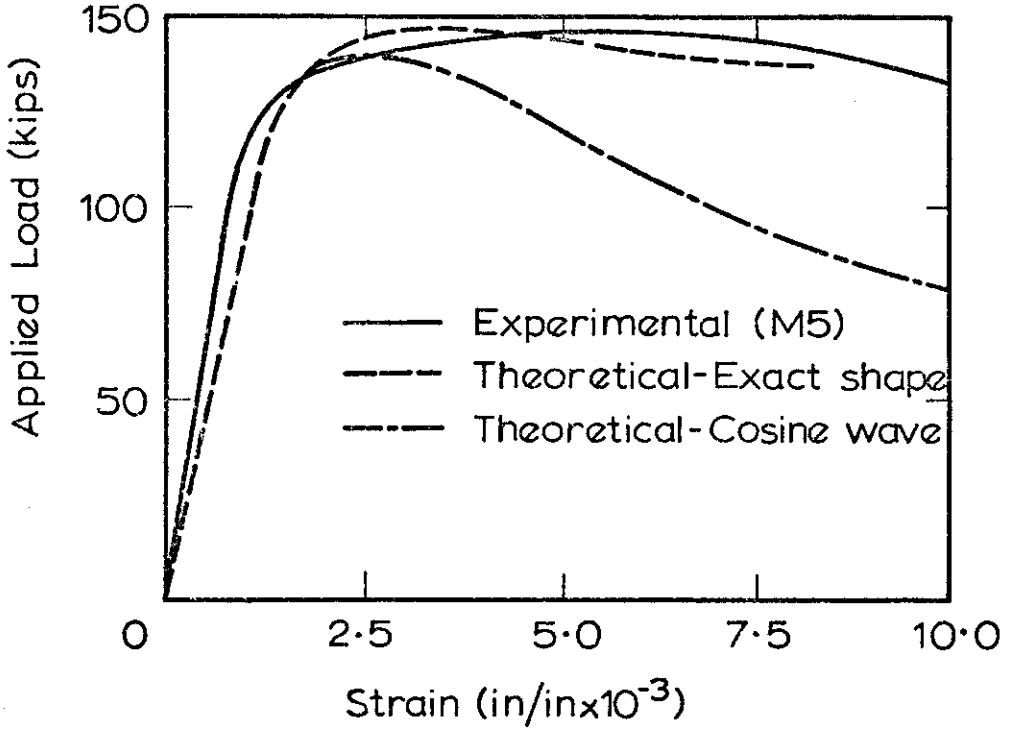

FIG. 2·18 LOAD-STRAIN CURVE FOR ECCENTRICALLY LOADED CONCRETE FILLED TUBE.(Neogi Et. Al.)

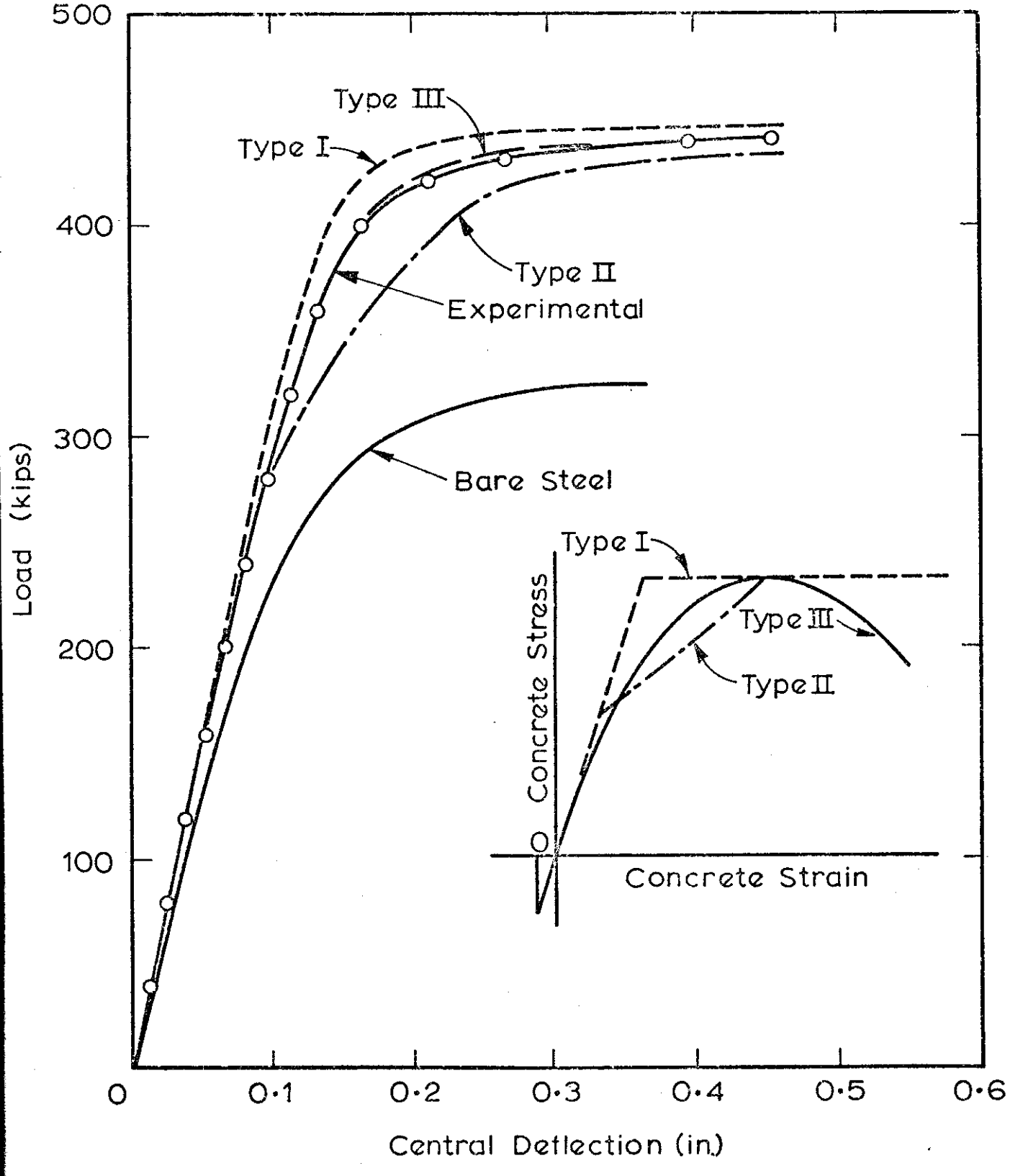

FIG. 3·1 EFFECT OF STRESS-STRAIN CHARACTERISTICS ON THEORETICAL COLUMN BEHAVIOUR FOR COLUMN SHC-1

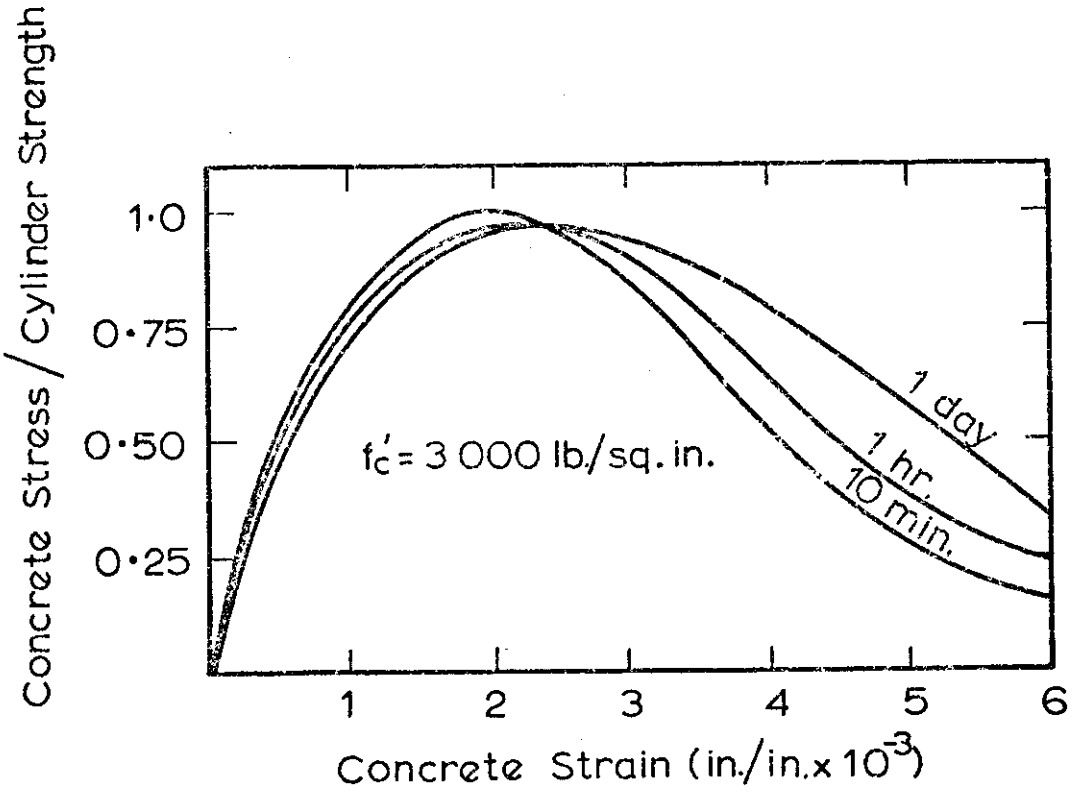

FIG. 3·2 STRESS-STRAIN RELATIONSHIPS FOR CONSTANT STRAIN RATE AT VARIOUS DURATIONS OF LOADING (RUSCH)

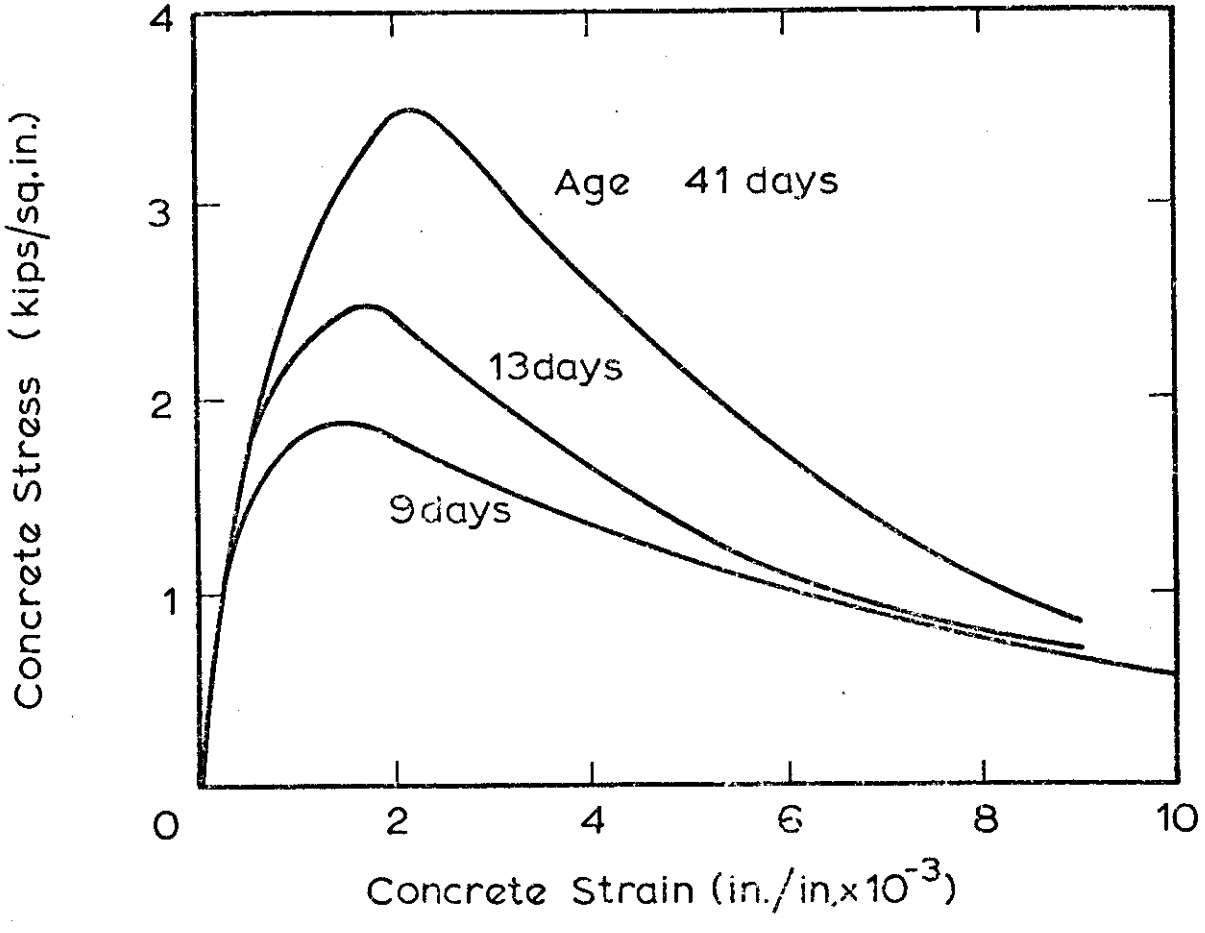

FIG. 3·3 CONCENTRIC COMPRESSION TESTS ON 6 IN. BY 3 IN. DIAMETER CYLINDERS (U.S. BUREAU OF RECLAMATION)

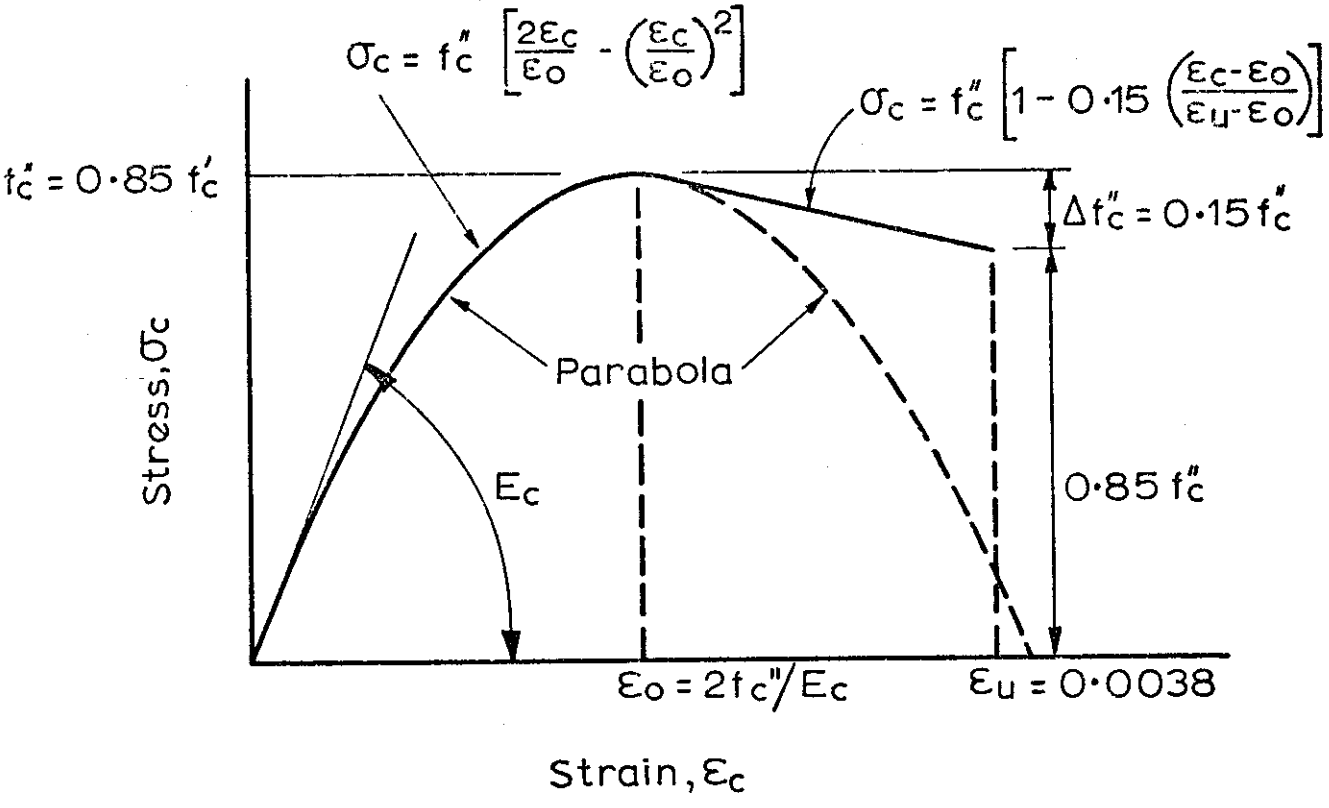

FIG 3·4 ASSUMED STRESS-STRAIN RELATIONSHIP FOR SHORT TERM LOADING (HOGNESTAD)

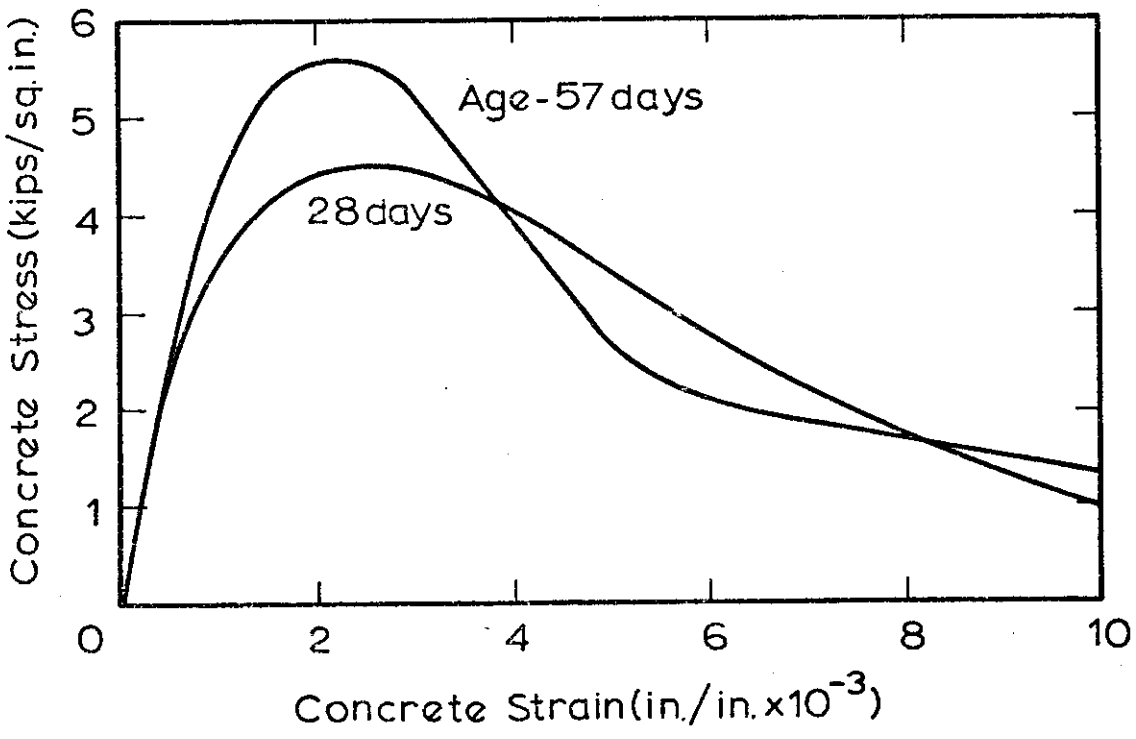

FIG. 3·5 CONCENTRIC COMPRESSION TESTS ON 3 BY 3 BY 9 IN. PRISMS (BARNARD)

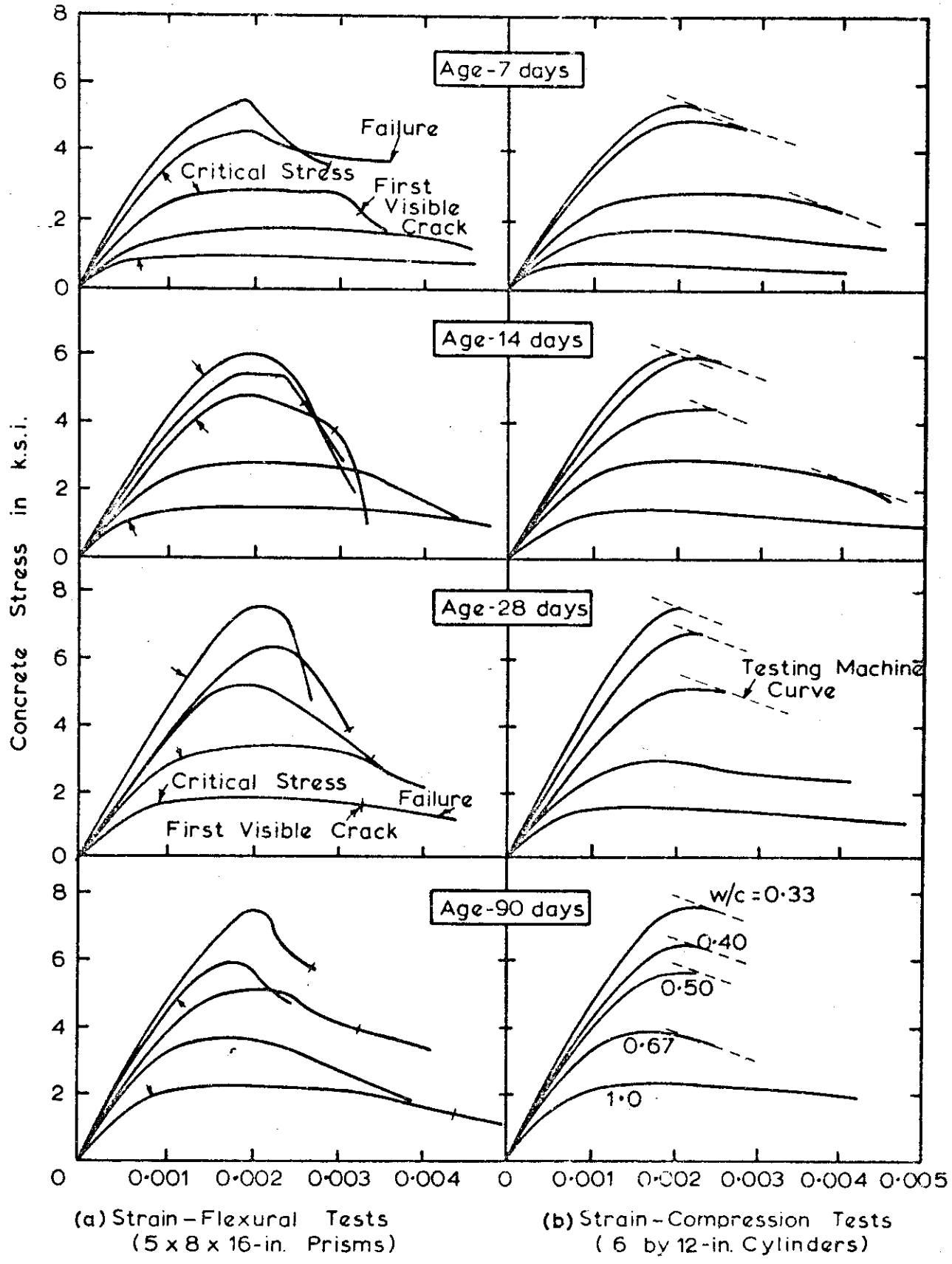

FIG. 3·6 STRESS STRAIN RELATIONSHIPS FOR CONCRETE IN FLEXURE (STRAIN GRADIENT) AND CONCENTRIC COMPRESSION (HOGNESTAD ET AL.)

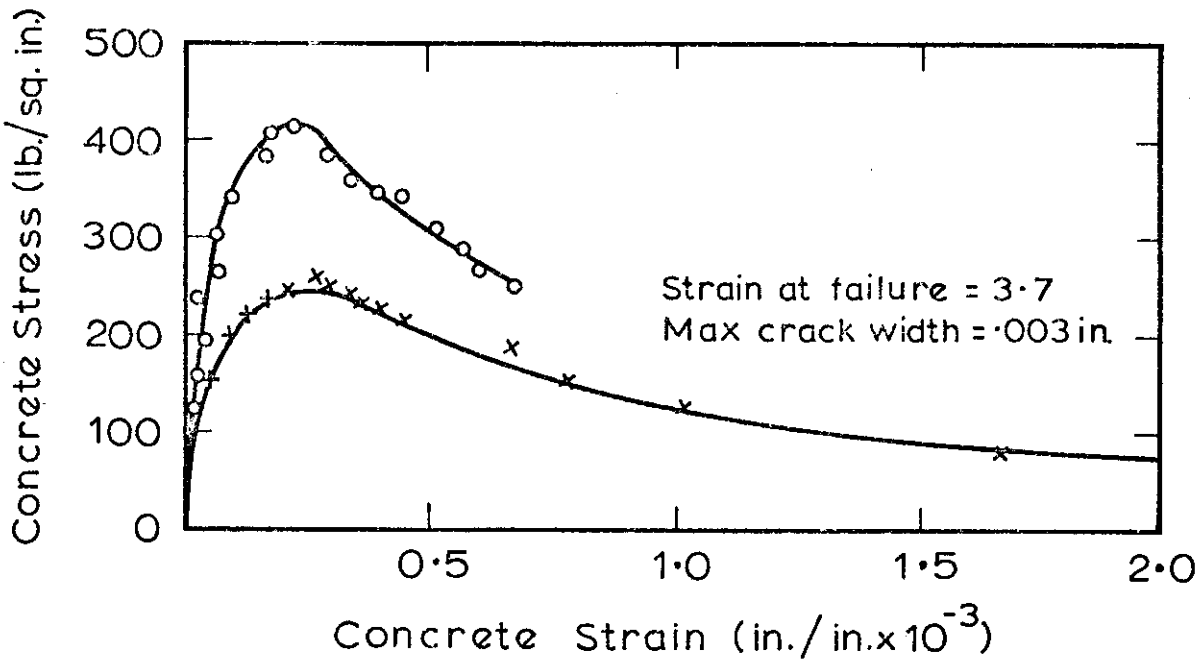

FIG. 3·7 TENSILE STRESS-STRAIN BEHAVIOUR. (EVANS AND MARATHE)

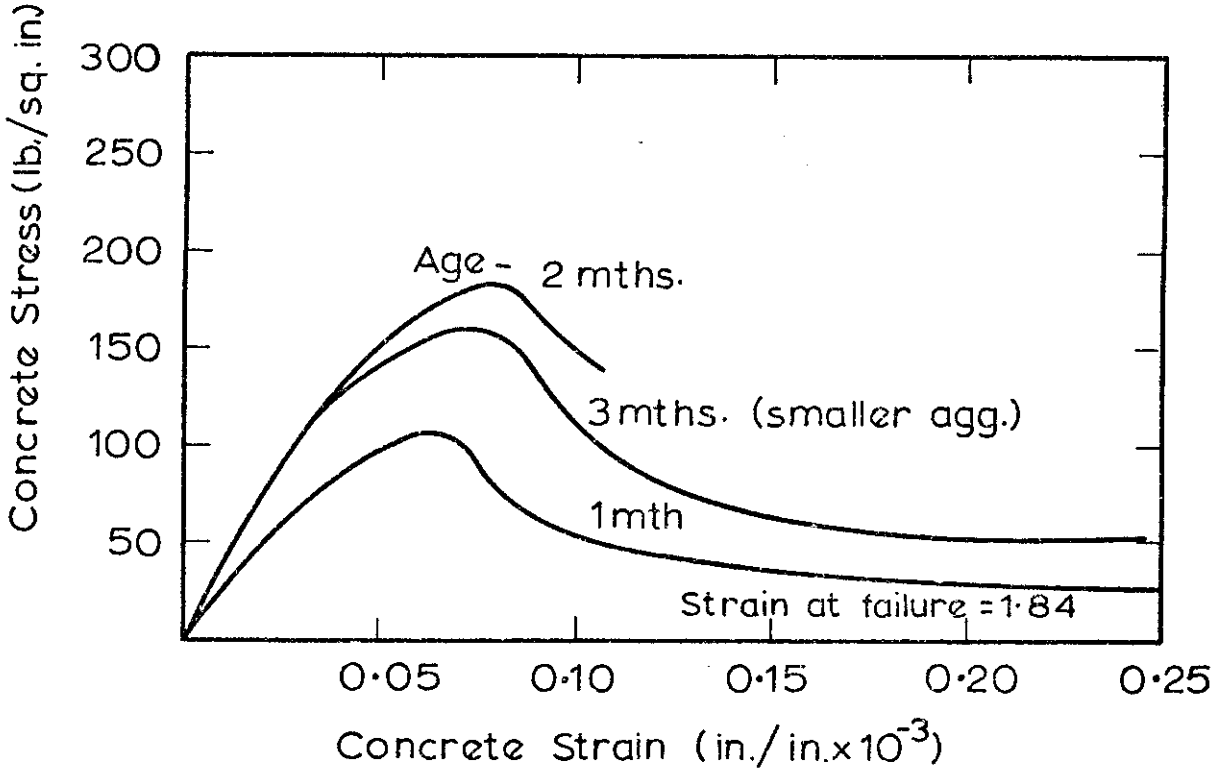

FIG. 3·8 TENSILE STRESS-STRAIN BEHAVIOUR. (HUGHES AND CHAPMAN)

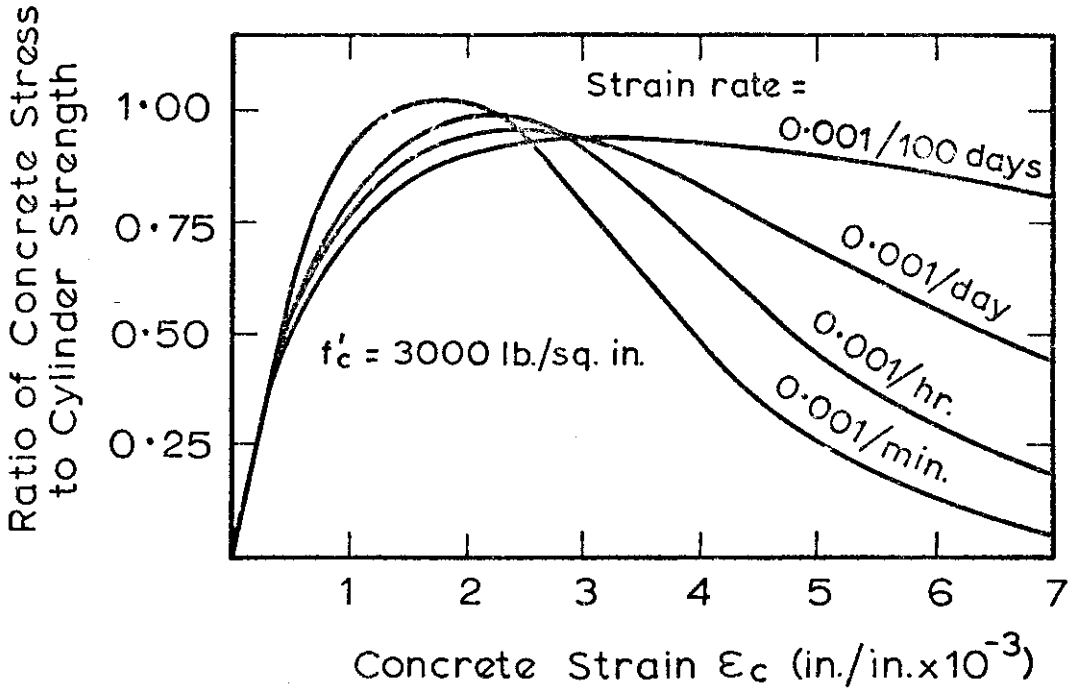

FIG. 3·9 STRESS-STRAIN CURVES FOR VARIOUS STRAIN RATES OF CONCENTRIC LOADING ON SQUARE PRISMS (RUSCH)

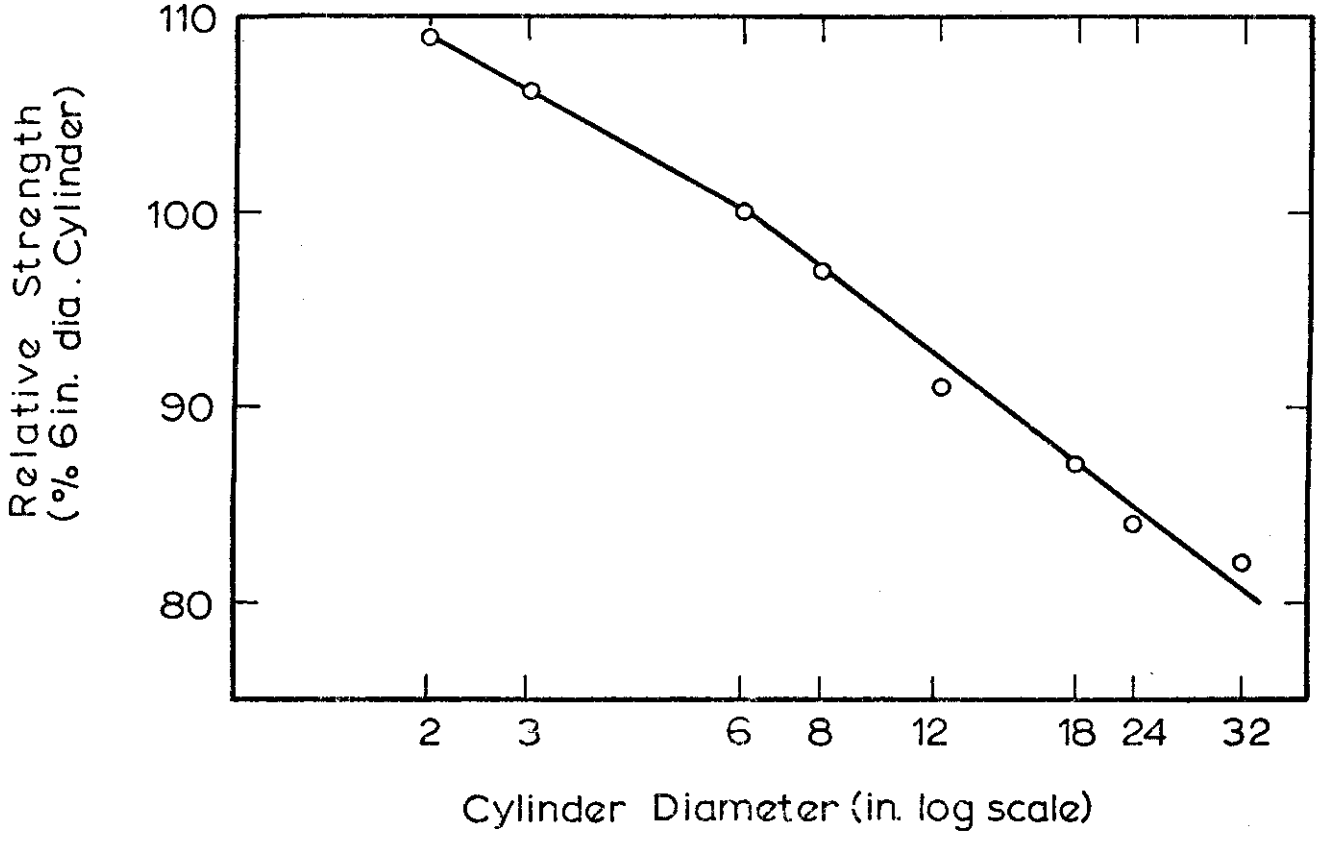

FIG. 3·10 EFFECT OF SIZE ON RELATIVE CYLINDER STRENGTH (BLANKS AND McNAMARA)

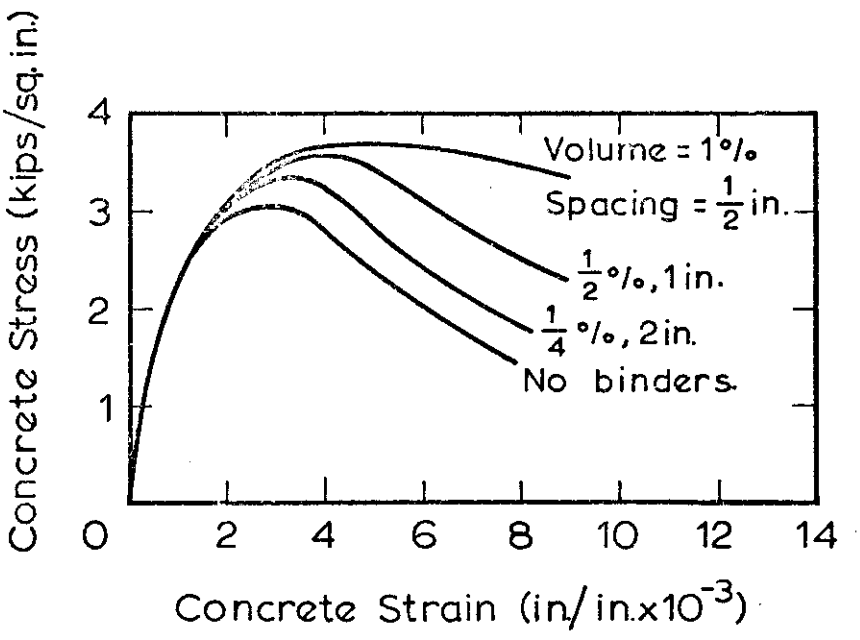

FIG. 3·11 THE EFFECT OF BINDER SPACING FOR COMPRESSION TESTS ON 10x2x2 IN. PRISMS WITH A CONSTANT BINDER SIZE. (SHAH AND VIJAY RANGAN)

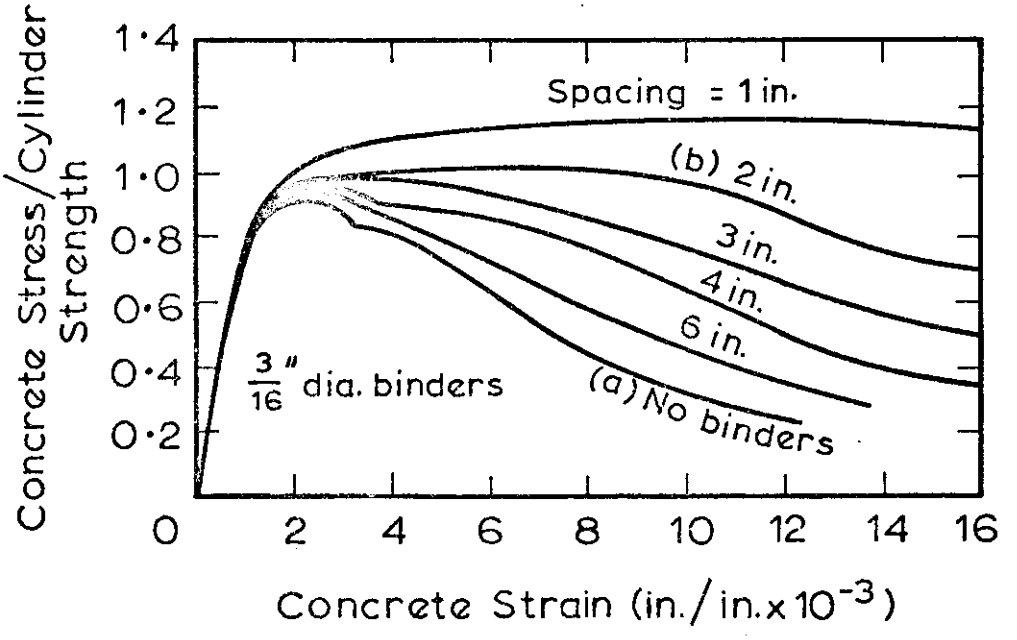

FIG. 3·12 THE EFFECT OF BINDER SPACING FOR FLEXURAL TESTS ON 6x4 IN. PRISMS WITH A CONSTANT BINDER SIZE, (SOLIMAN)

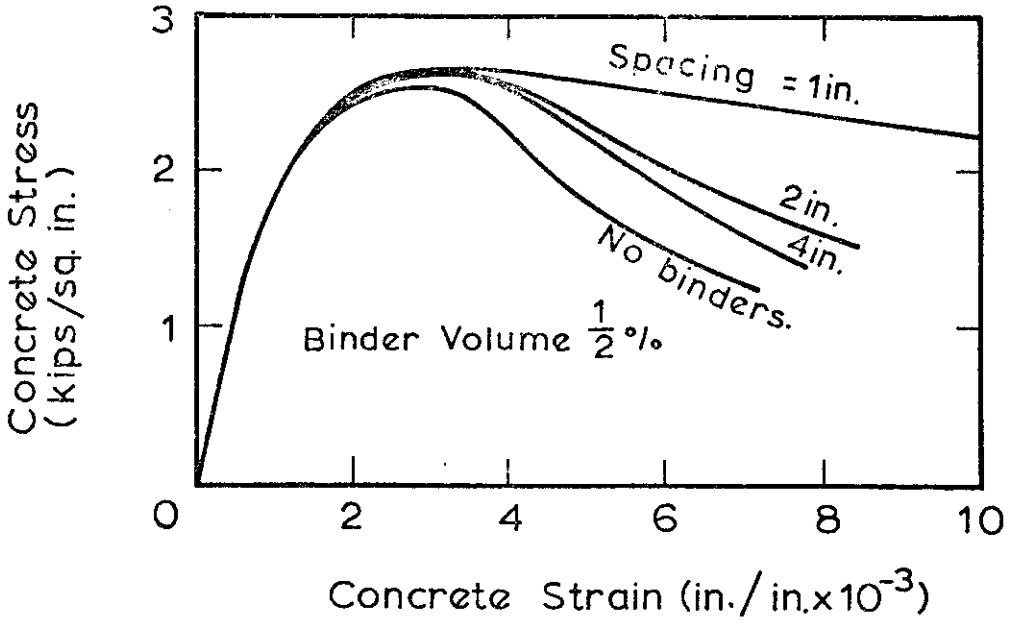

FIG.3·13 THE EFFECT OF BINDER SPACING FOR COMPRESSION TESTS ON 10x2x2 IN PRISMS WITH A CONSTANT BINDER VOLUME (SHAH AND VIJAY RANGAN)

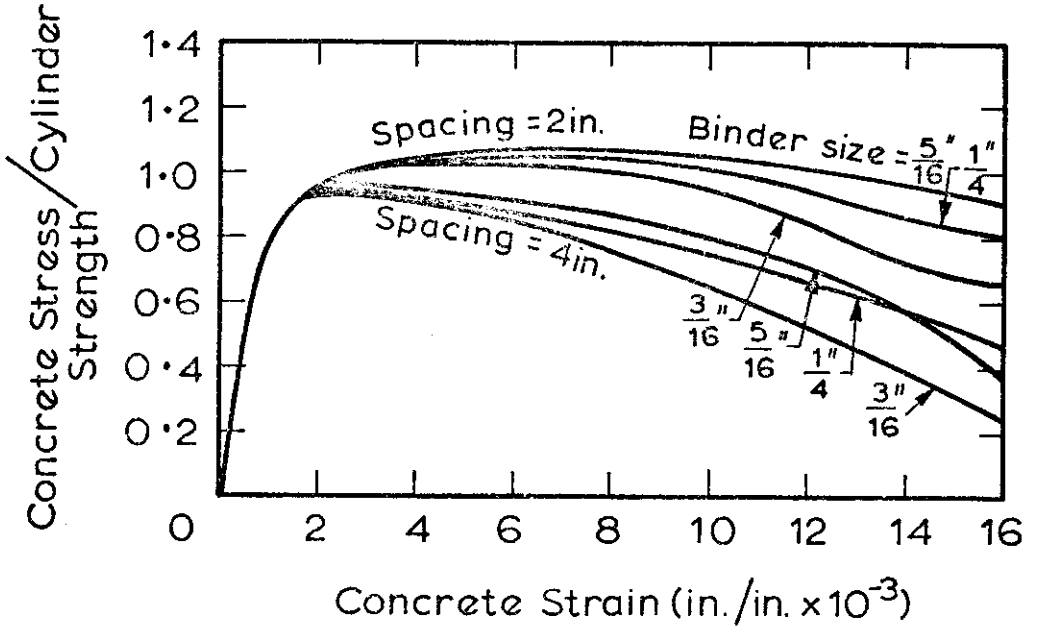

FIG.3·14 THE EFFECT OF BINDER SIZE FOR FLEXURAL TESTS ON 6x4 IN. PRISMS WITH A CONSTANT BINDER SPACING. (SOLIMAN)

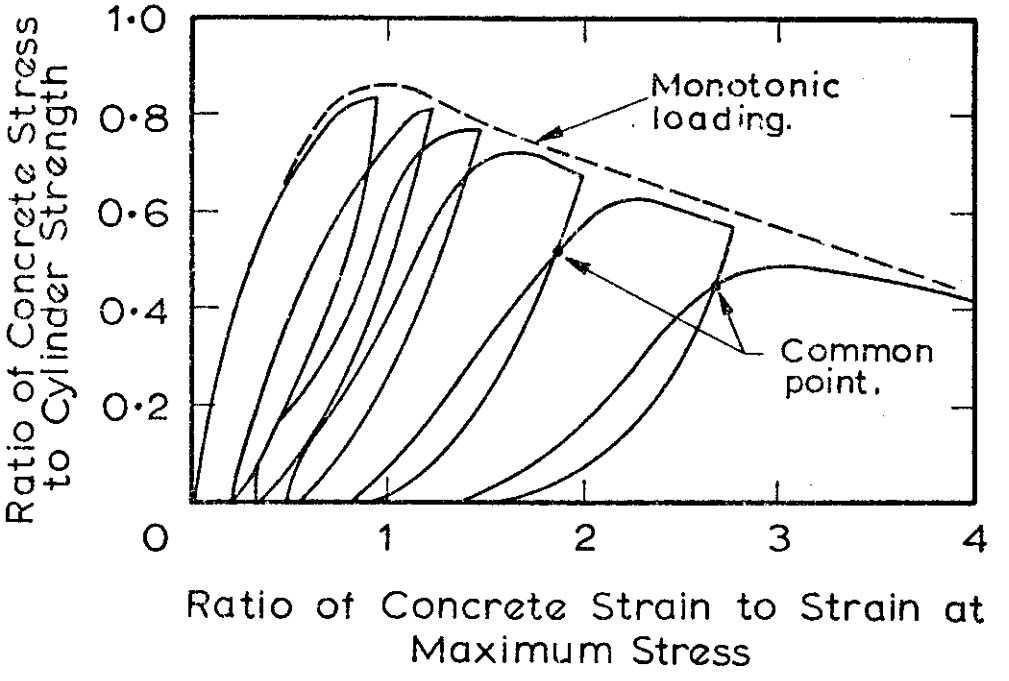

FIG. 3·15 CYCLIC LOADING IN CONCENTRIC COMPRESSION ON 5 x 3 IN. CONCRETE PRISIMS. (KARSAN & JIRSA)

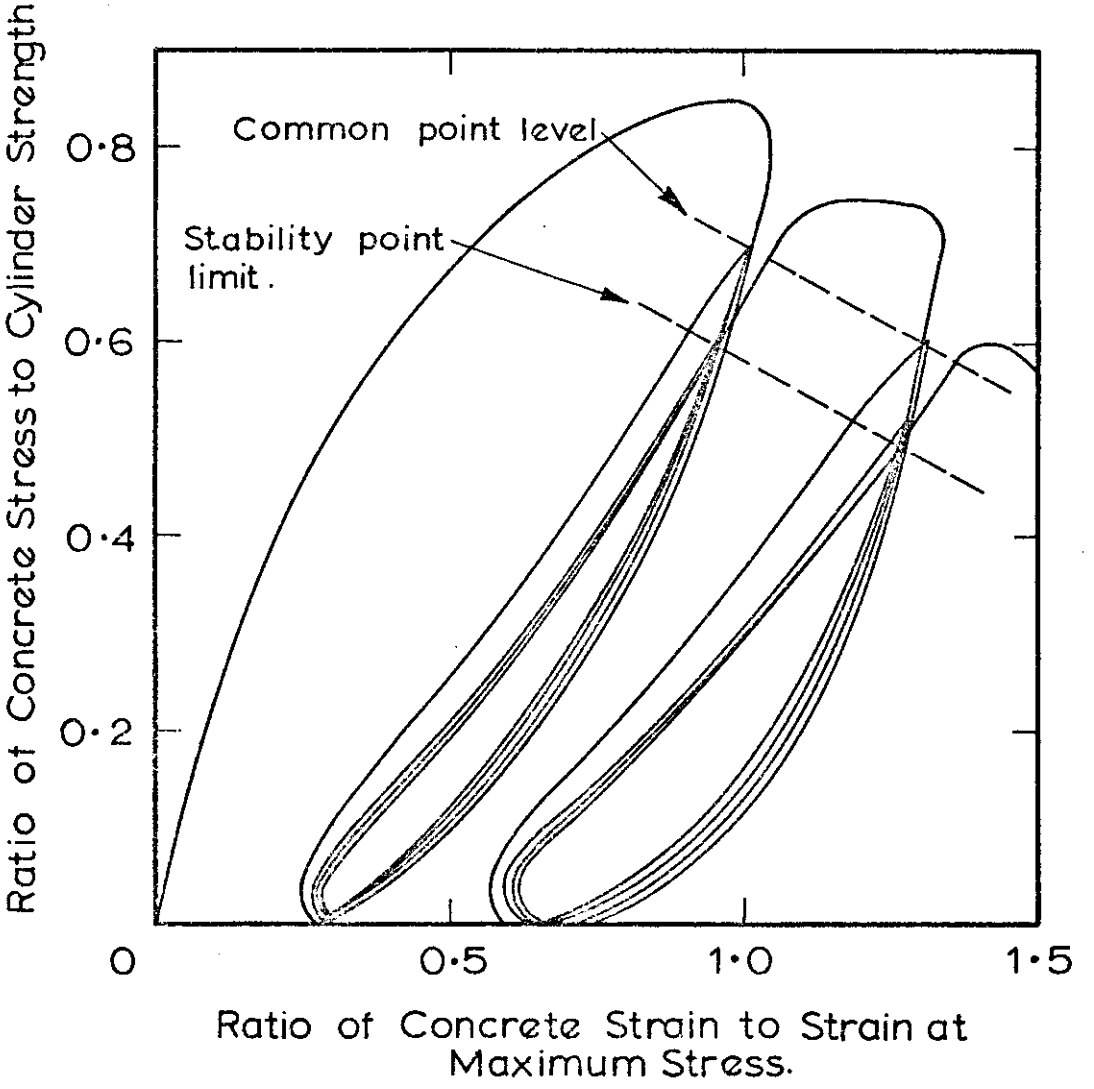

FIG. 3·16 CYCLIC LOADING UNTIL STRAINS STABILIZE (KARSAN & JIRSA)

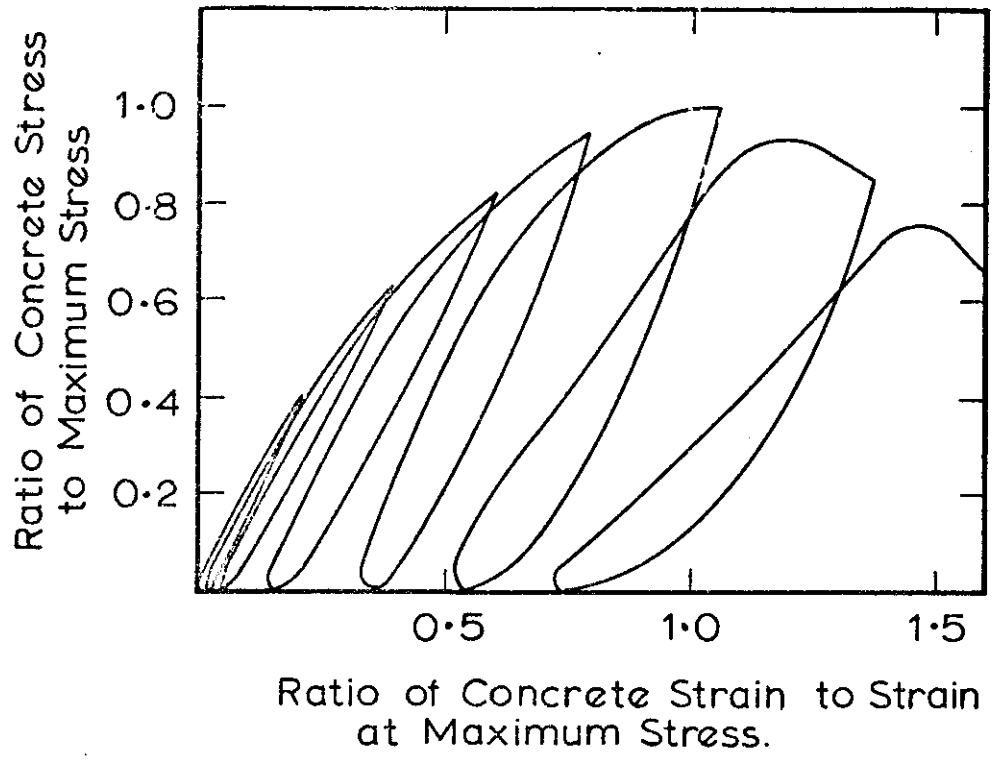

FIG. 3·17 TYPICAL CONCRETE UNLOADING CURVES FOR A RANGE OF STRESS LEVELS.

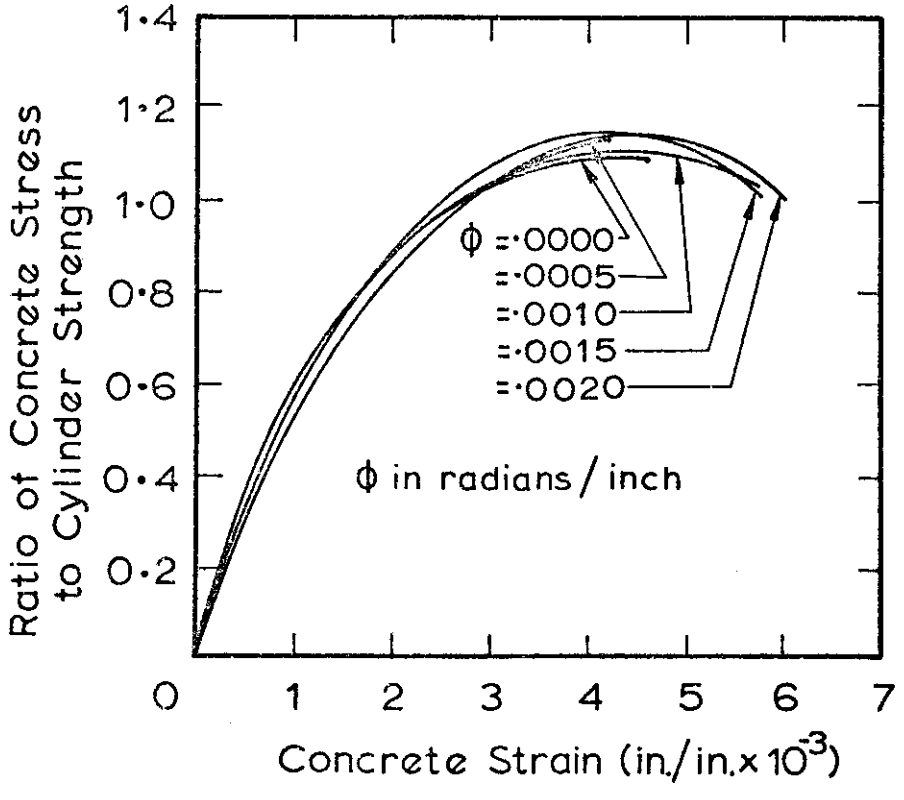

FIG. 3·18 STRESS-STRAIN CURVES FOR 2x2 IN. CONCRETE PRISMS SUBJECTED TO VARIOUS STRAIN GRADIENTS, ϕ. (CLARK ET AL.)

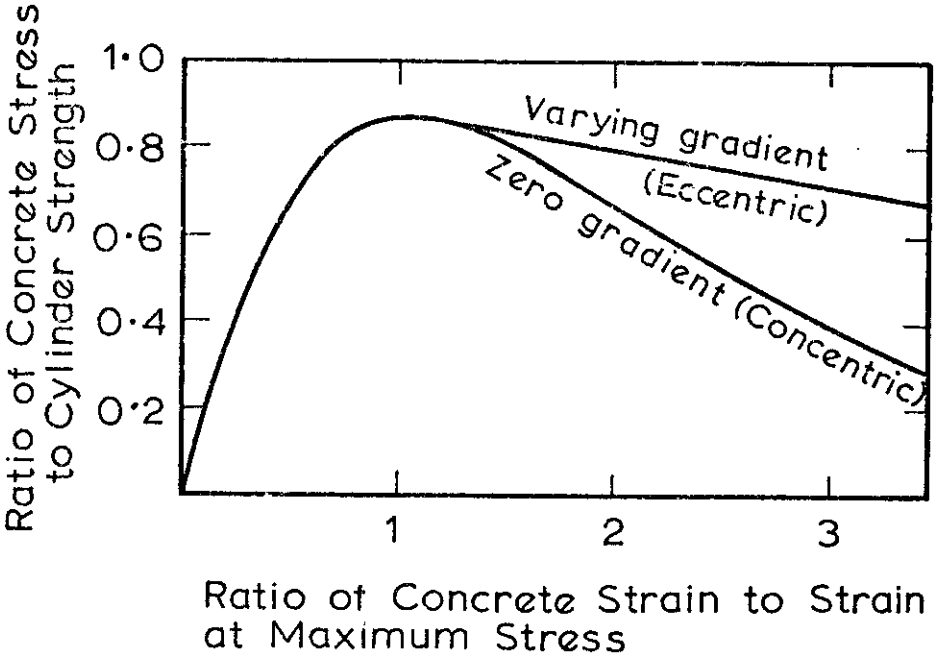

FIG.3·19 STRESS-STRAIN CURVES FOR 5x3 IN. PRISMS UNDER CONCENTRIC & ECCENTRIC LOADING. (KARSAN & JIRSA)

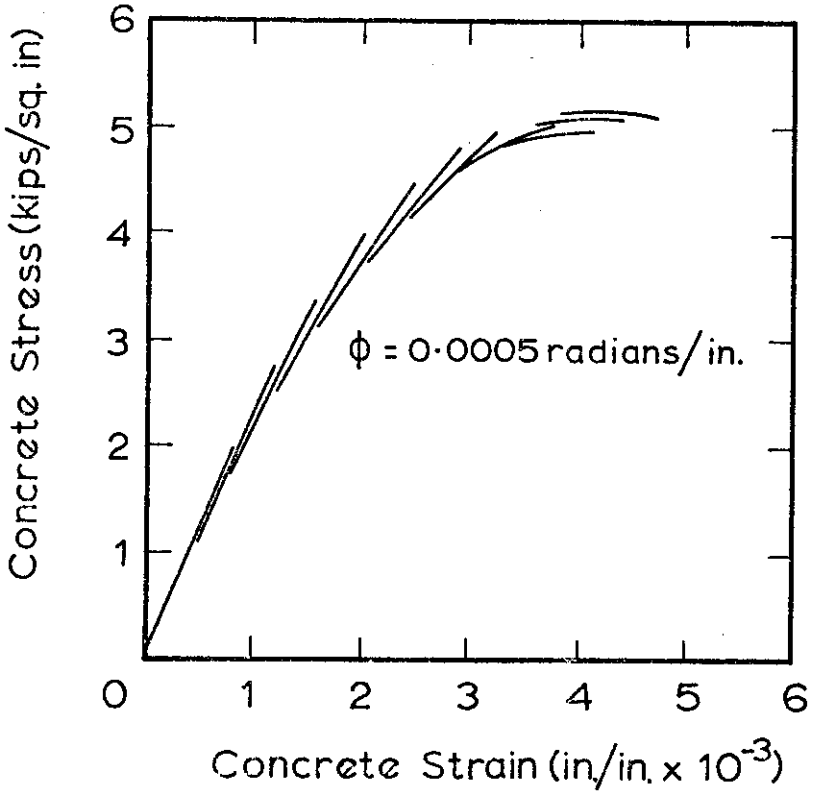

FIG.3·20 STRESS-STRAIN CURVE OF PARABOLIC SEGMENTS. SPECIMEN UNDER A CONSTANT STRAIN GRADIENT. (CLARK ET. AL)

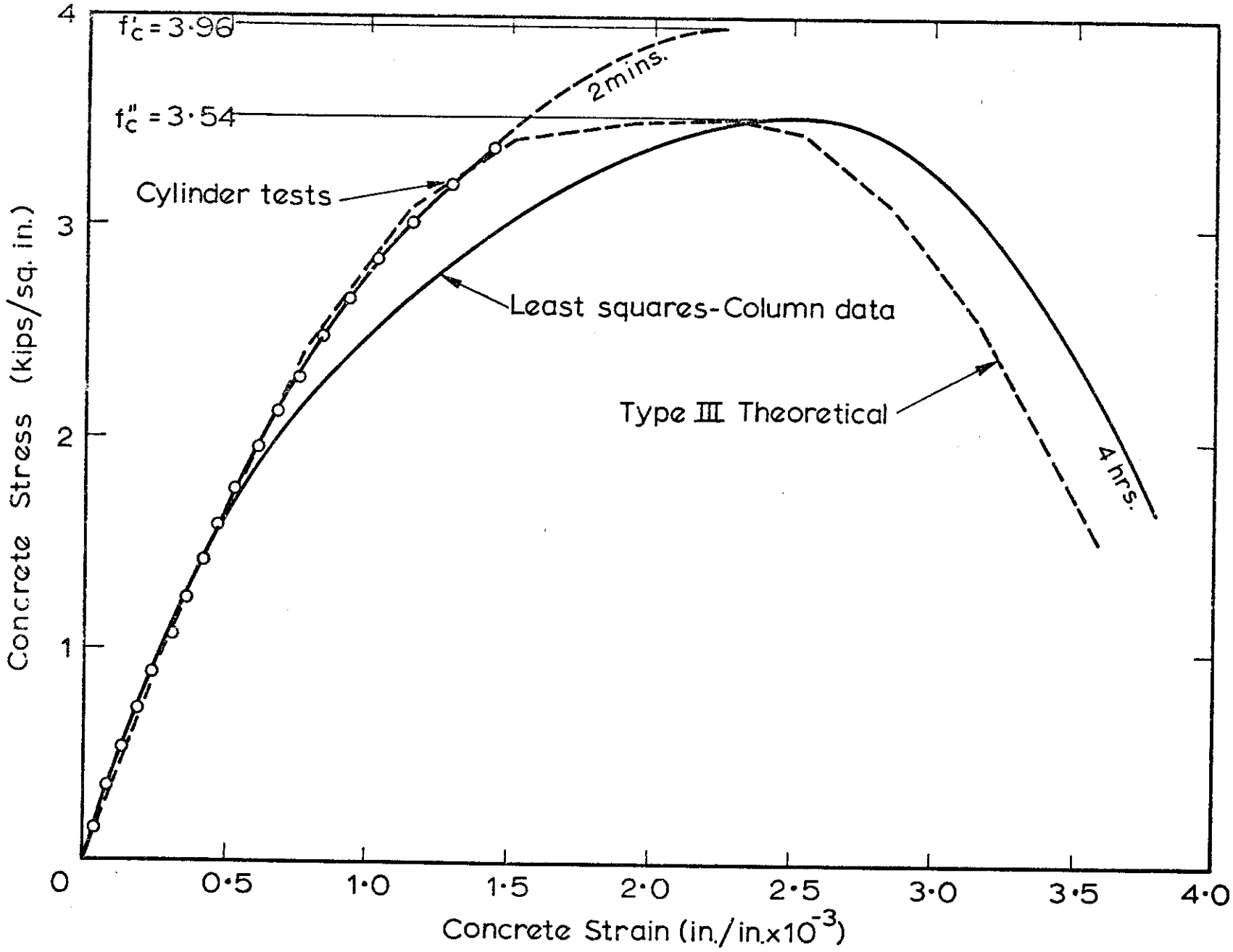

FIG. 3·21 CONCRETE STRESS-STRAIN CURVES FOR COLUMN CC1

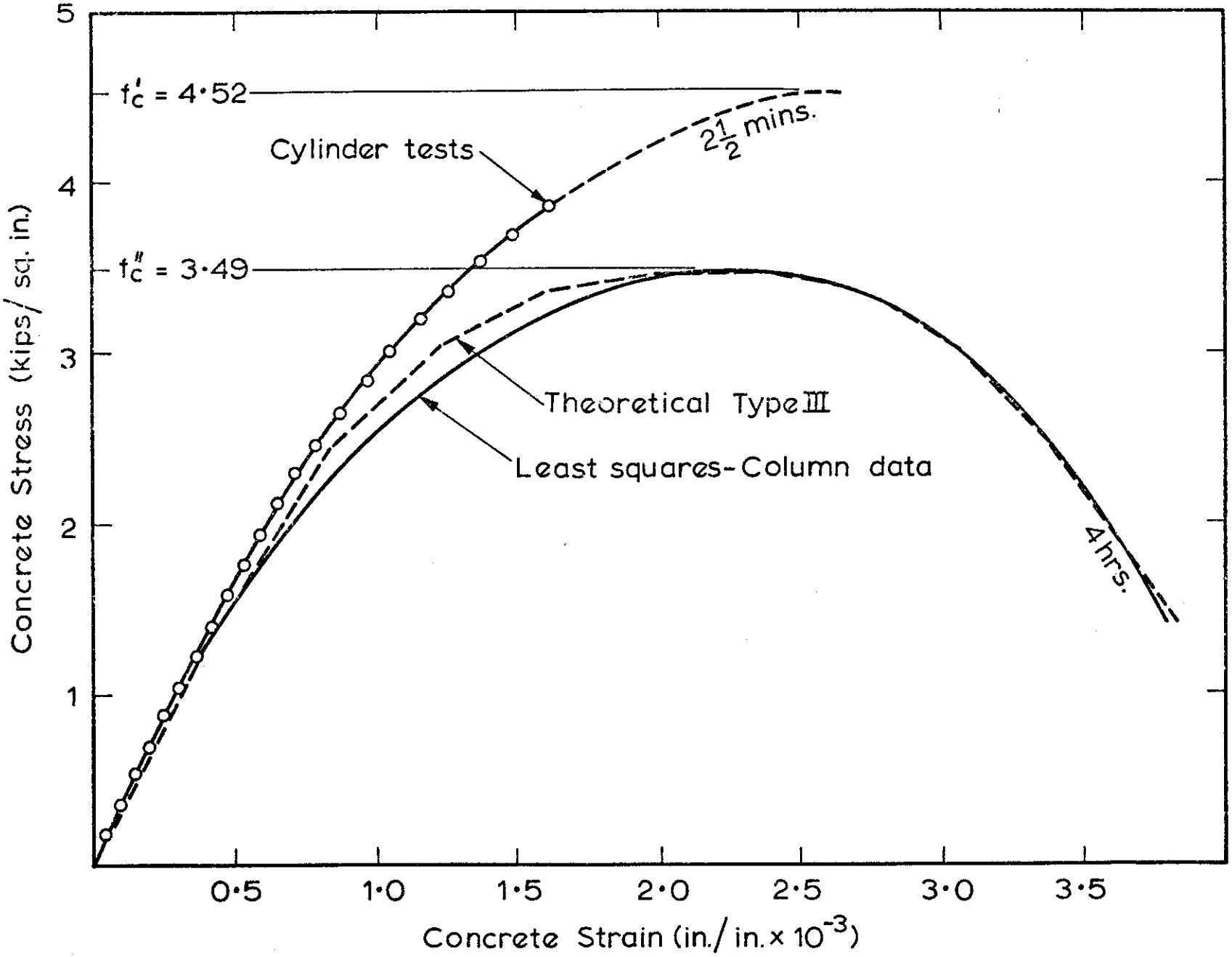

FIG. 3·22 CONCRETE STRESS-STRAIN CURVES FOR COLUMN CC2

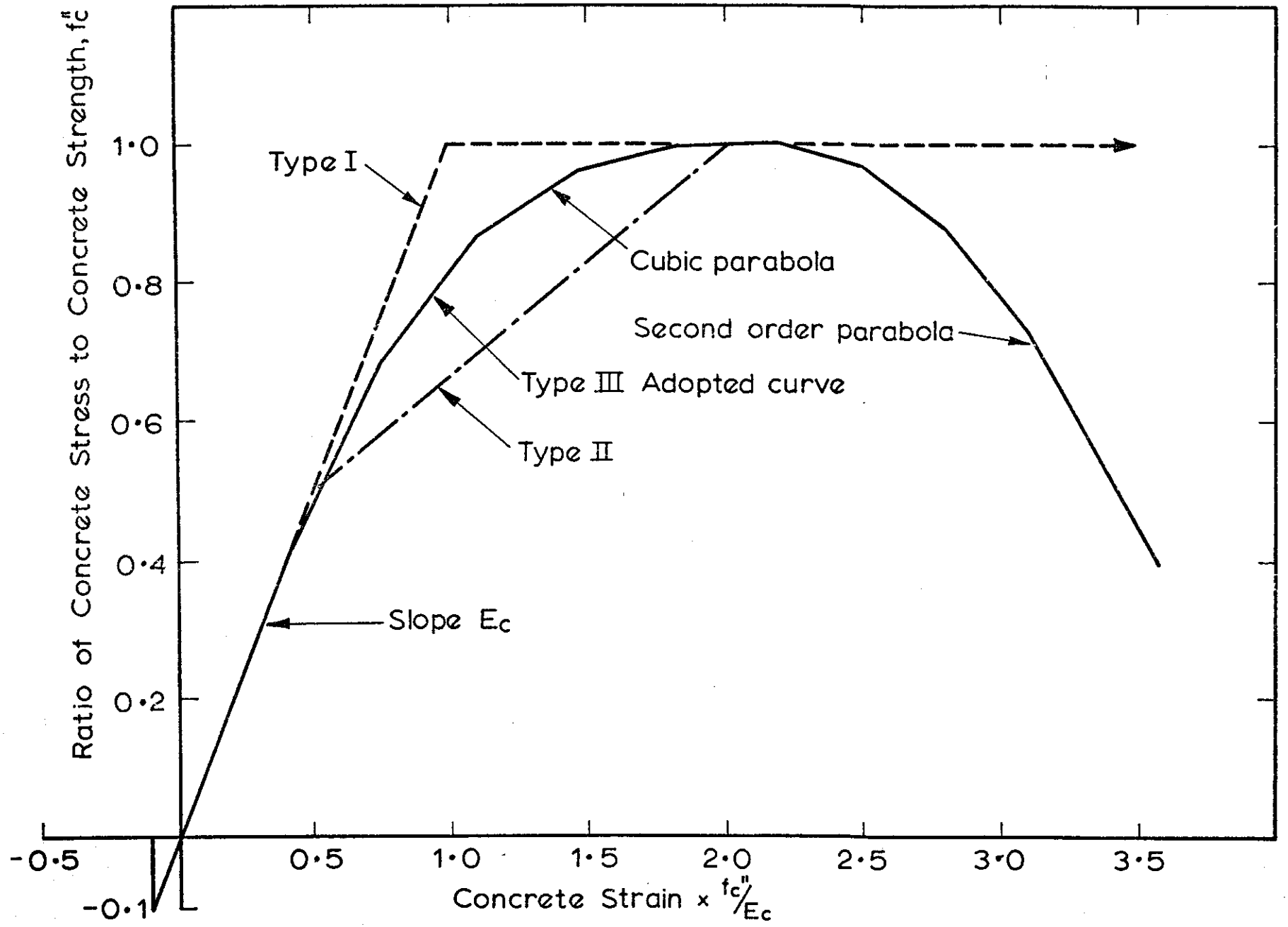

FIG. 3·23 THEORETICAL CONCRETE STRESS-STRAIN CURVES FOR SHORT TERM LOADING

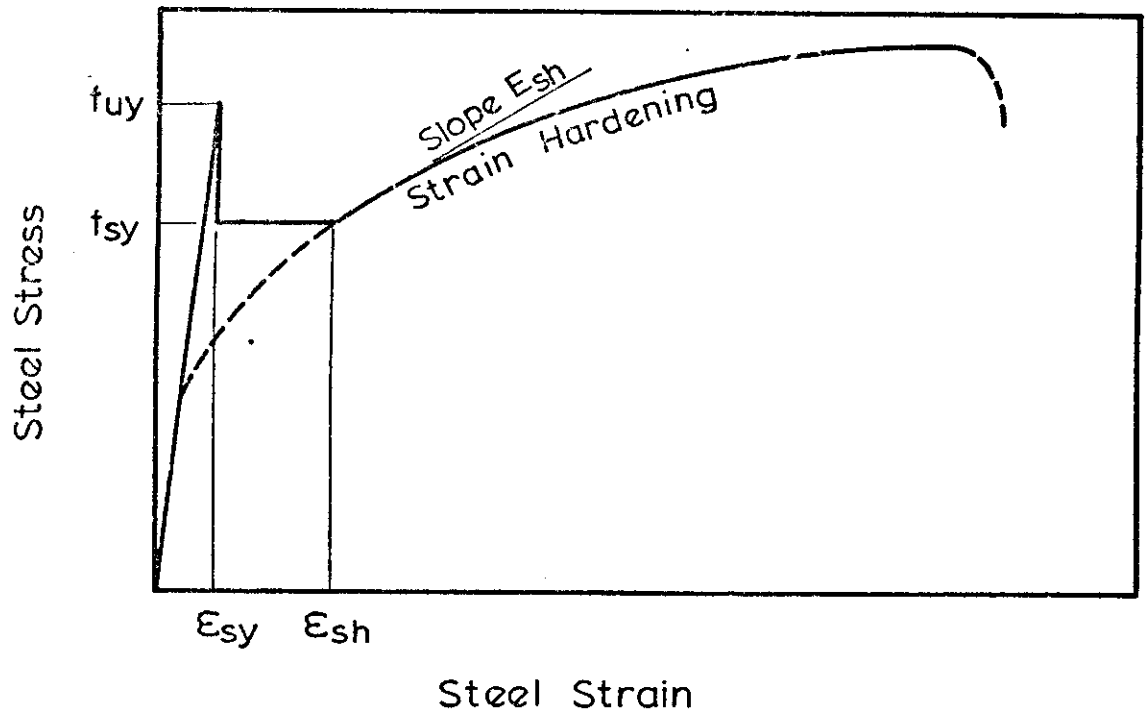

FIG. 3·24 DIAGRAMMATIC STRESS-STRAIN CURVE FOR MILD STEEL

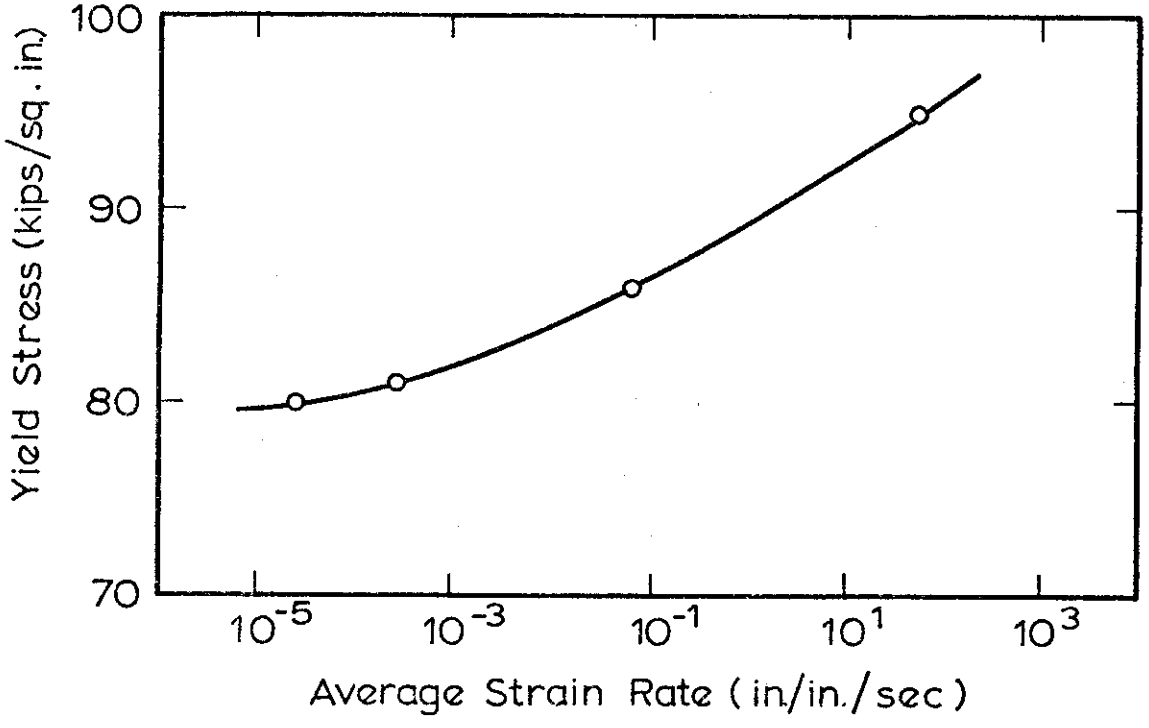

FIG. 3·25 EFFECT OF STRAIN RATE ON YIELD STRESS FOR COLD-ROLLED 1018 STEEL (STEIDEL & MAKEROV)

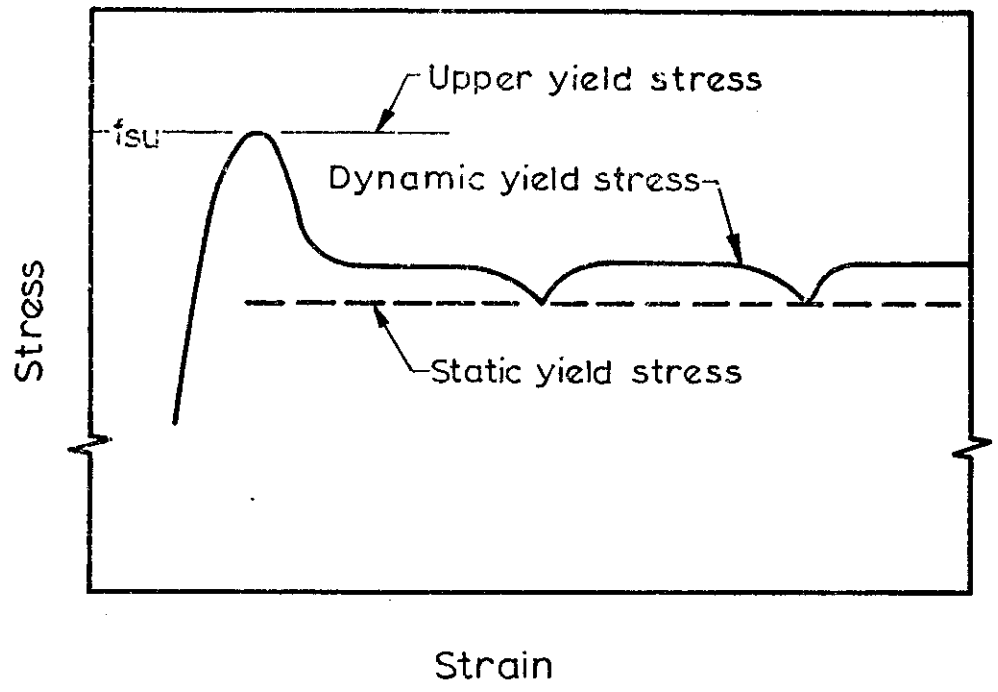

FIG. 3·26 DIAGRAMMATIC YIELD PLATEAU FOR MILD STEEL

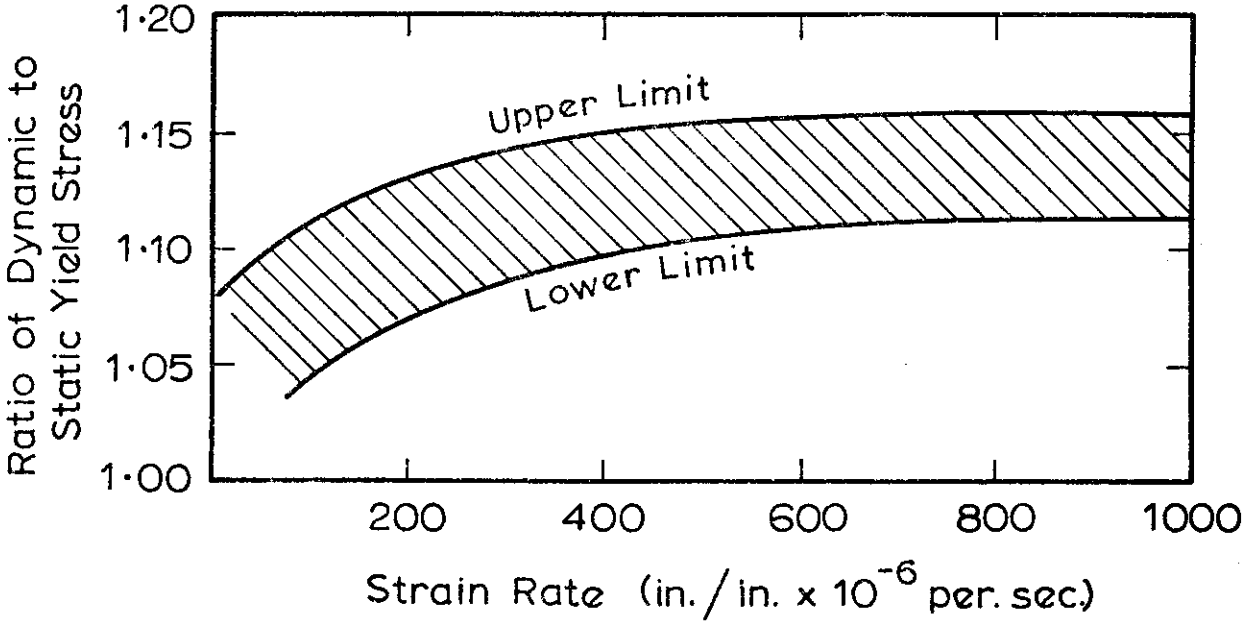

FIG. 3·27 RELATION BETWEEN DYNAMIC & STATIC YIELD STRESSES & STRAIN RATE.

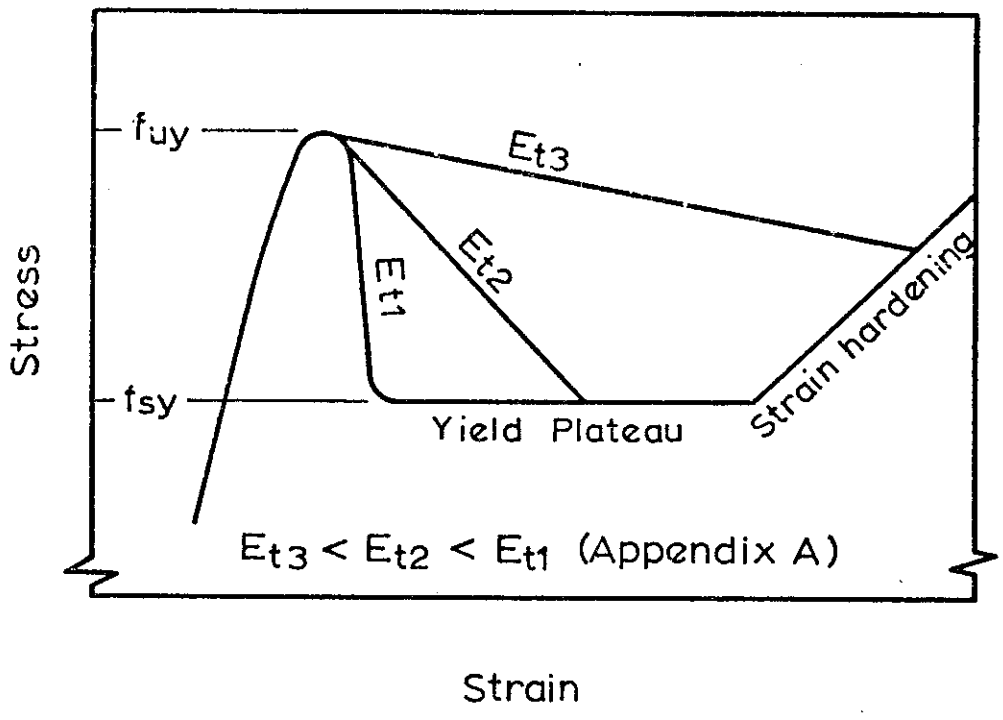

FIG. 3·28 THE EFFECT OF TEST STIFFNESS ON YIELD BEHAVIOUR OF STEEL.

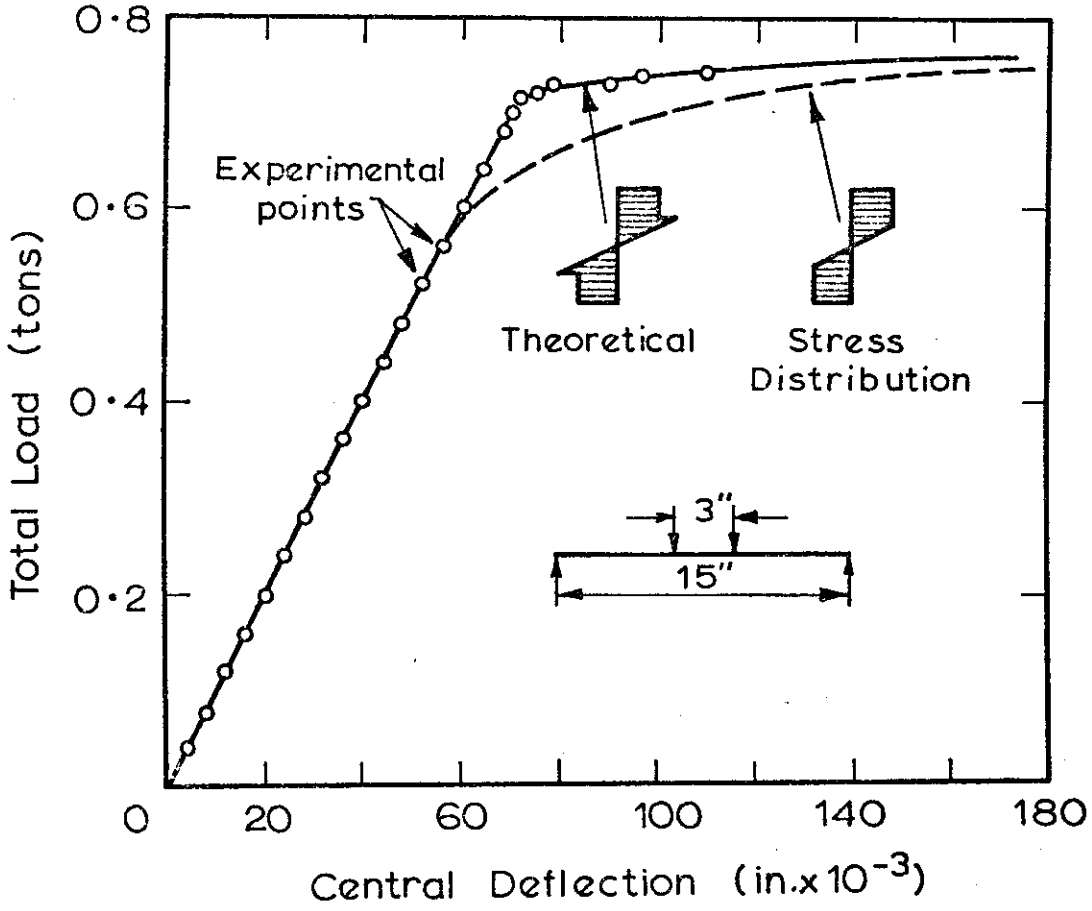

FIG. 3·29 LOAD-DEFLECTION CURVES FOR TESTS ON 7/8 x 7/8 IN. NORMALIZED STEEL BEAMS (RODERICK)

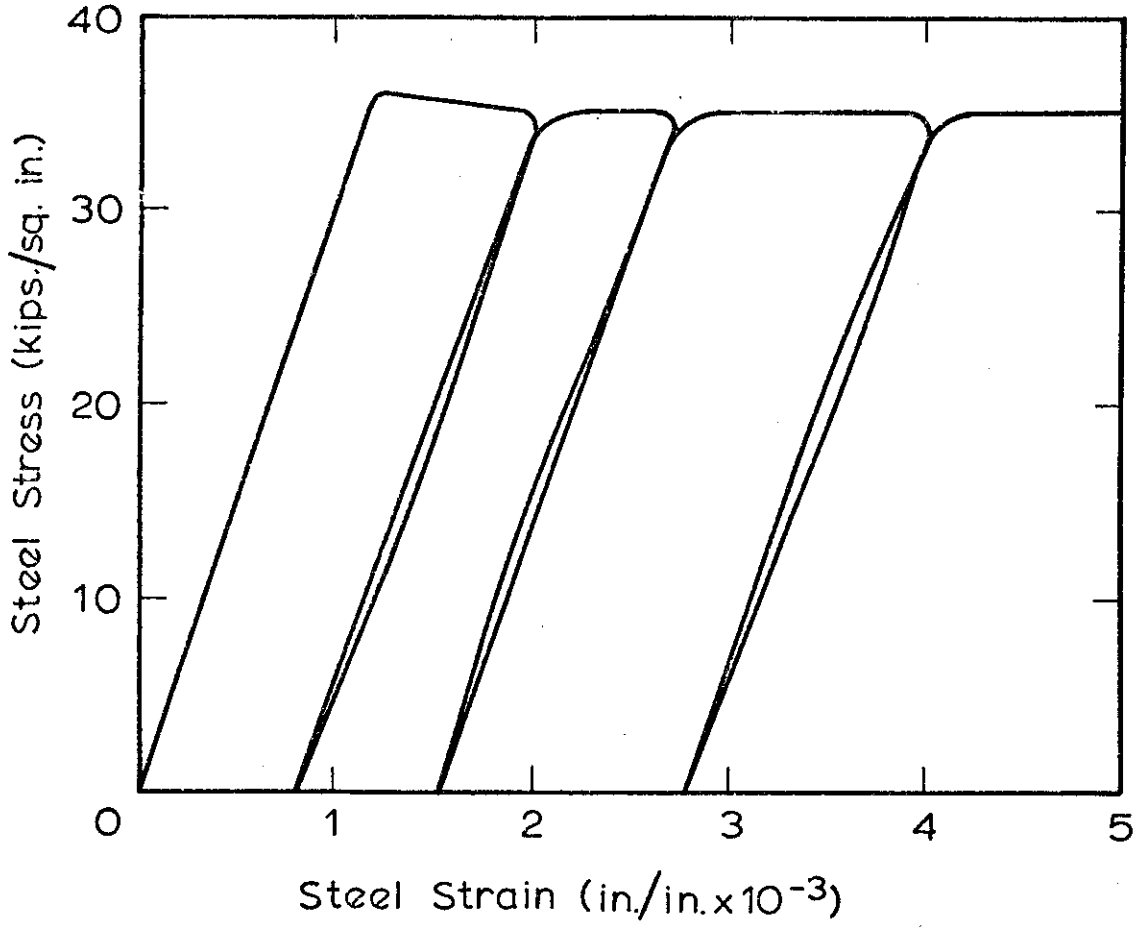

FIG. 3·30 LOADING AND UNLOADING CURVES FOR MILD STEEL (DALBY).

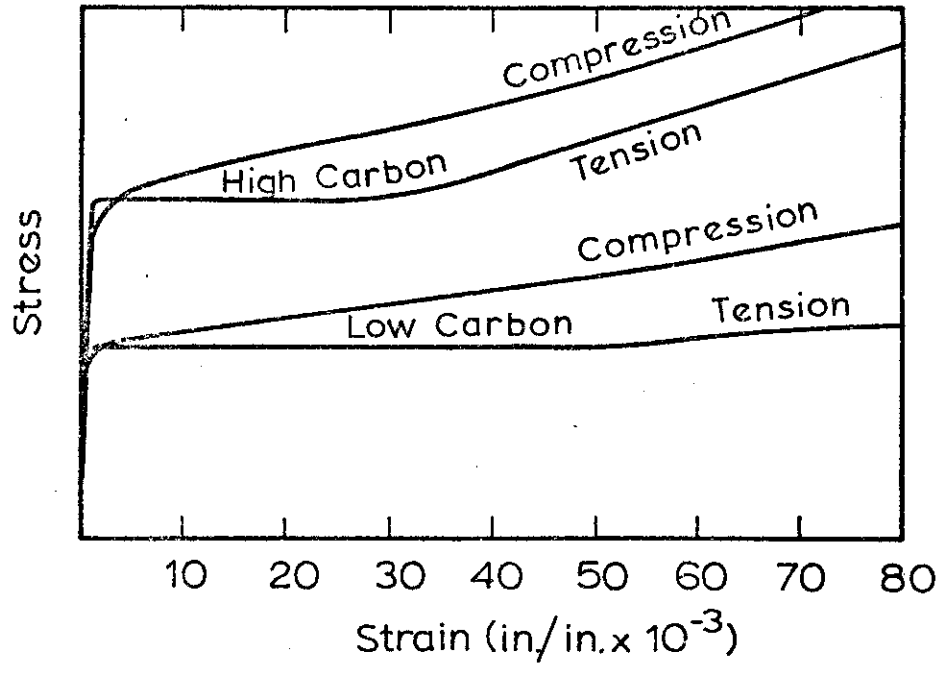

FIG. 3·31 STRESS-STRAIN CURVES FOR NORMALIZED STEEL SPECIMENS UNDER UNIAXIAL TENSION AND COMPRESSION (LIKHAREV)

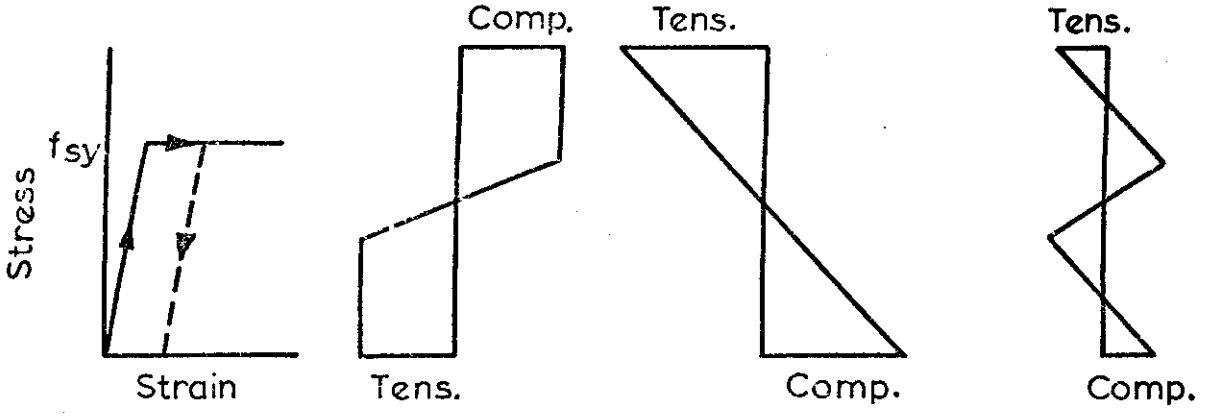

FIG. 3·32 RESIDUAL STRESS DEVELOPMENT FOR A PLASTICALLY BENT BEAM.

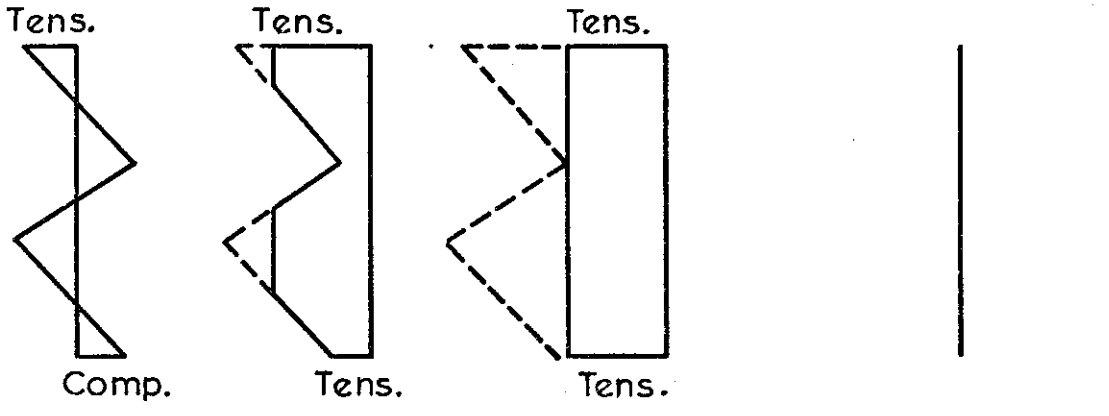

FIG. 3·33 REMOVAL OF RESIDUAL STRESS BY UNIFORM TENSILE EXTENSION.

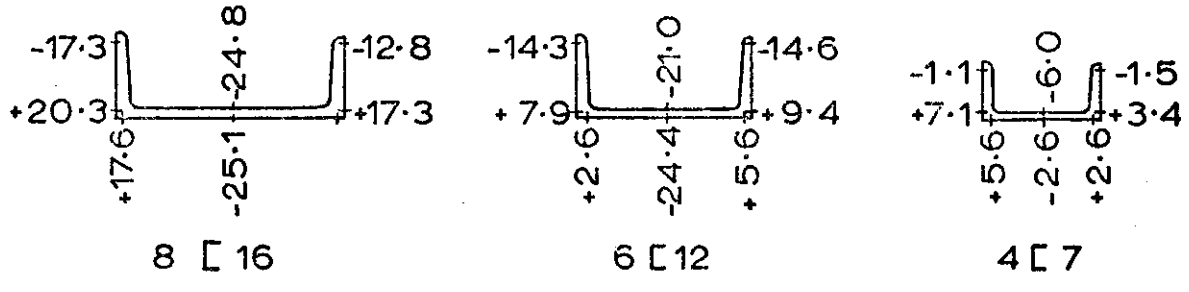

Stresses in kips/sq. in. Tensile Stresses +ve

FIG. 3·34 MEASURED RESIDUAL STRESSES FOR CHANNEL SECTIONS (O'CONNOR).

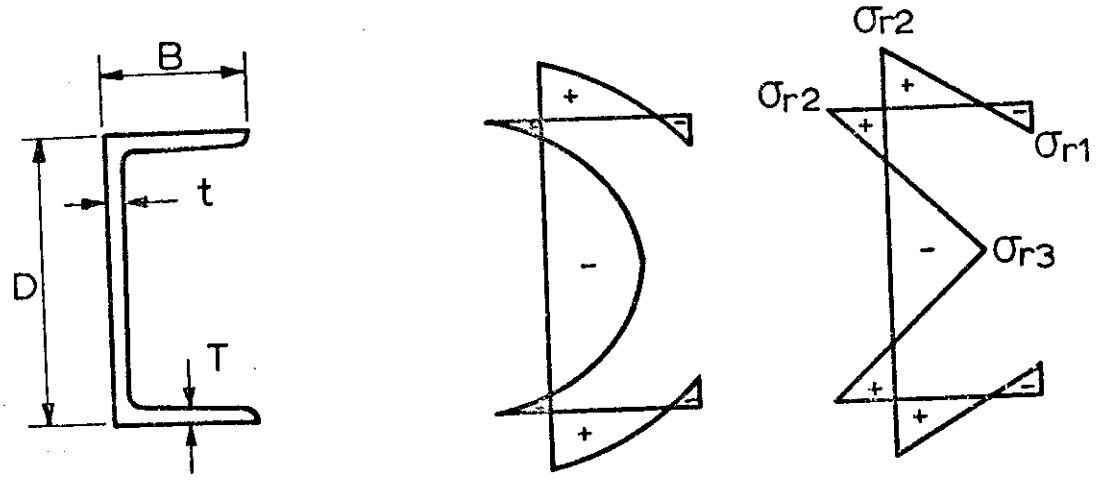

FIG. 3·35 RESIDUAL STRESS DISTRIBUTIONS FOR CHANNEL SECTIONS (TENSILE STRESSES +ve).

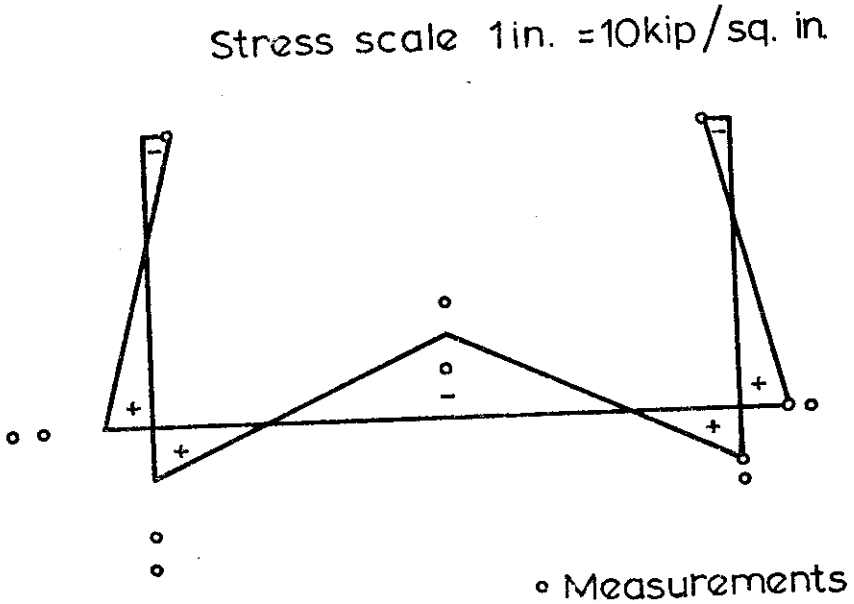

FIG. 3·36 COMPARISON OF THE THEORETICAL STRESS DISTRIBUTION WITH VALUES MEASURED BY O'CONNOR

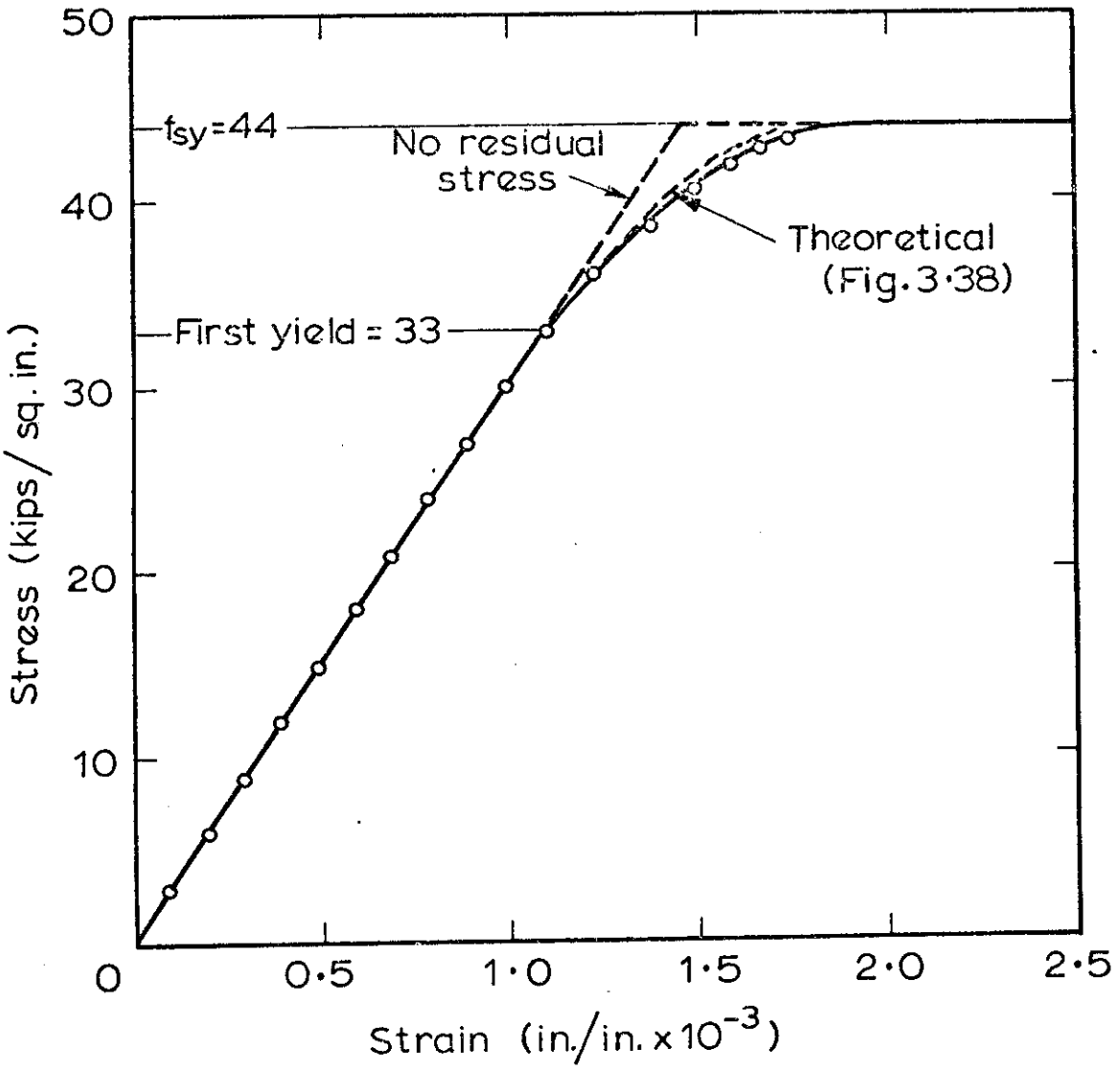

FIG. 3·37 STRESS-STRAIN CURVE FROM STUB COLUMN TEST FOR COLUMN CC1 SHOWING RESIDUAL STRESS EFFECT.

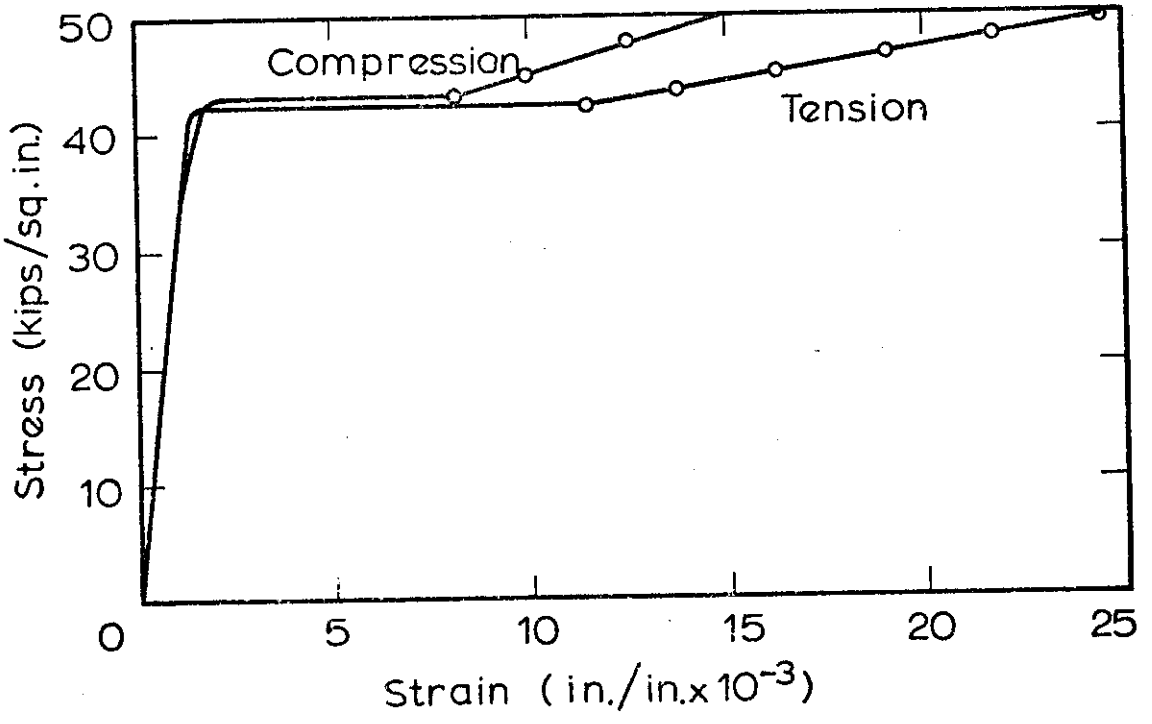

FIG. 3·38 COMPARISON OF STUB COLUMN AND TENSION TEST COUPON RESULTS FOR COLUMN CC1.

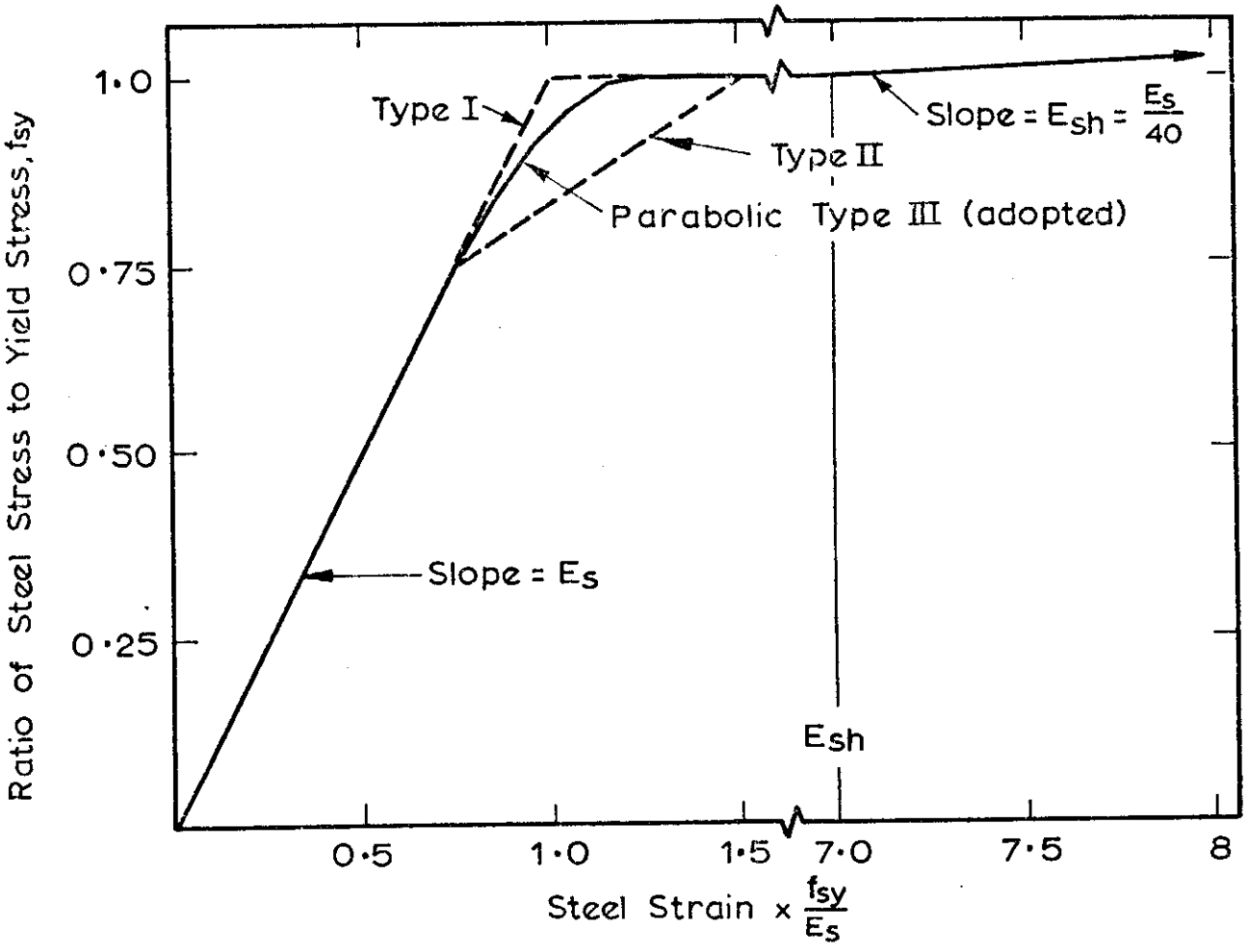

FIG·3·39 THEORETICAL AVERAGE STRESS-STRAIN CURVE FOR MILD STEEL.

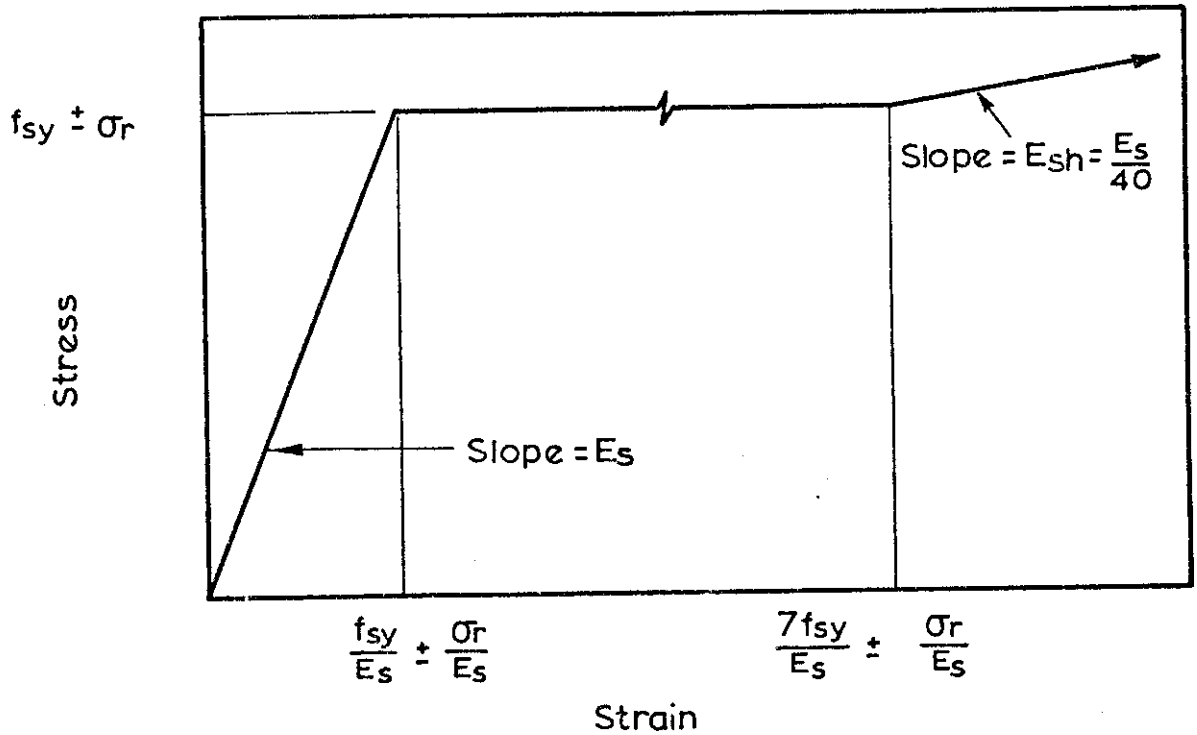

FIG. 3·40 STRESS - STRAIN CURVE FOR STEEL ELEMENT CONTAINING A UNIFORM RESIDUAL STRESS σr

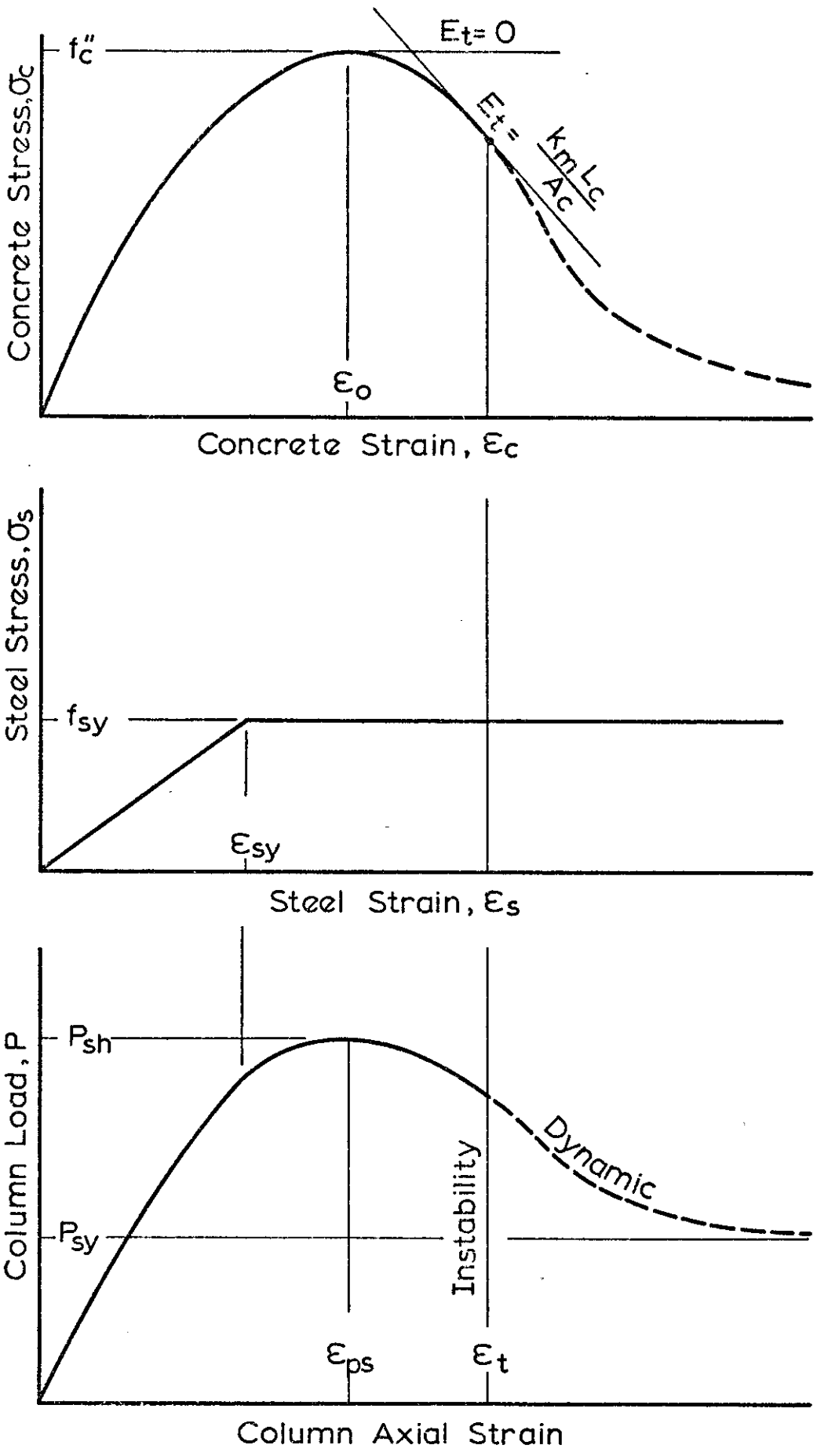

FIG. 4·1 BEHAVIOUR OF A CONCENTRICALLY LOADED SHORT COMPOSITE COLUMN RELATED TO ITS MATERIAL PROPERTIES.

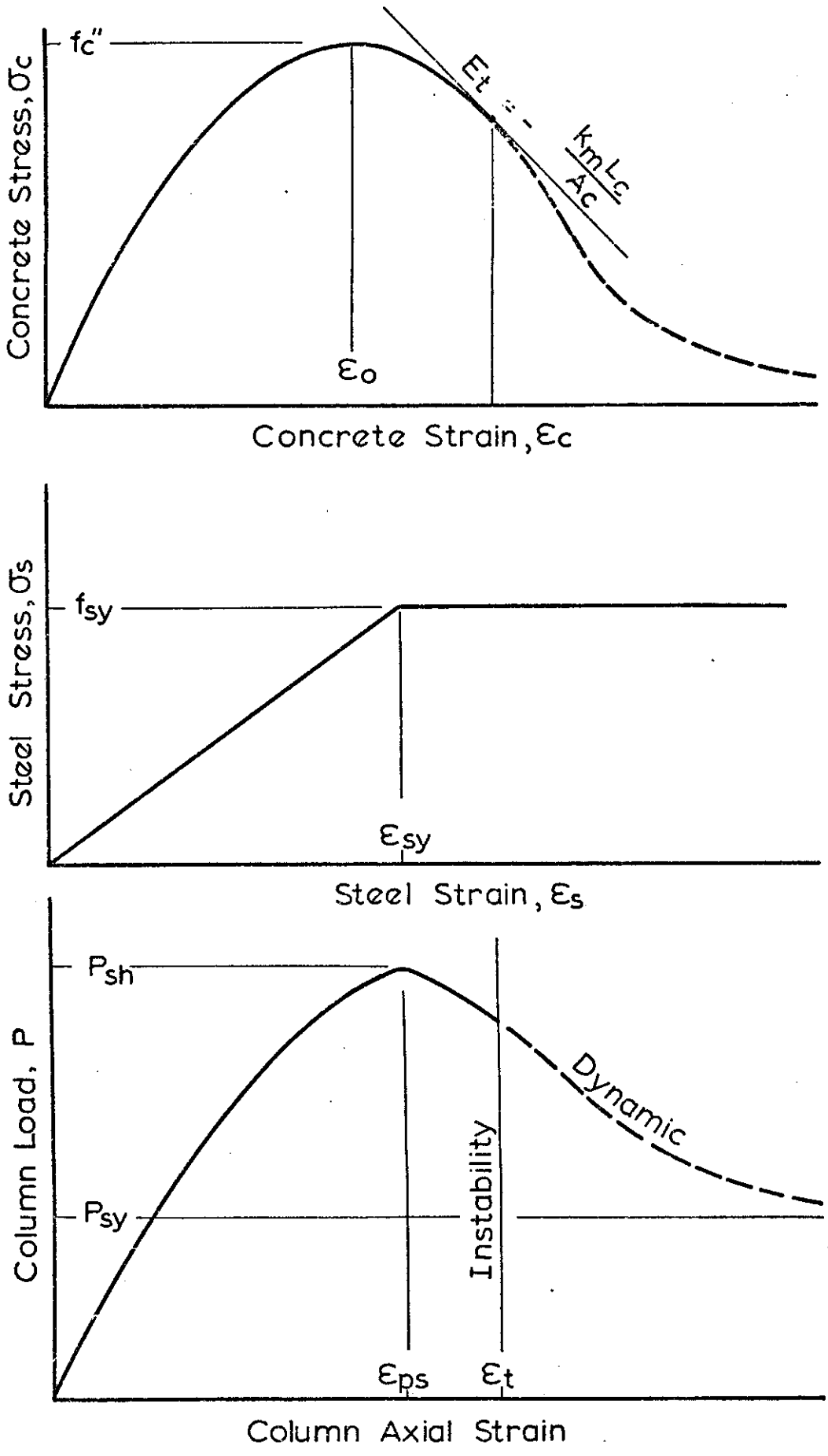

FIG.4·2 BEHAVIOUR OF A CONCENTRICALLY LOADED SHORT COMPOSITE COLUMN RELATED TO ITS MATERIAL PROPERTIES

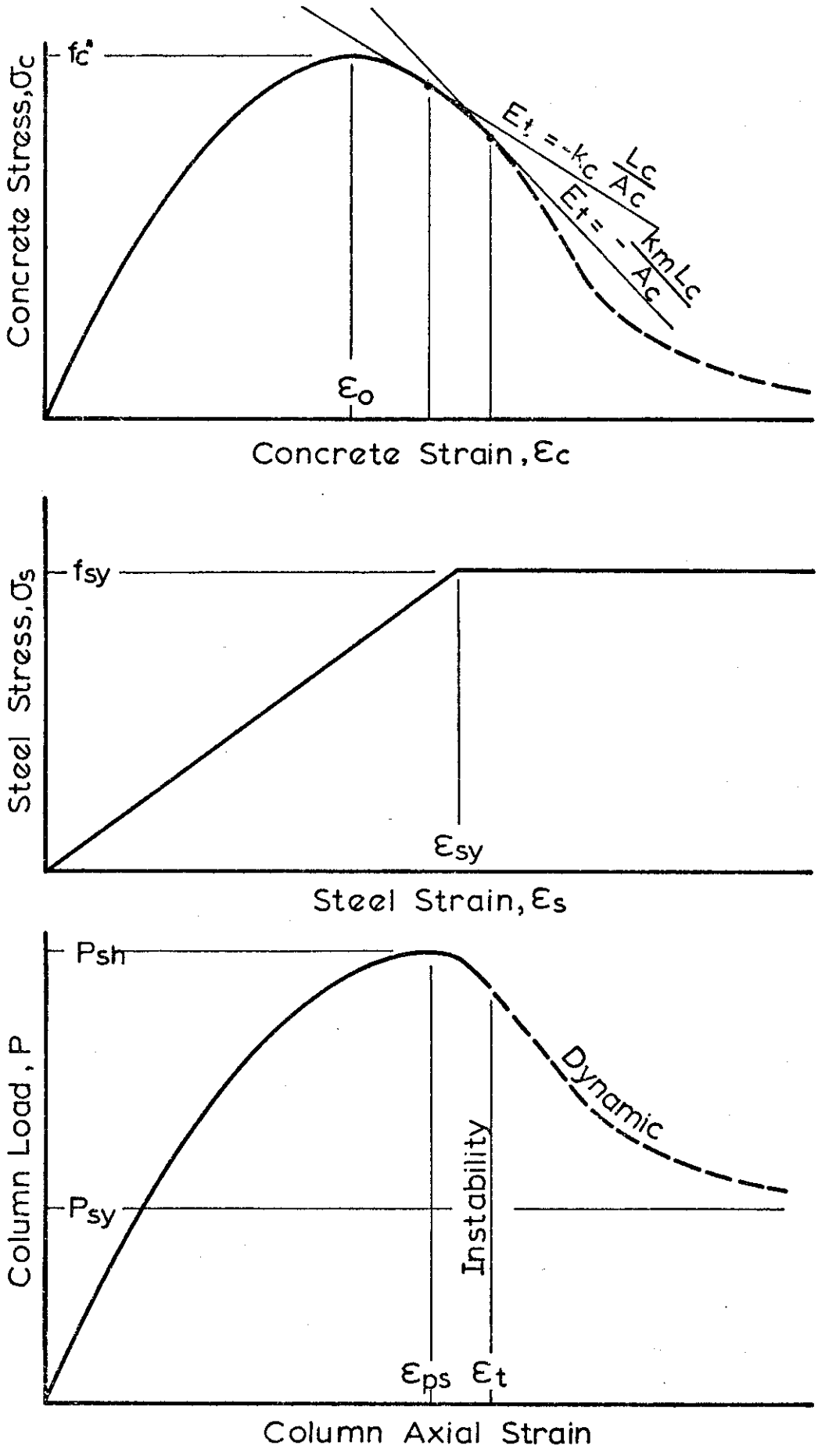

FIG. 4·3 BEHAVIOUR OF A CONCETRICALLY LOADED SHORT COMPOSITE COLUMN RELATED TO MATERIAL PROPERTIES.

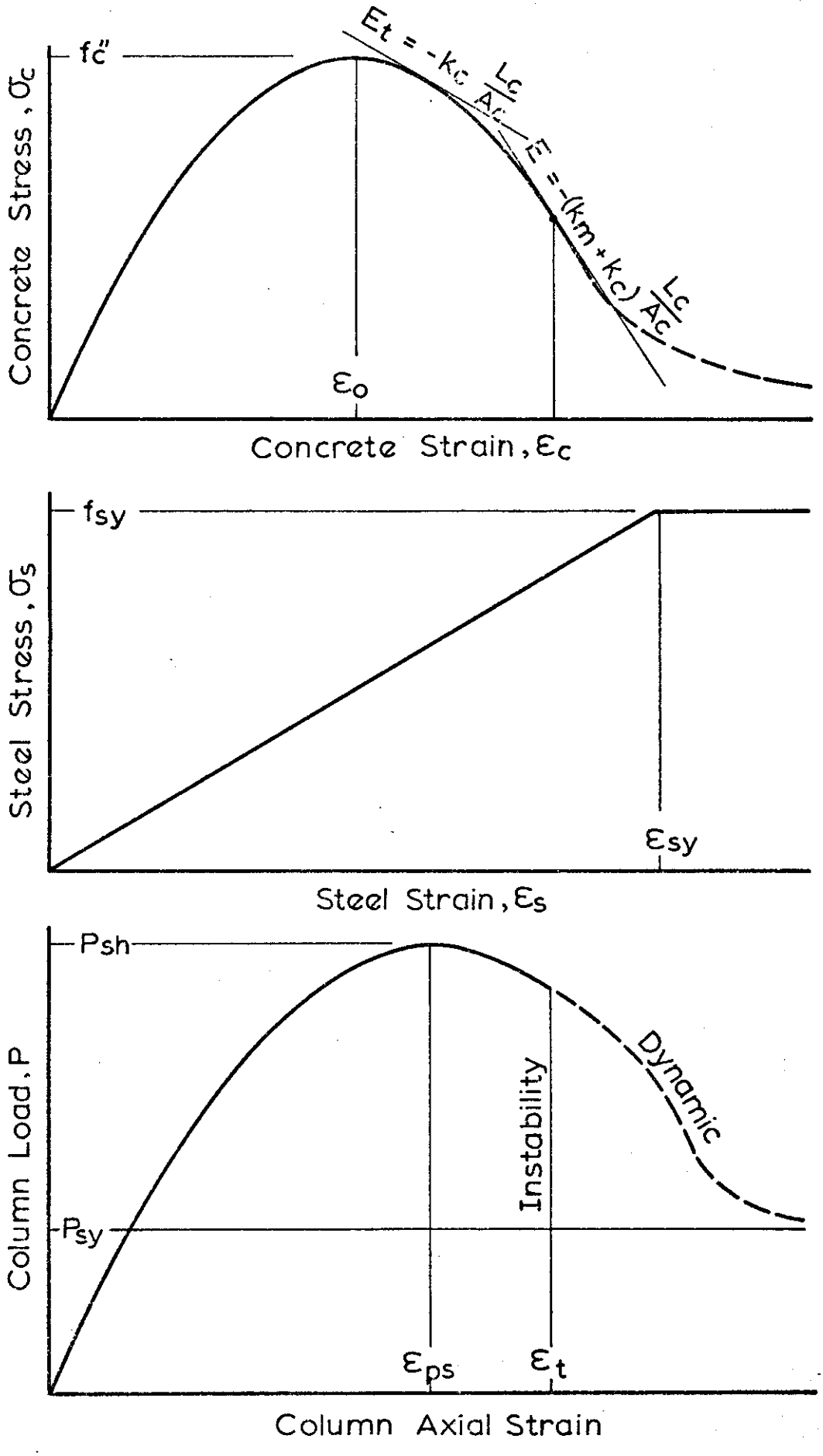

FIG. 4·4 BEHAVIOUR OF A CONCENTRICALLY LOADED SHORT COMPOSITE COLUMN RELATED TO ITS MATERIAL PROPERTIES

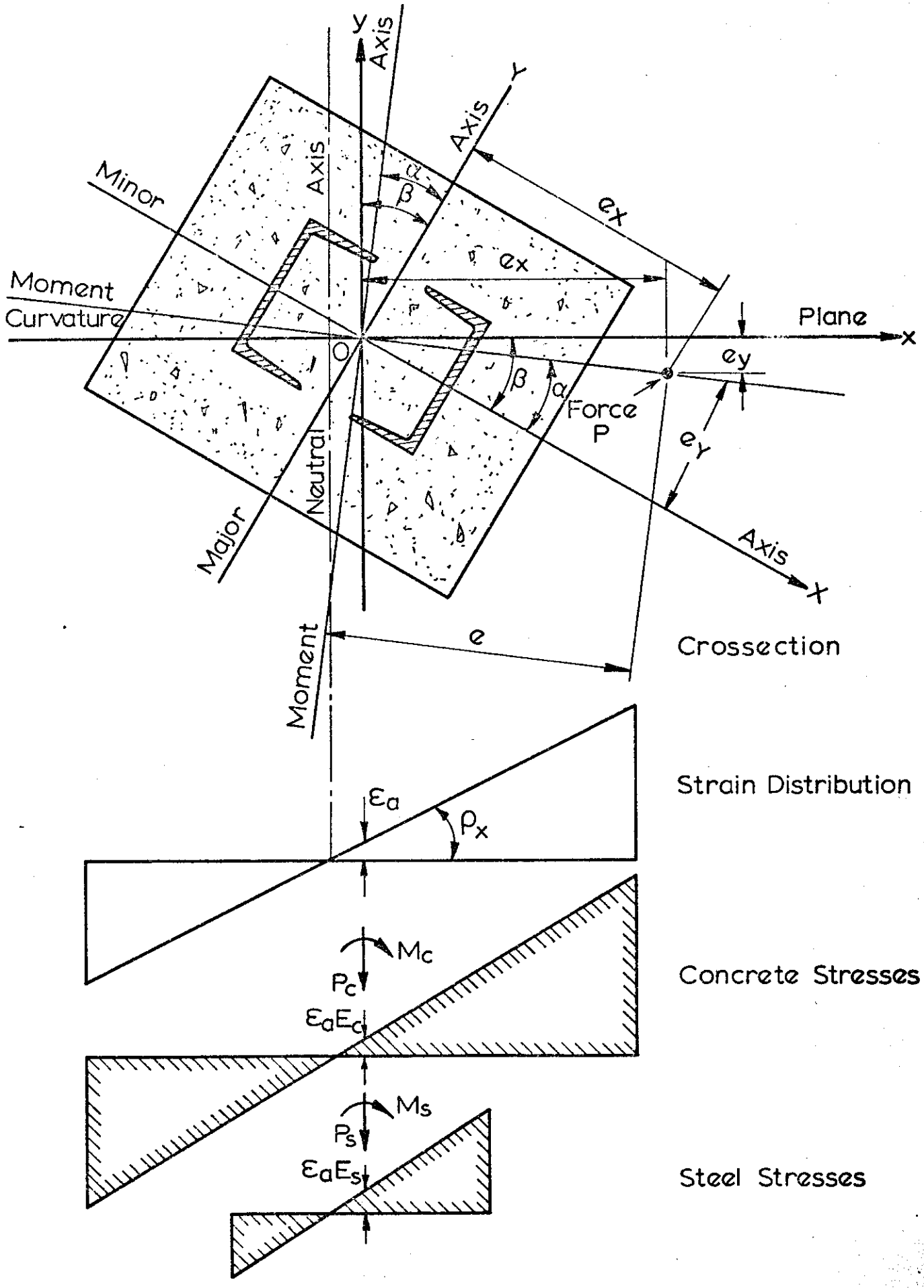

FIG. 4·5 STRESS DISTRIBUTION AT AN ELASTIC SECTION OF A COMPOSITE COLUMN BENT ABOUT BOTH PRINCIPAL AXES.

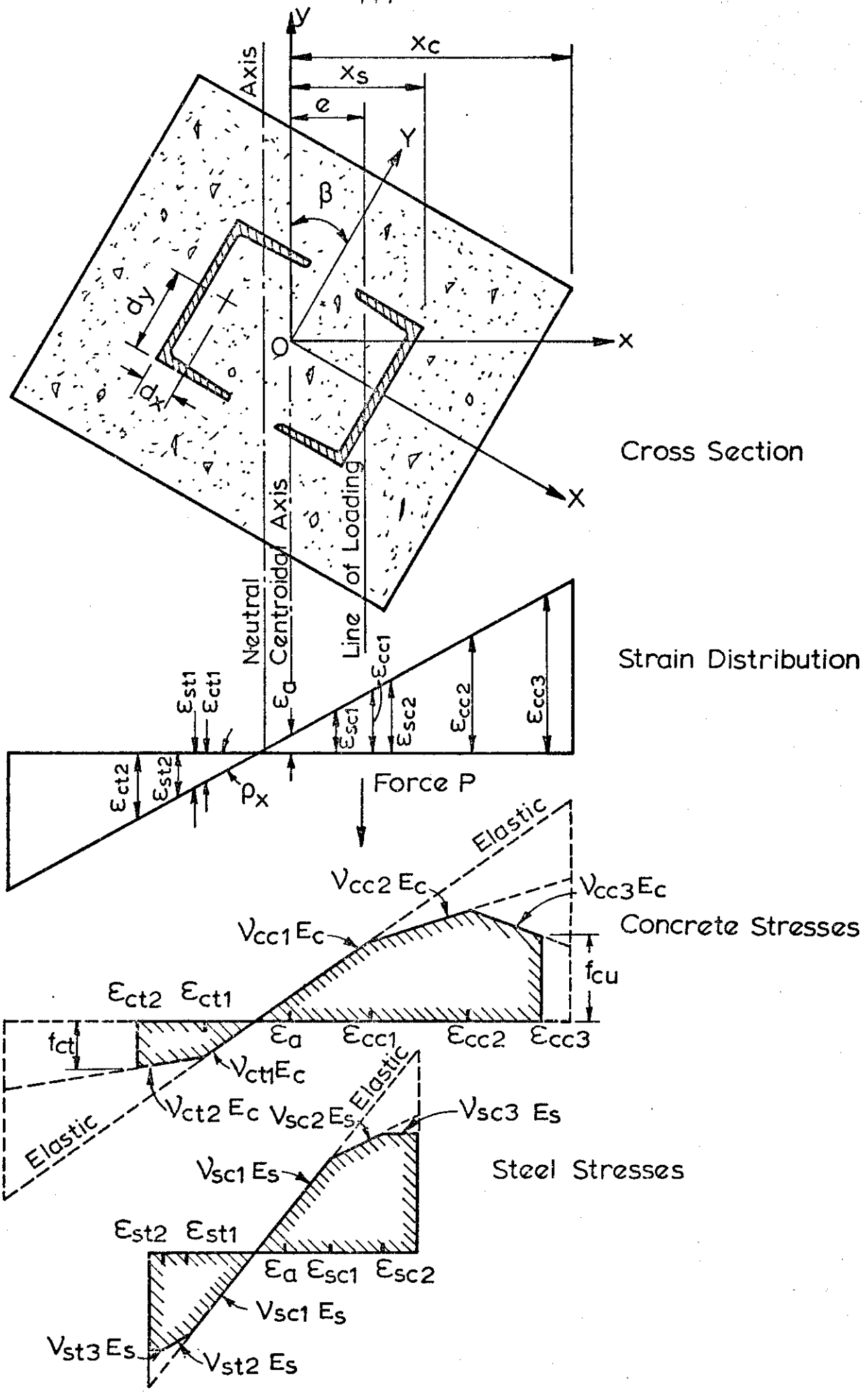

FIG. 4·6 STRESS DISTRIBUTION AT AN INELASTIC SECTION OF A COMPOSITE COLUMN BENT ABOUT BOTH AXES.

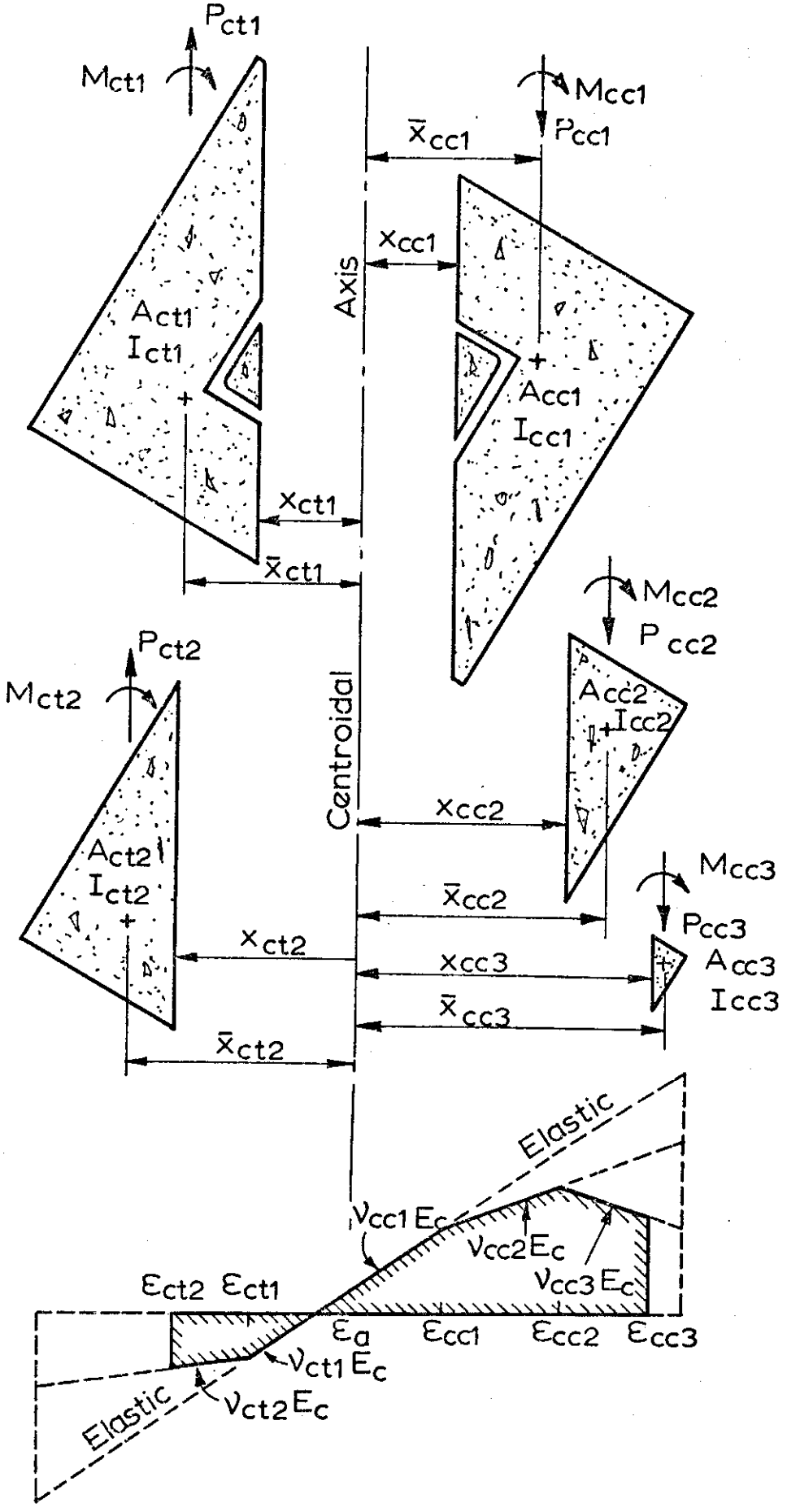

FIG. 4·7 FORCES AND MOMENTS PRODUCED BY THE TRIANGULAR & TRAPEZOIDAL CONCRETE STRESS BLOCKS IN DASHED LINES ACTING ON THEIR CORRESPONDING CONCRETE AREAS

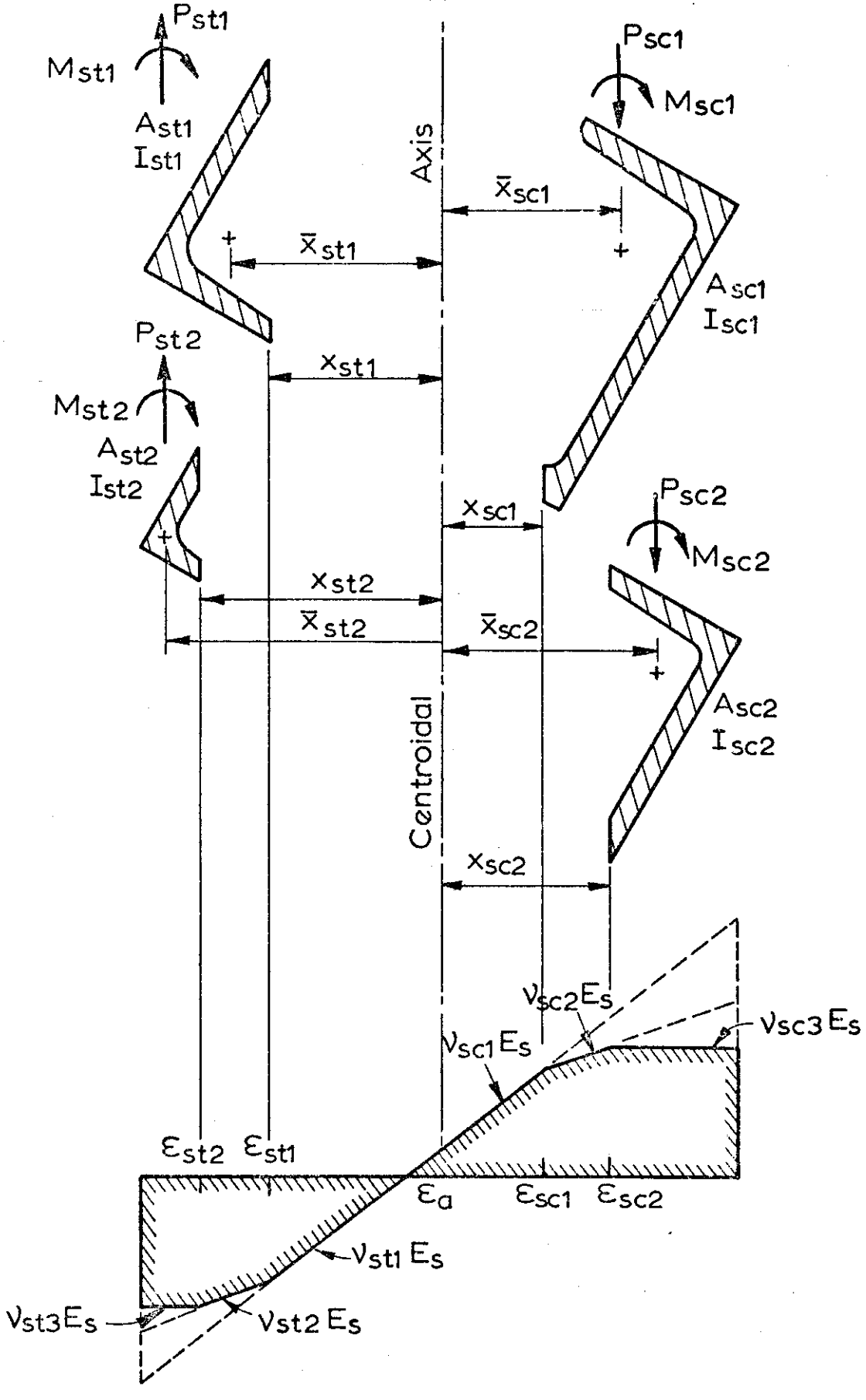

FIG. 4·8 FORCES AND MOMENTS PRODUCED BY THE TRIANGULAR STEEL STRESS BLOCKS IN DASHED LINES ACTING ON THEIR CORRESPONDING STEEL AREAS.

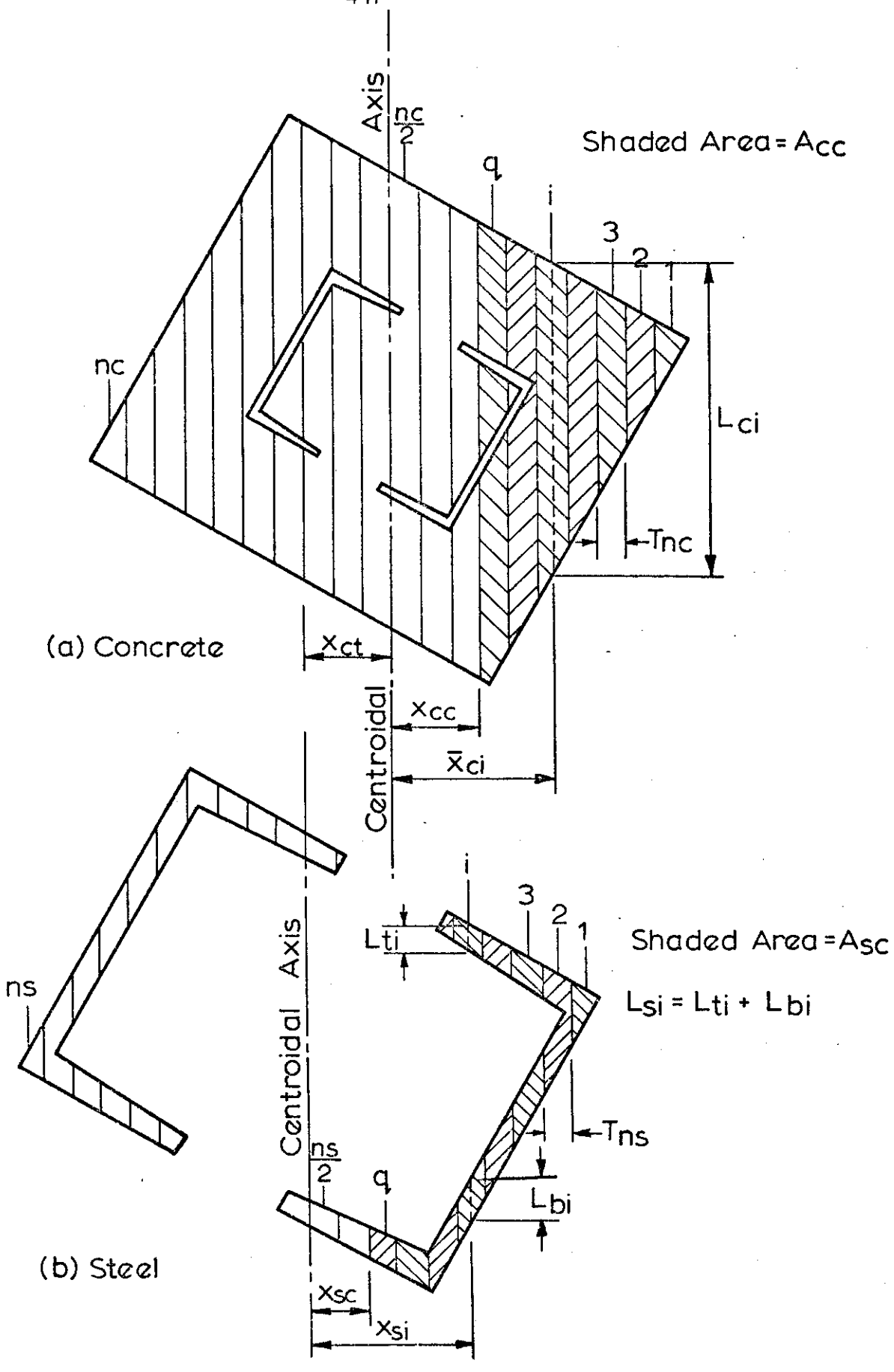

FIG. 4·9 DIVISION OF CONCRETE AND STEEL AREAS INTO STRIPS FOR DETERMINATION OF GEOMETRICAL PROPERTIES.

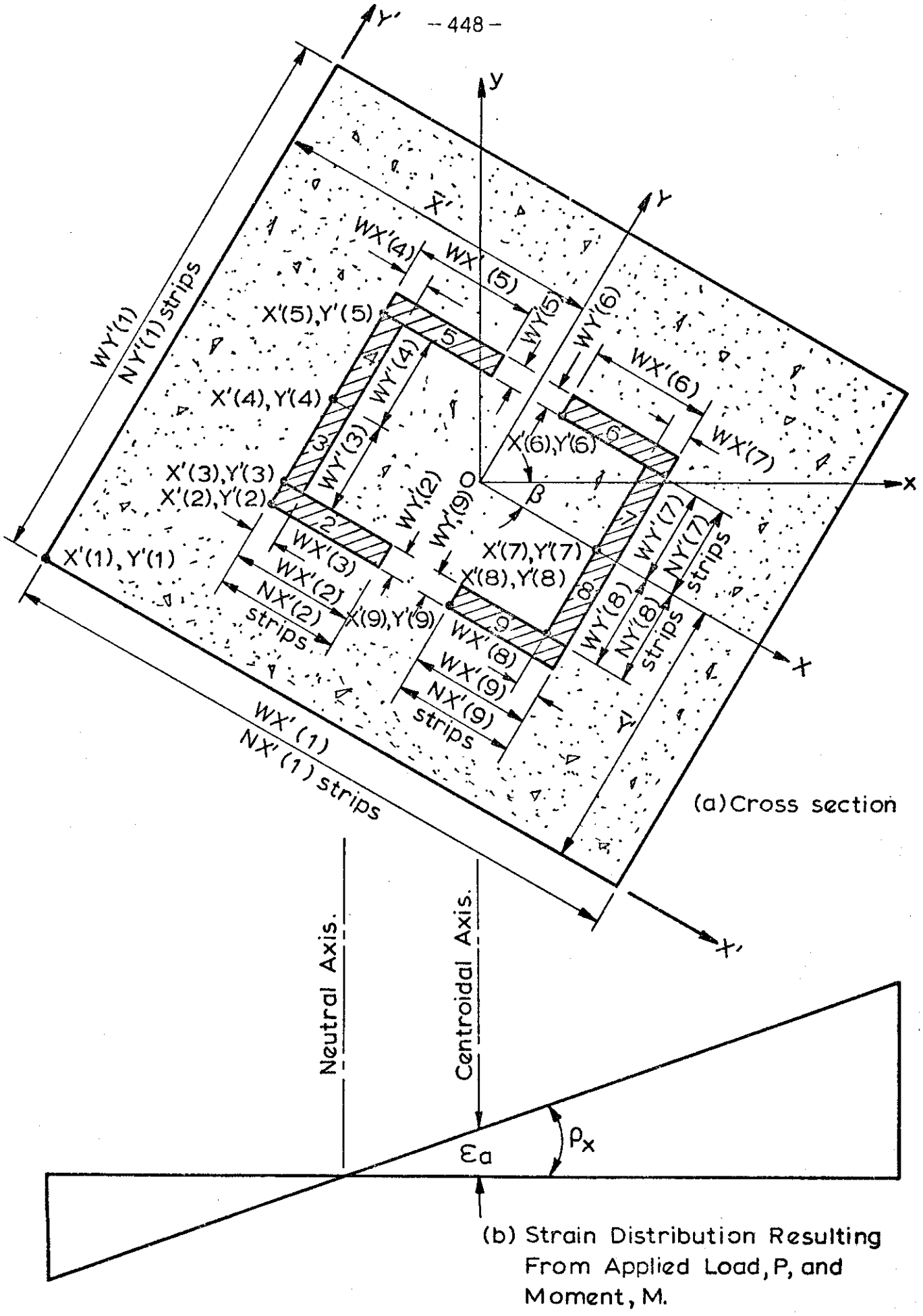

FIG. 4·10 DIVISION OF CROSS SECTION INTO SEGMENTS AND ELEMENTS FOR DETERMINATION OF LOAD-MOMENT-CURVATURE RELATIONSHIP INCLUDING RESIDUAL STRESS EFFECTS.

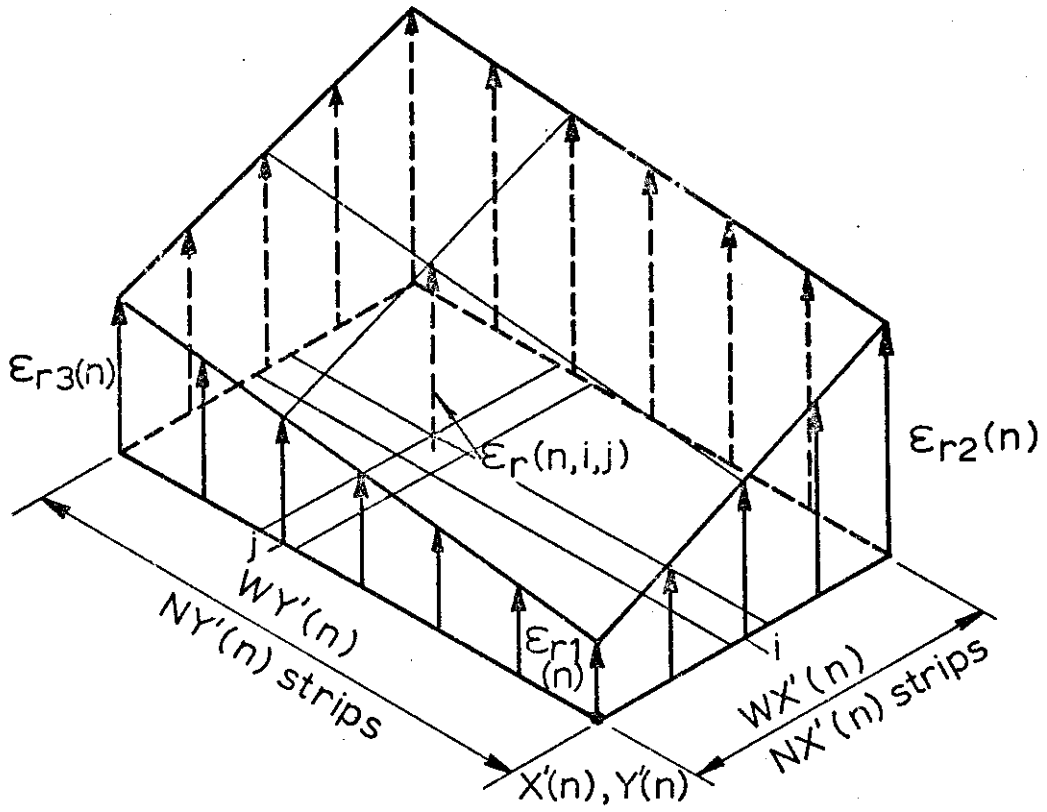

FIG. 4·11 RESIDUAL STRAIN DISTRIBUTION OVER n th SEGMENT OF CROSS SECTION.

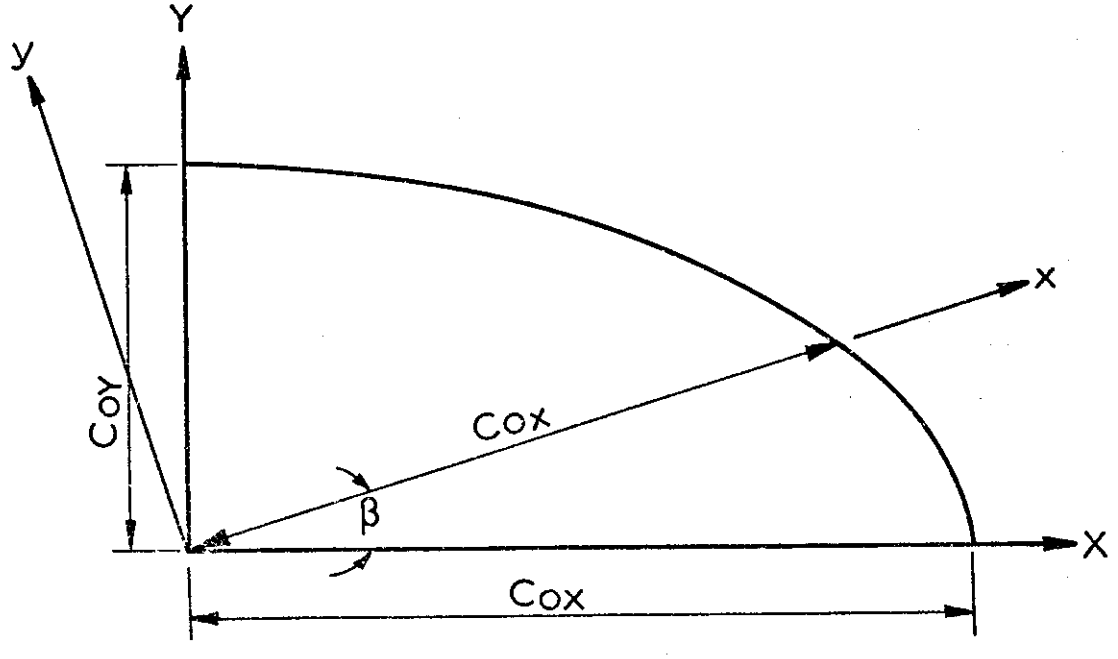

FIG. 4·12 VARIATION IN INITIAL IMPERFECTION AT MID-HEIGHT OF COLUMN WITH ROTATION OF AXES

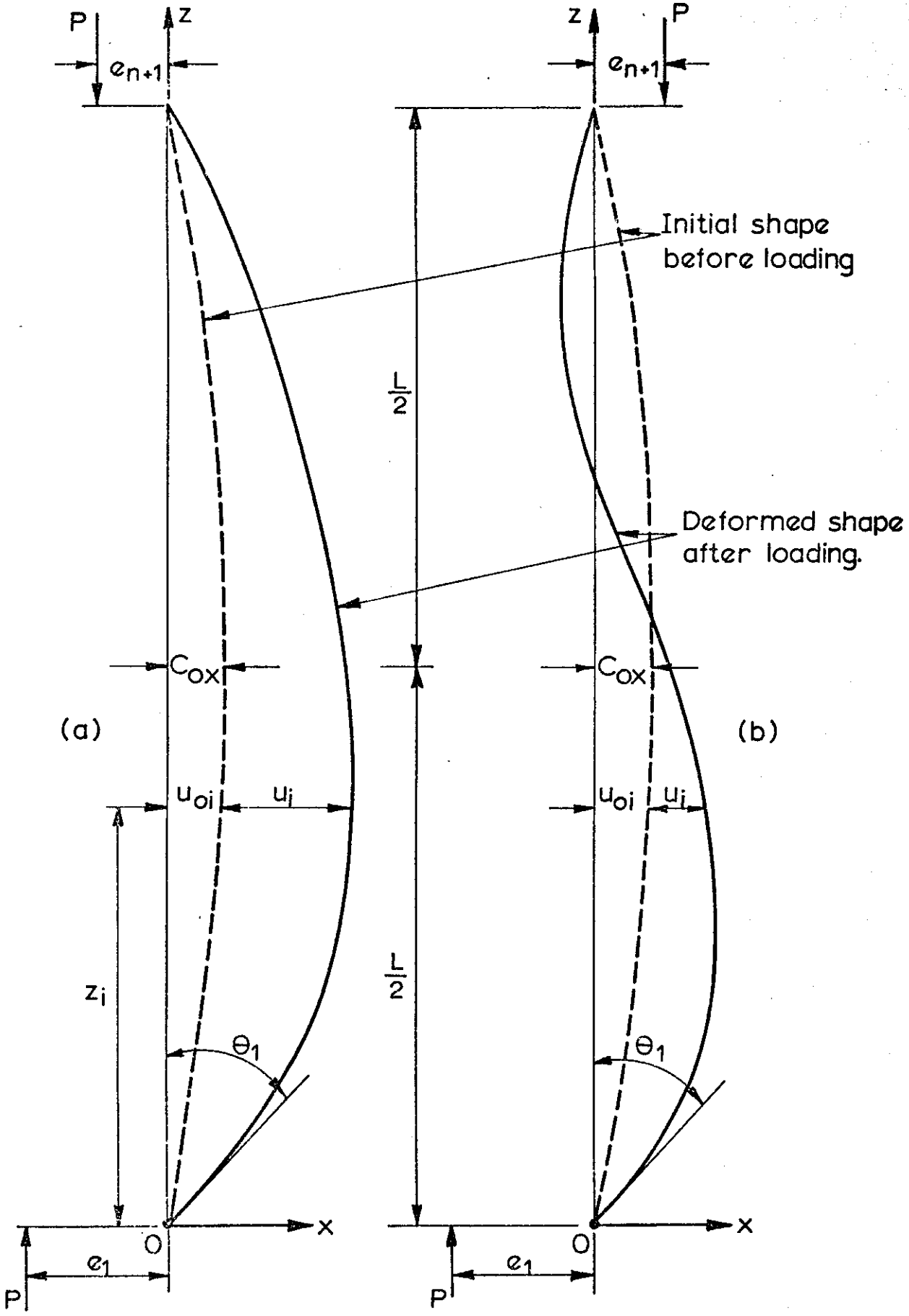

FIG. 4·13 DEFORMED SHAPES OF COLUMNS UNDER ECCENTRIC LOADING

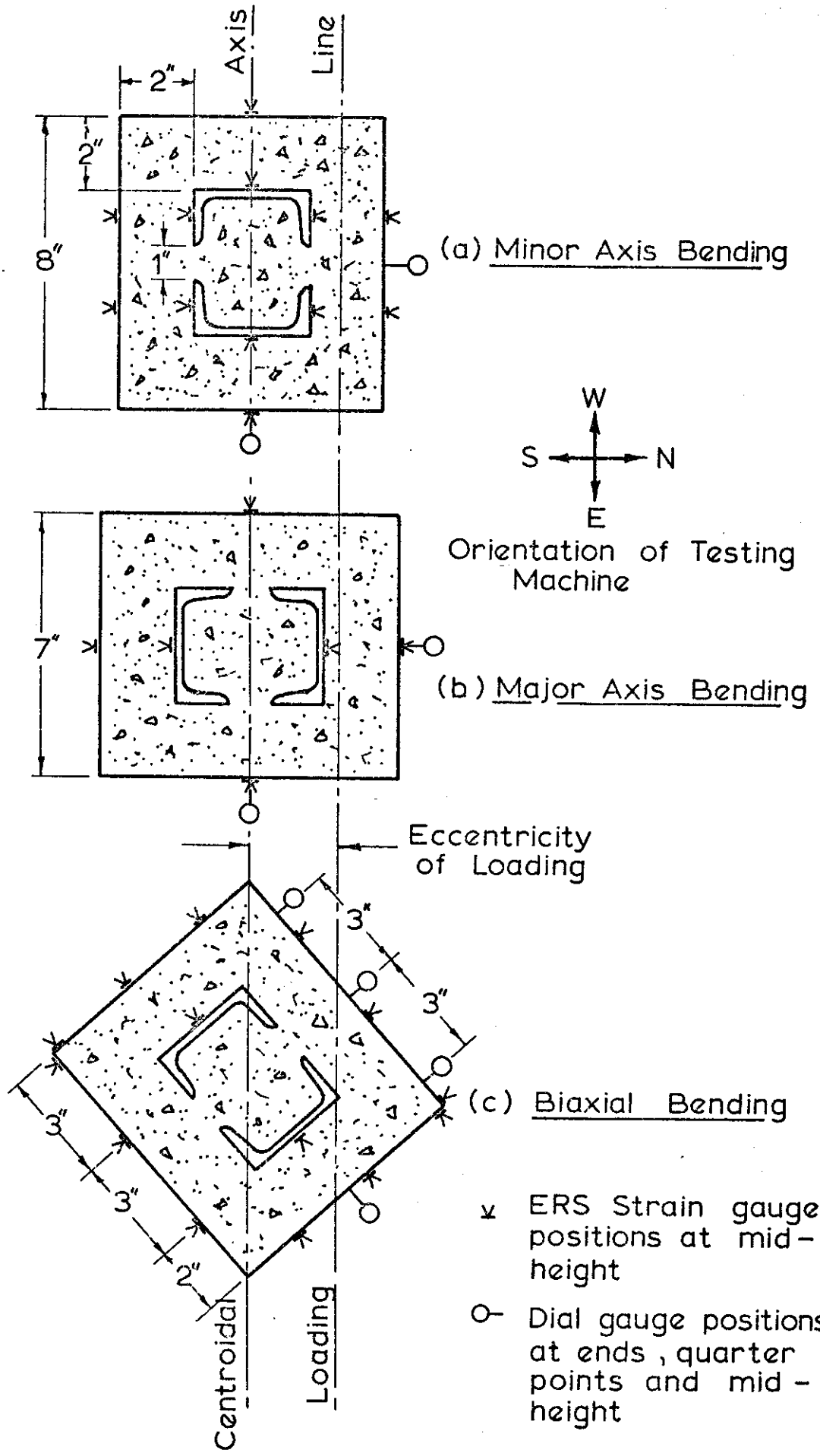

FIG. 5·1 CROSSECTIONAL DETAILS OF CC SERIES COMPOSITE COLUMNS

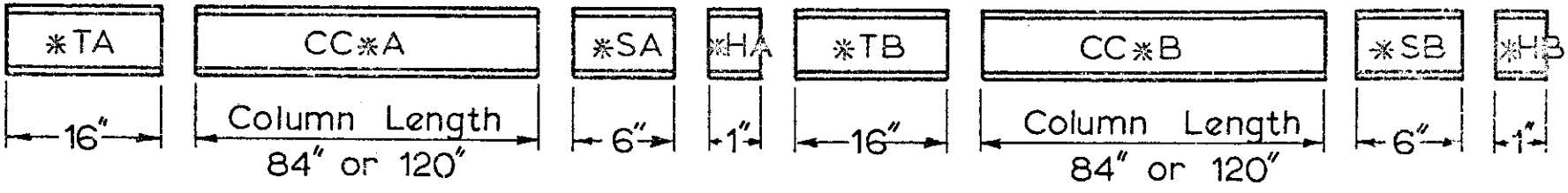

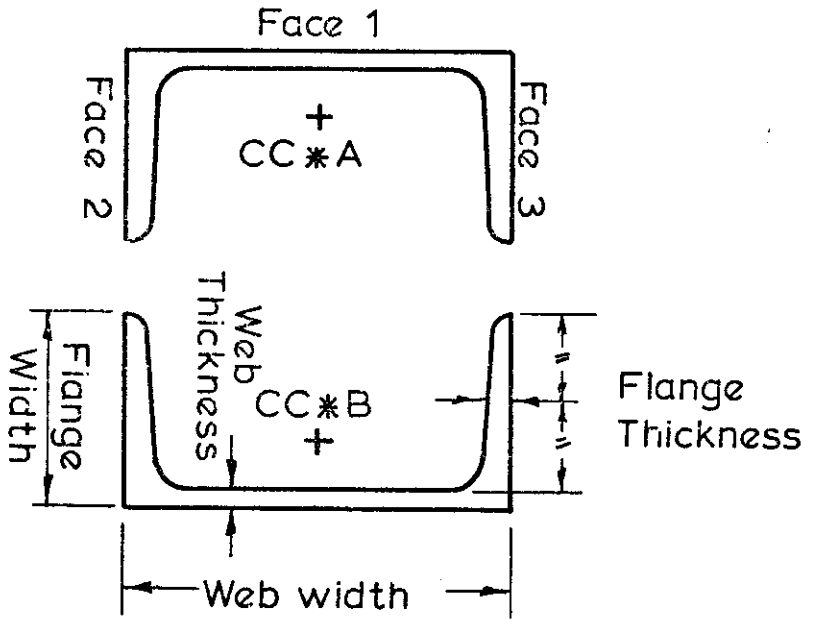

* Column No.

* TA, * TB — Tension Tests

* SA, * SB — Squat Compression Tests

* HA, * HB — Hounsfield Tests

CC* A, CC* B — Column Core Lengths

FIG 5·2 TEST PIECES CUT FROM A SINGLE LENGTH OF CHANNEL FOR EACH COLUMN TEST

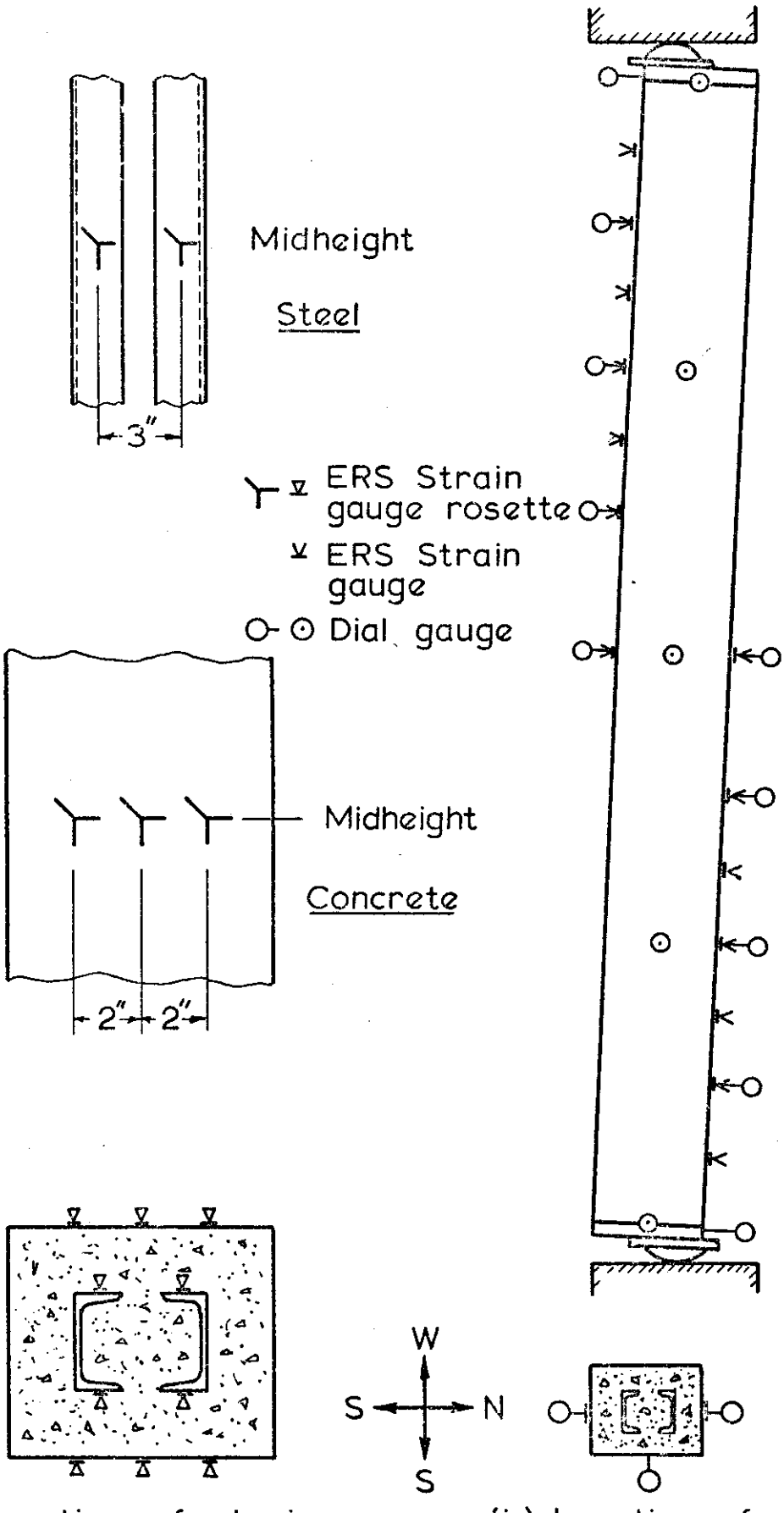

(a) Location of strain rosettes at mid-height

(b) Location of strain and dial gauges along length

FIG. 5·3 INSTRUMENTATION FOR COLUMN CC11

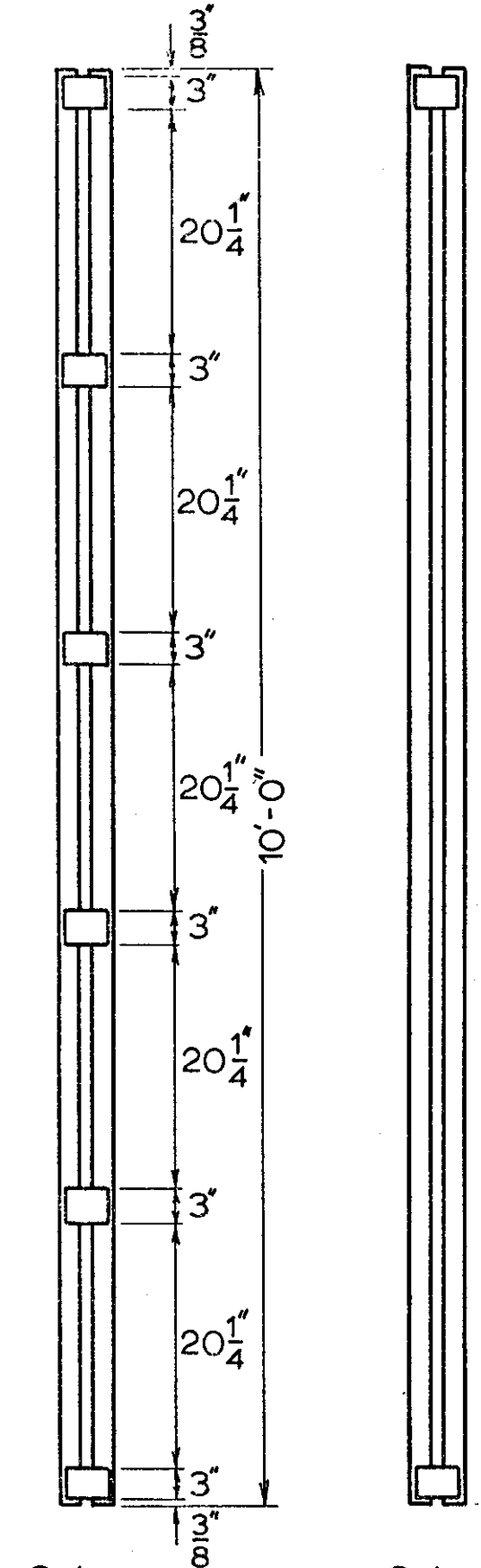

Columns
CC14, CC15

Column
CC13, CC13R

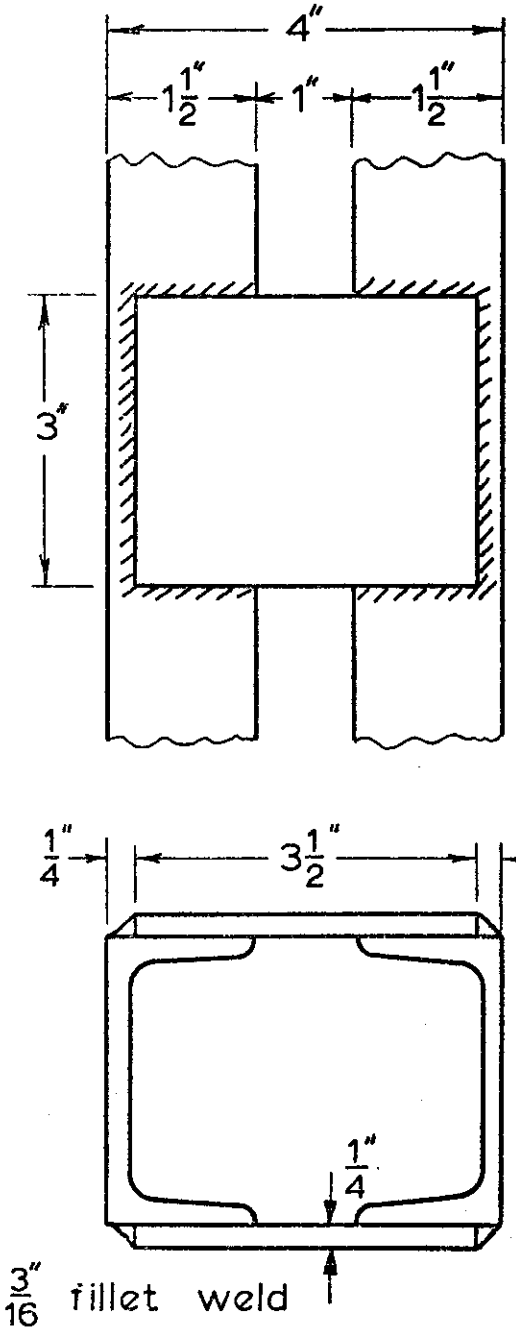

Details of batten plates

FIG. 5·4 DETAILS OF BATTENED COLUMNS

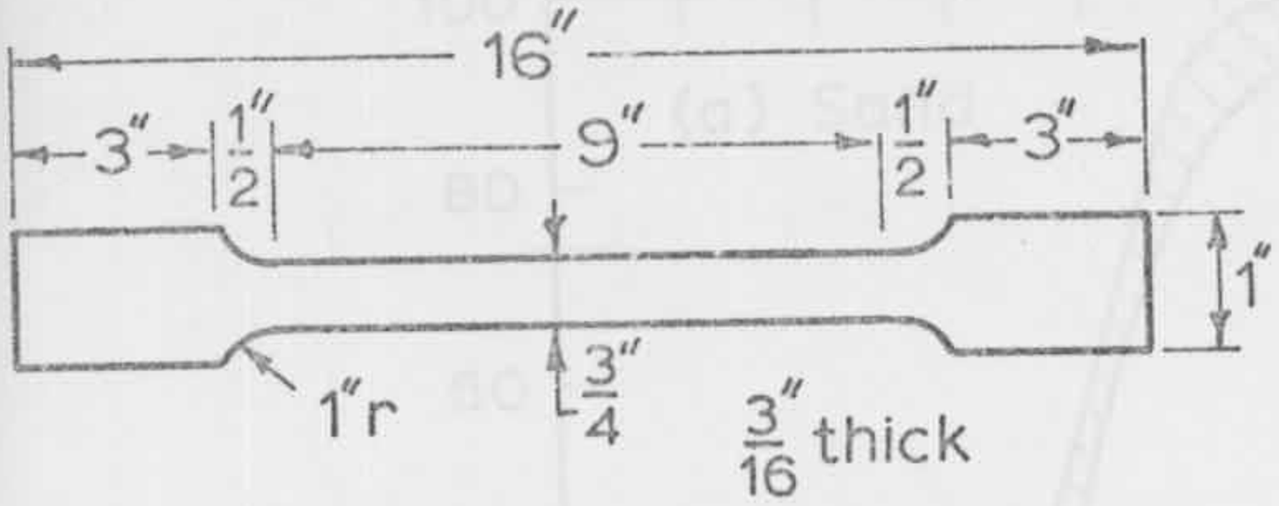

(a) Coupon dimension

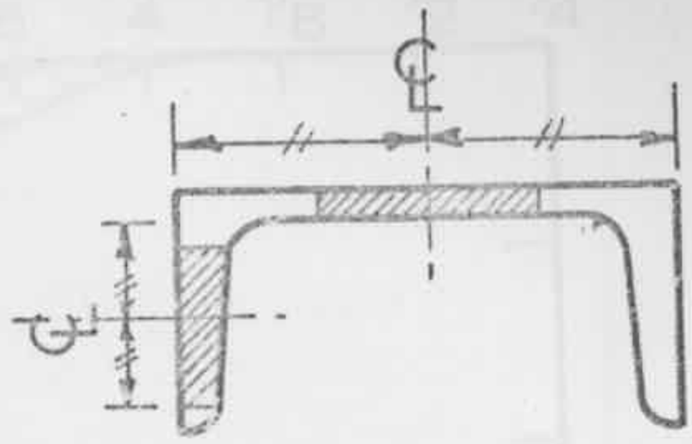

(b) Location of Coupons

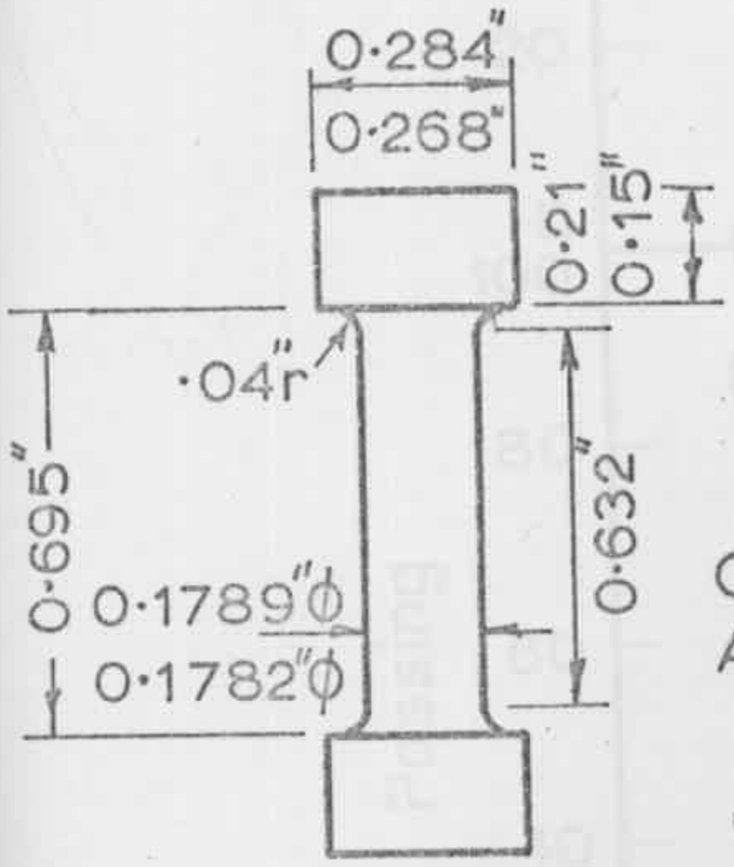

Crossectional Area = $\frac{1}{40}$ sq. in.

(c) Hounsfield Test Piece No 12

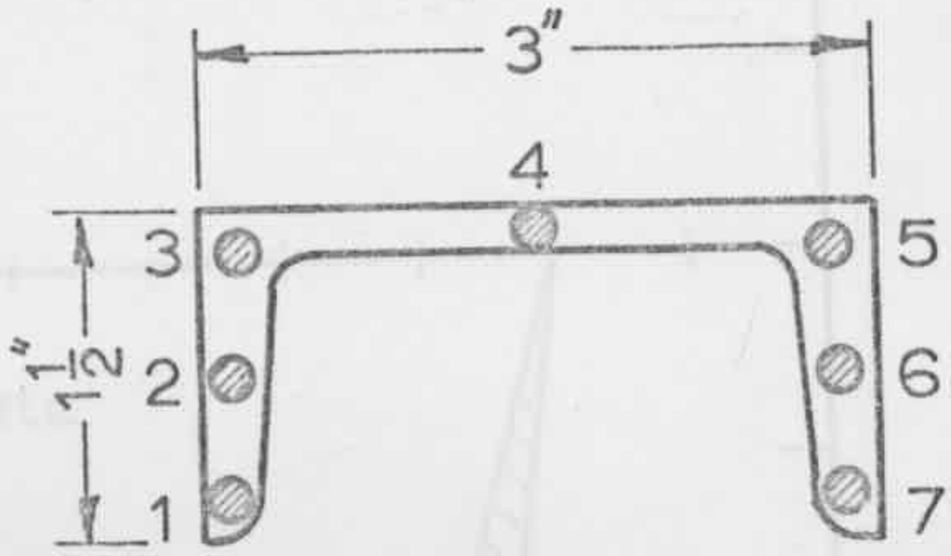

(d) Position of Hounsfield Test Pieces

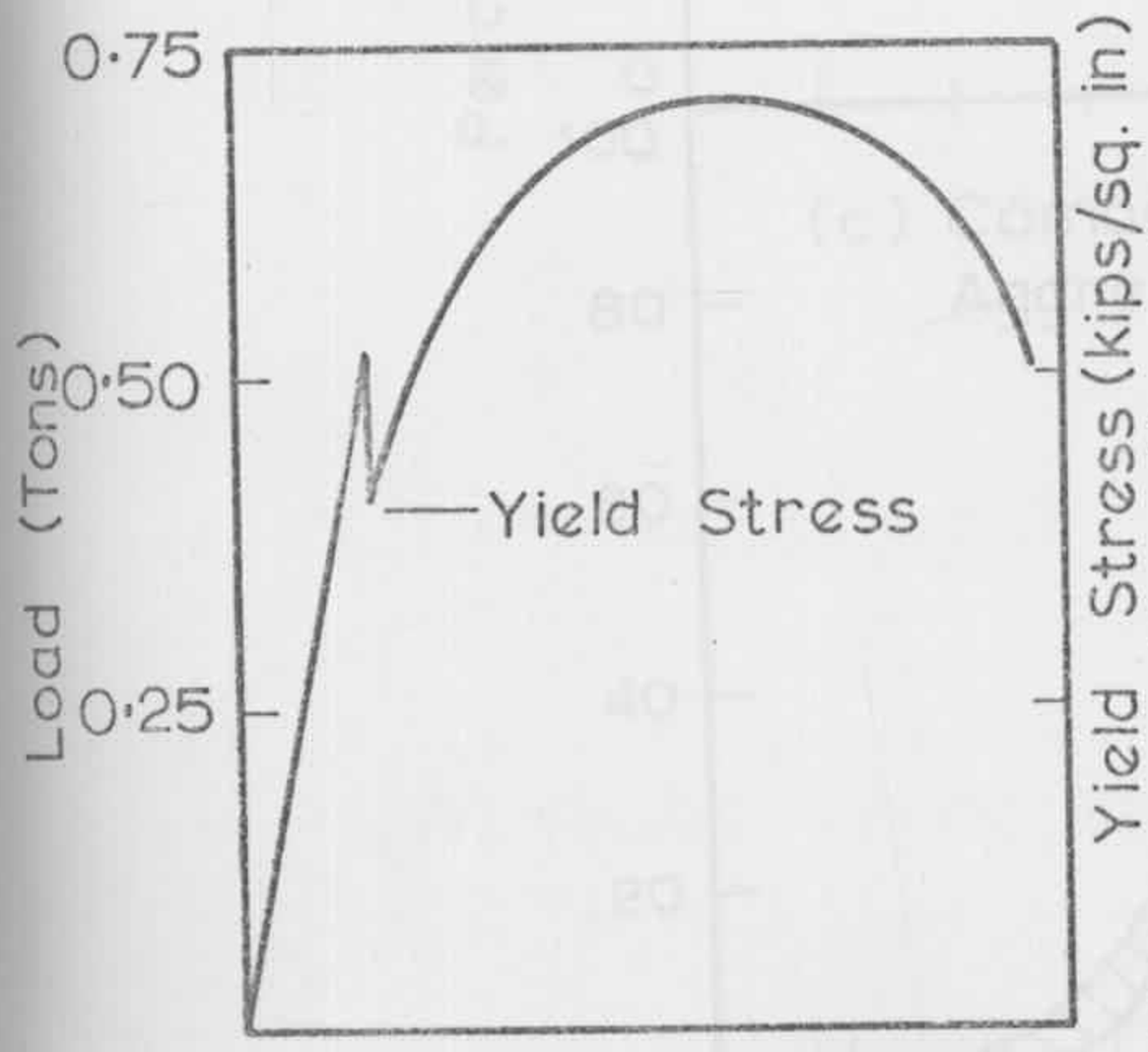

(e) Typical Hounsfield Plot

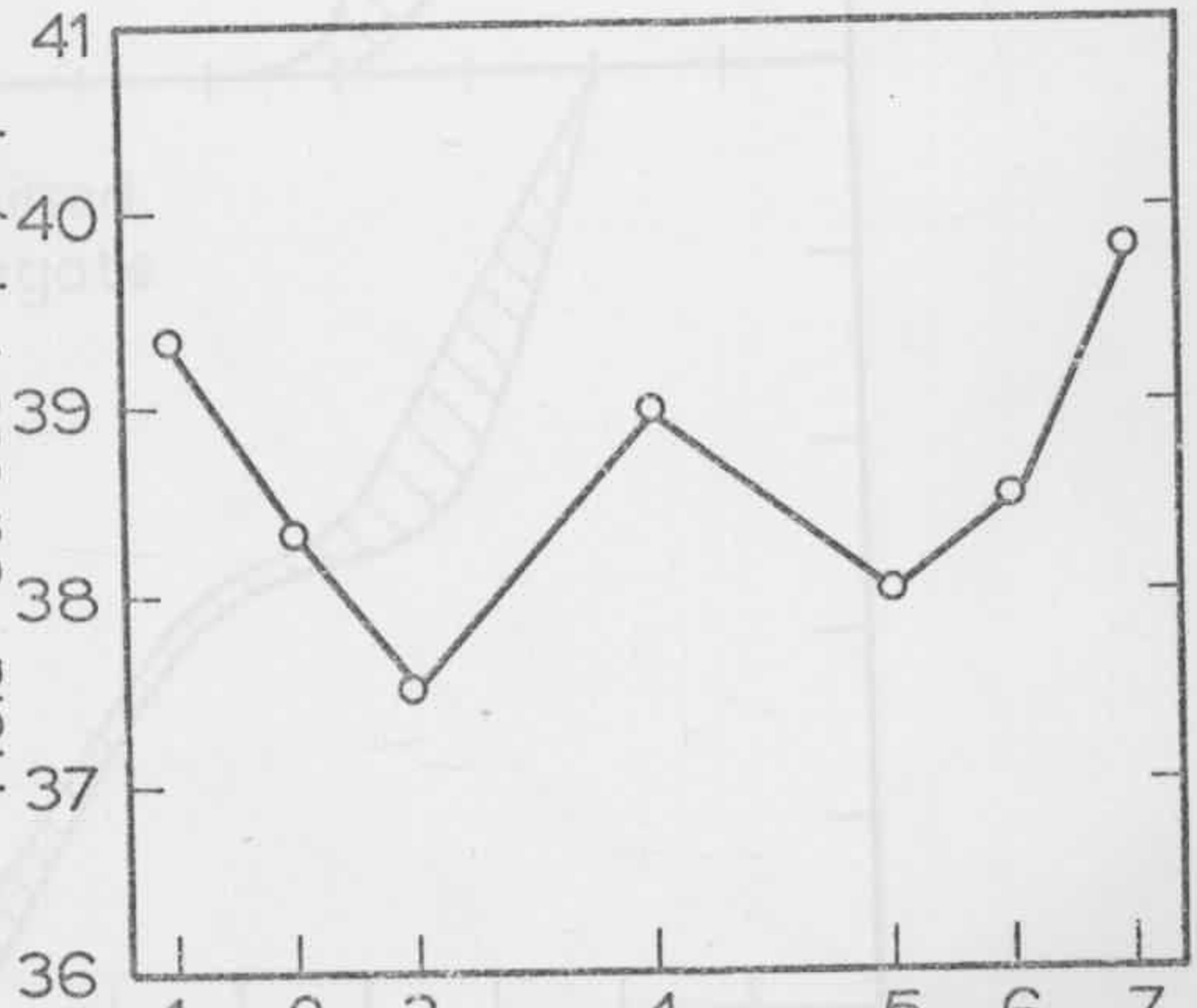

(f) Variation of Yield Stress with Position

FIG. 5·5 STEEL CONTROL TESTS

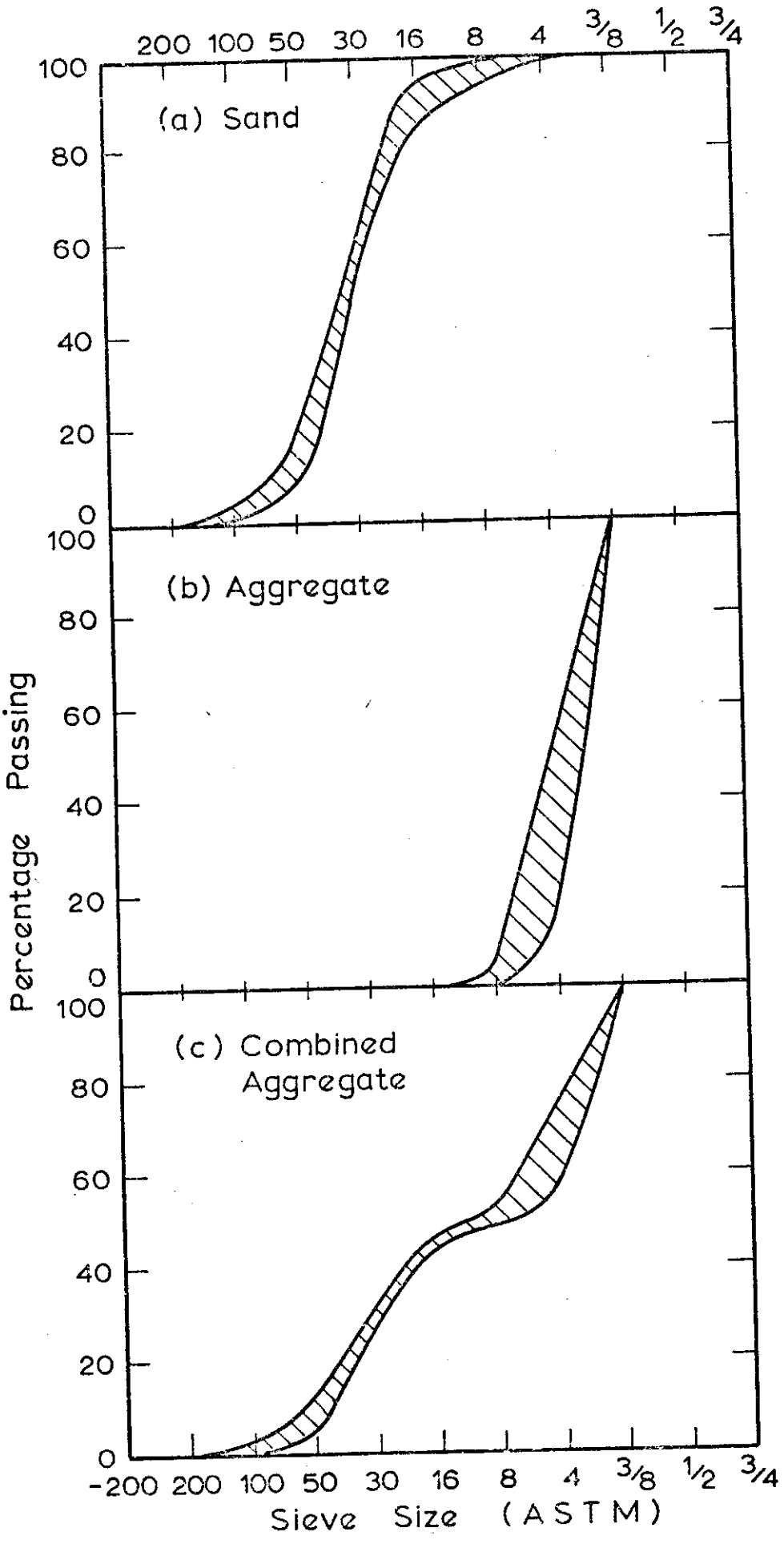

FIG. 5·6 AGGREGATE GRADING CURVES

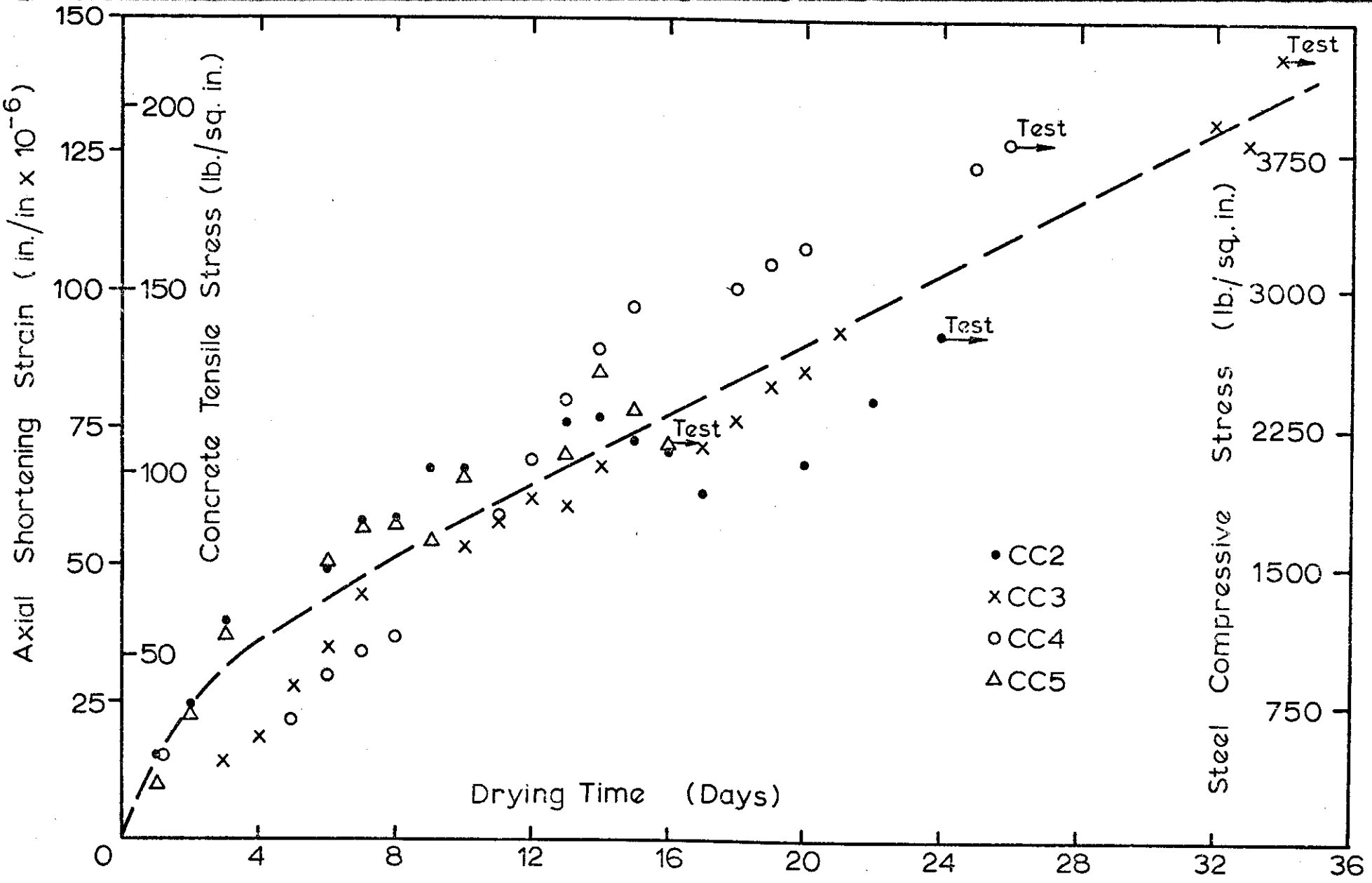

FIG. 5·7 AXIAL SHORTENING WITH TIME DUE TO SHRINKAGE FOR CC SERIES COMPOSITE COLUMNS WITH DIFFERENT AND VARYING TEMPERATURE AND HUMIDITIES

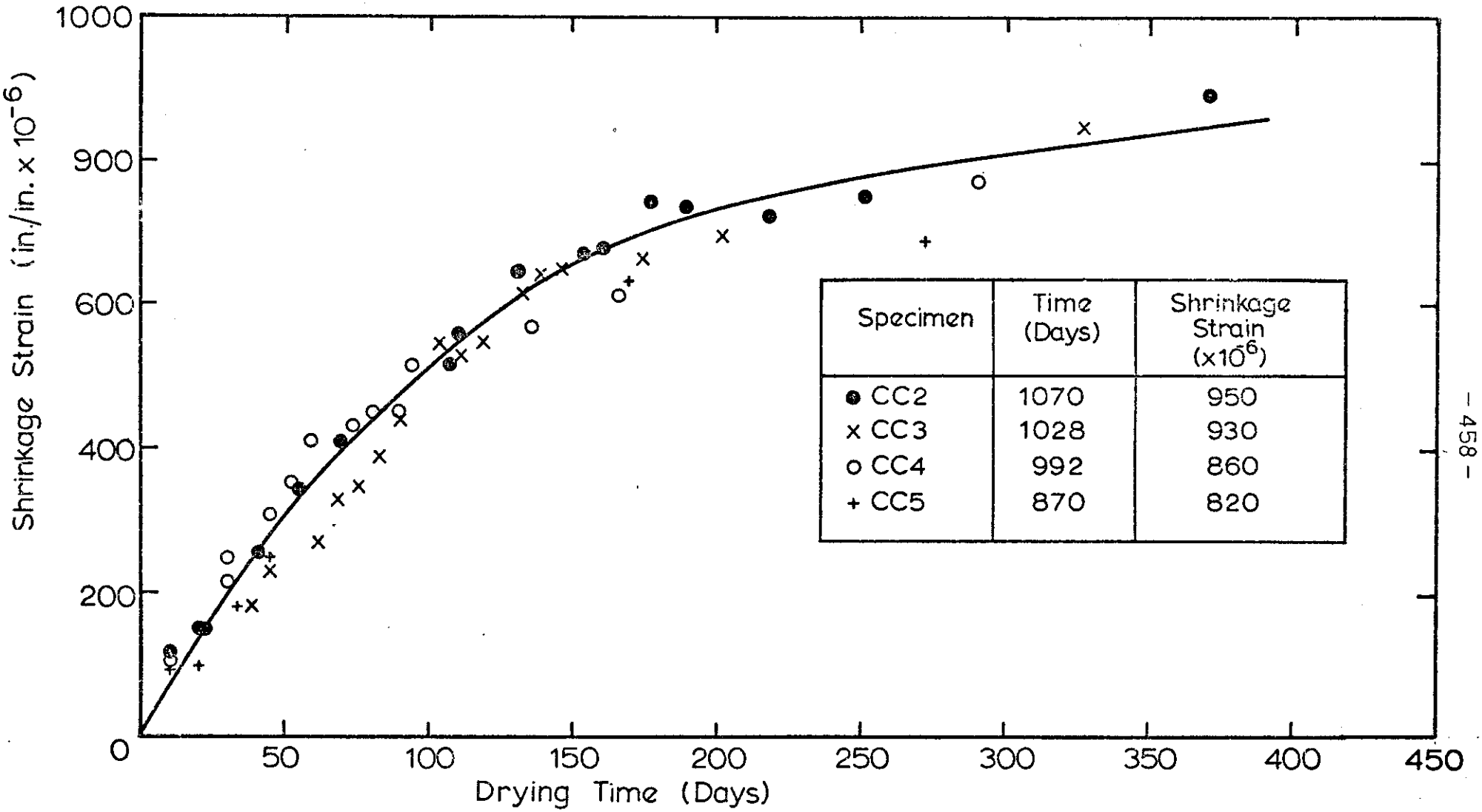

FIG.5·8 SHRINKAGE STRAIN -TIME WITH VARYING HUMIDITY AND TEMPERATURE FOR CONCRETE SPECIMEN OF 8 IN. BY 7 IN. CROSS SECTION.

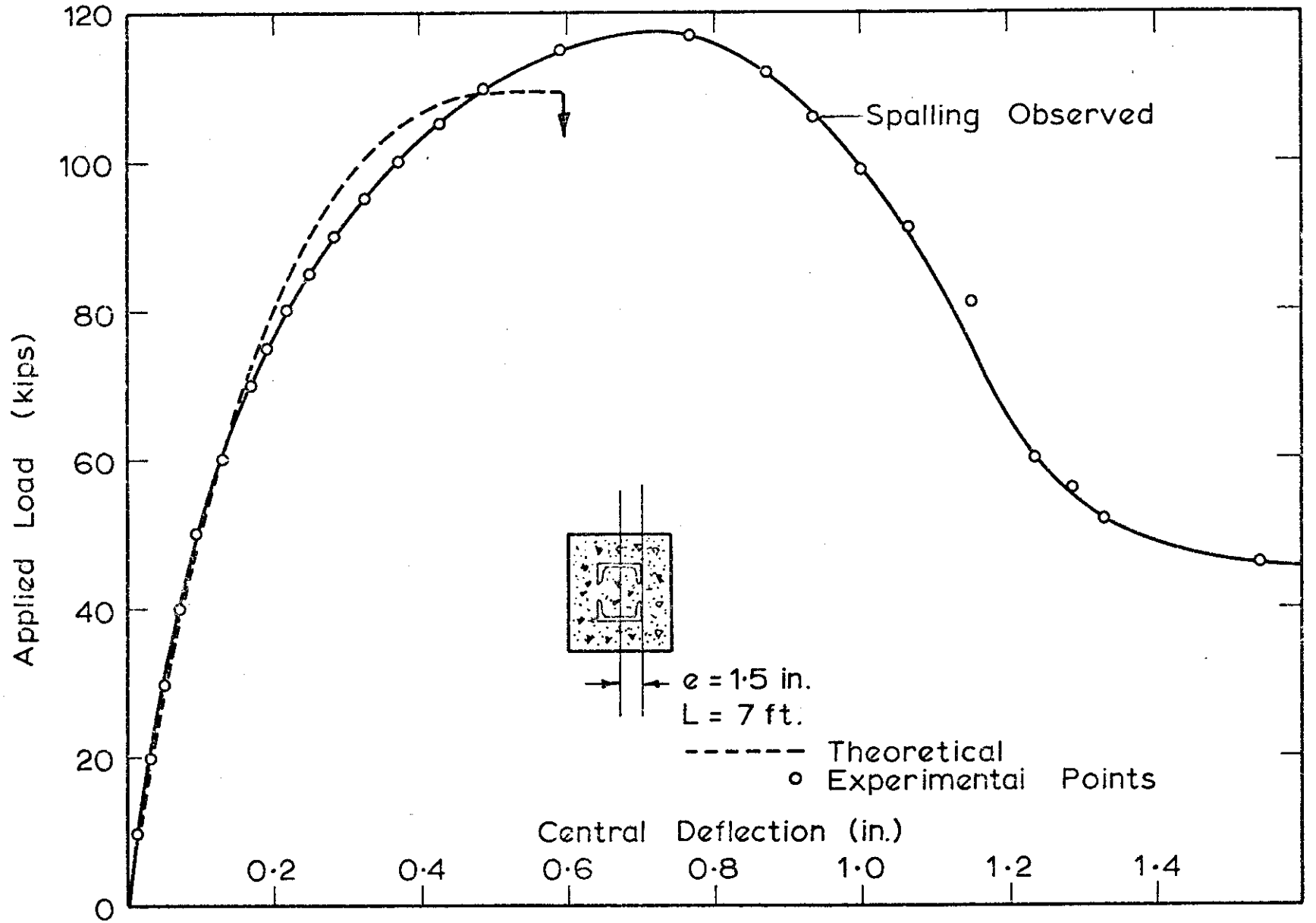

FIG. 5·9 LOAD - DEFLECTION RELATIONSHIP FOR 7FT. COLUMN CC1 BENT ABOUT THE MINOR AXIS

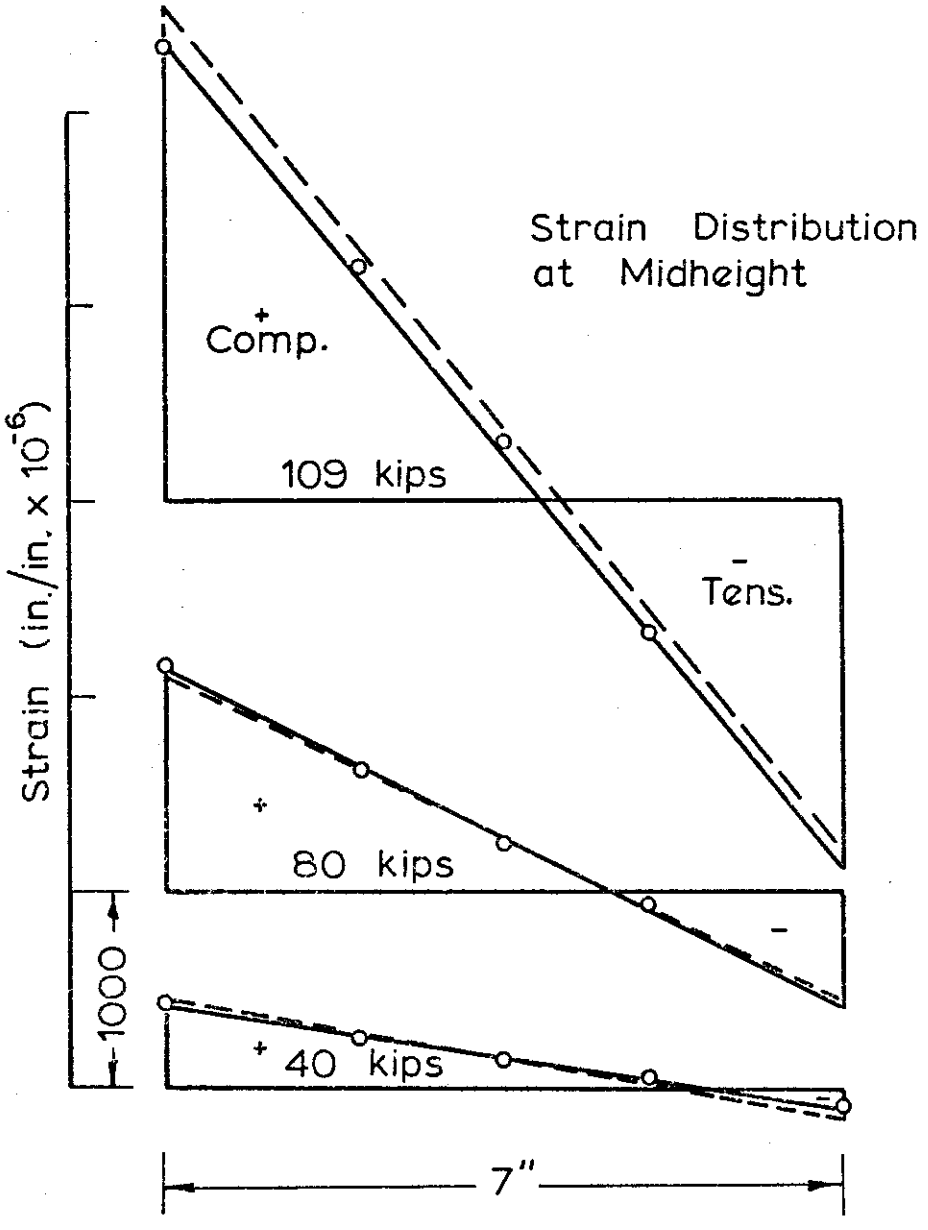

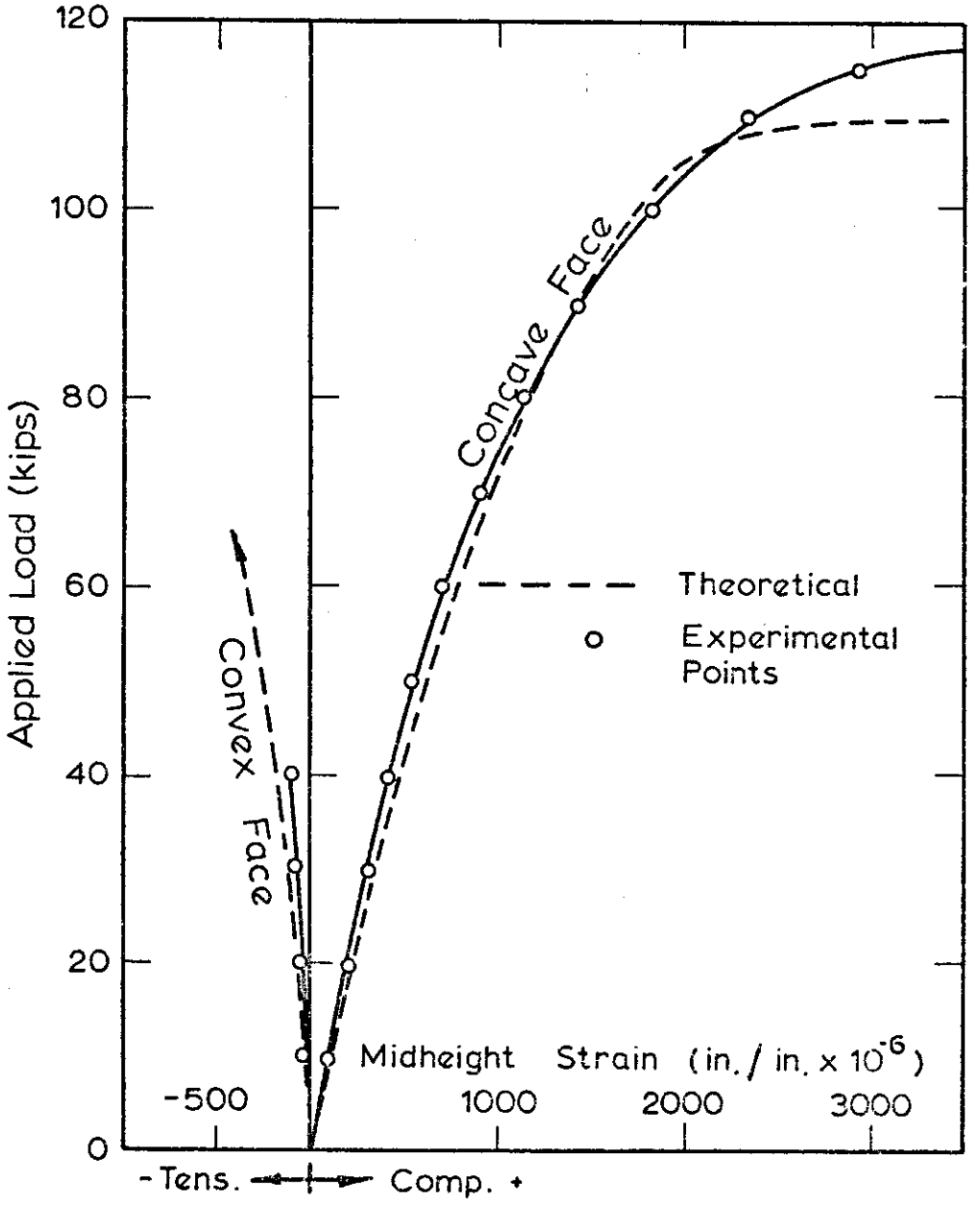

FIG. 5·10 STRAIN RESULTS FOR 7FT. COLUMN CC1 BENT ABOUT MINOR AXIS

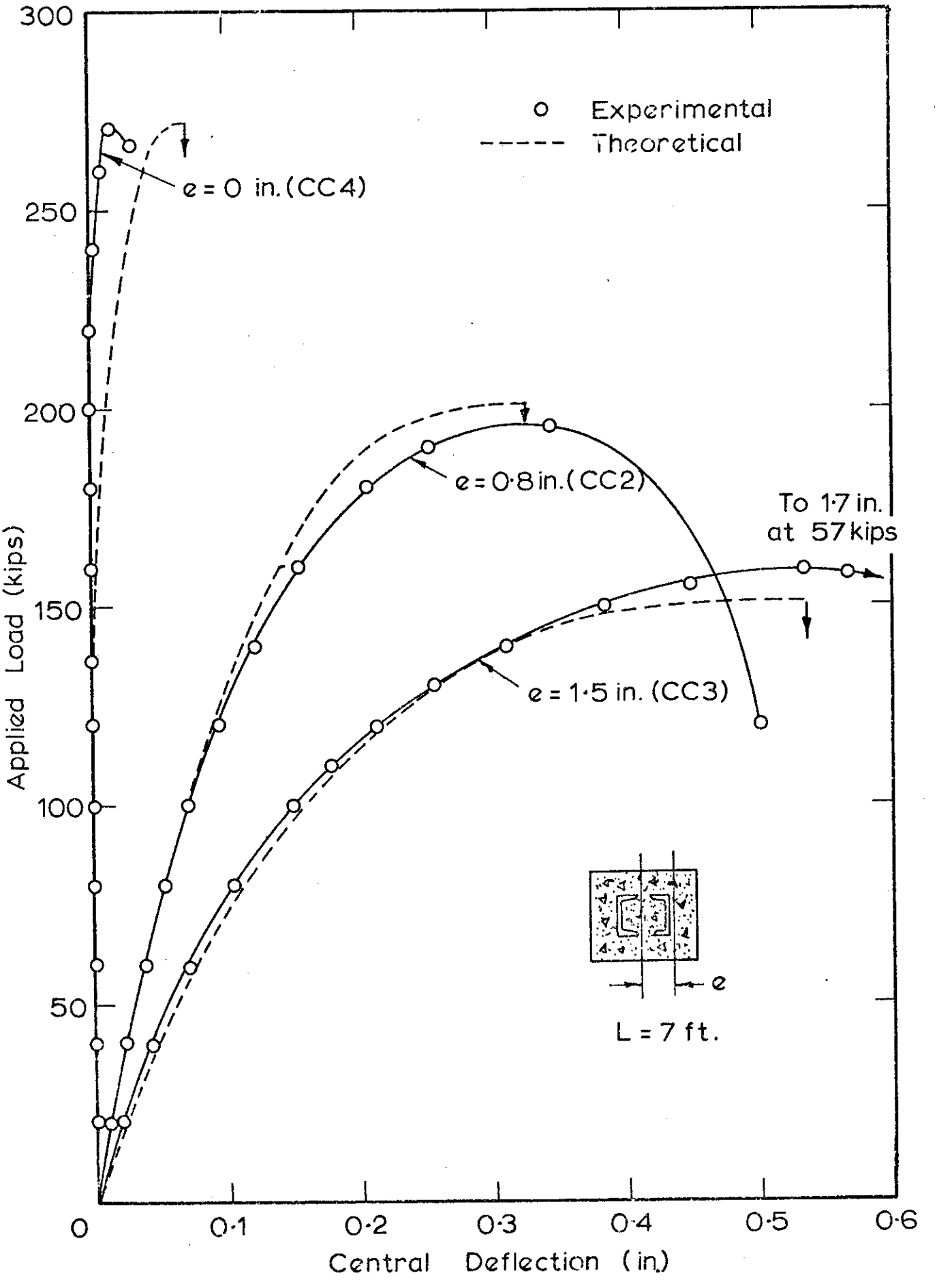

FIG. 5·11 LOAD - DEFLECTION RELATIONSHIPS FOR 7 FT. COLUMNS CC2, CC3 AND CC4 BENT ABOUT THE MAJOR AXIS.

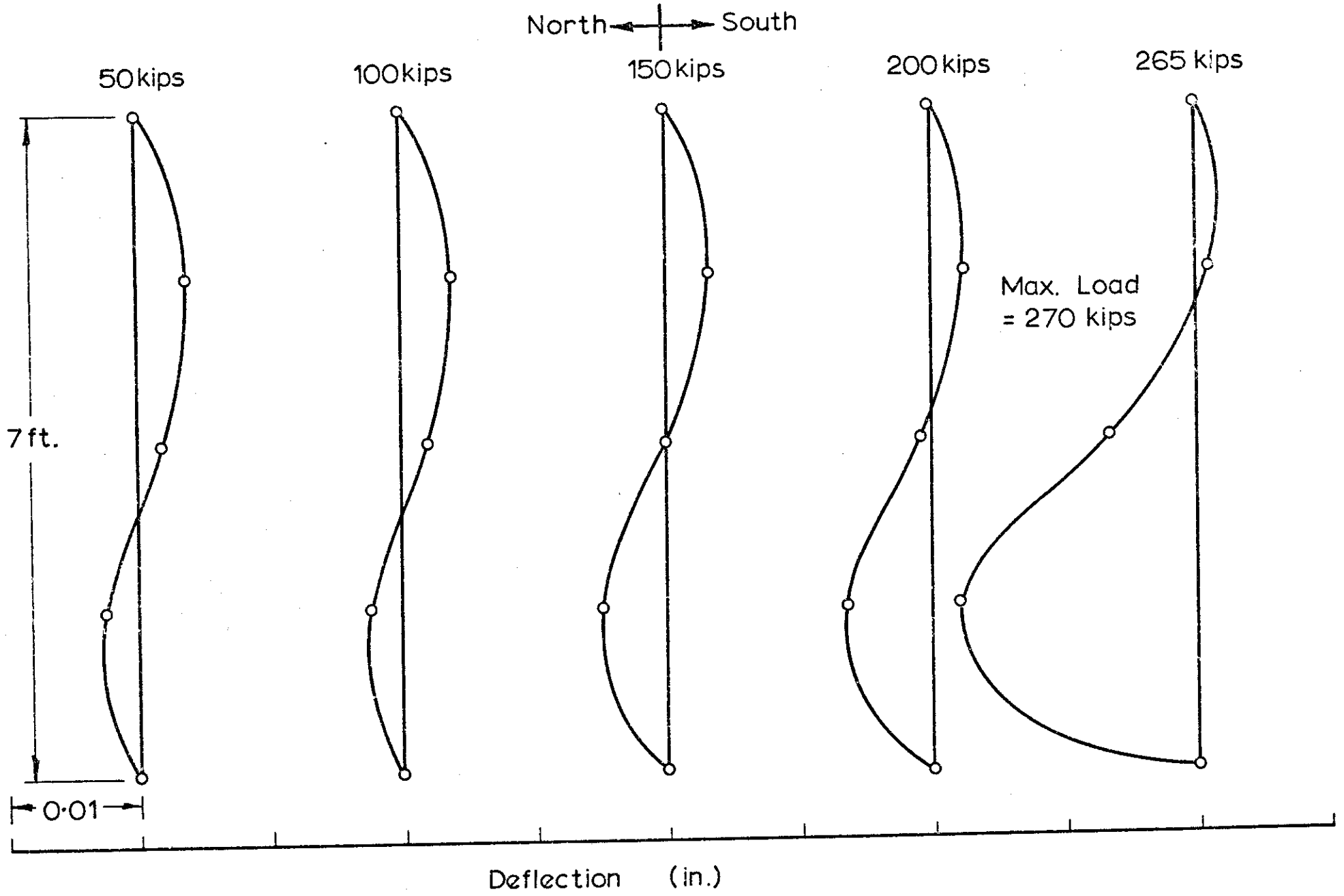

FIG. 5·12 DEFLECTION PROFILES FOR CONCENTRICALLY LOADED COLUMN CC4

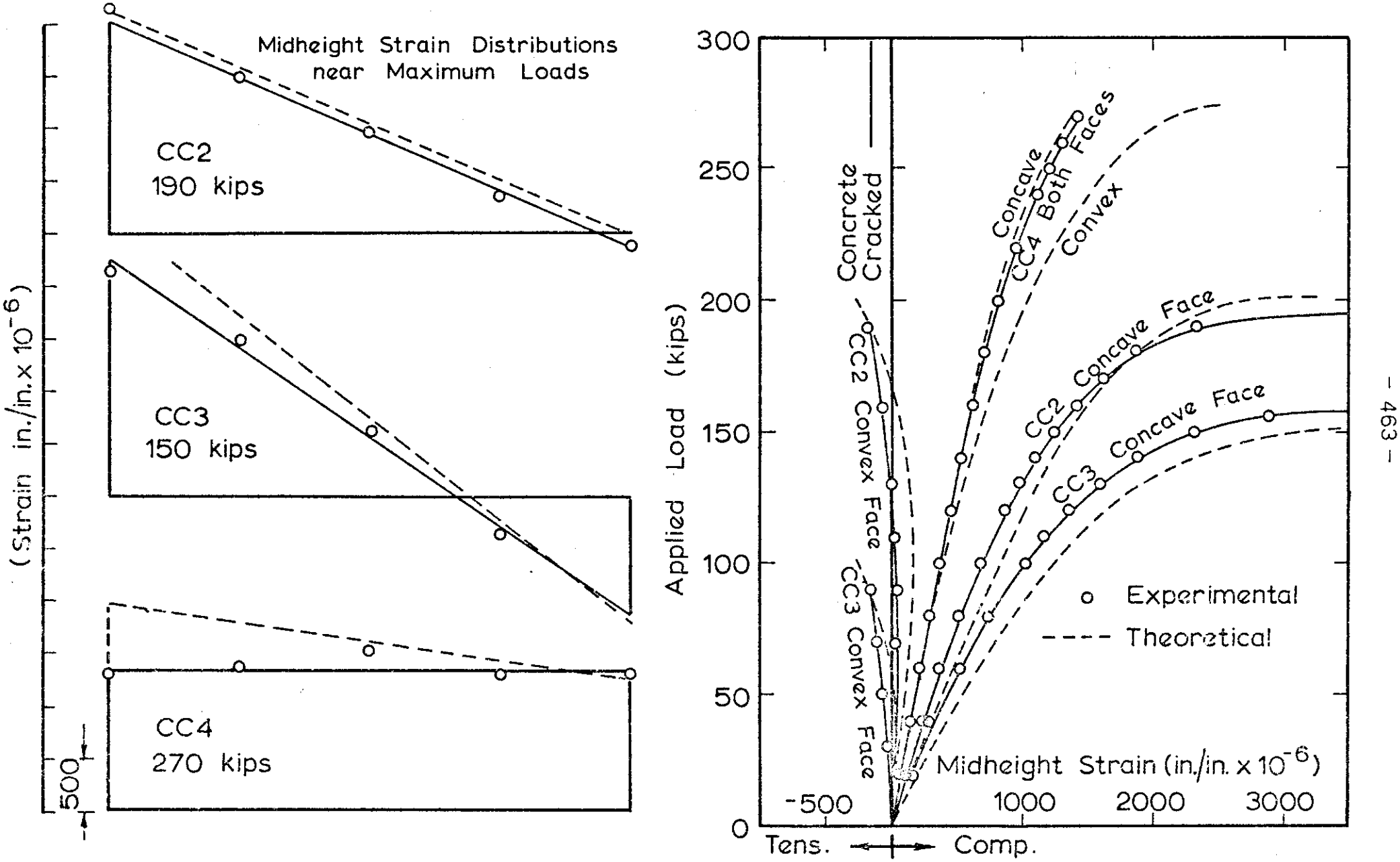

FIG. 5·13 STRAIN RESULTS FOR 7 FT. COLUMNS CC2, CC3 AND CC4 BENT ABOUT THE MAJOR AXIS

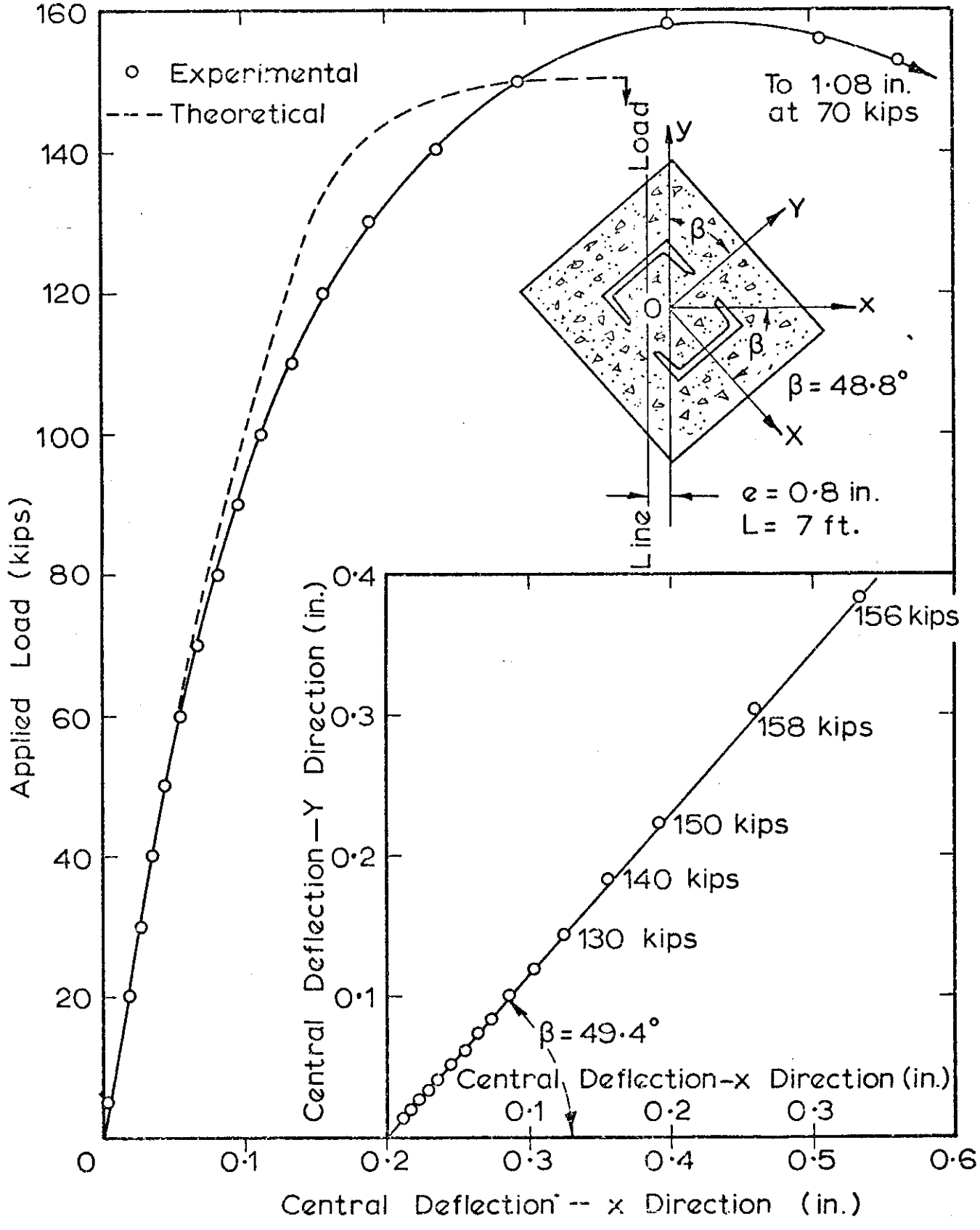

FIG. 5·14 LOAD-DEFLECTION RELATIONSHIP FOR 7FT. COLUMN CC5 BENT BIAXIALLY ABOUT A DIAGONAL AXIS

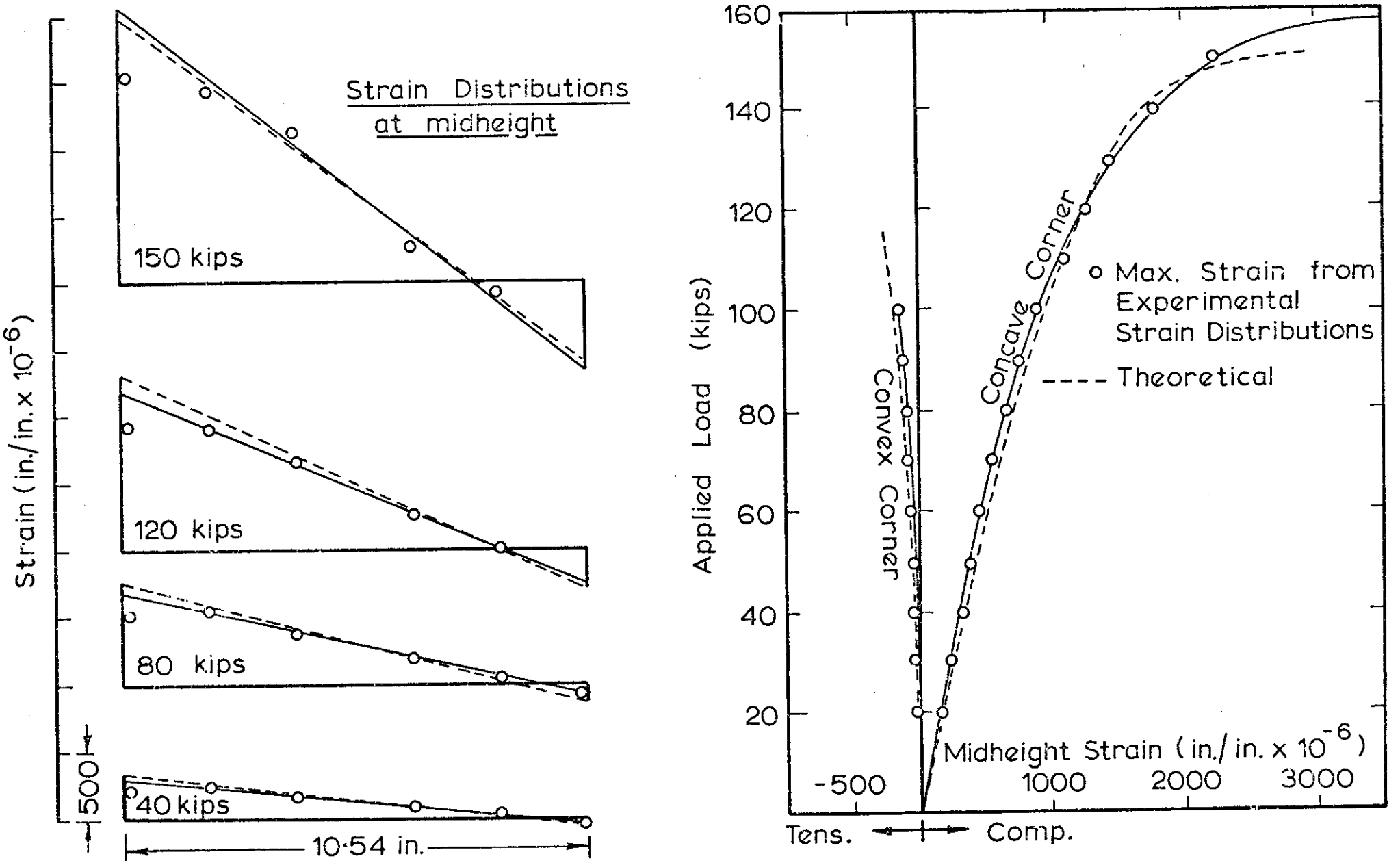

FIG. 5·15 STRAIN RESULTS FOR 7FT. COLUMN CC5 BENT BIAXIALLY ABOUT A DIAGONAL AXIS

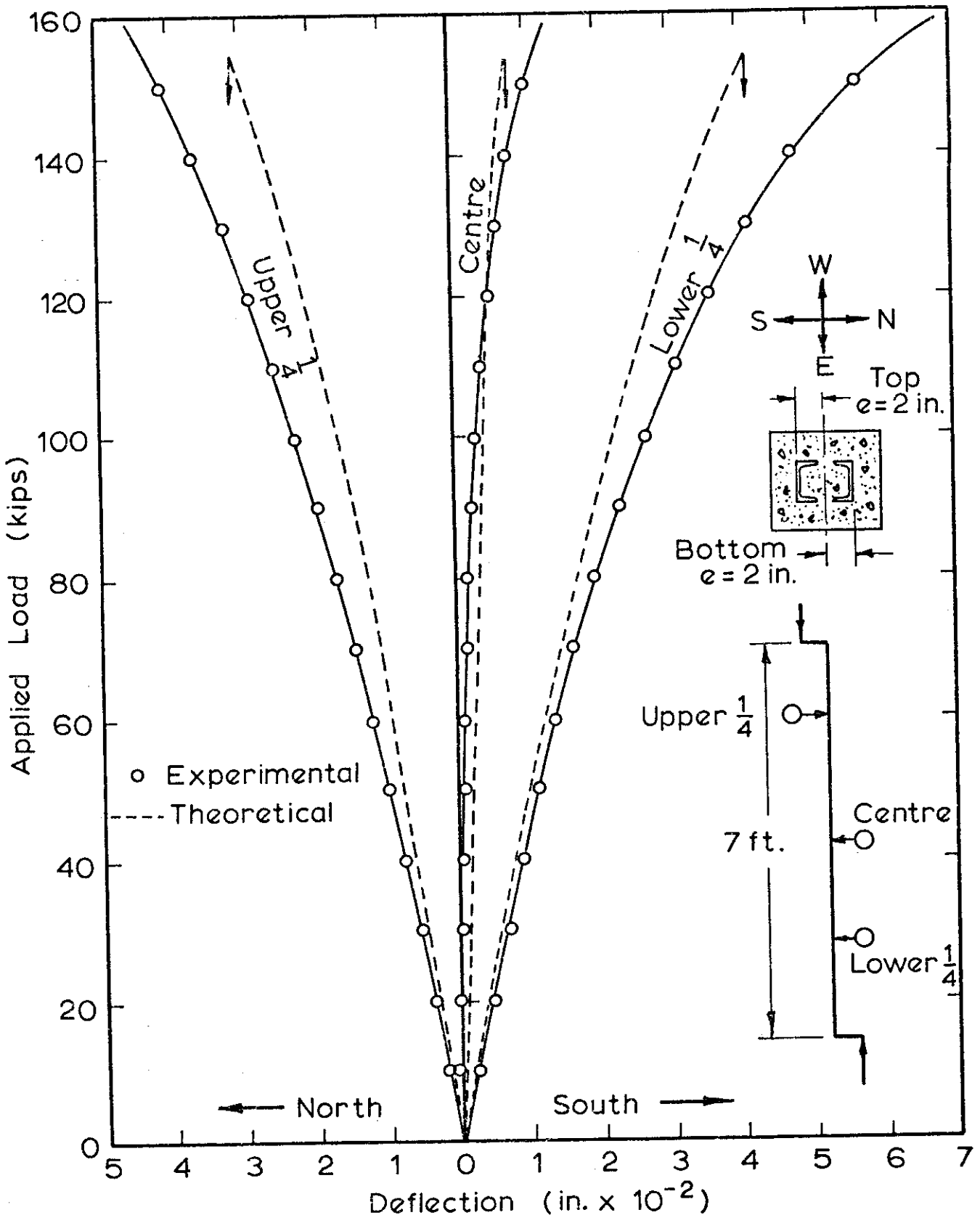

FIG. 5·16 LOAD - DEFLECTION RELATIONSHIPS FOR 7FT. COLUMN CC11 BENT ABOUT THE MAJOR AXIS IN DOUBLE CURVATURE

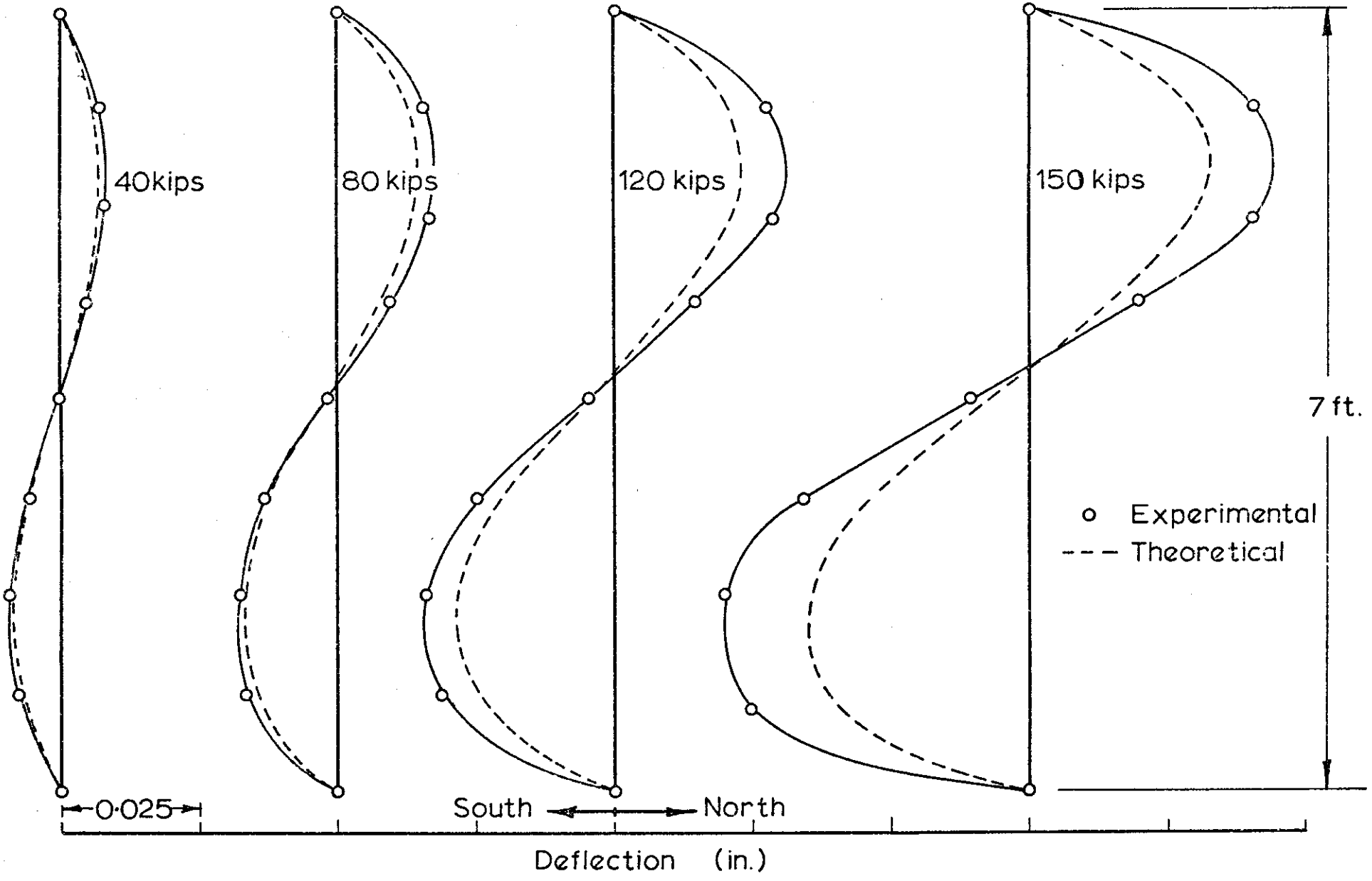

FIG. 5·17 DEFLECTION PROFILES FOR 7FT. COLUMN CC11 BENT ABOUT THE MAJOR AXIS IN DOUBLE CURVATURE

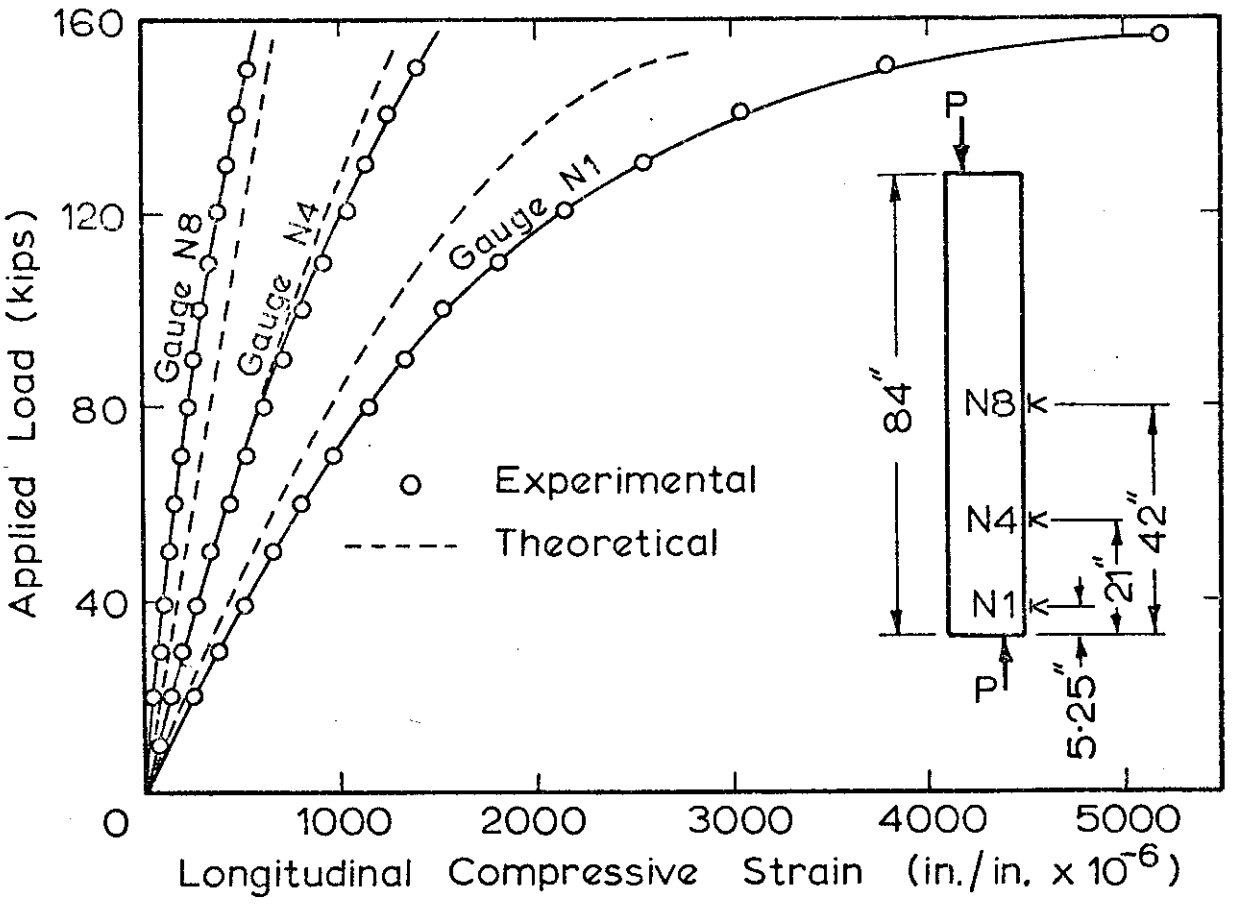

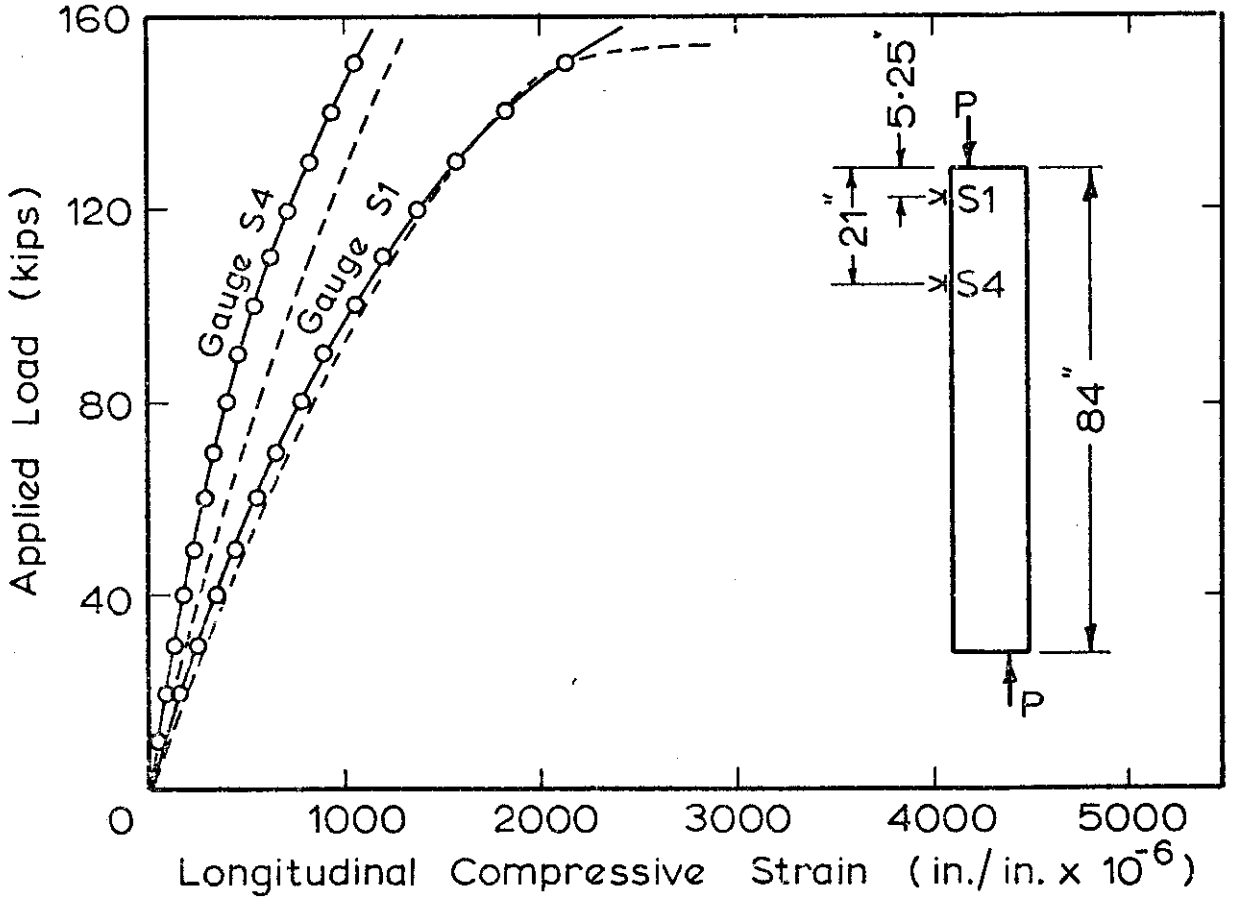

FIG. 5·18 STRAIN RESULTS FOR 7FT. COLUMN CC11 BENT ABOUT THE MAJOR AXIS IN DOUBLE CURVATURE.

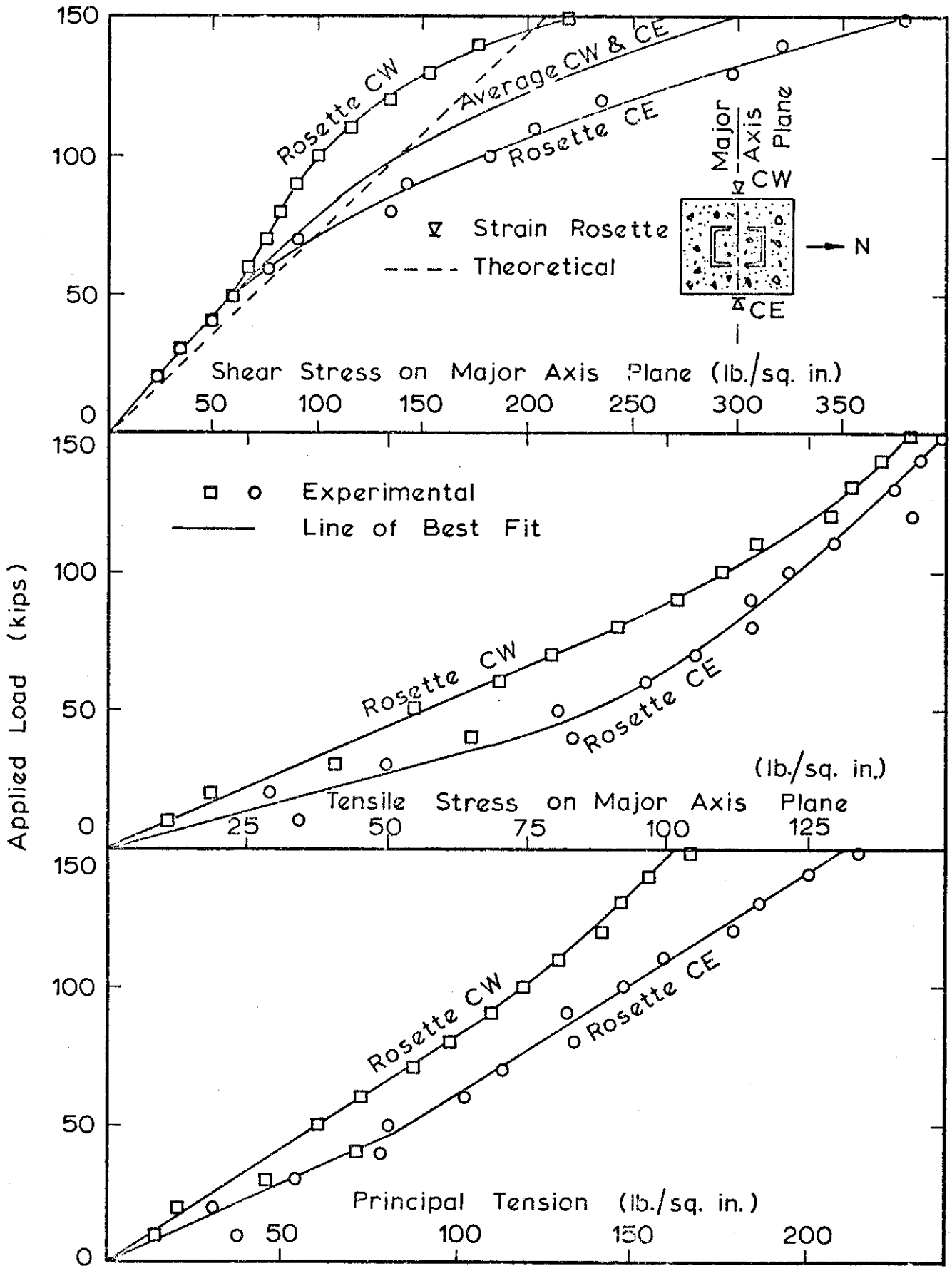

FIG. 5·19 STRESS CONDITION AT MIDHEIGHT FOR 7FT. COLUMN CC11 BENT IN DOUBLE CURVATURE ABOUT THE MAJOR AXIS

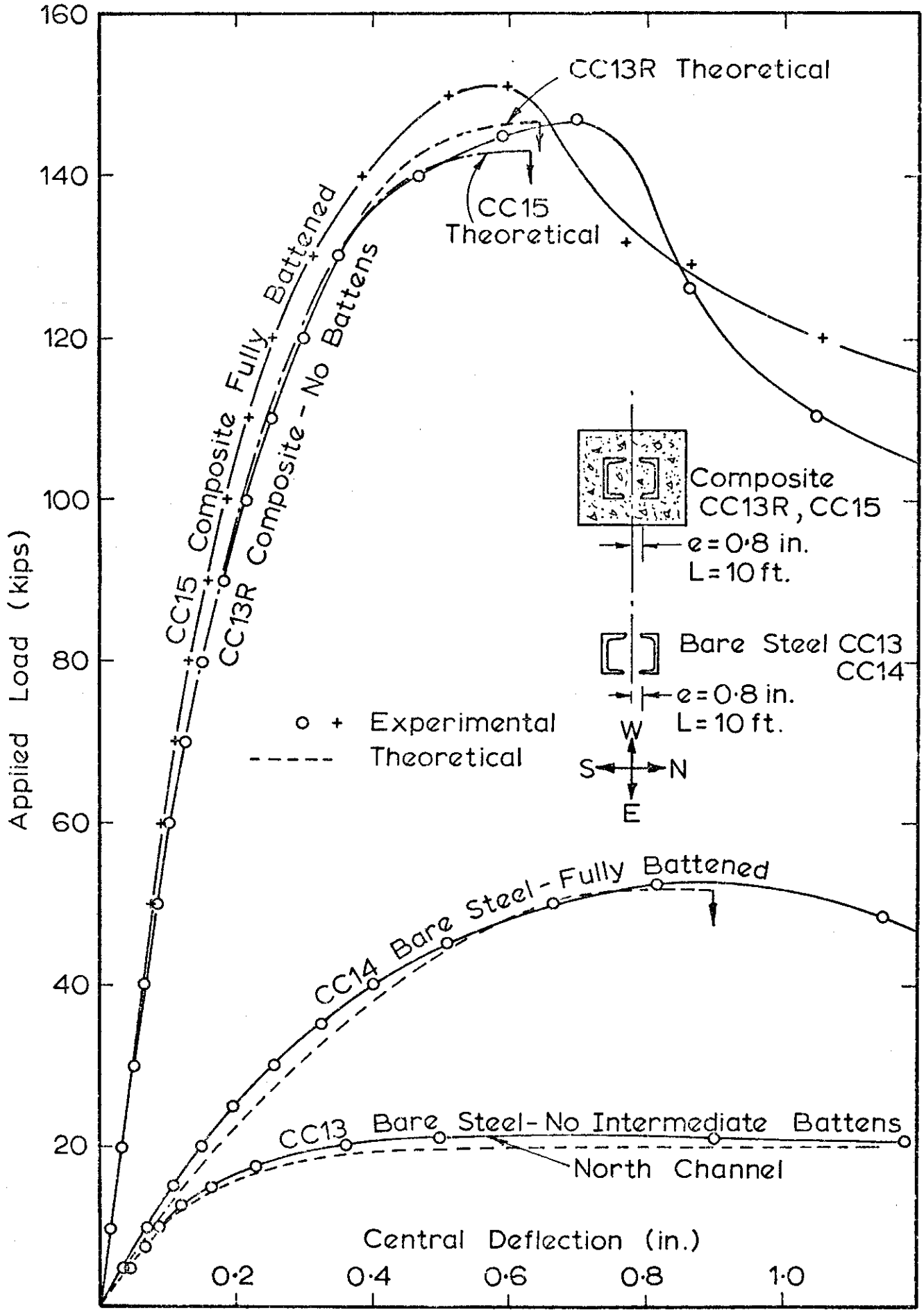

FIG. 5·20 LOAD – DEFLECTION RELATIONSHIPS FOR 10 FT. COLUMNS CC13, CC13R, CC14 AND CC15 BENT ABOUT THE MAJOR AXIS

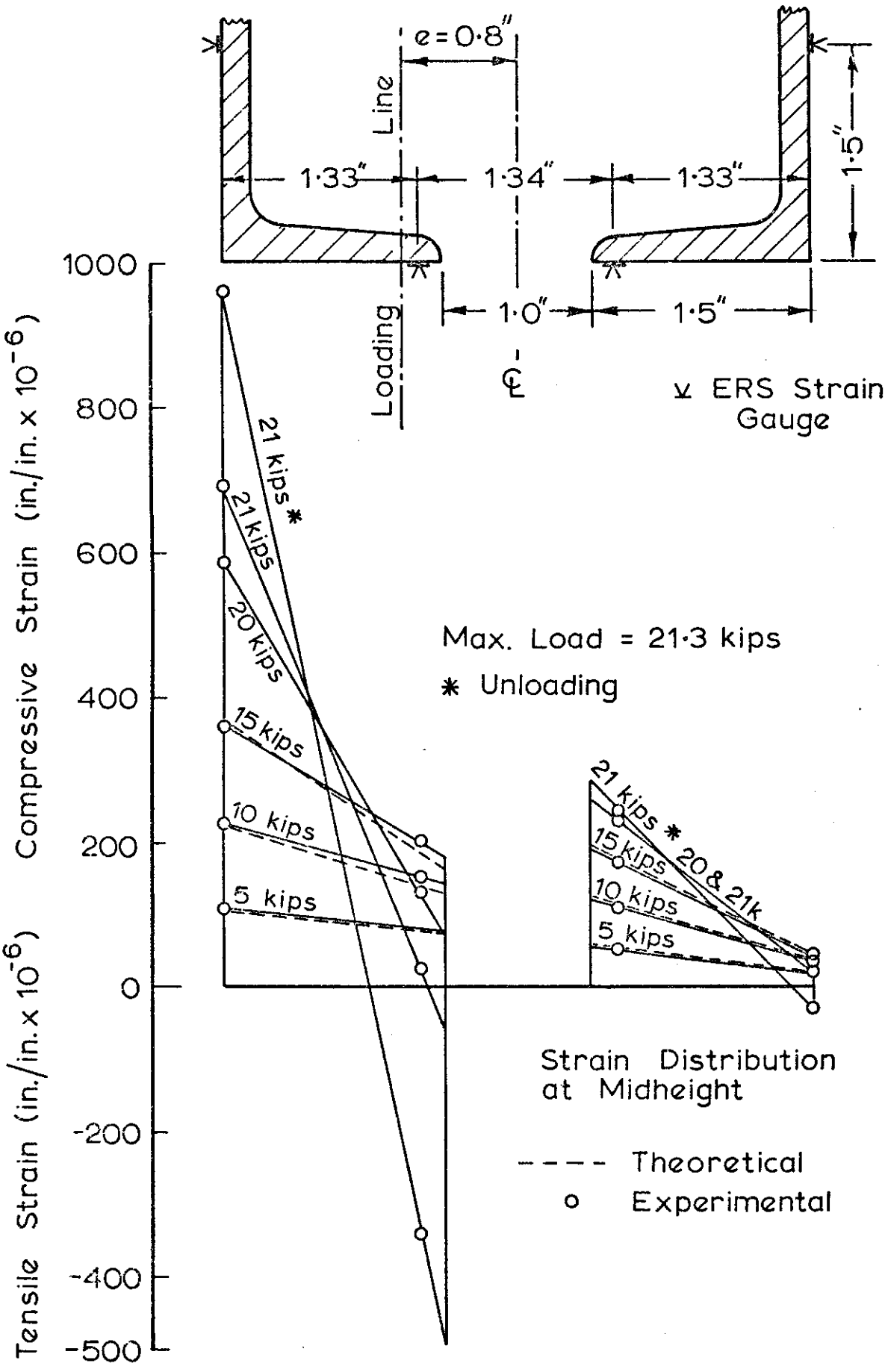

FIG. 5·21 STRAIN RESULTS FOR 10 FT. BARE STEEL UNBATTENED COLUMN CC13 BENT ABOUT THE MAJOR AXIS

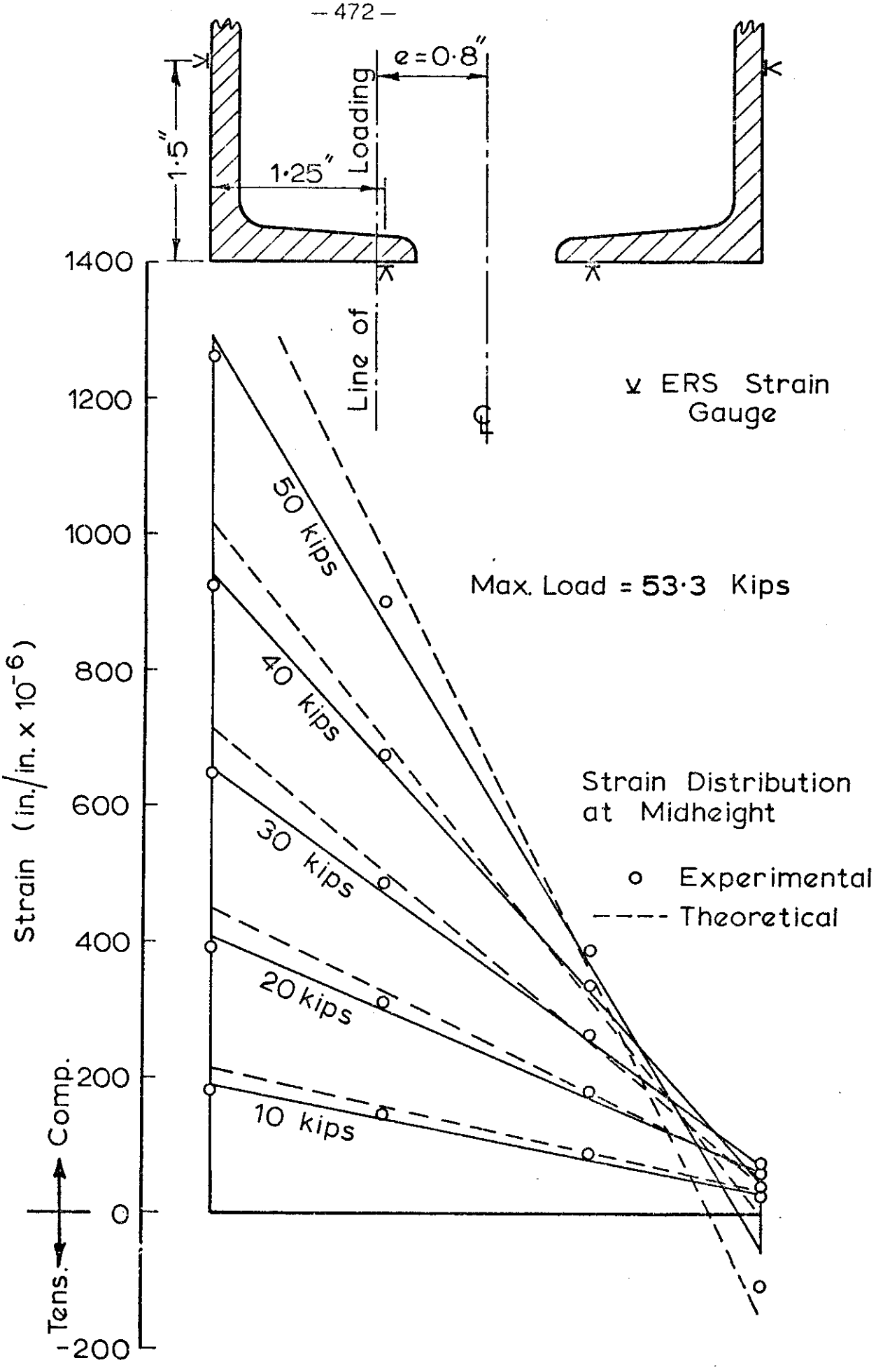

FIG 5·22 STRAIN RESULTS FOR 10 FT BARE STEEL BATTENED COLUMN CC14 BENT ABOUT THE MAJOR AXIS

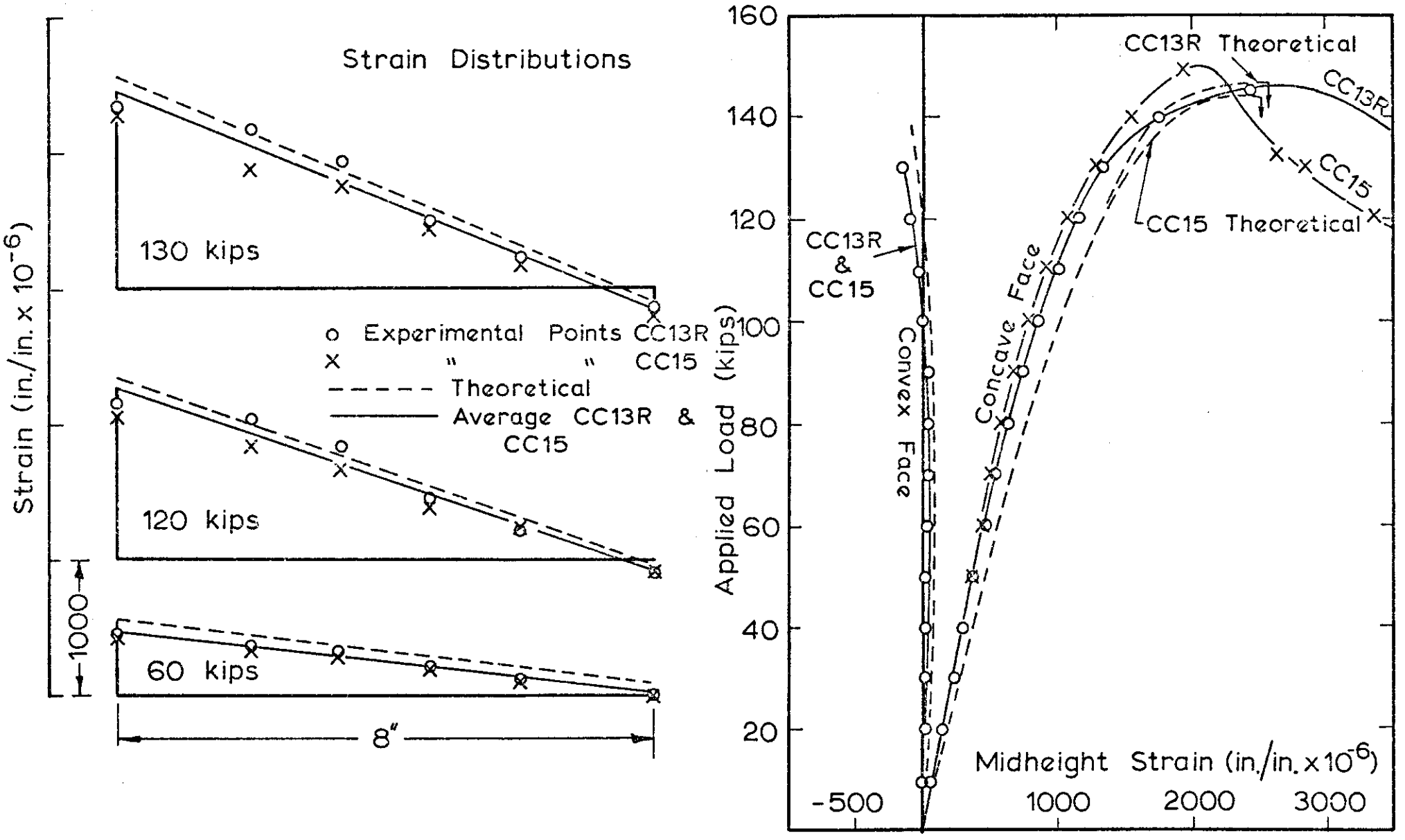

FIG. 5·23 STRAIN RESULTS FOR 10 FT. COMPOSITE COLUMNS CC13R, CC15 BENT ABOUT THE MAJOR AXIS

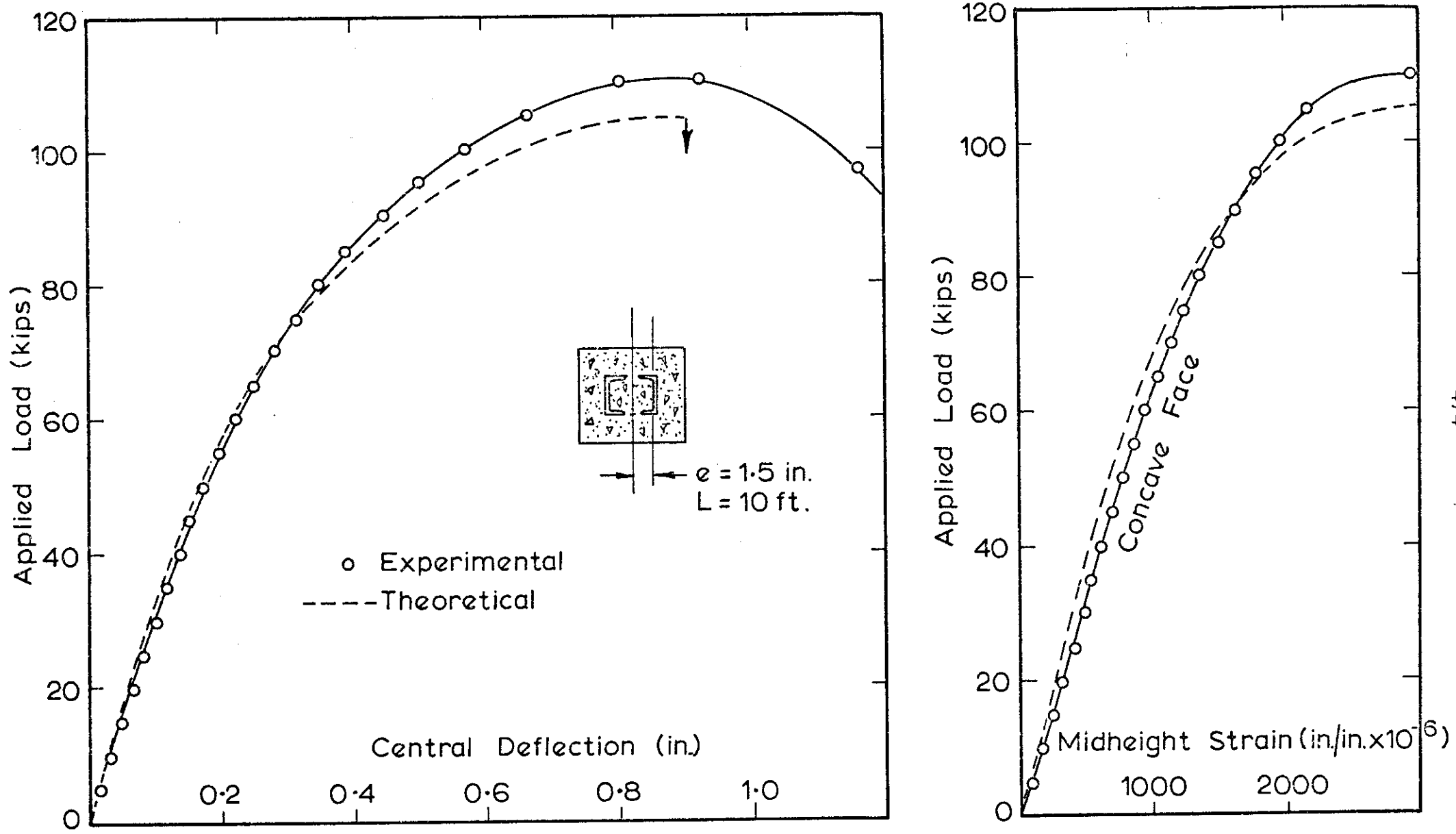

FIG. 5·24 LOAD – DEFLECTION AND STRAIN RESULTS FOR COLUMN CC16 BENT ABOUT THE MAJOR AXIS

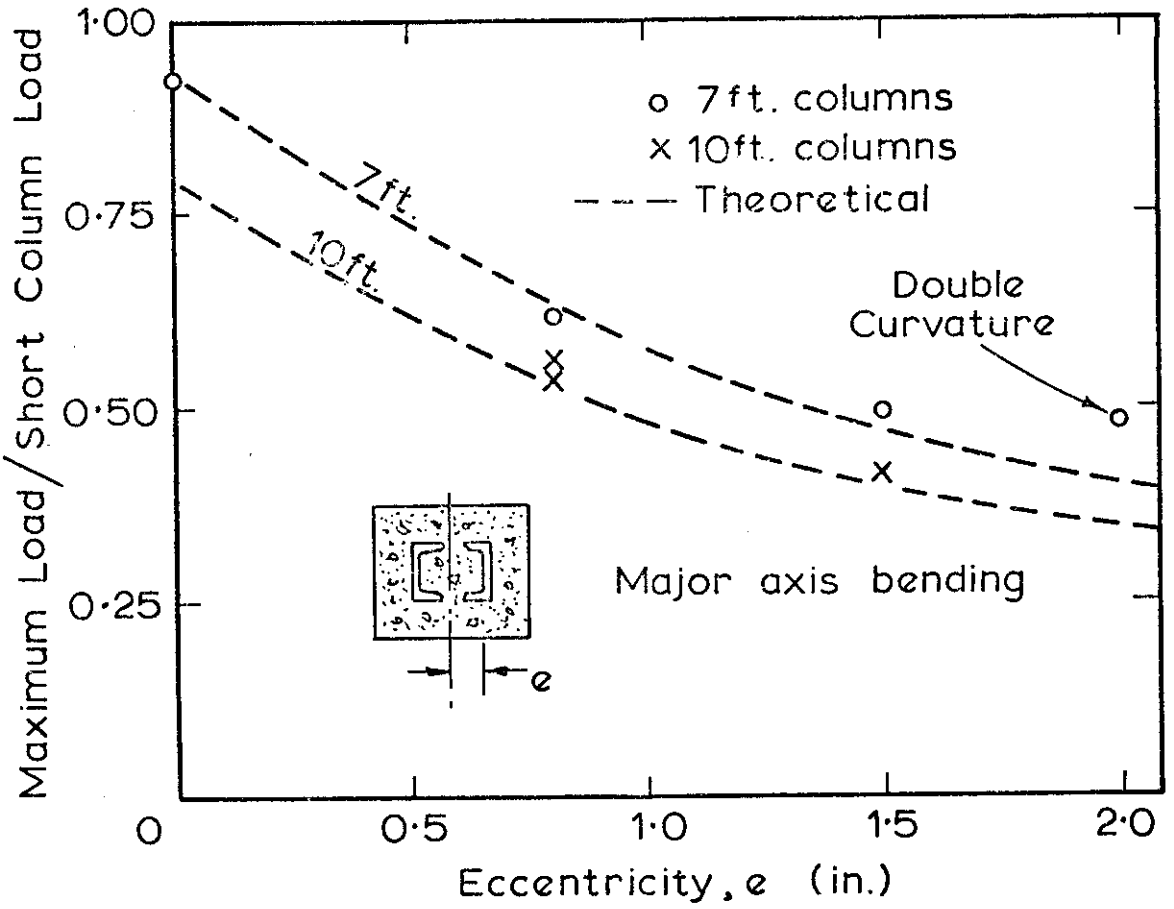

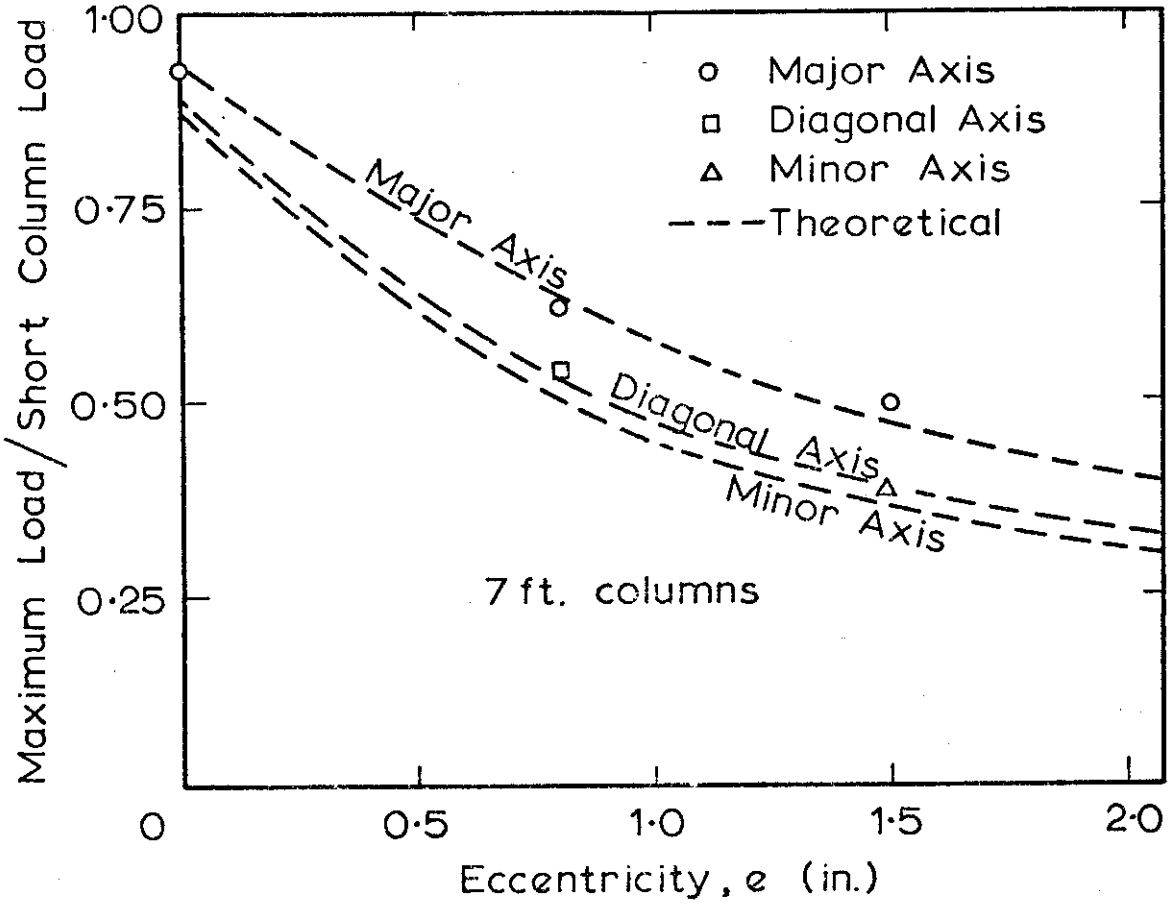

FIG 5·25 RELATIONSHIP BETWEEN DIMENSIONLESS MAXIMUM LOAD AND ECCENTRICITY FOR CC SERIES COMPOSITE COLUMNS

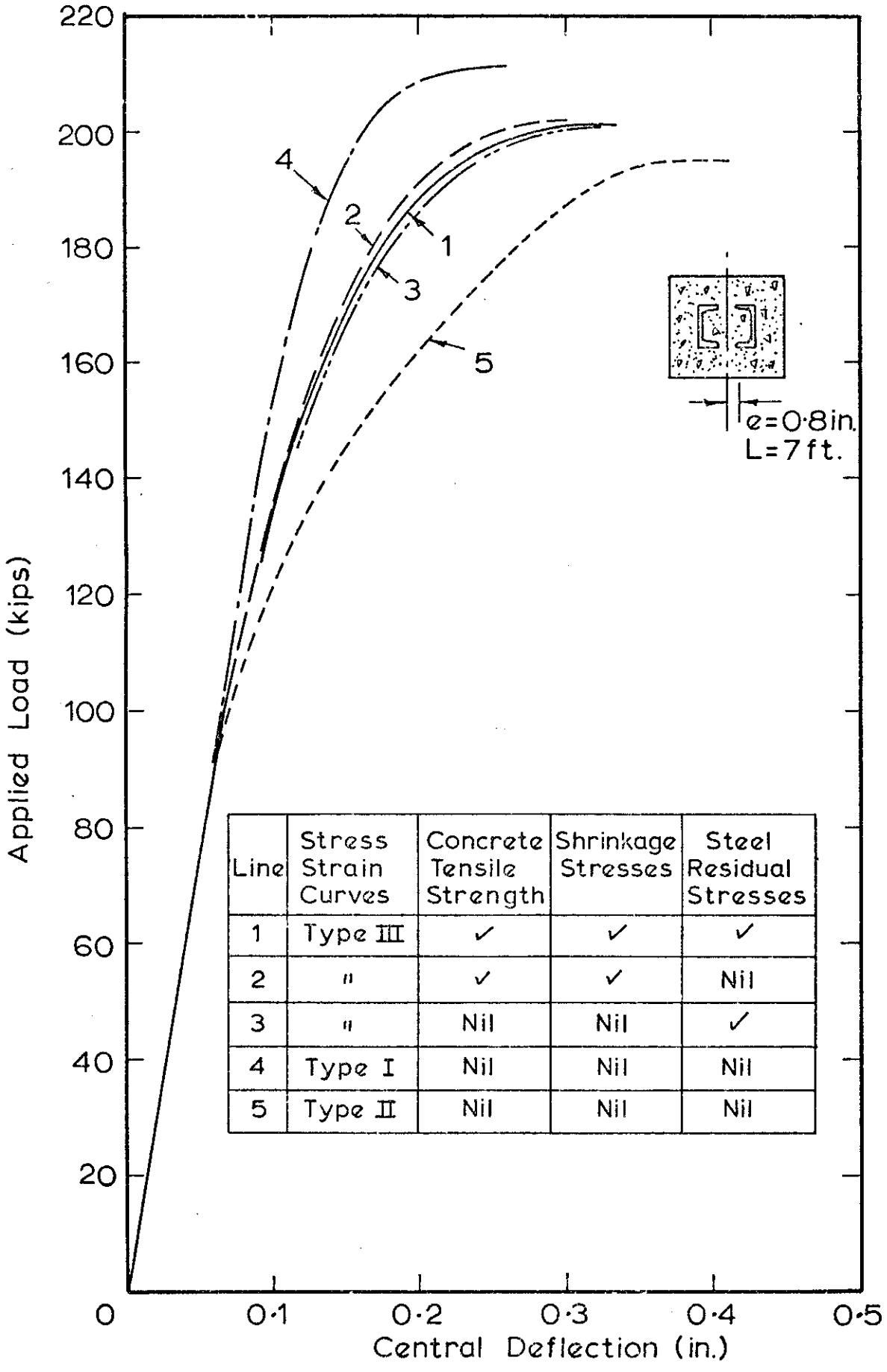

Line	Stress Strain Curves	Concrete Tensile Strength	Shrinkage Stresses	Steel Residual Stresses
1	Type III	✓	✓	✓
2	"	✓	✓	Nil
3	"	Nil	Nil	✓
4	Type I	Nil	Nil	Nil
5	Type II	Nil	Nil	Nil

FIG. 5·26 THEORETICAL LOAD – DEFLECTION RELATIONSHIPS FOR 7 FT COLUMN CC2 BENT ABOUT THE MAJOR AXIS.

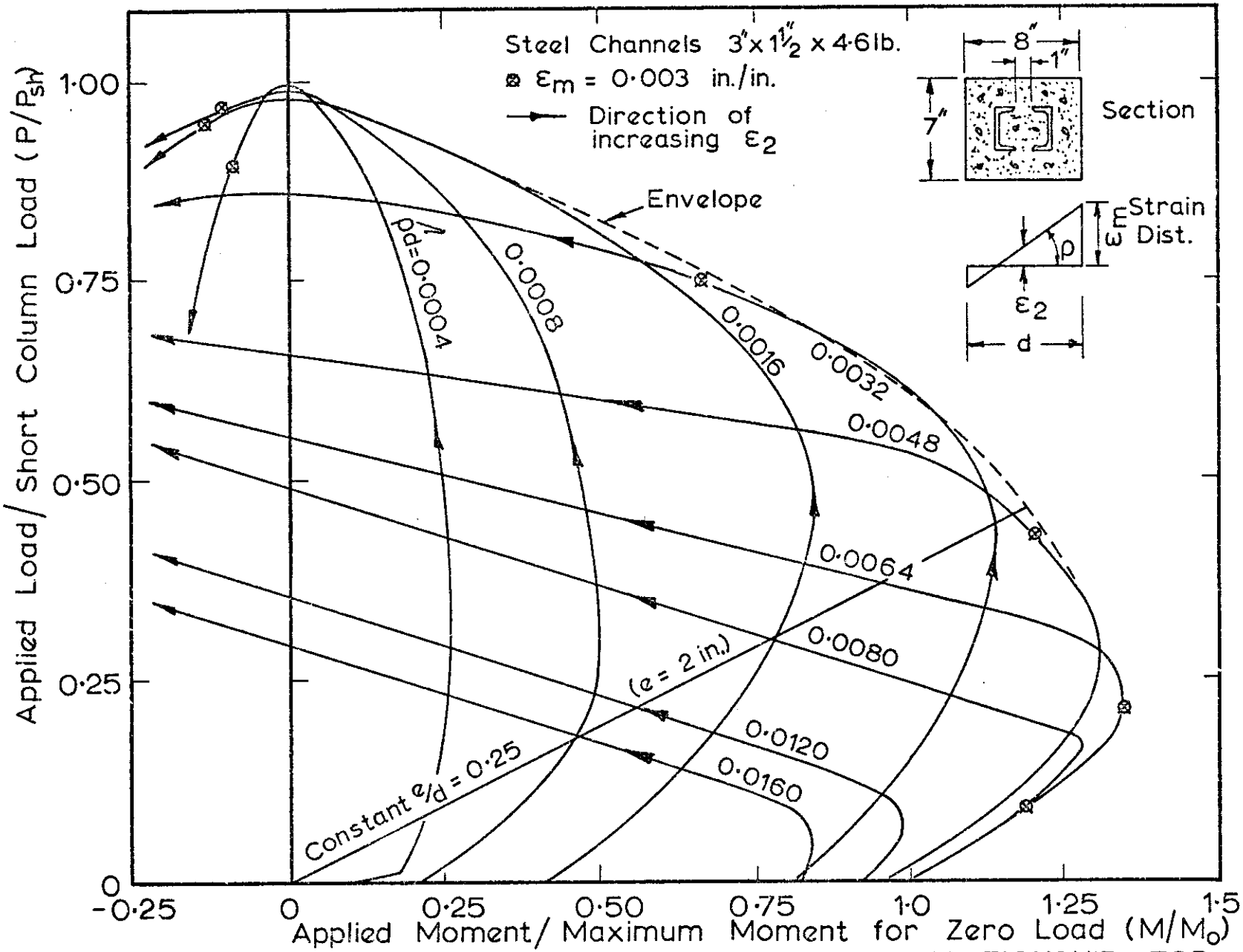

FIG. 5·27 DIMENSIONLESS LOAD - MOMENT- CURVATURE RELATIONSHIP FOR CC SERIES COMPOSITE SECTION WITH MOMENT ABOUT THE MAJOR AXIS

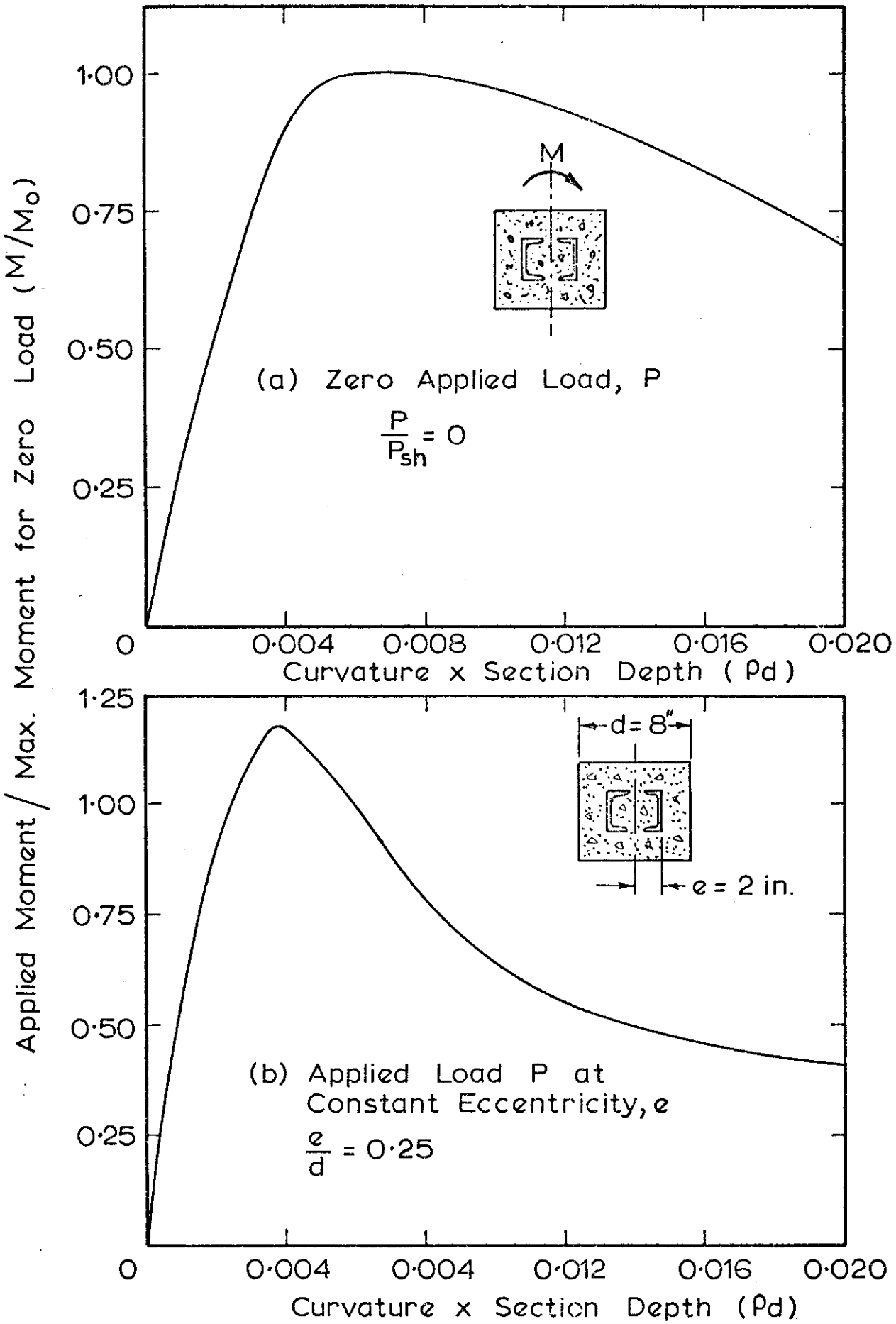

FIG. 5·28 DIMENSIONLESS MOMENT - CURVATURE RELATIONSHIPS FOR CC SERIES COMPOSITE SECTION

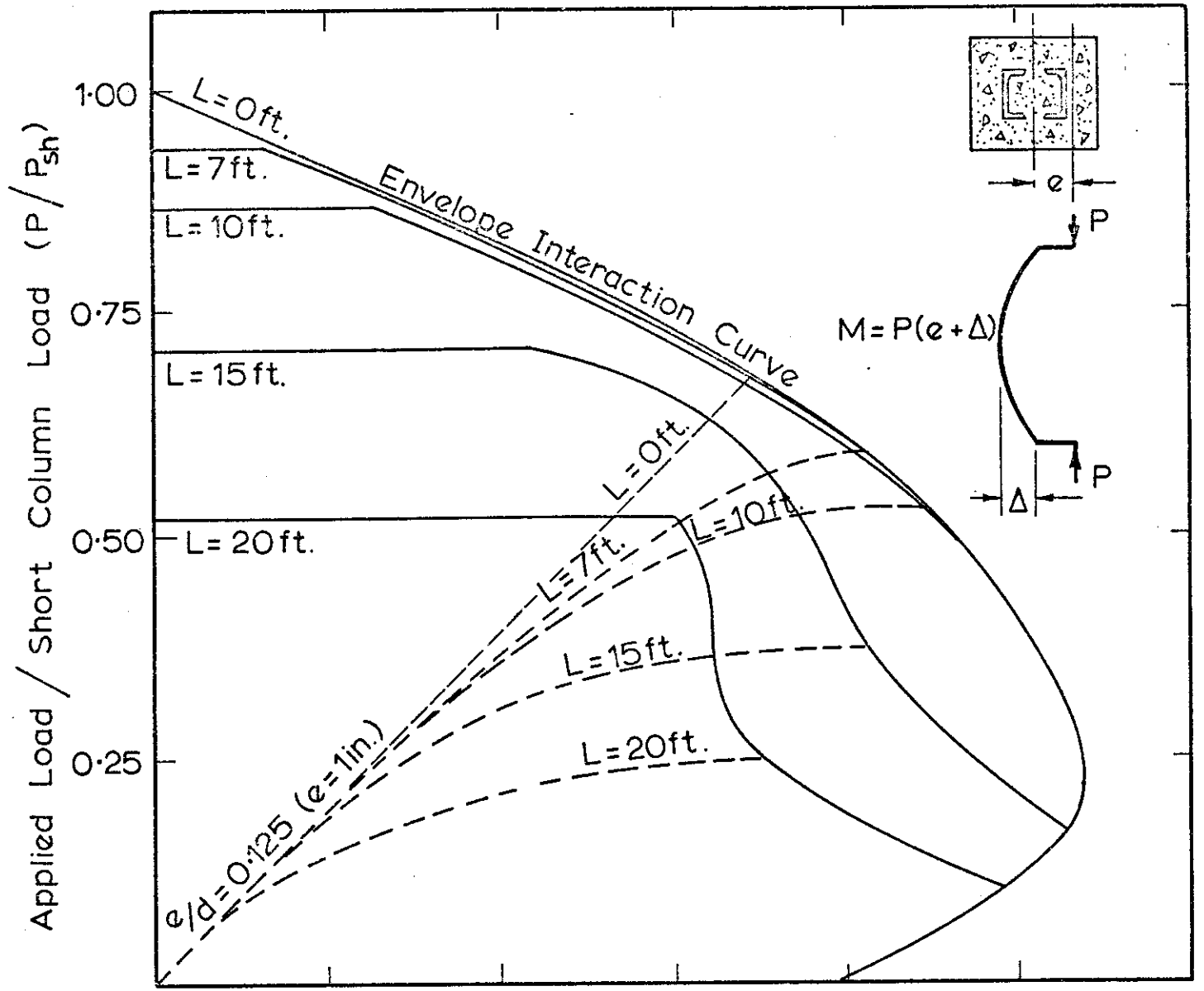

FIG 5·29 DIMENSIONLESS LOAD-MOMENT INTERACTION CURVES FOR CC SERIES COMPOSITE COLUMNS

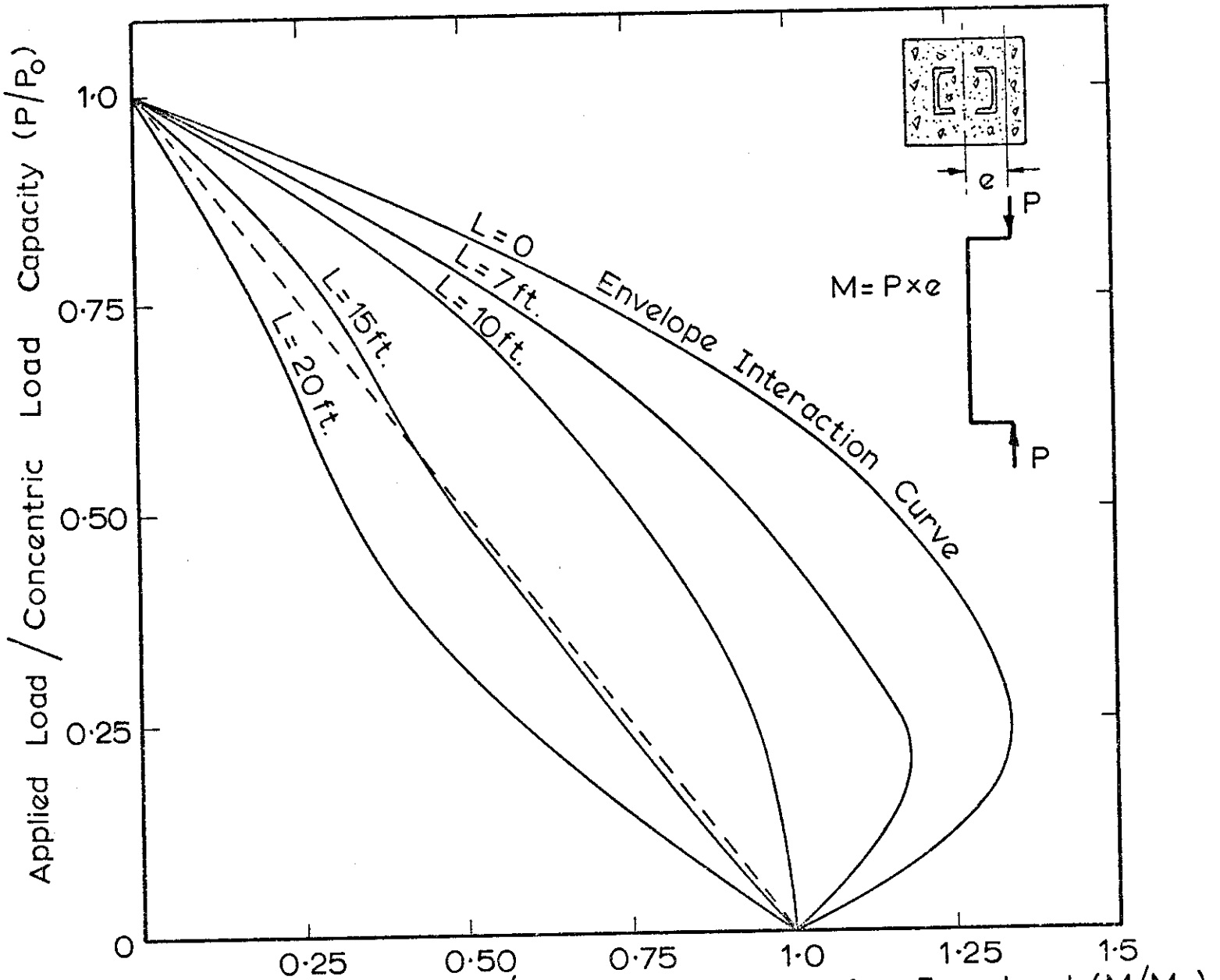

FIG. 5·30 DIMENSIONLESS LOAD-MOMENT INTERACTION CURVES FOR CC SERIES COMPOSITE COLUMNS

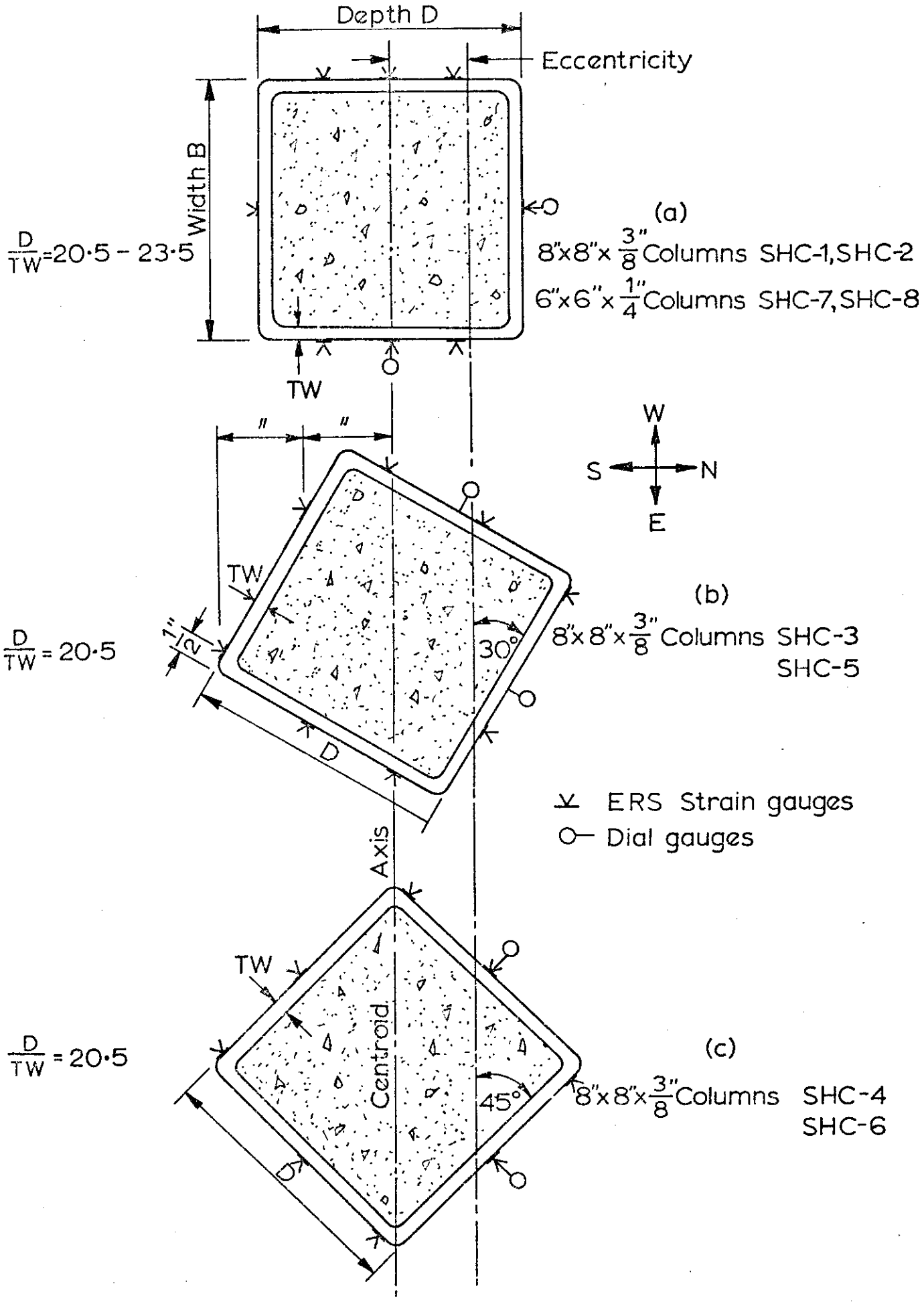

FIG. 6·1 CROSS SECTIONAL AND LOADING DETAILS FOR CONCRETE FILLED SQUARE TUBES. SHC COLUMN SERIES.

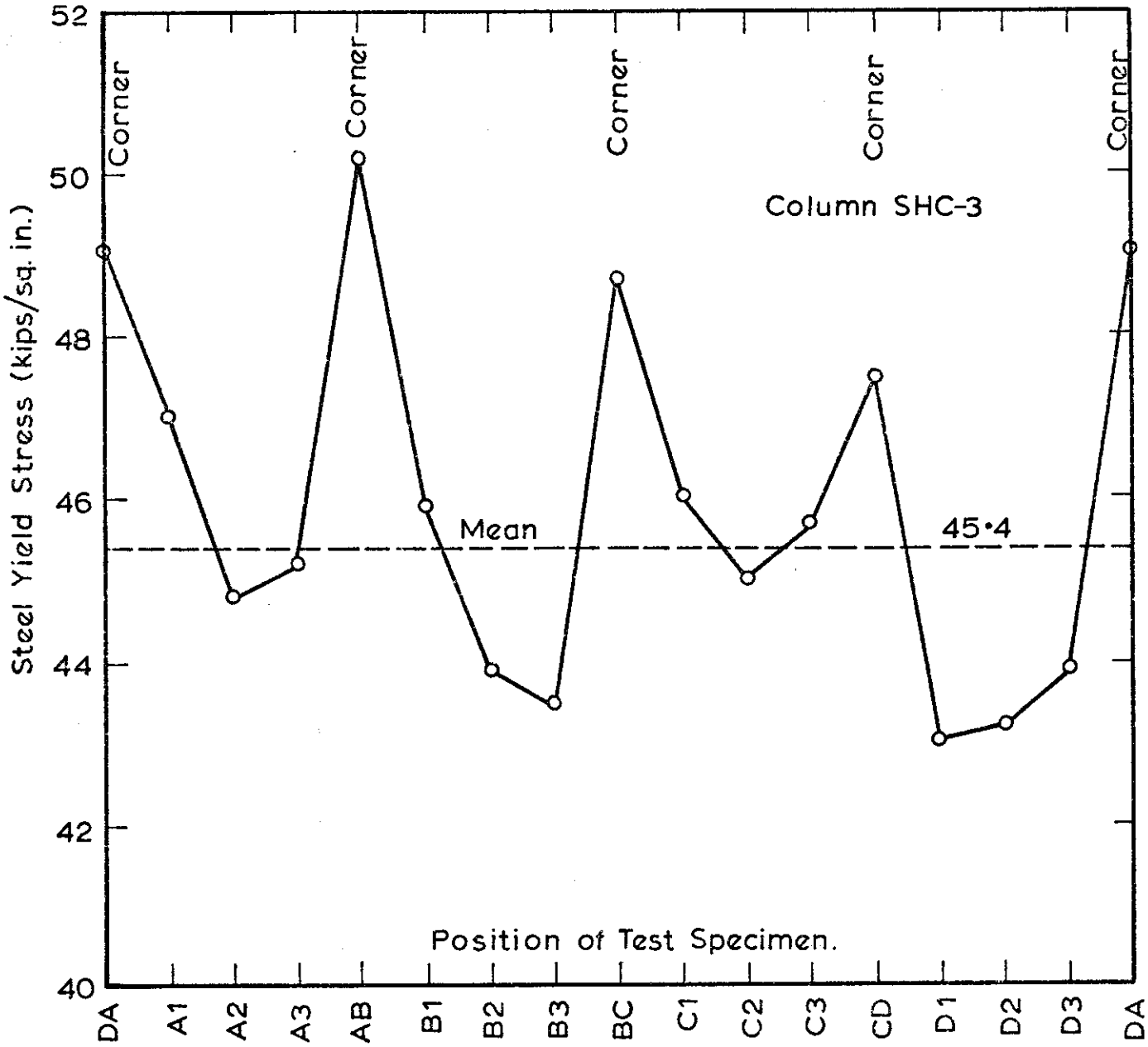

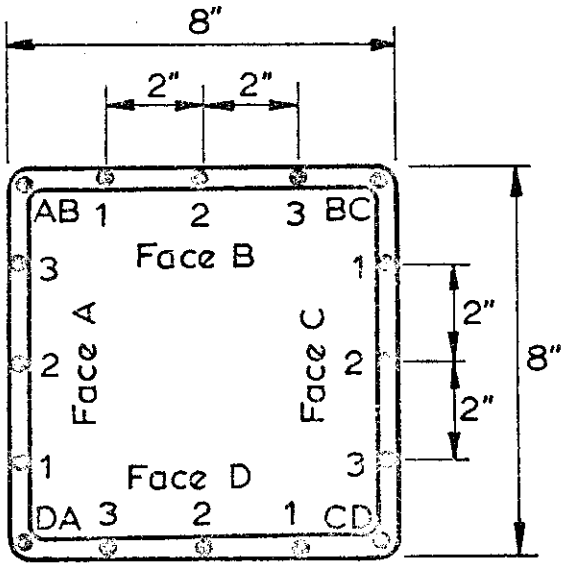

Position of Specimen

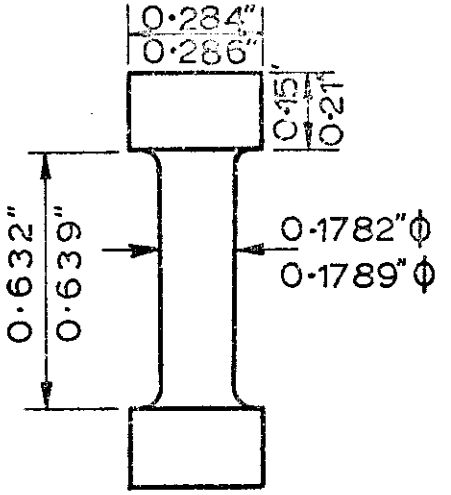

Hounsfield Test Piece No.12

FIG. 6·2 VARIATION OF STEEL YIELD STRESS WITH POSITION ON TUBE.

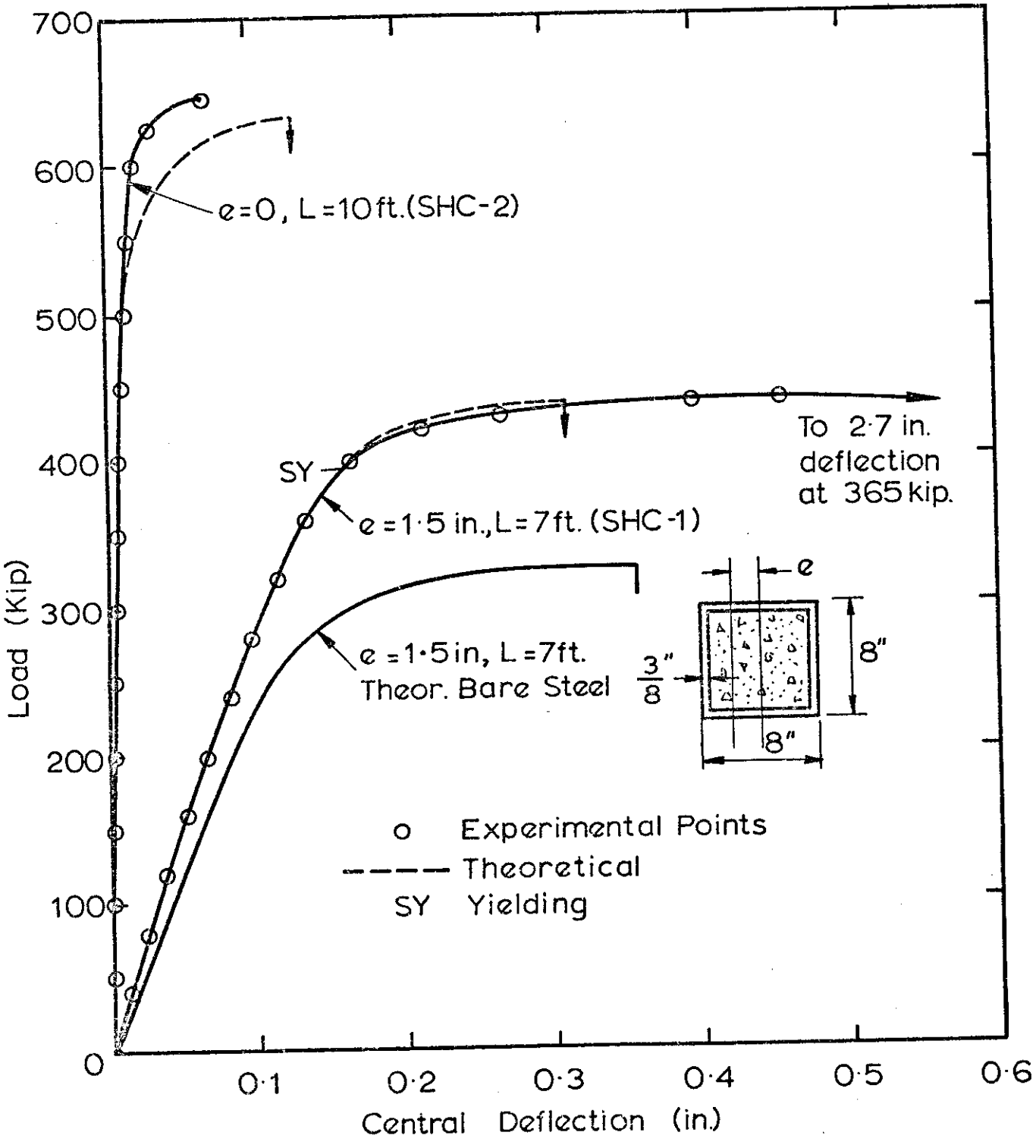

FIG. 6·3 LOAD-CENTRAL DEFLECTION CURVES FOR COLUMNS SHC-1 AND SHC-2.

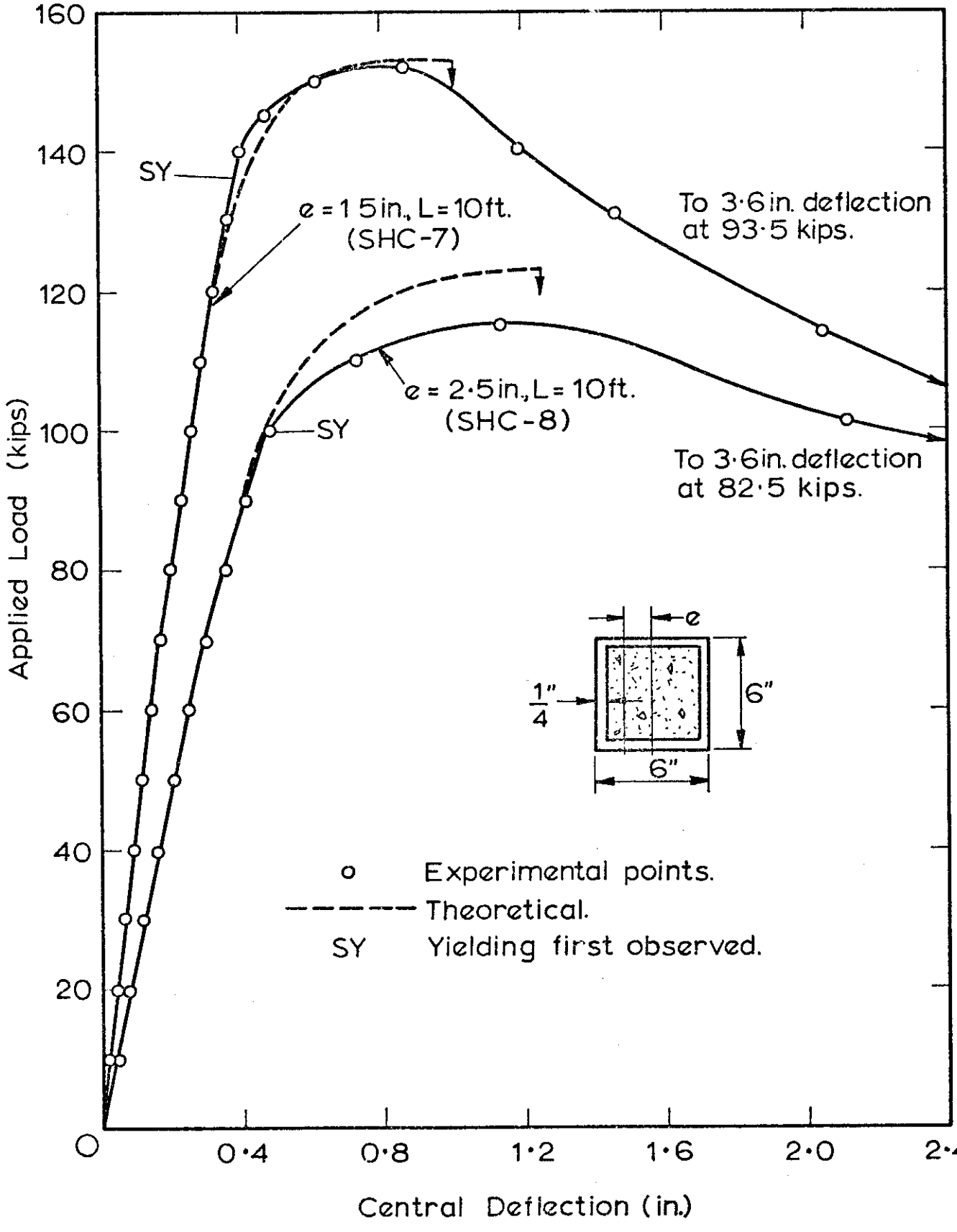

FIG. 6·4 LOAD CENTRAL DEFLECTION CURVES FOR COLUMNS SHC-7 AND SHC-8

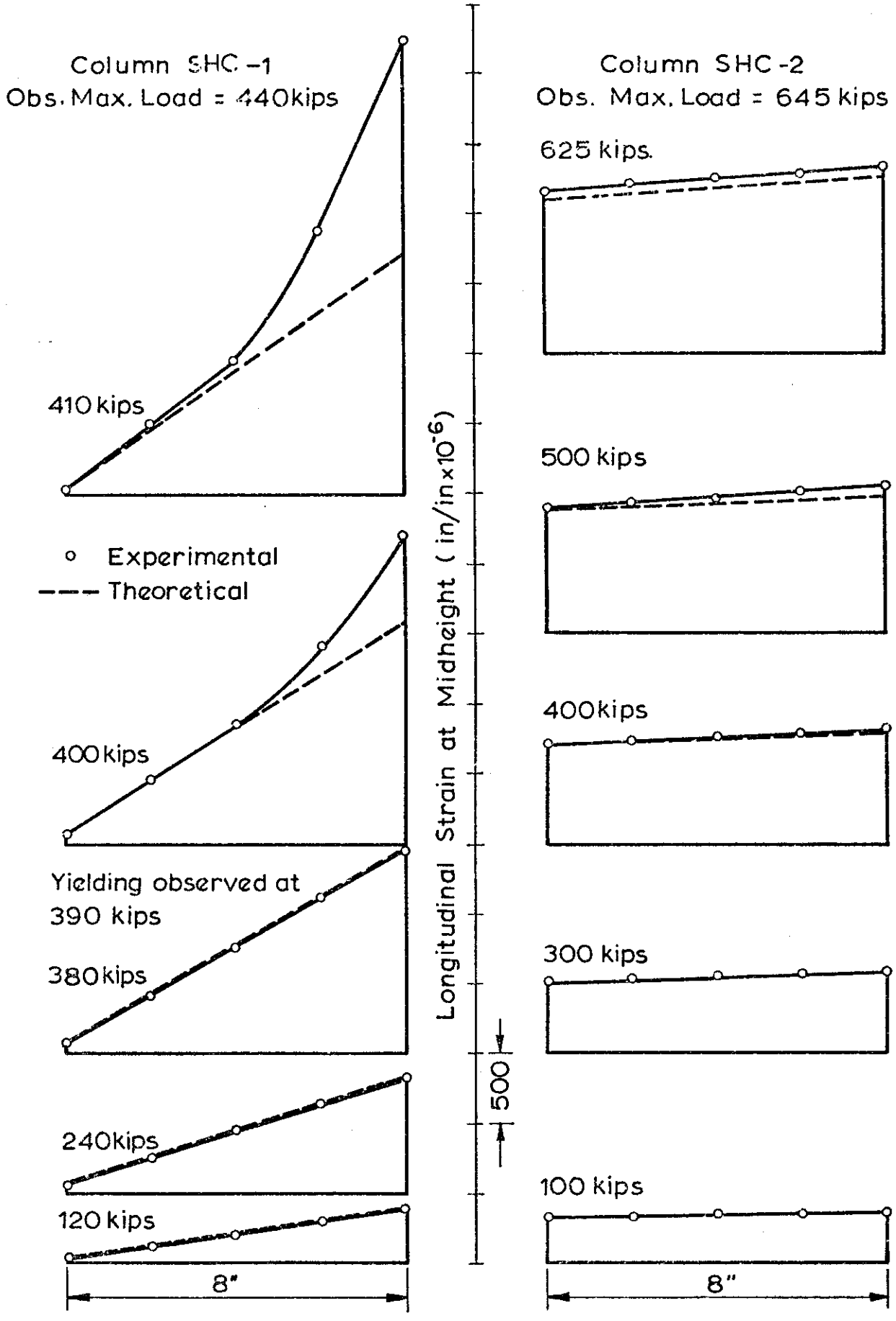

FIG. 6·5 MIDHEIGHT STRAIN DISTRIBUTIONS FOR 8IN. x 8IN. x 3/8 IN. CONCRETE FILLED TUBES WITH 0° LOADING AXIS INCLINATION.

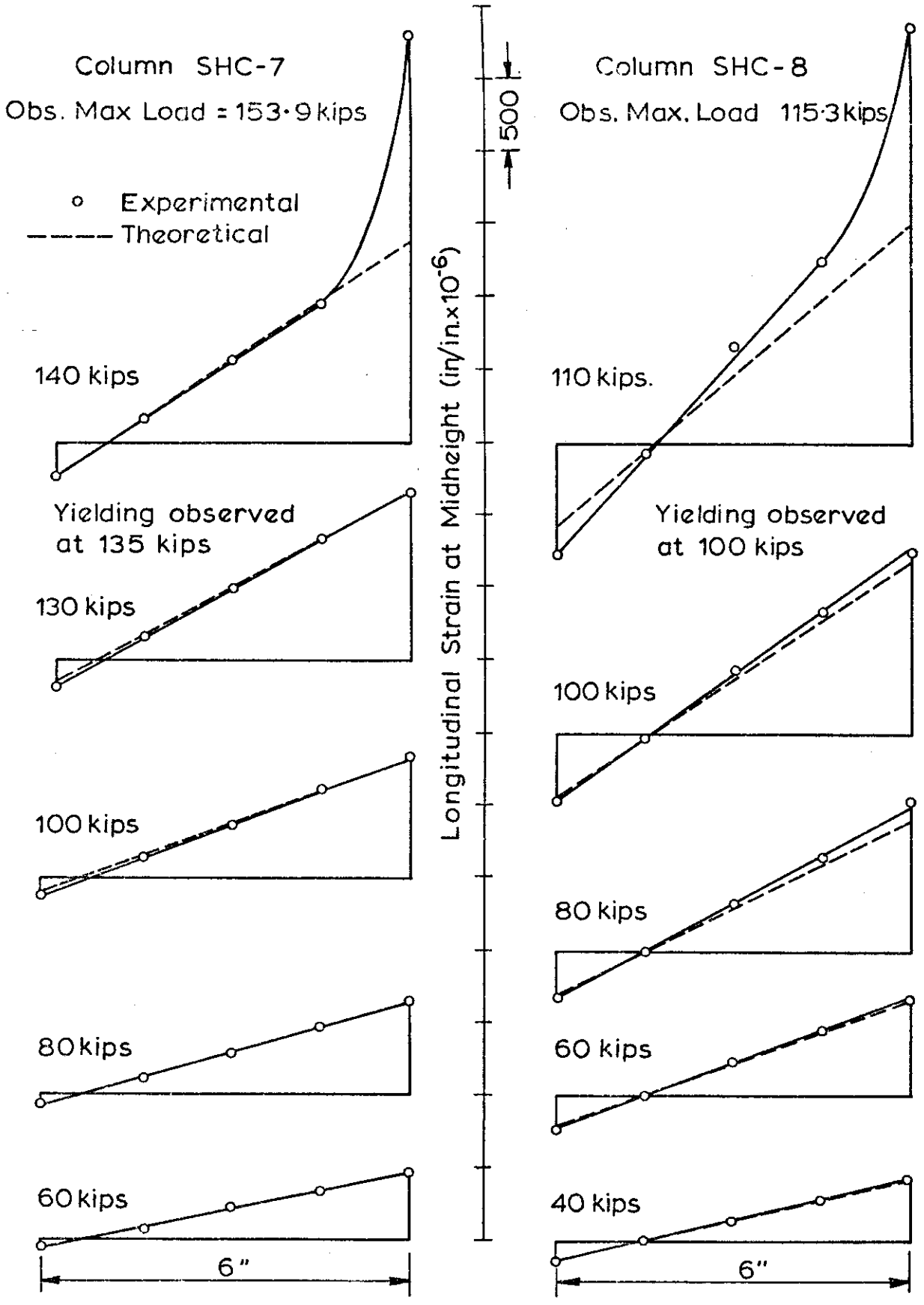

FIG. 6·6 MIDHEIGHT DISTRIBUTIONS FOR 6 IN. x 6 IN. x $\frac{1}{4}$ IN. CONCRETE FILLED TUBES WITH 0° LOADING AXIS INCLINATION.

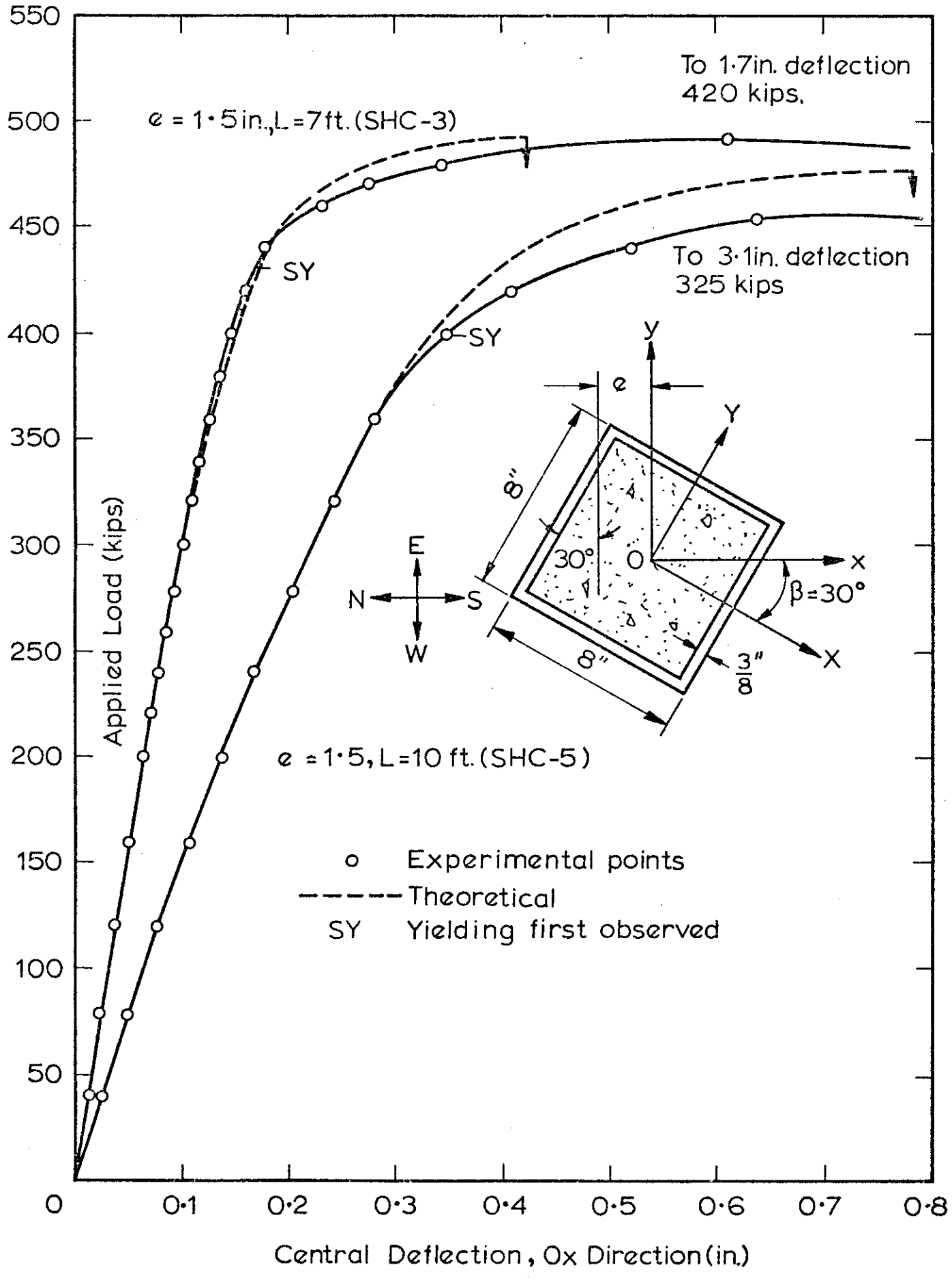

FIG. 6·7 LOAD DEFLECTION RELATIONSHIPS FOR 8 IN. x 8 IN. x $\frac{3}{8}$ IN. CONCRETE FILLED TUBES WITH 30° LOADING AXIS INCLINATION.

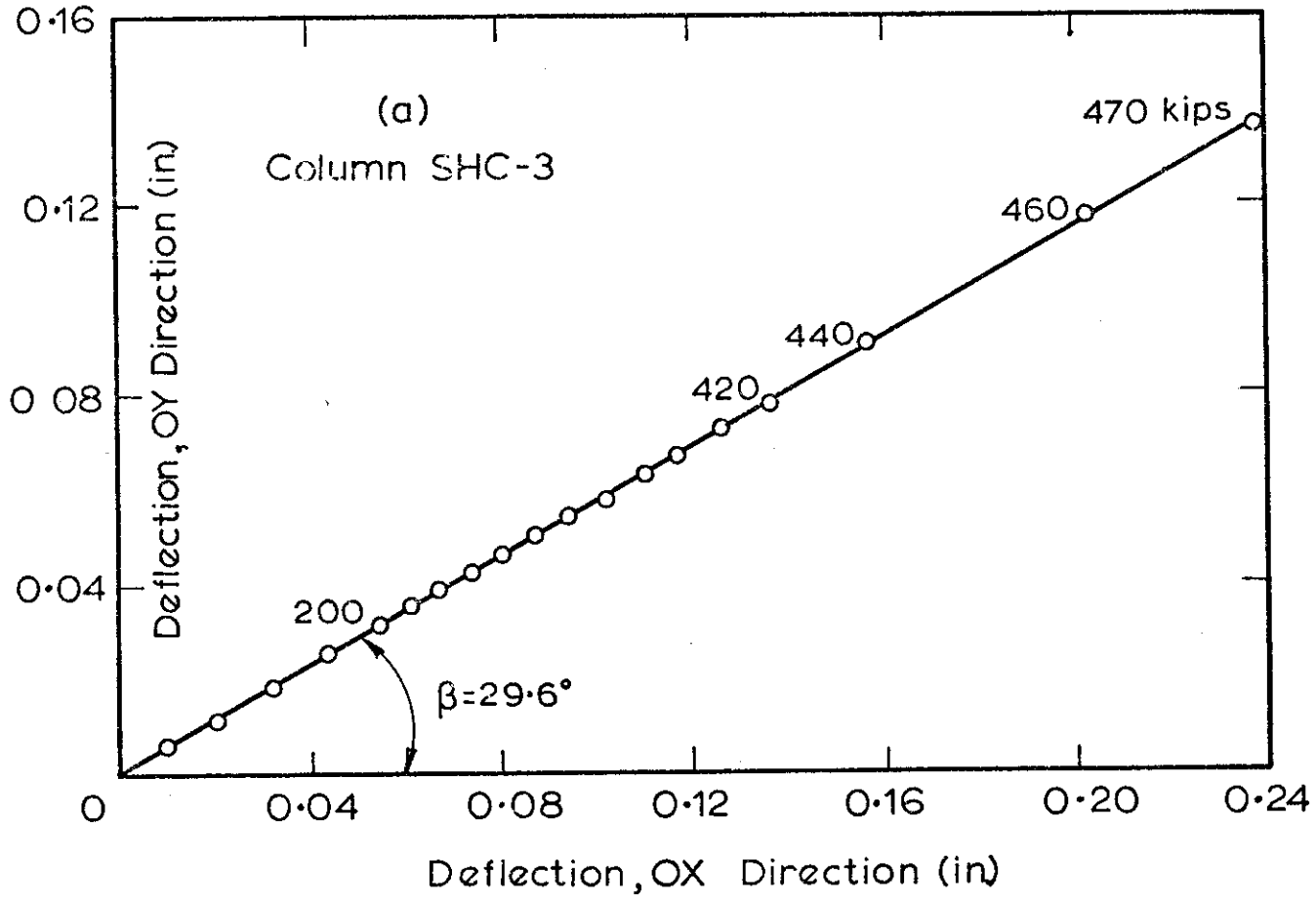

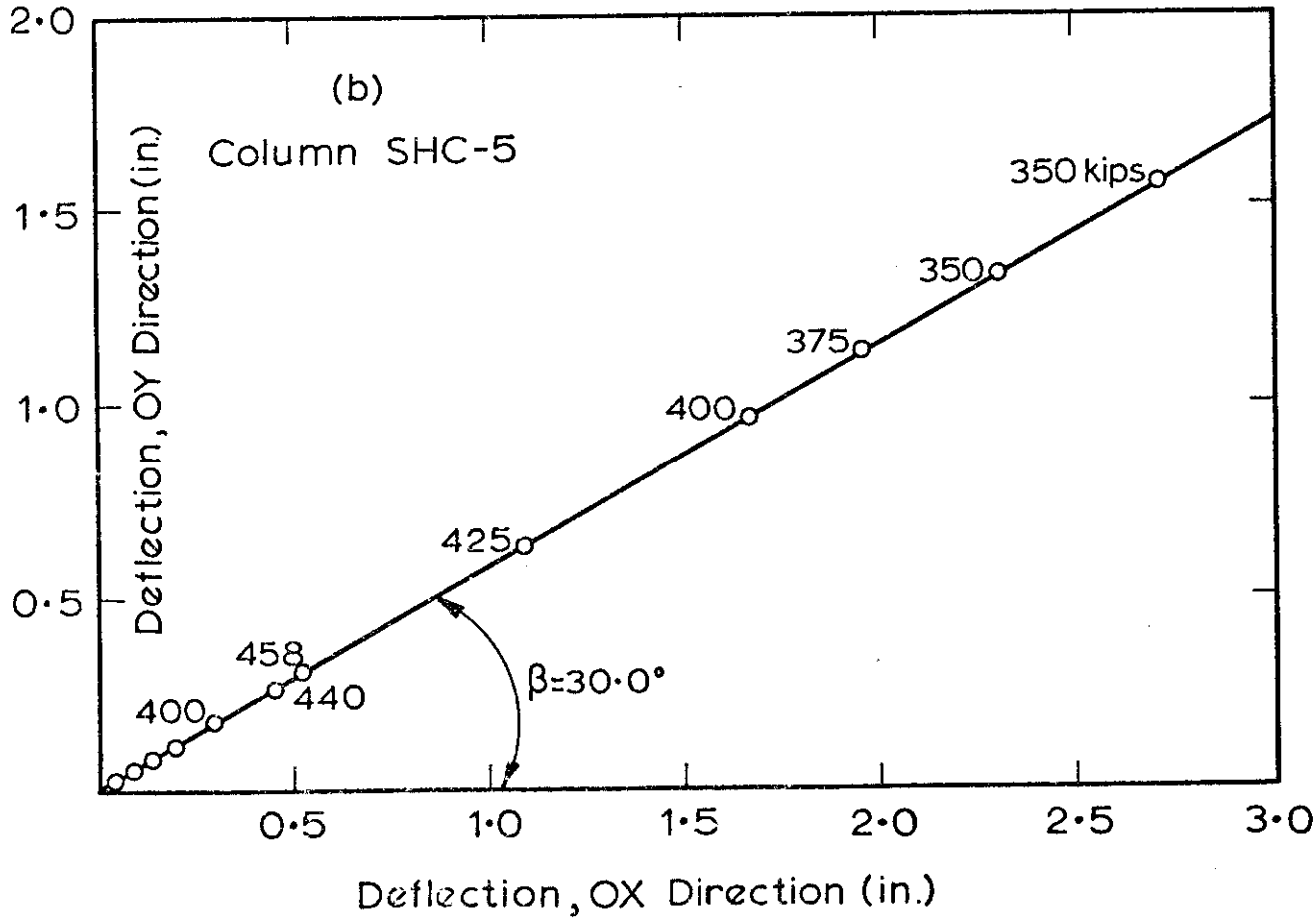

FIG. 6·8 RELATIONSHIP BETWEEN DEFLECTIONS IN THE TWO PRINCIPAL DIRECTIONS FOR 8IN. x 8IN. x $\frac{3}{8}$ IN. CONCRETE FILLED TUBES WITH 30° LOADING AXIS INCLINATION.

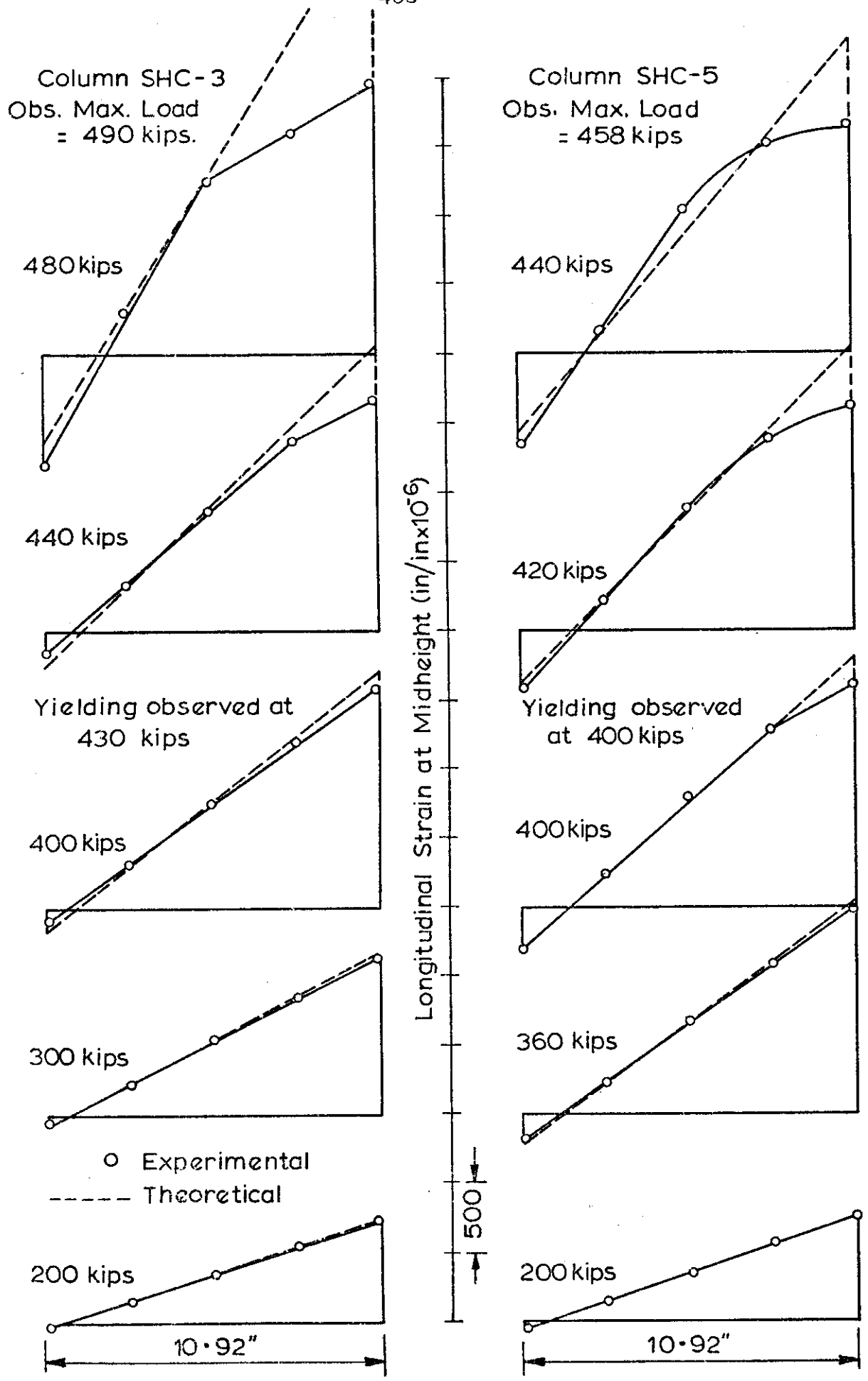

FIG. 6·9 MIDHEIGHT STRAIN DISTRIBUTIONS FOR 8 IN x 8 IN x $\frac{3}{8}$ IN. CONCRETE FILLED TUBES WITH 30° LOADING AXIS INCLINATION.

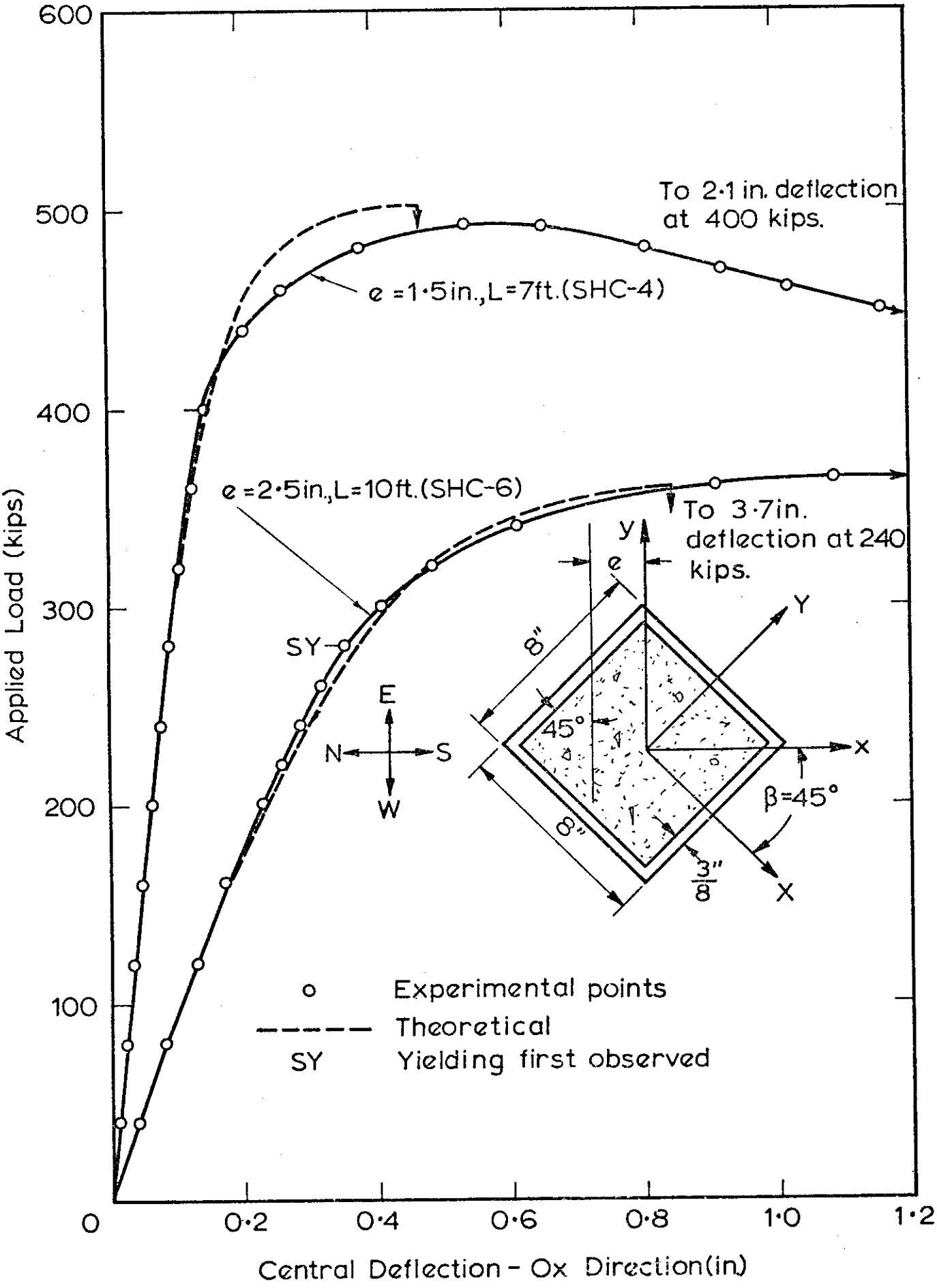

FIG. 6·10 LOAD-DEFLECTION RELATIONSHIPS 8IN.x 8IN.x $\frac{3}{8}$ IN. CONCRETE FILLED TUBES WITH 45° LOADING AXIS INCLINATION.

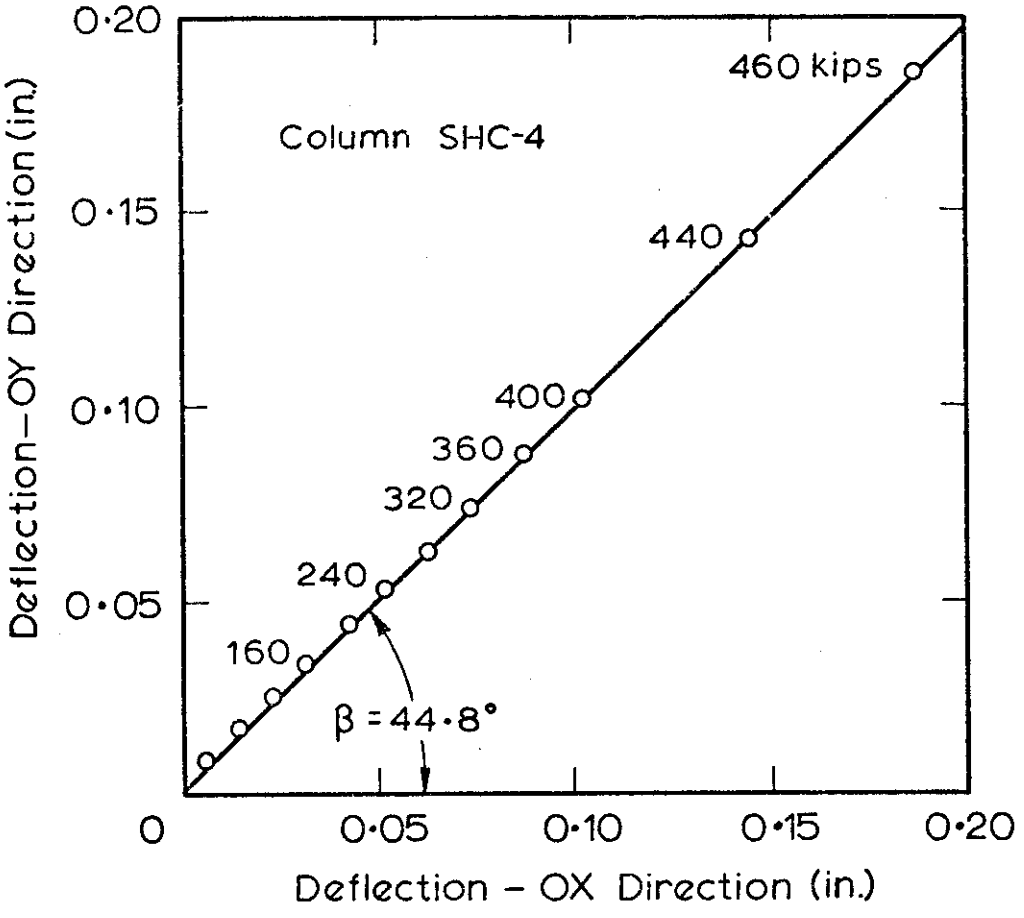

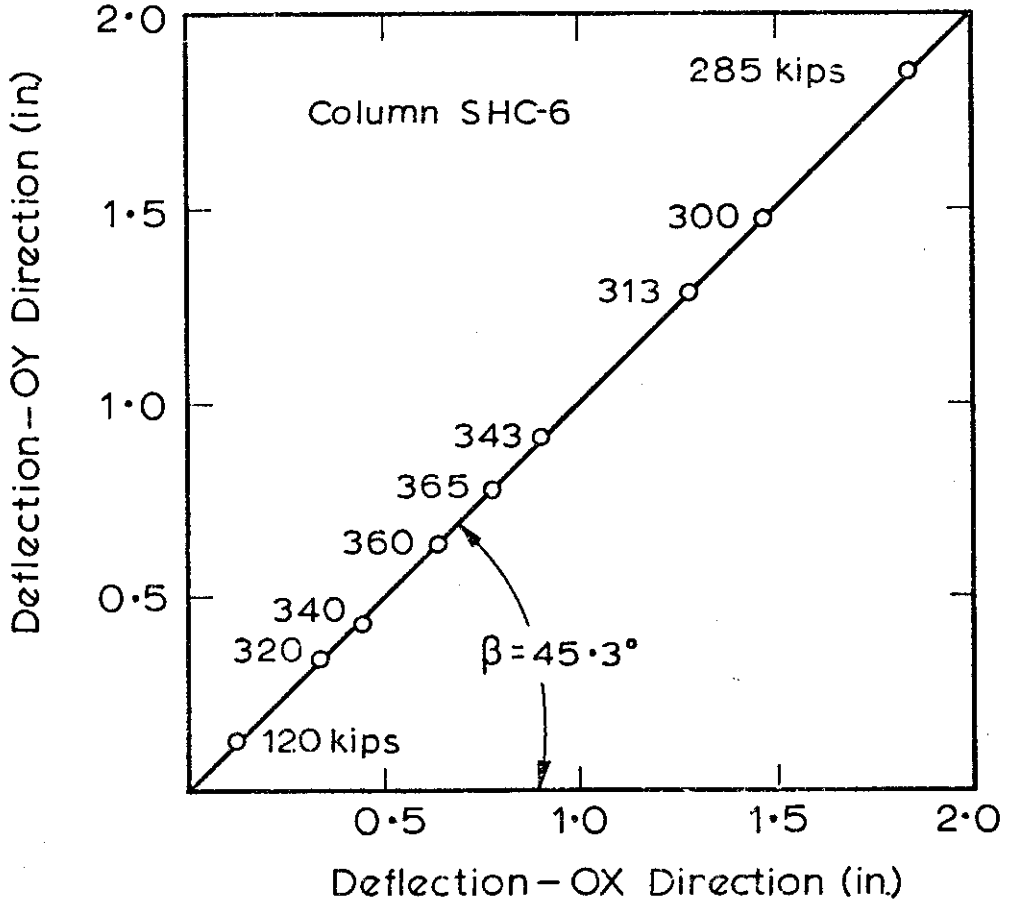

FIG. 6·11 RELATIONSHIP BETWEEN DEFLECTION IN THE TWO PRINCIPAL DIRECTION FOR 8 IN. x 8 IN. x $\frac{3}{8}$ IN. CONCRETE FILLED TUBES WITH 45° LOADING AXIS INCLINATION.

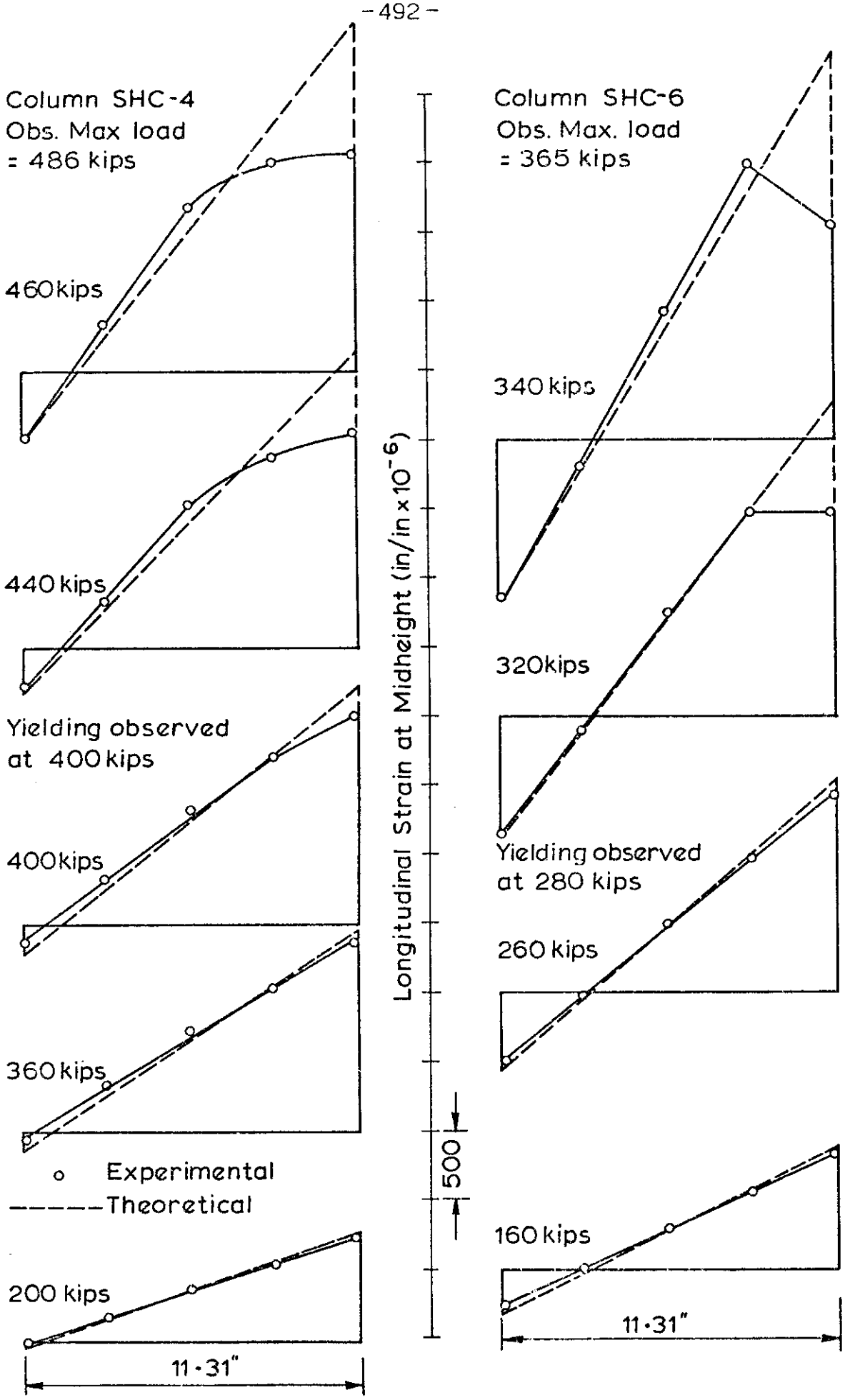

FIG. 6·12 MIDHEIGHT STRAIN DISTRIBUTION FOR 8 IN. x 8 IN. x $\frac{3}{8}$ IN. CONCRETE FILLED TUBES WITH 45° LOADING AXIS INCLINATION.

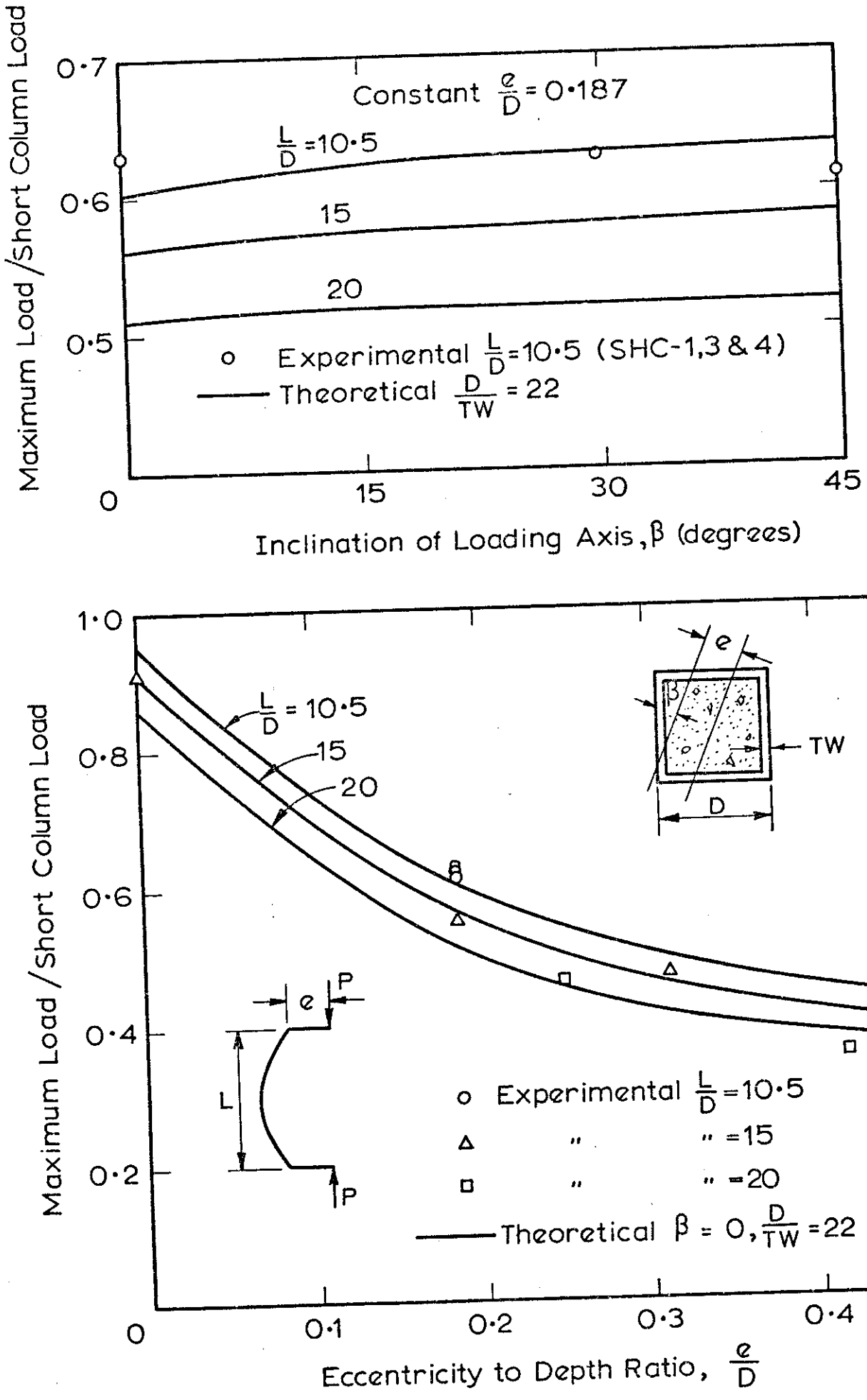

FIG.6·13 SUMMARY OF RESULTS FOR TESTS ON CONCRETE FILLED SQUARE STEEL TUBES.

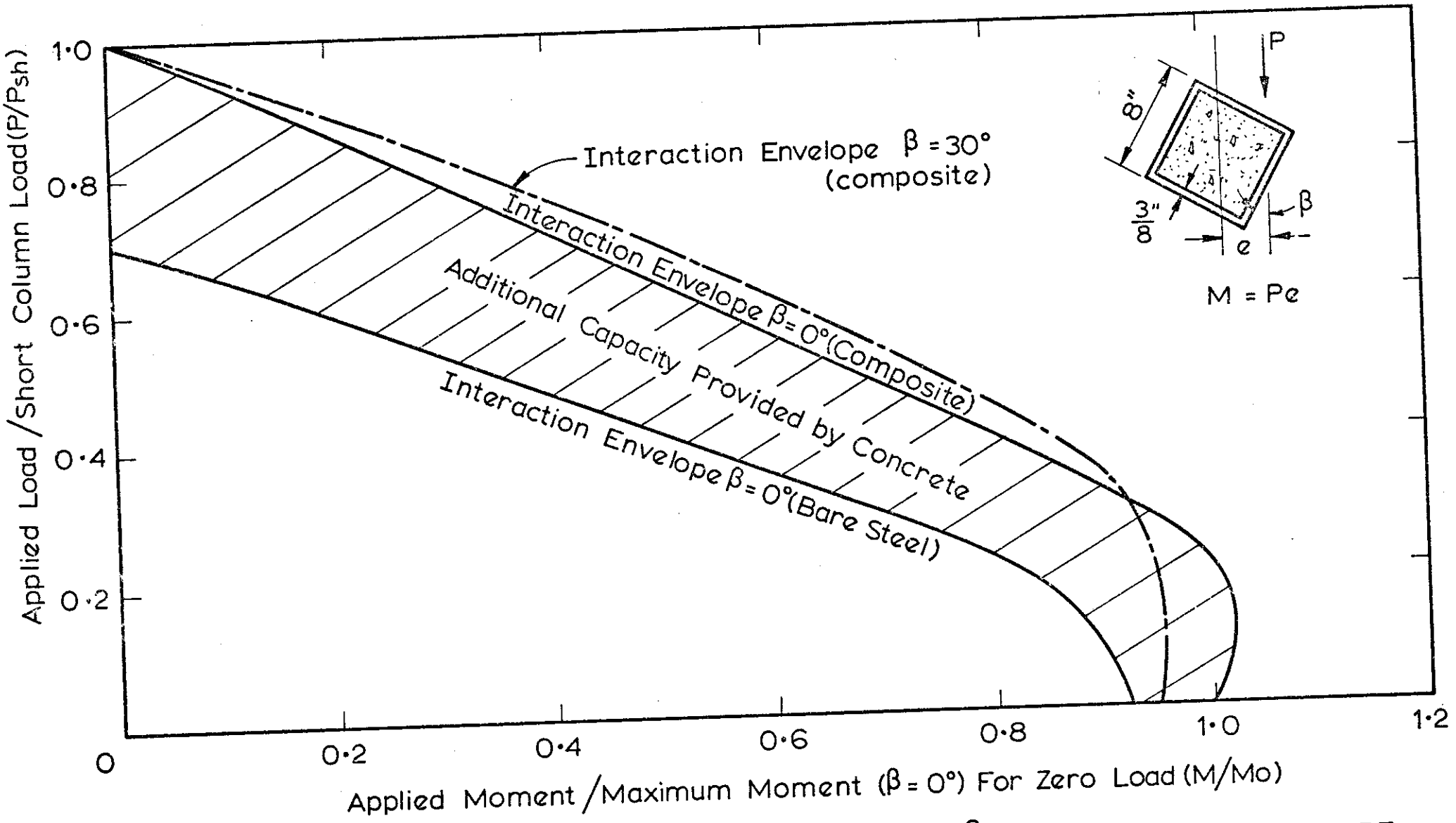

FIG. 6·14 LOAD-MOMENT INTERACTION FOR 8 IN. × 8 IN. × $\frac{3}{8}$ IN. CONCRETE FILLED TUBE SECTION

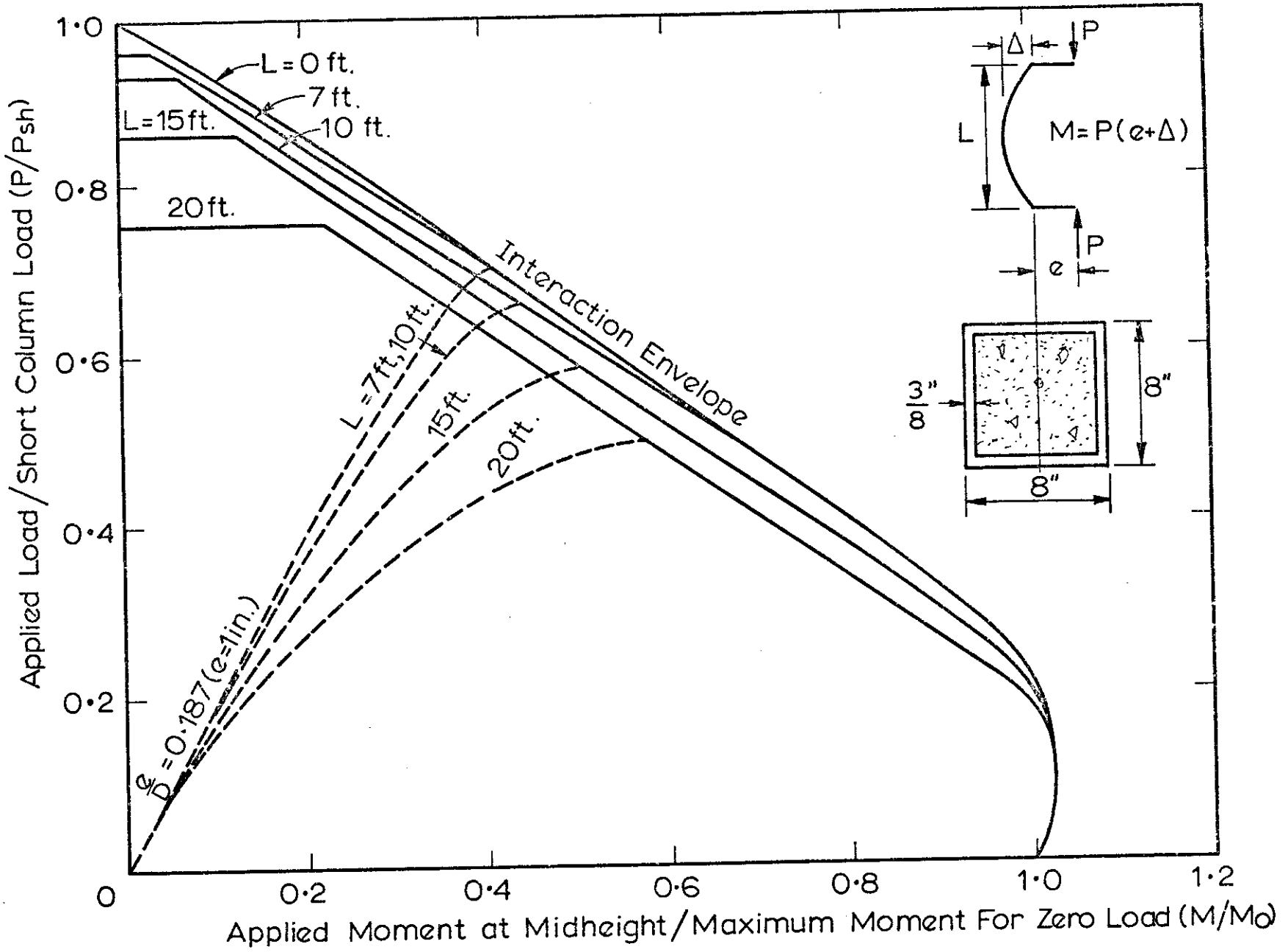

FIG. 6·15 LOAD-MAXIMUM MOMENT INTERACTION FOR SHC SERIES COLUMNS.

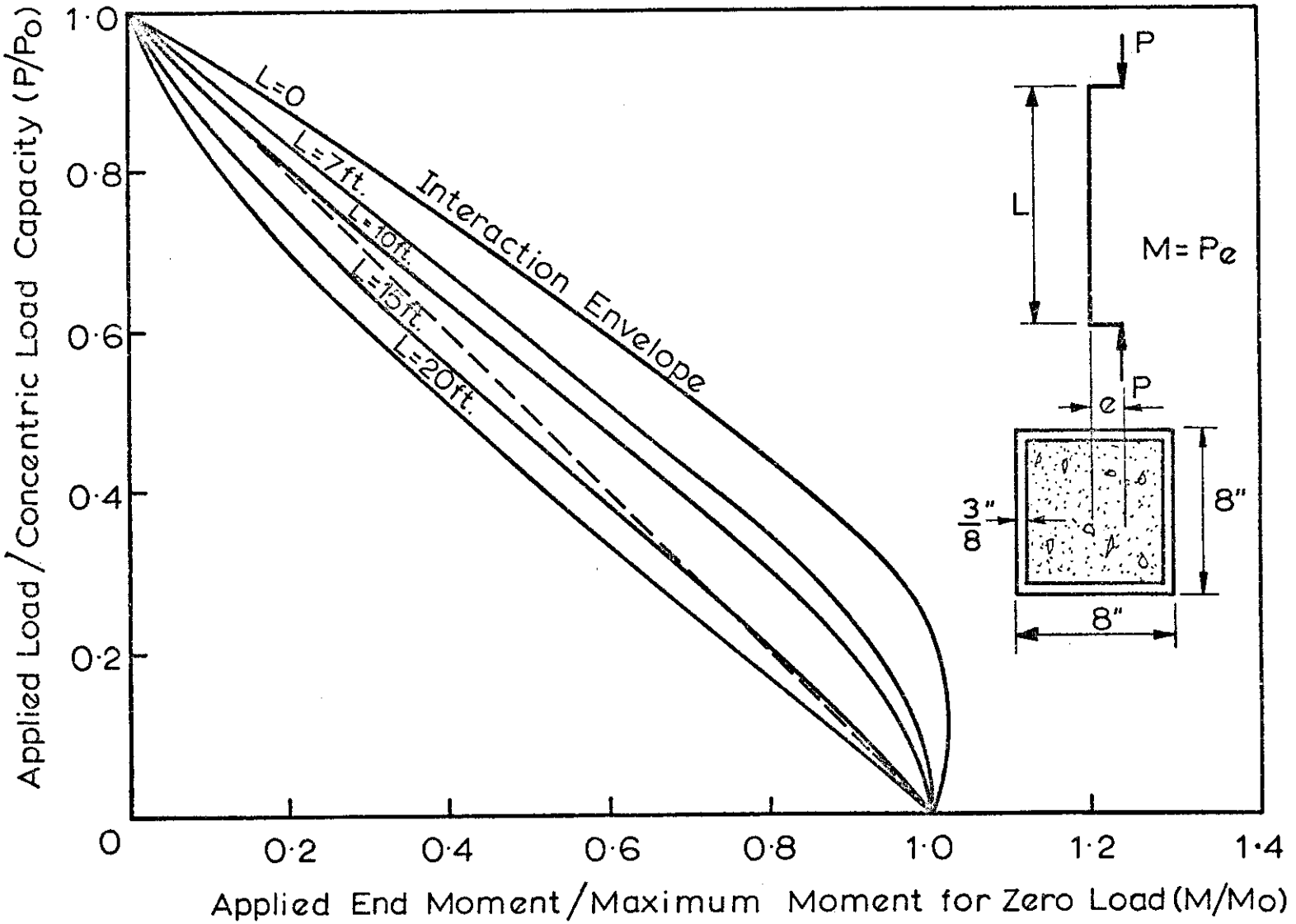

FIG. 6·16 LOAD-END MOMENT INTERACTION FOR SHC SERIES COLUMNS.

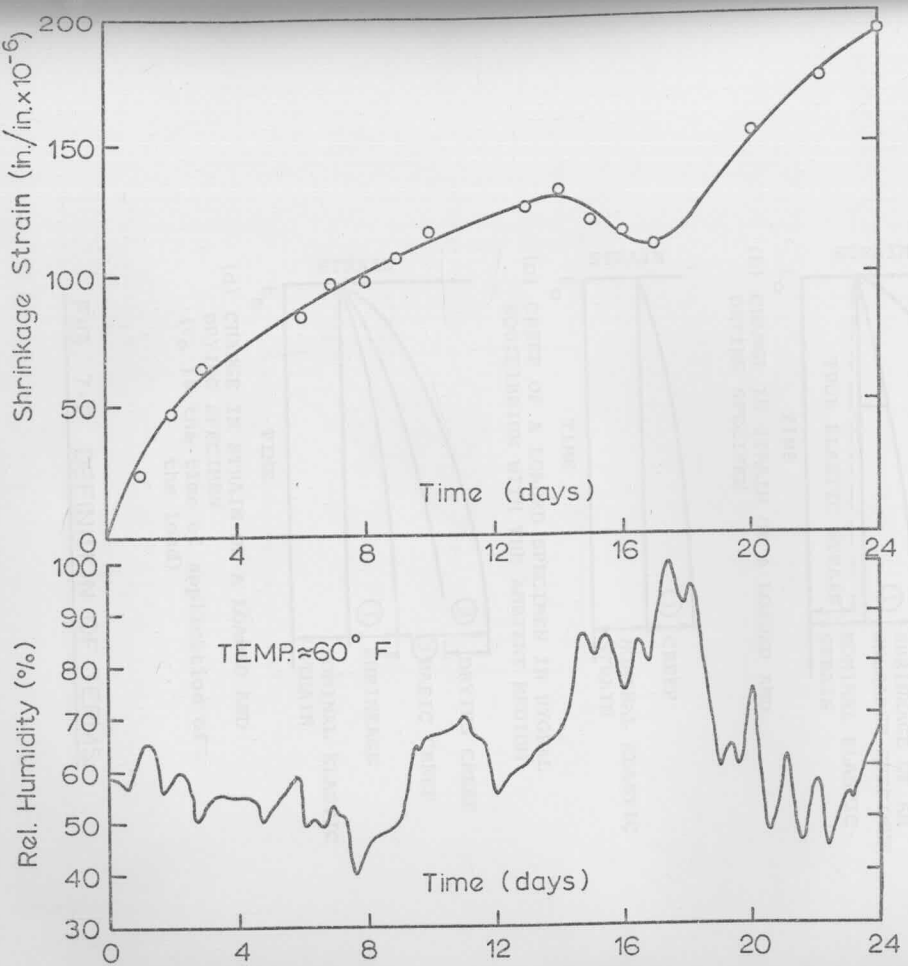

FIG. 7·1 EFFECT OF HUMIDITY ON CONCRETE SHRINKAGE FOR A SPECIMEN OF 8"x 7" CROSS SECTION. (CC2)

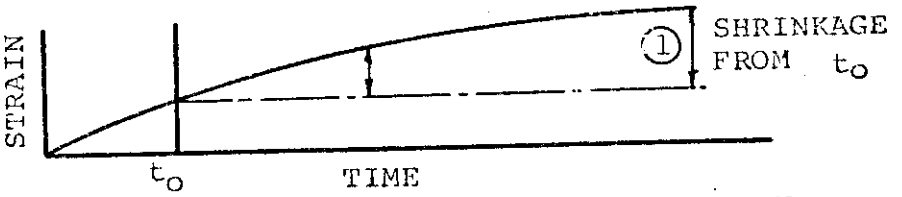

(a) SHRINKAGE OF AN UNLOADED SPECIMEN

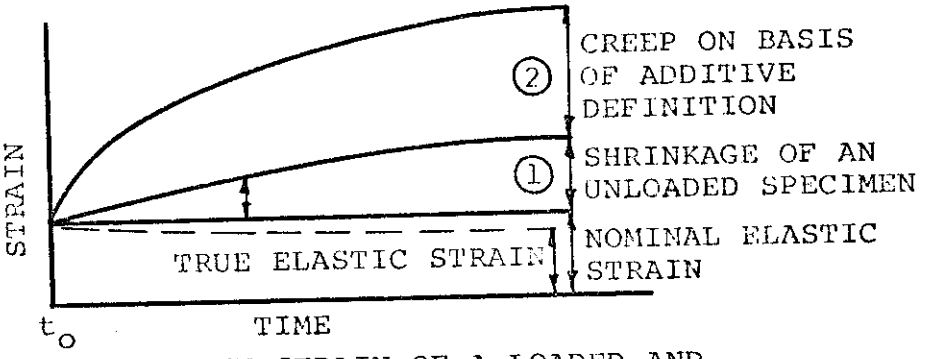

(b) CHANGE IN STRAIN OF A LOADED AND DRYING SPECIMEN

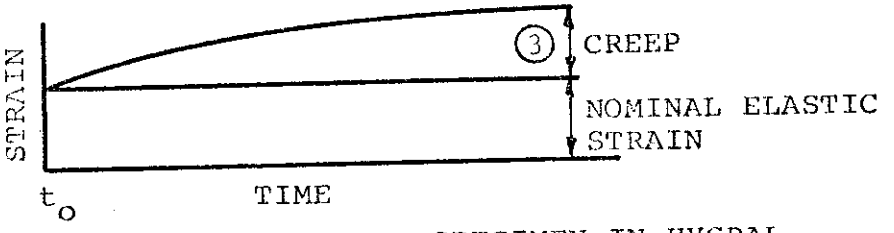

(c) CREEP OF A LOADED SPECIMEN IN HYGRAL EQUILIBRIUM WITH THE AMBIENT MEDIUM

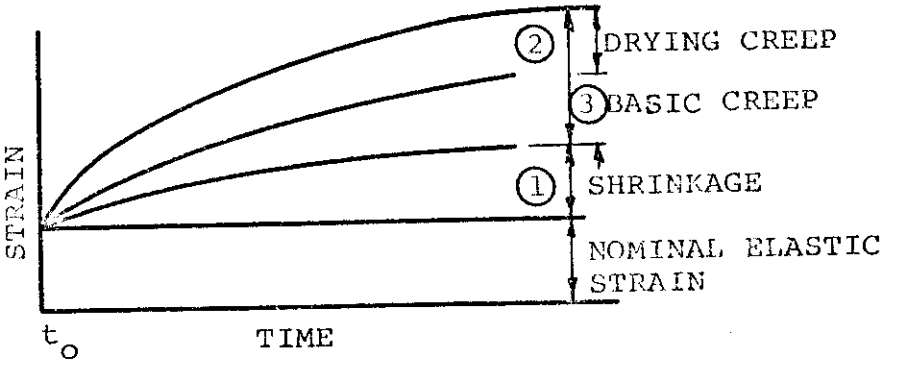

(d) CHANGE IN STRAIN OF A LOADED AND DRYING SPECIMEN
(t_o is the time of application of the load)

FIG. 7·2 DEFINITION OF TERMS.

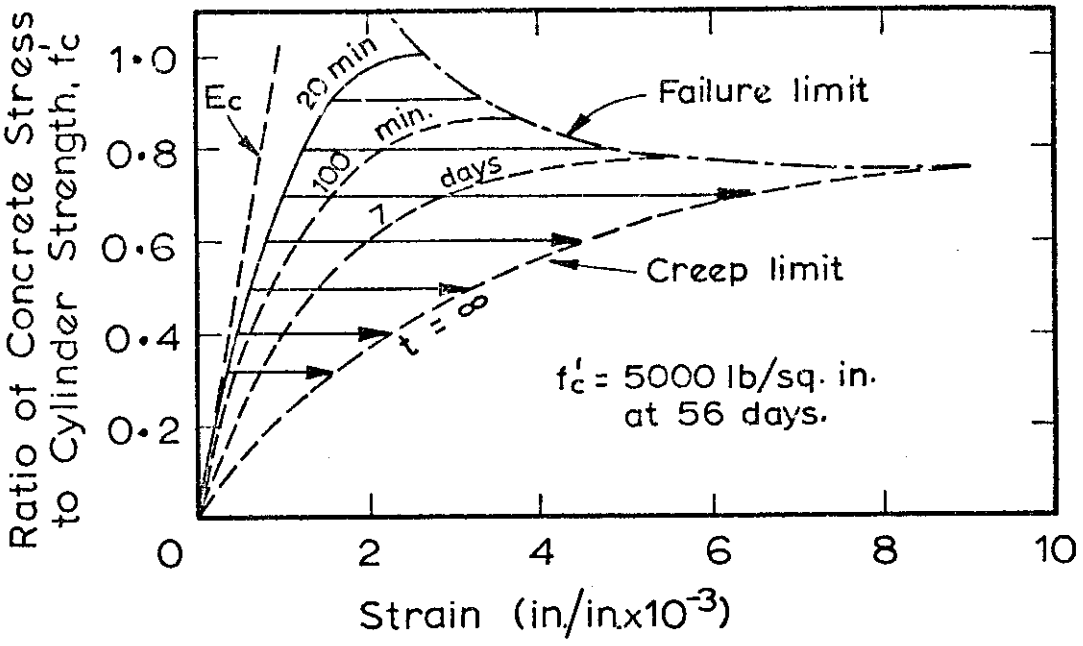

FIG. 7·3 INFLUENCE OF LOAD INTENSITY AND DURATION ON CONCRETE STRAIN. (RUSCH)

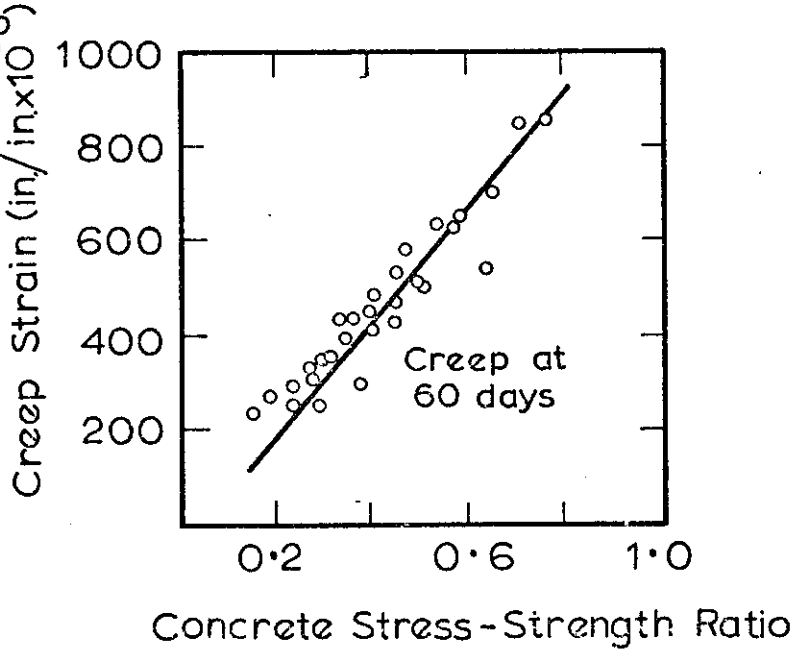

FIG. 7·4 RELATION BETWEEN CREEP OF MORTAR AND STRESS-STRENGTH RATIO FOR DIFFERENT MIXES & STRESSES (NEVILLE)

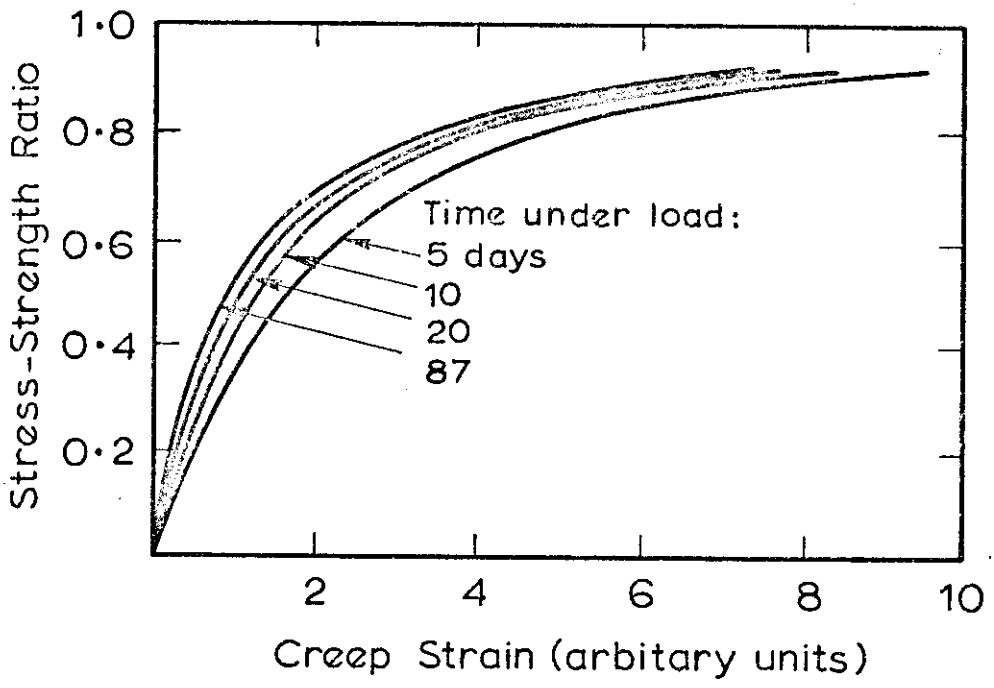

FIG. 7·5 RELATION BETWEEN CREEP AND STRESS-STRENGTH RATIO.(GVOZDEV).

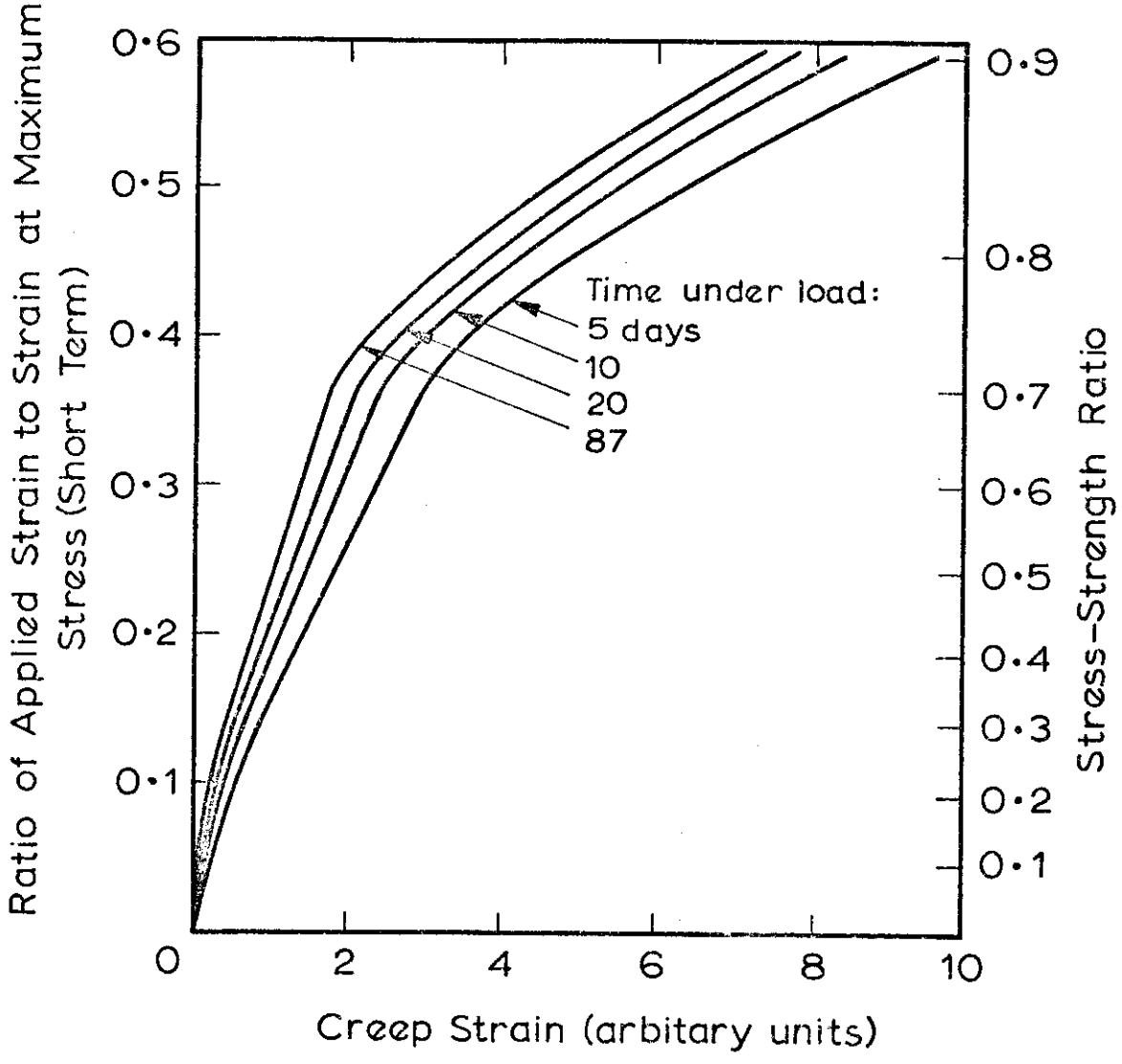

FIG. 7·6 FIG. 7·5 REPLOTTED SHOWING RELATIONSHIP BETWEEN SHORT TERM STRAIN AND CREEP STRAIN.

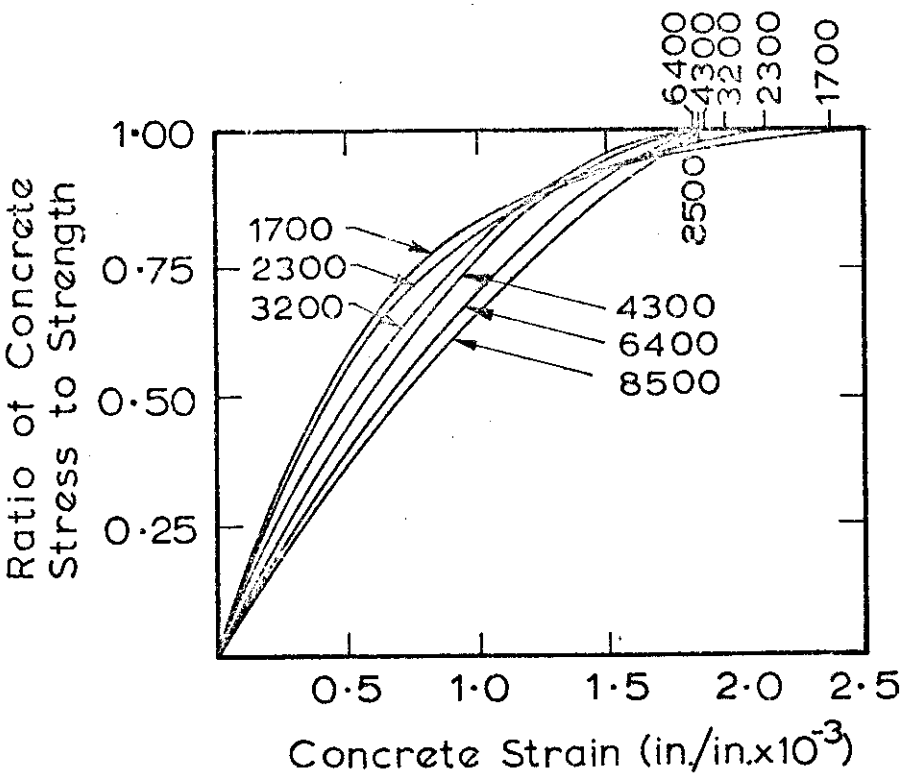

FIG. 7·7 RELATION BETWEEN STRESS-STRENGTH RATIO AND STRAIN FOR CONCRETES OF DIFFERENT STRENGTHS (RUSCH).

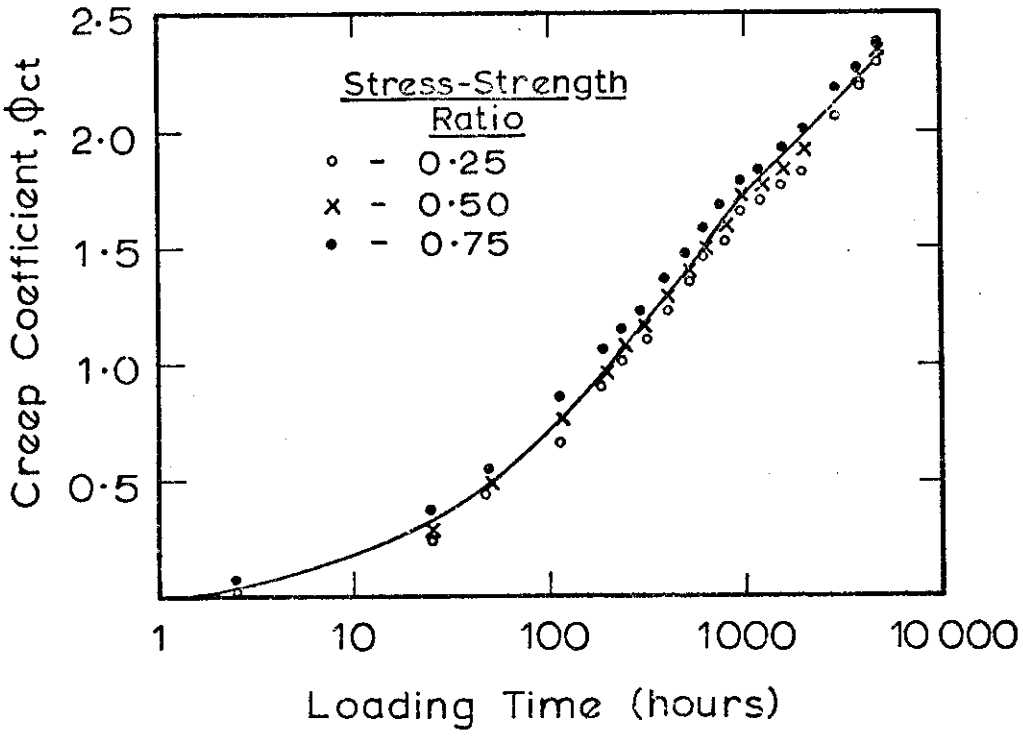

FIG. 7·8 VARIATION OF CREEP COEFFICIENT WITH TIME FOR VARIOUS STRESS LEVELS (GOYAL & JACKSON).

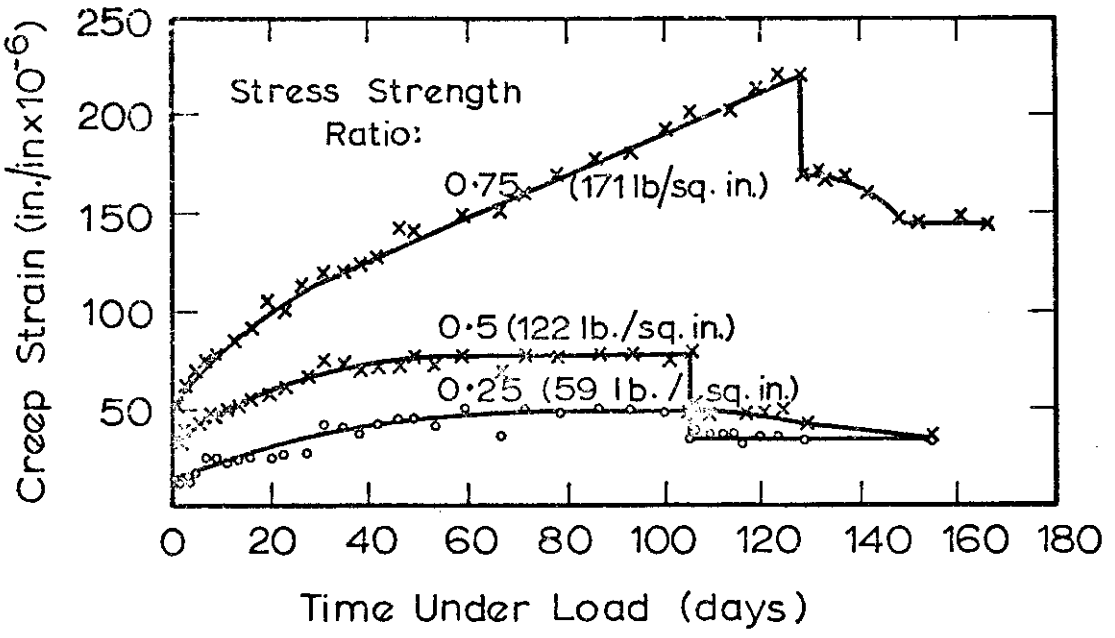

FIG. 7·9 CREEP IN TENSION FOR DIFFERENT STRESS STRENGTH RATIOS (ILLSTON)

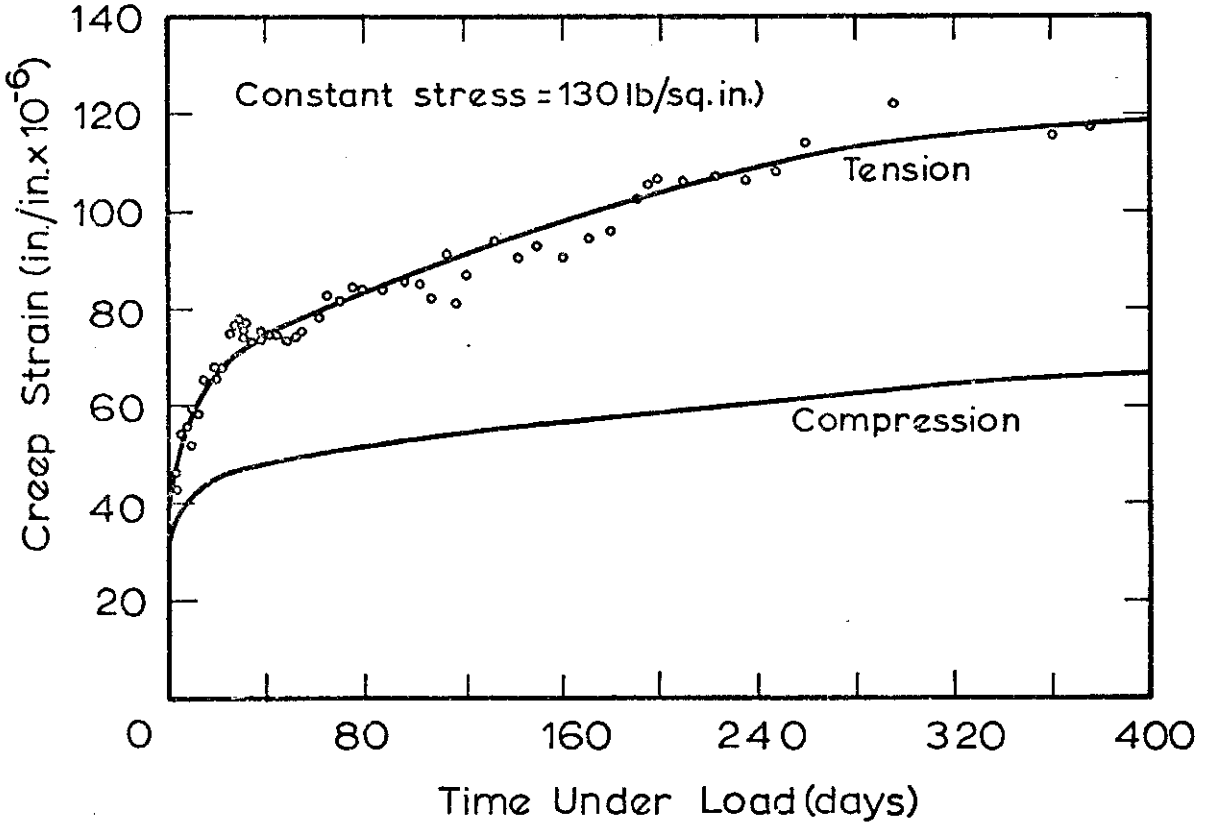

FIG. 7·10 CREEP IN TENSION AND COMPRESSION FOR SAME APPLIED STRESS (ILLSTON)

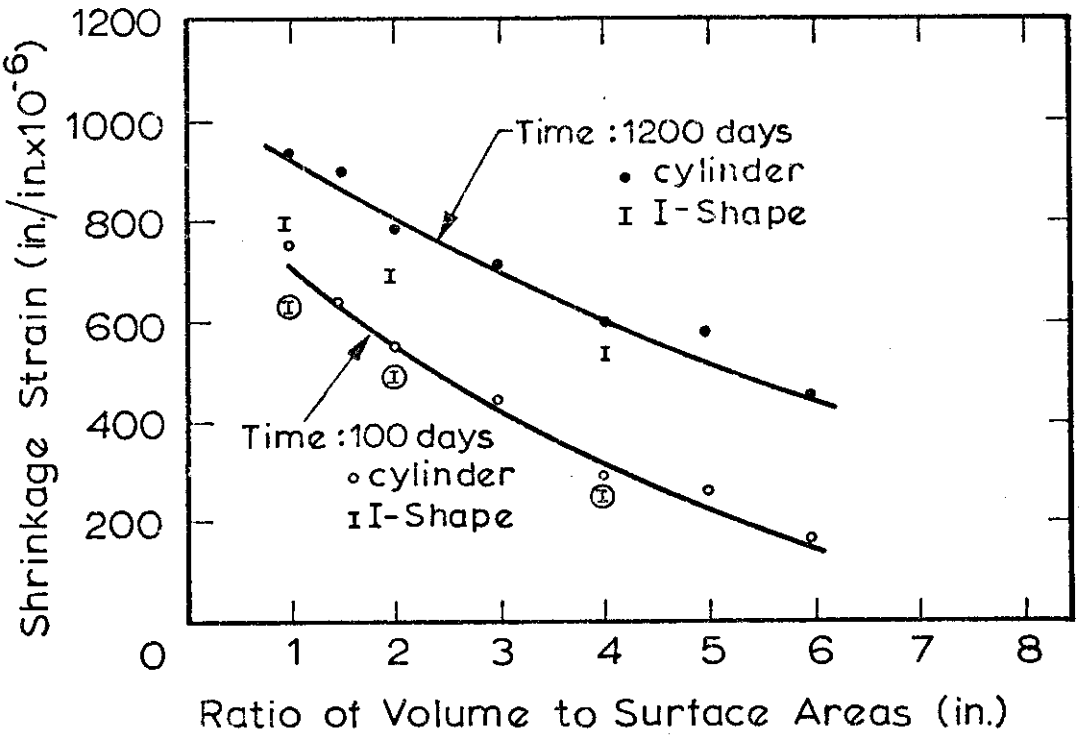

FIG. 7·11 THE INFLUENCE OF VOLUME / SURFACE-AREA RATIO ON SHRINKAGE (HANSEN & MATTOCK)

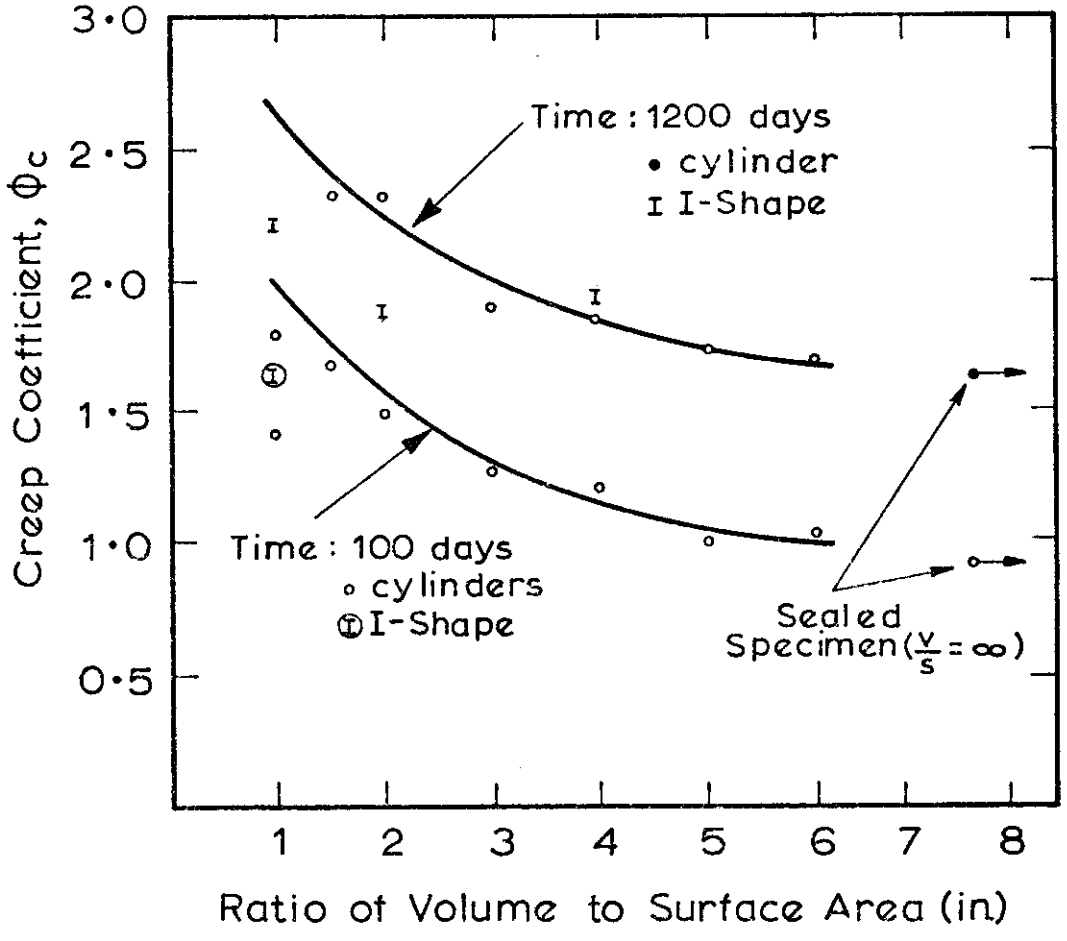

FIG. 7·12 THE INFLUENCE OF VOLUME / SURFACE-AREA RATIO ON CREEP (HANSEN & MATTOCK)

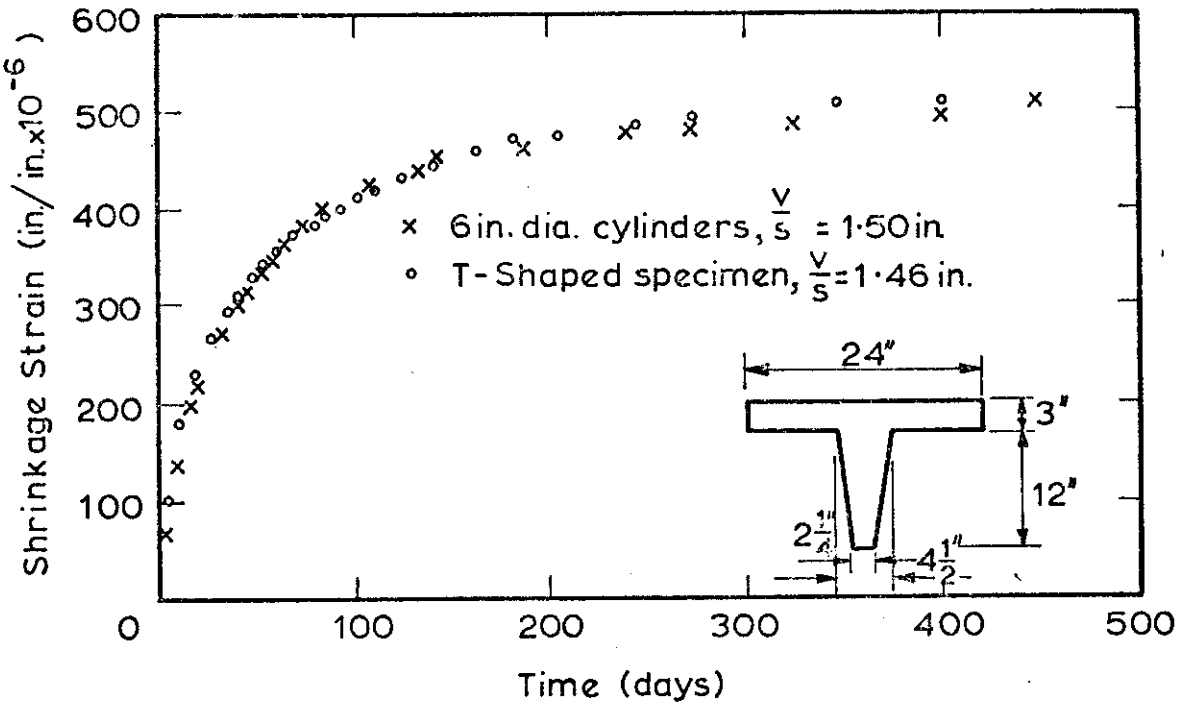

FIG. 7·13 COMPARISON OF SHRINKAGE OF DIFFERENT SHAPED SPECIMENS HAVING THE SAME VOLUME TO SURFACE-AREA RATIOS (HANSEN & MATTOCK)

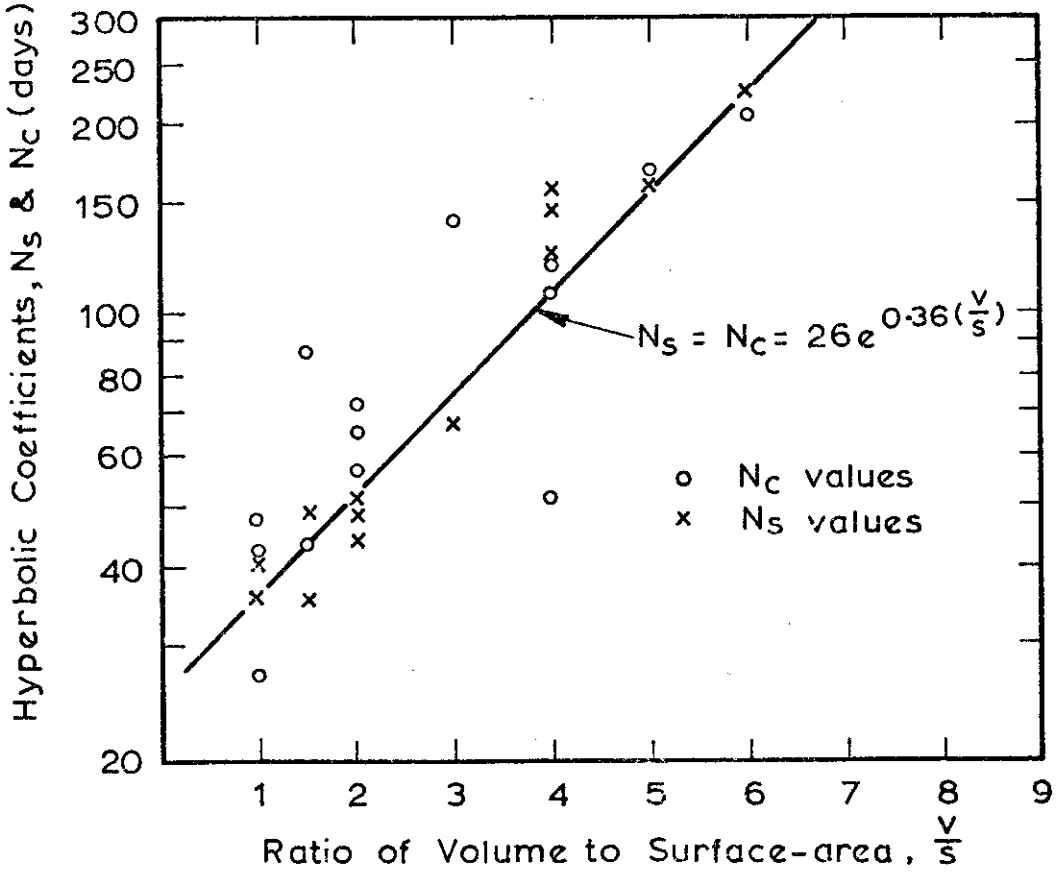

FIG. 7·14 COMPARISON OF COEFFICIENTS FOR HYPERBOLIC EQUATIONS TO REPRESENT THE VARIATION OF CREEP AND SHRINKAGE WITH TIME (HANSEN & MATTOCK)

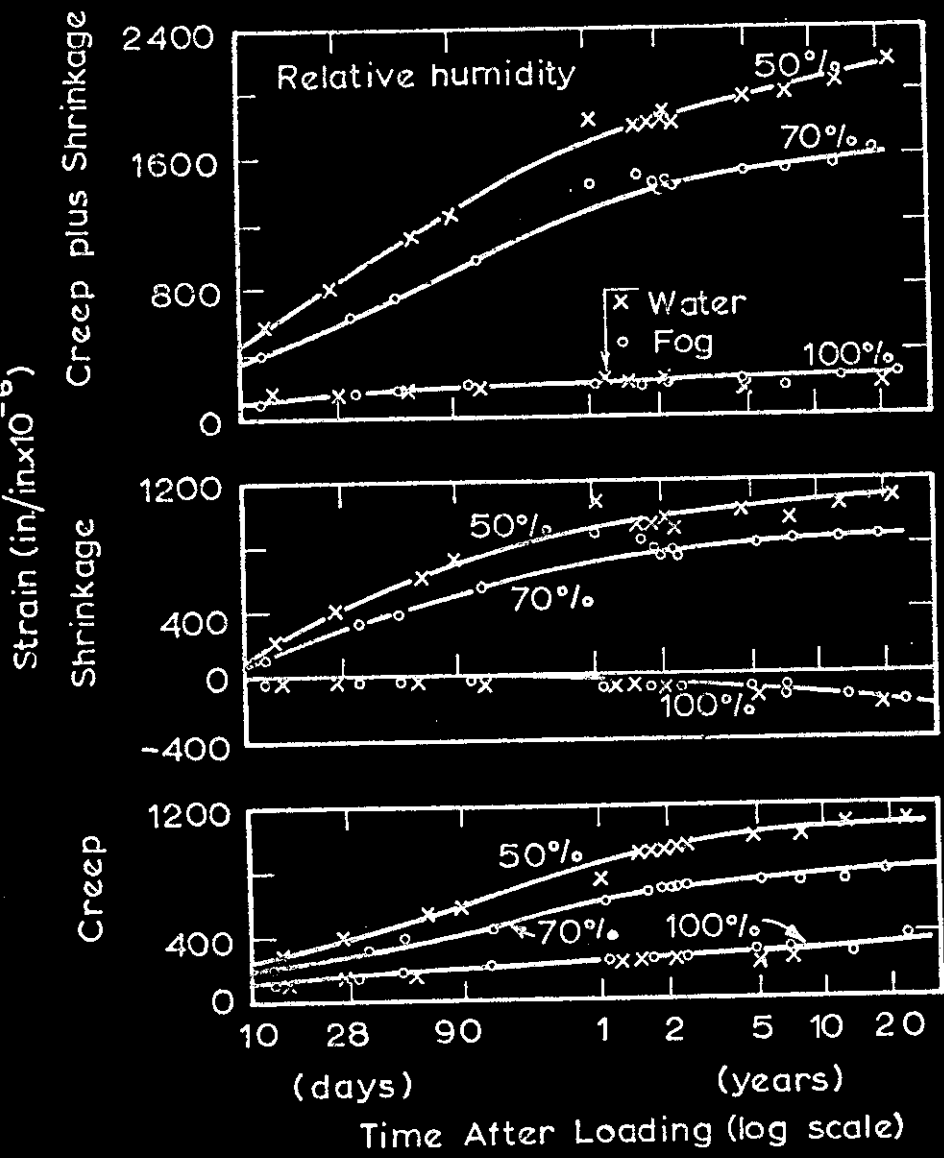

FIG. 7·15 THE EFFECT OF DRYING CONDITIONS (HUMIDITY) ON CREEP & SHRINKAGE (TROXELL ET AL)

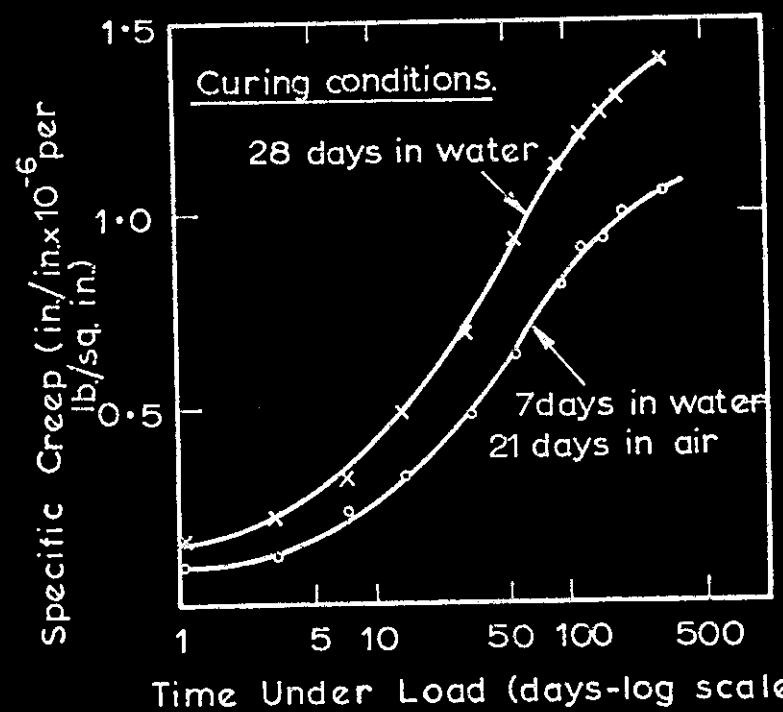

FIG. 7·16 THE EFFECT OF CURING CONDITIONS ON CREEP, SPECIMENS LOADED IN AIR (WIERIG)

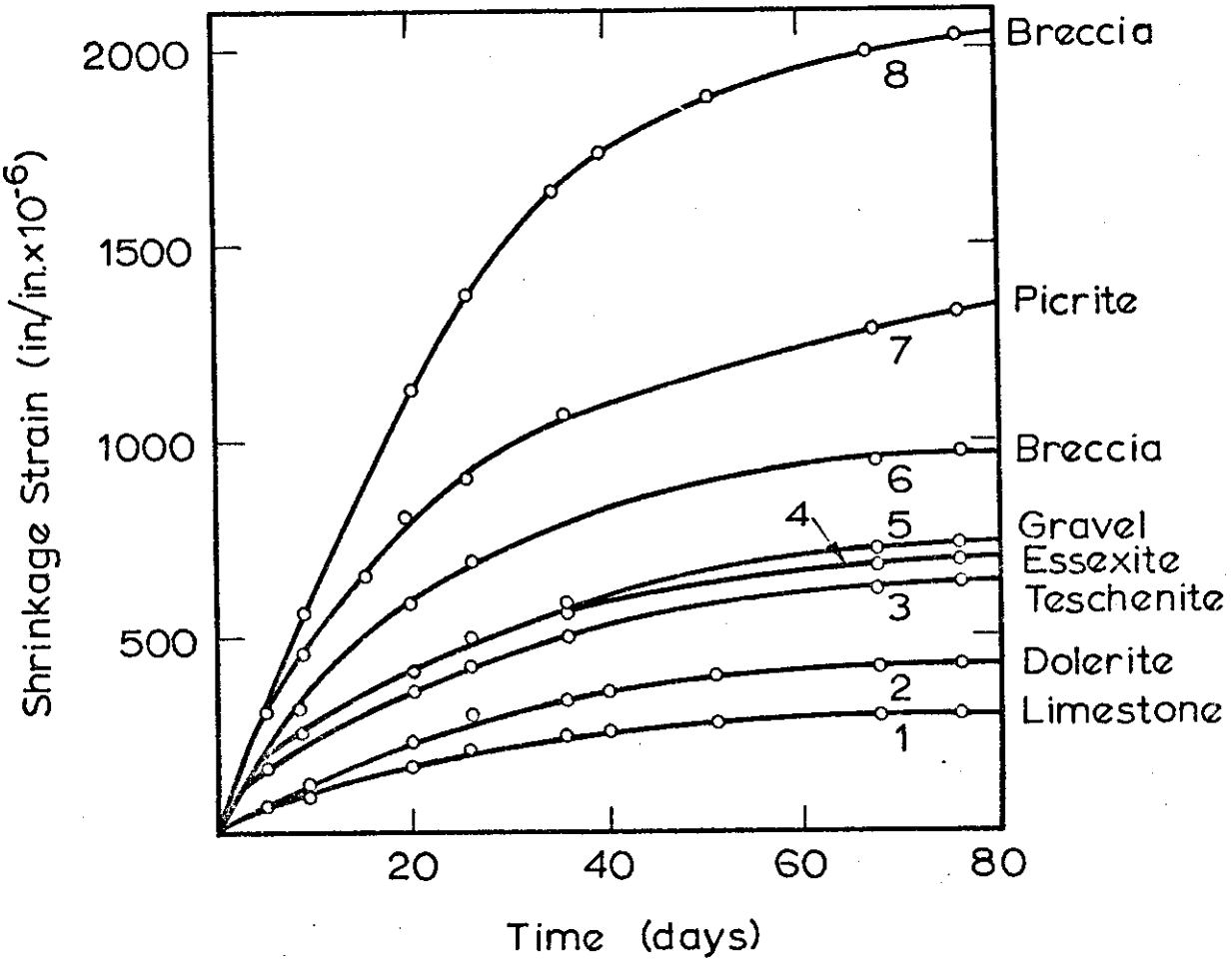

FIG. 7·17 THE EFFECT OF VARYING AGGREGATE TYPE ON SHRINKAGE FOR CONCRETE OF SAME MIX (ROPER)

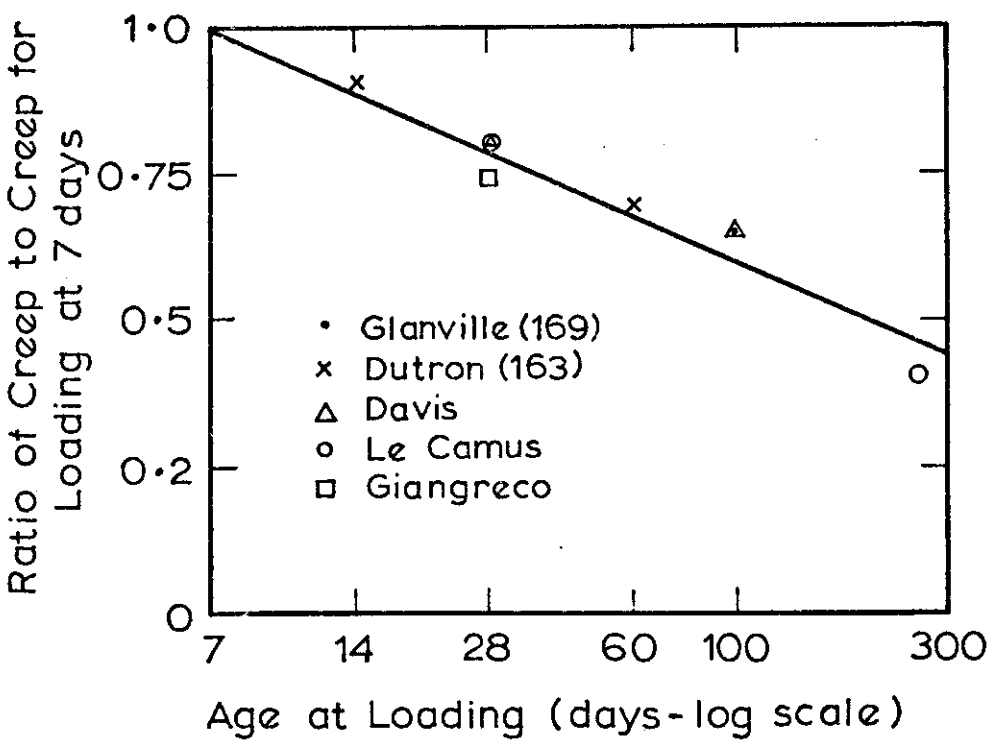

FIG. 7·18 THE EFFECT OF AGE AT LOADING ON CREEP (L'HERMITE)

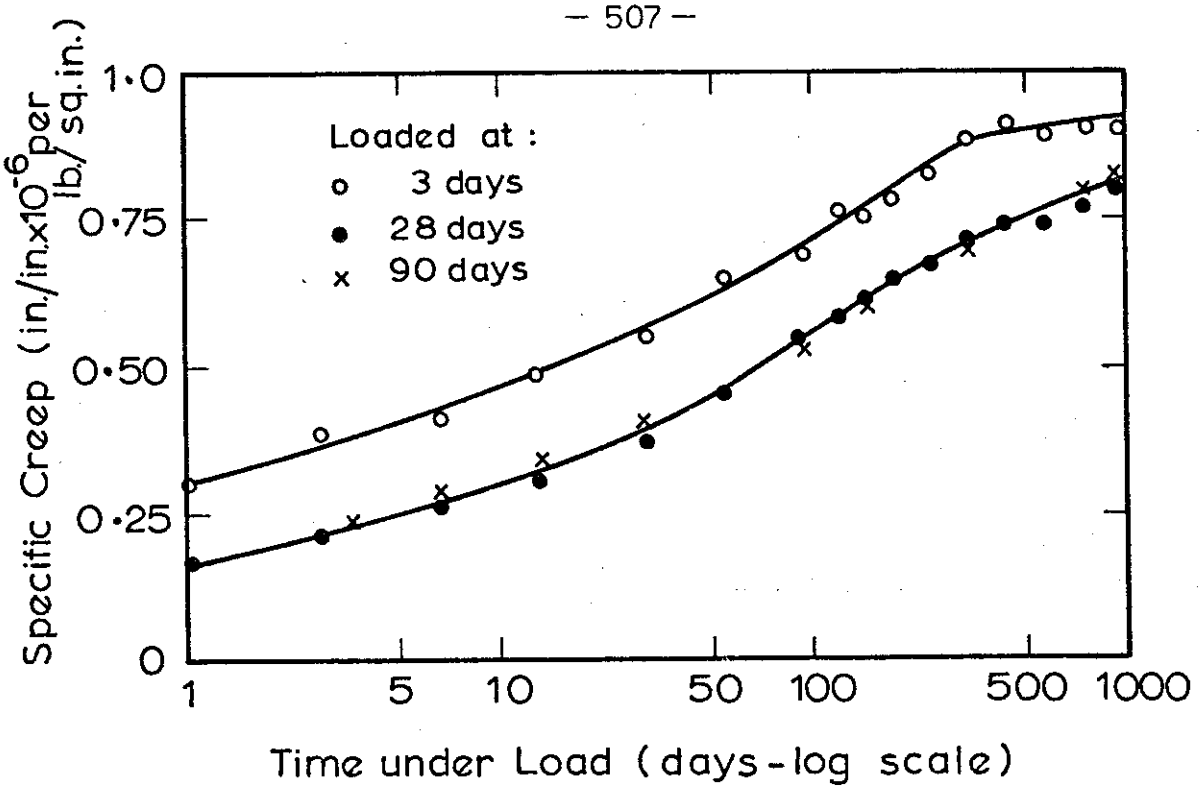

FIG. 7·19 THE EFFECT OF AGE AT LOADING ON CREEP (HUMMEL ET AL.)

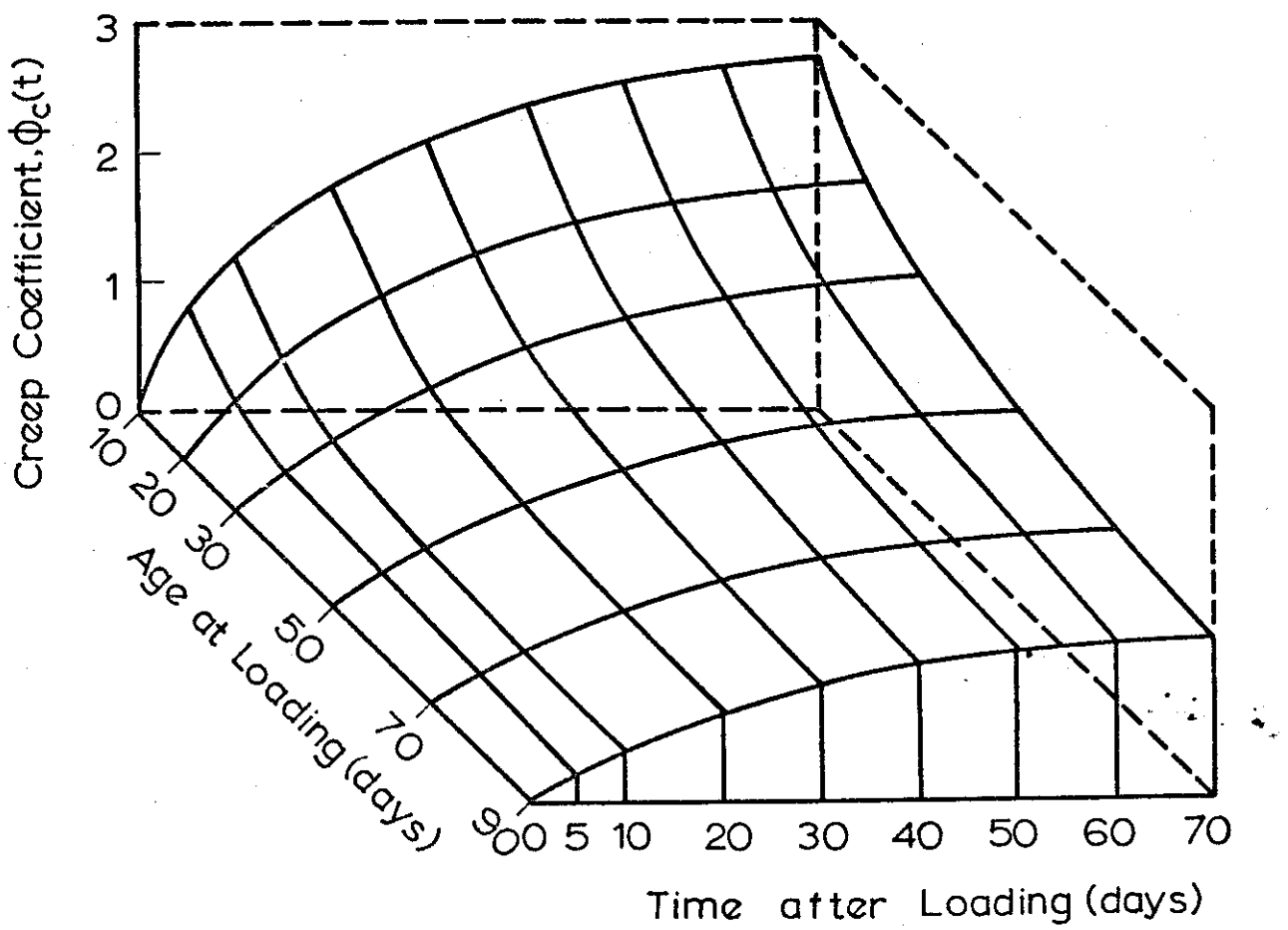

FIG. 7·20 CREEP SURFACE SHOWING VARIATION OF CREEP WITH AGE AT LOADING & TIME UNDER LOAD (McHENRY)

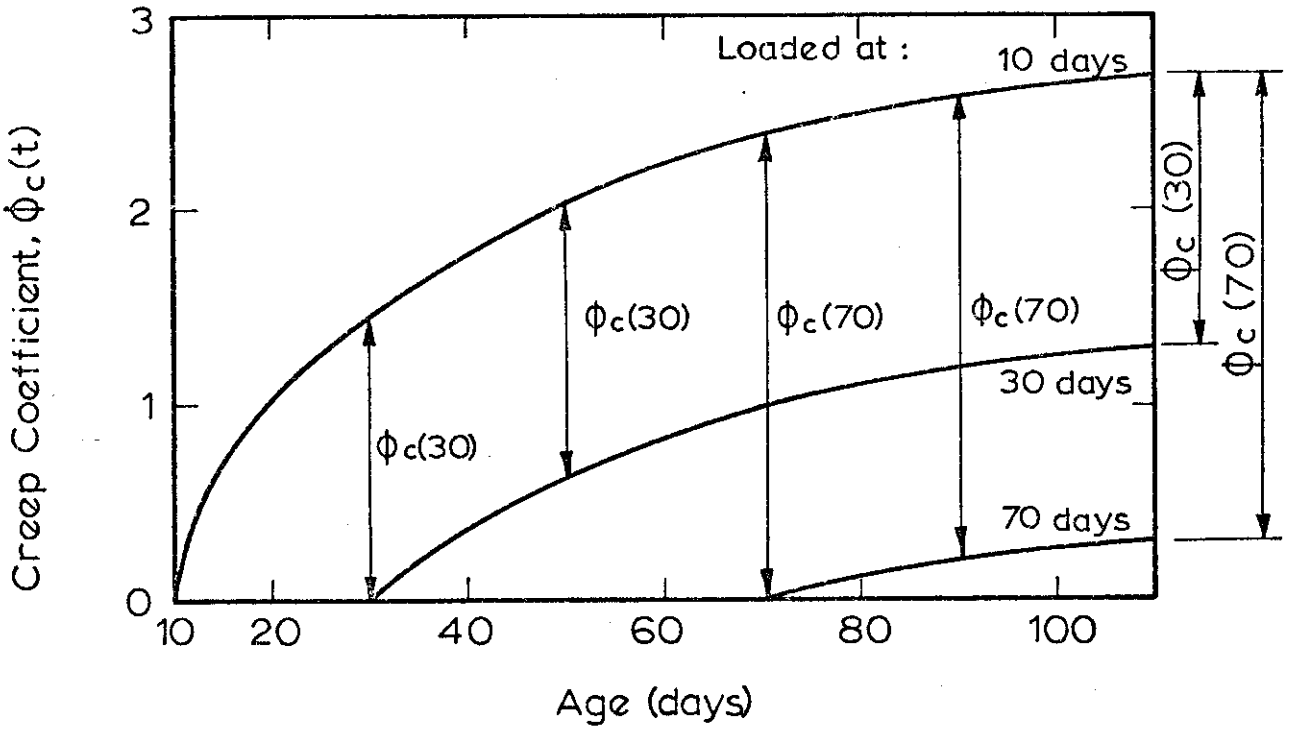

FIG. 7·21 VARIATION OF CREEP WITH AGE AT LOADING AND TIME UNDER LOAD (RATE OF CREEP METHOD)

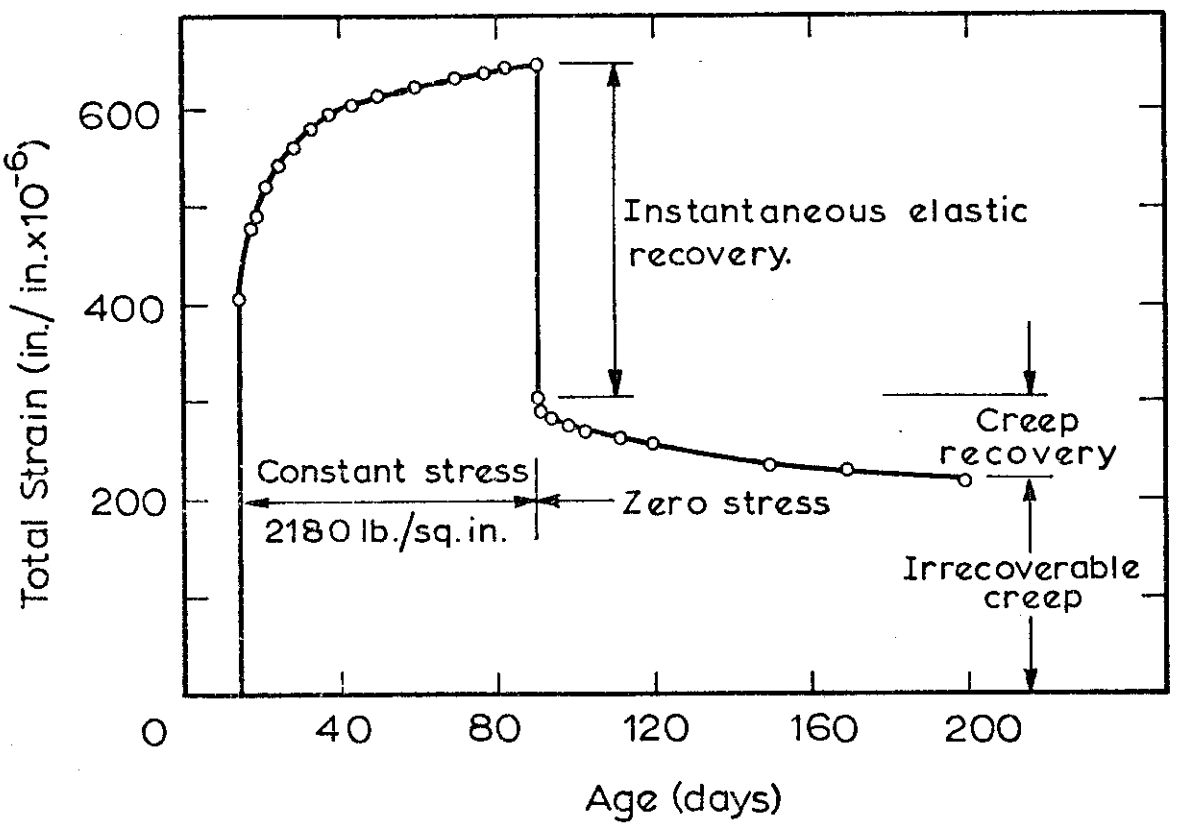

FIG. 7·22 STRAIN DURING AND AFTER A PERIOD OF CONSTANT SUSSTAINED STRESS (ROSS)

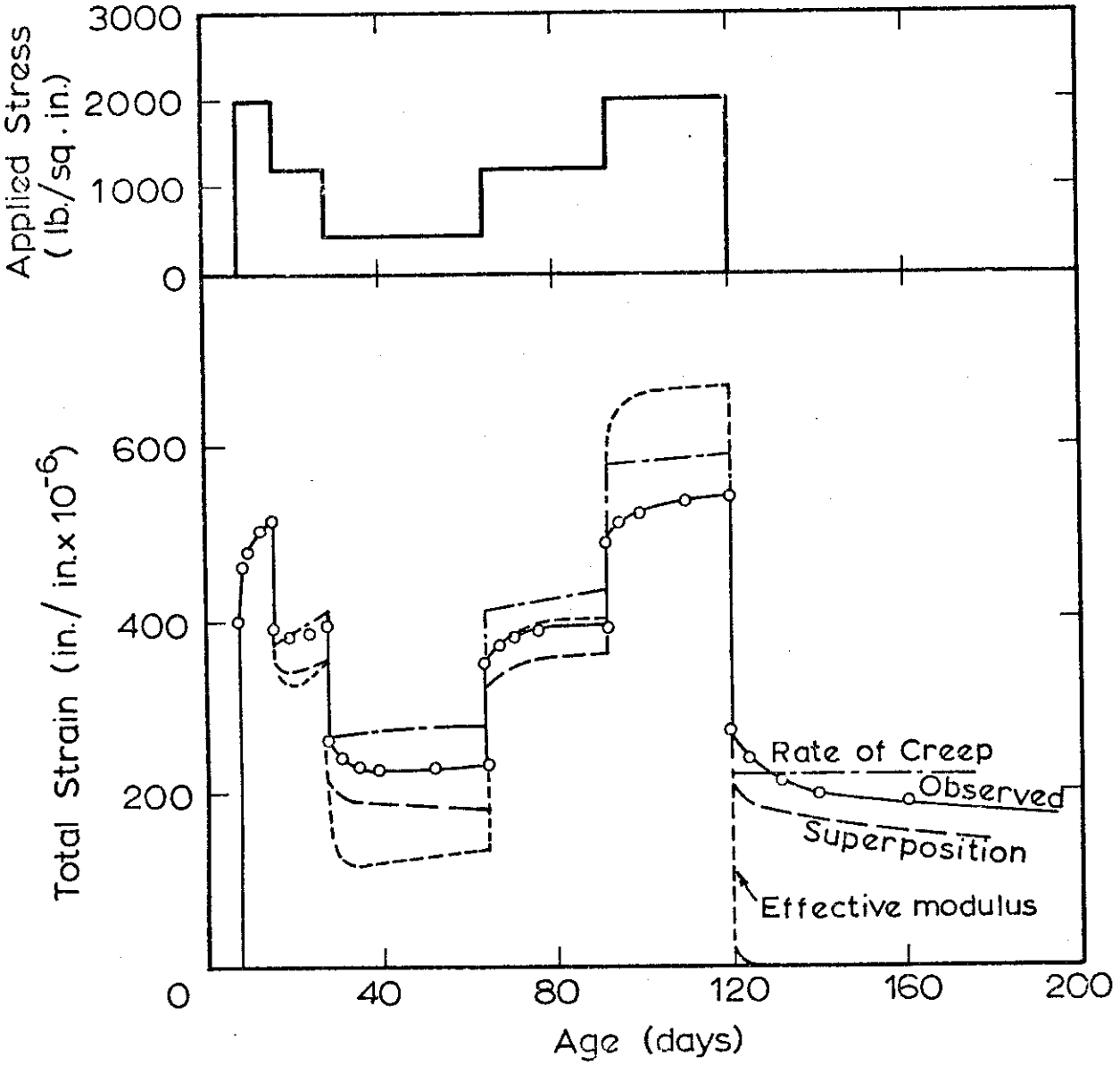

FIG. 7·23 COMPARISON OF METHODS FOR ESTIMATING CREEP FOR STRESS DECREMENTS & INCREMENTS (ROSS)

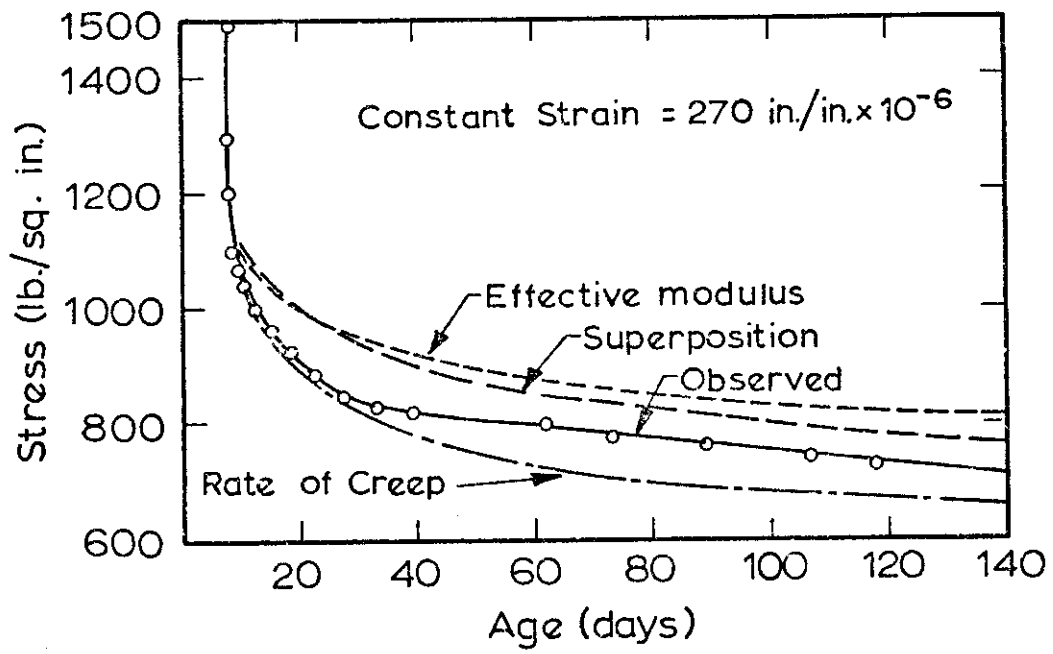

FIG. 7·24 COMPARISON OF METHODS FOR ESTIMATING CREEP FOR A GRADUALLY DECREASING STRESS BY RELAXATION UNDER CONSTANT STRAIN (ROSS)

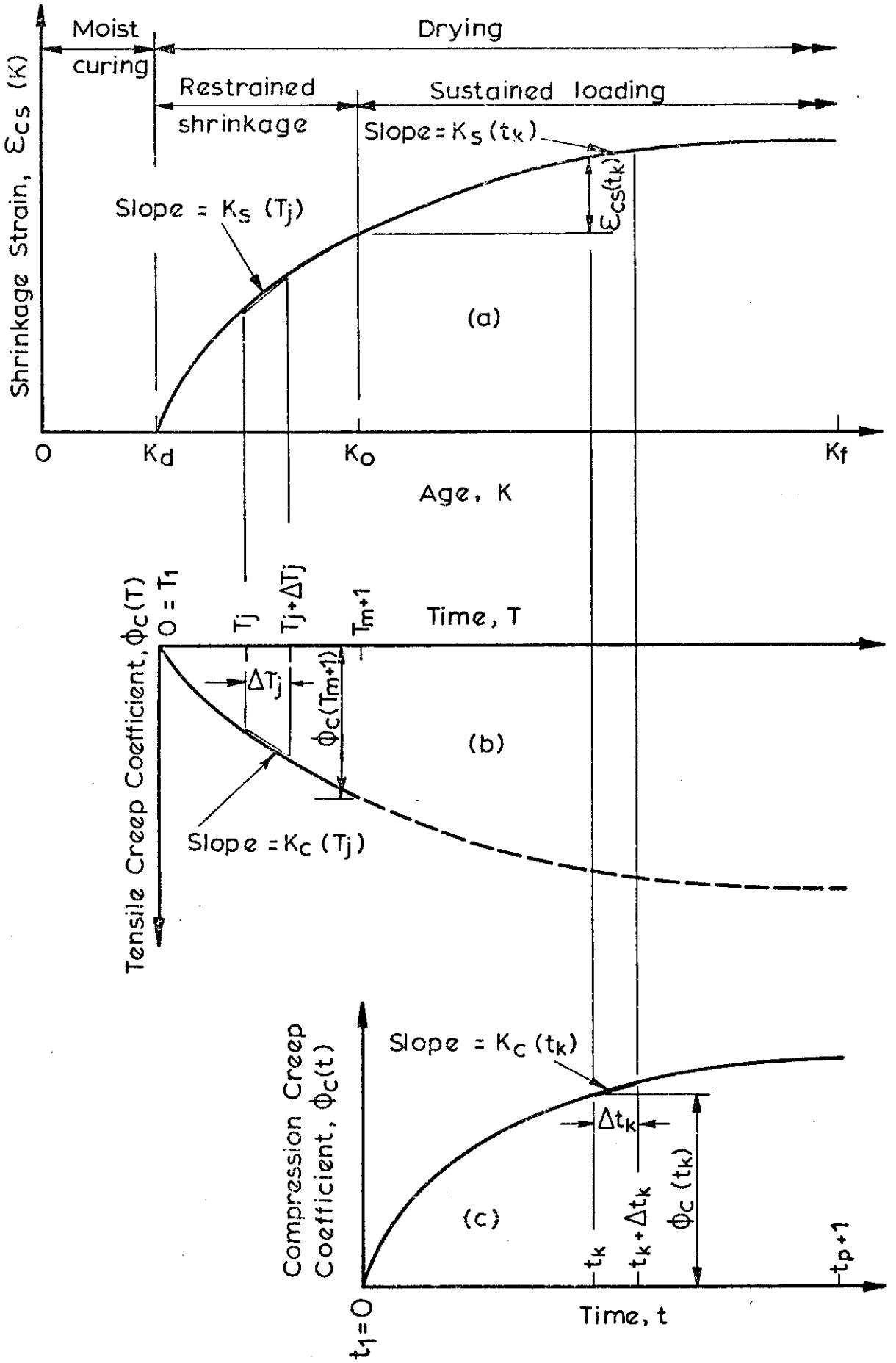

FIG. 8·1 SHRINKAGE AND CREEP DATA FOR ANALYSIS OF LONG TERM BEHAVIOUR.

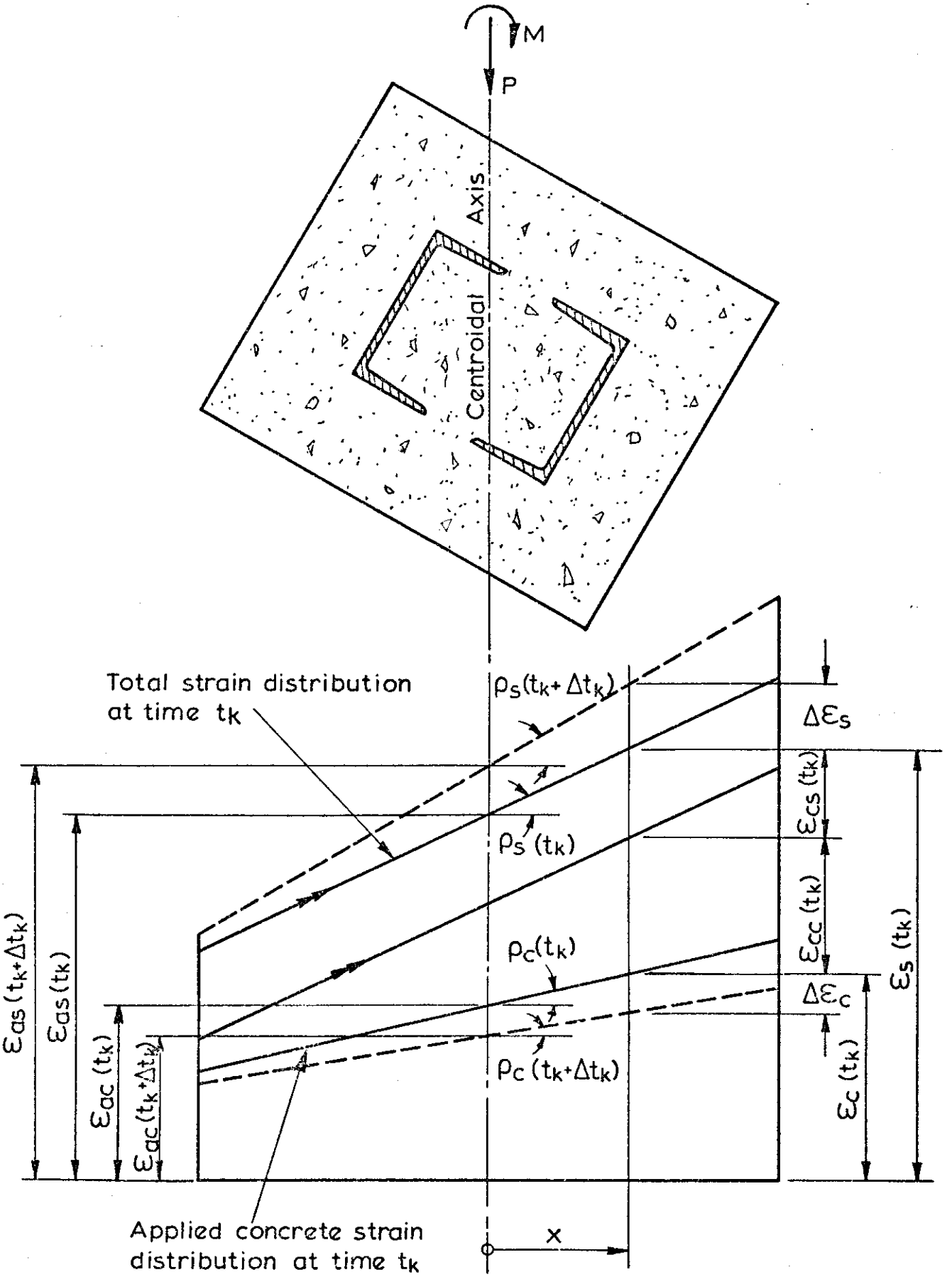

FIG. 8·2 SHRINKAGE AND CREEP STRAINS AT A COMPOSITE SECTION UNDER A SUSTAINED APPLIED LOAD AND MOMENT.

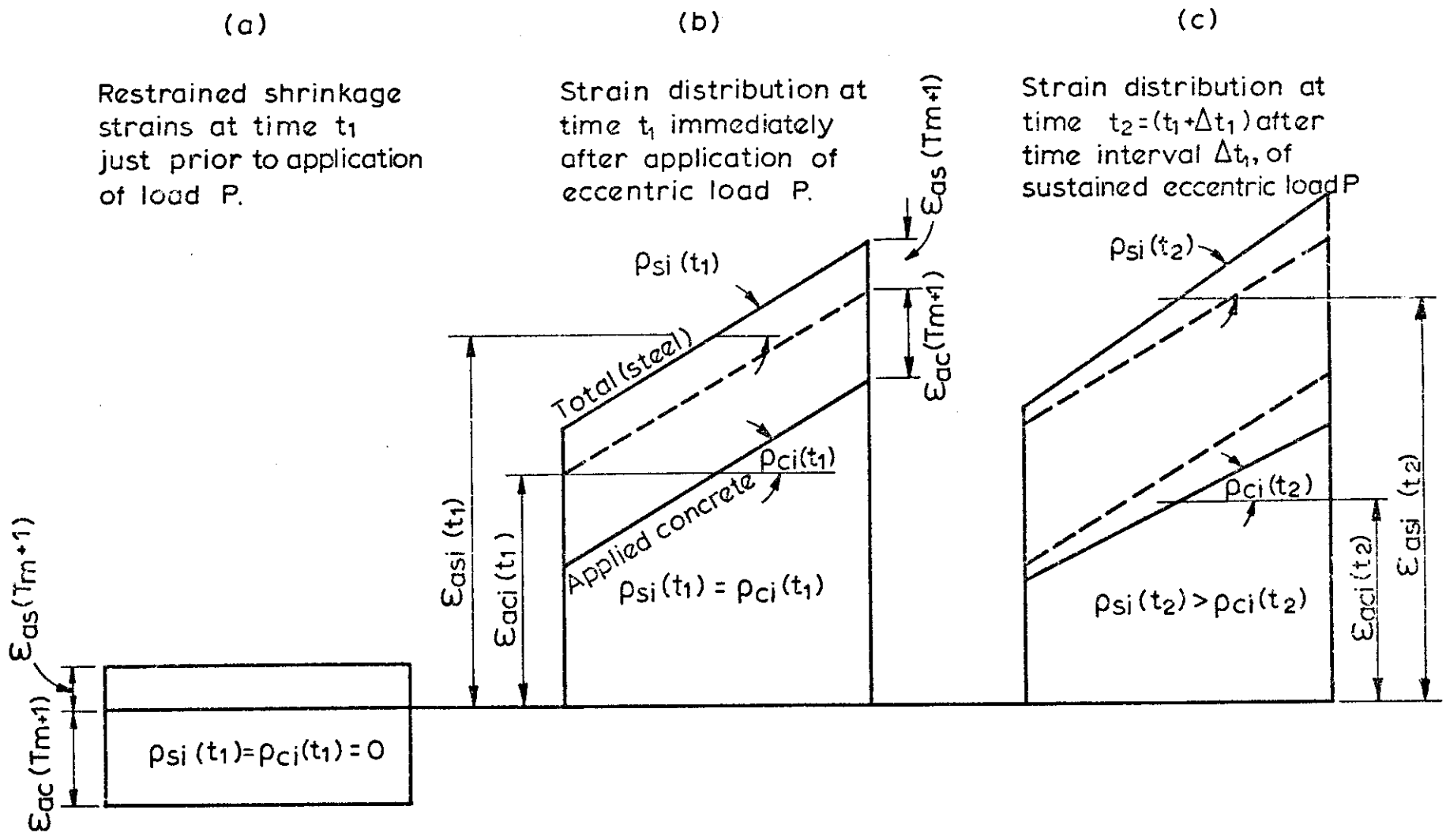

FIG. 8·3 EFFECT OF RESTRAINED SHRINKAGE, LOADING AND TIME UNDER LOAD ON THE STRAIN DISTRIBUTION.

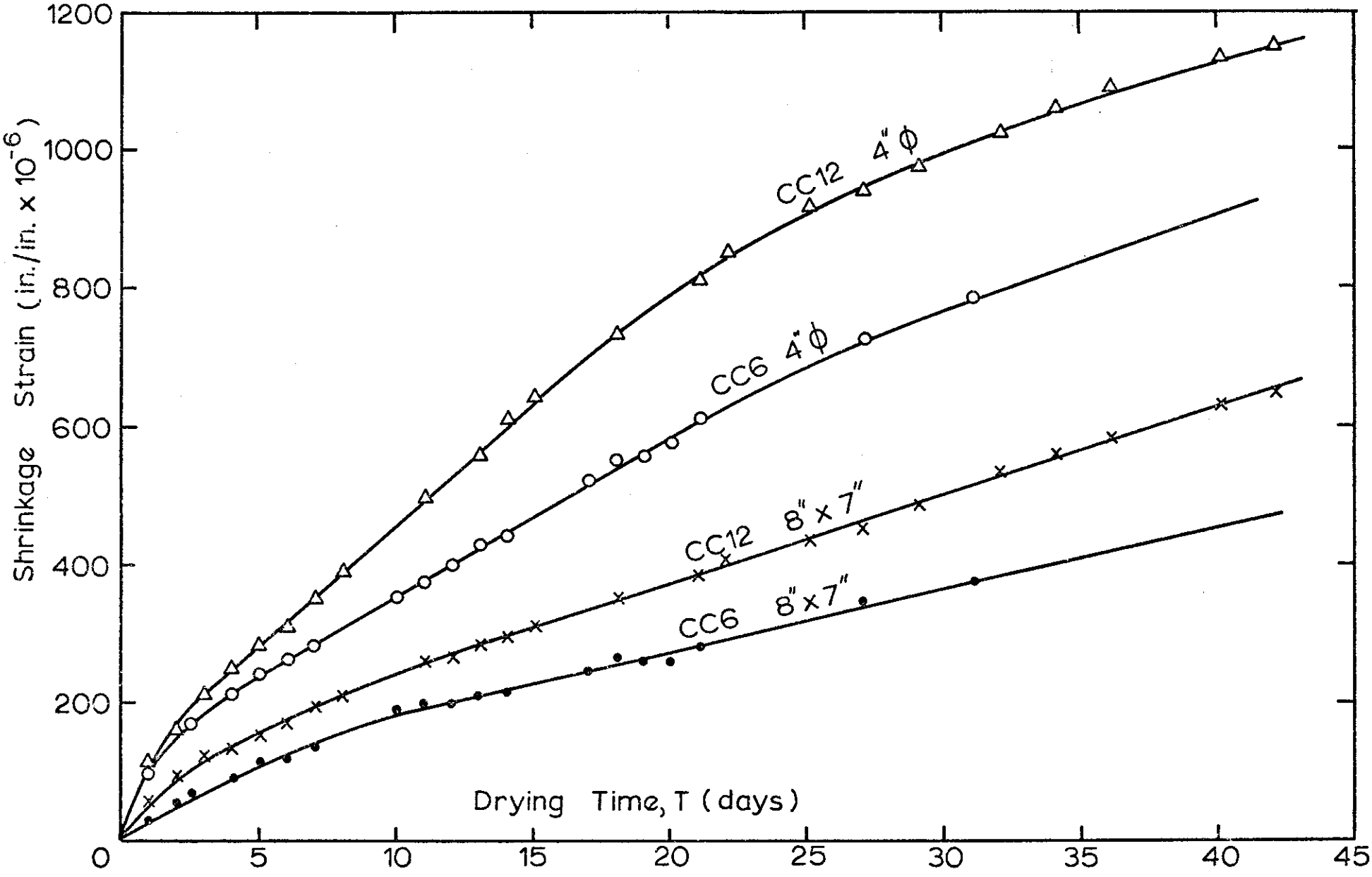

FIG. 9·1 EFFECT OF SIZE ON SHRINKAGE STRAINS

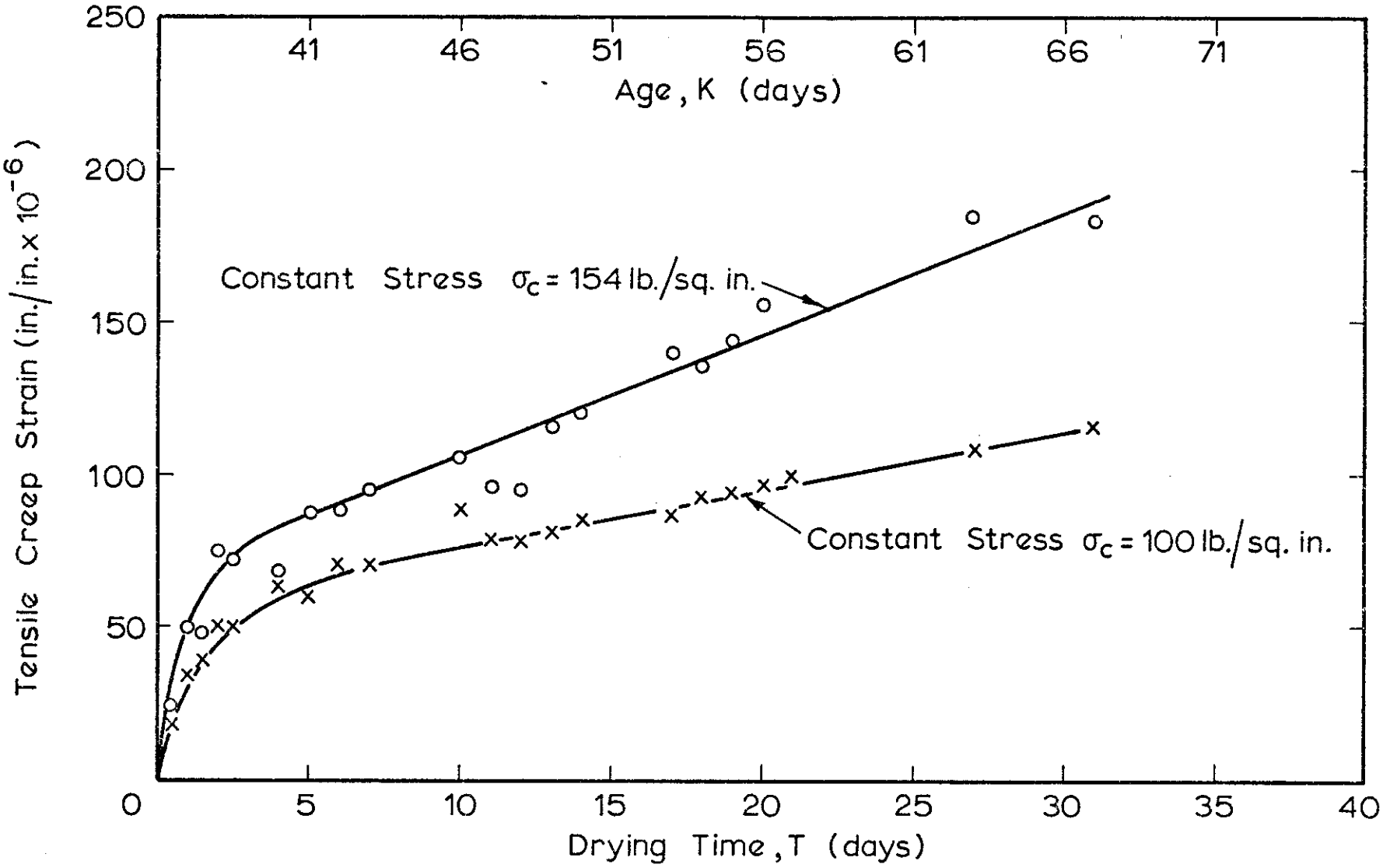

FIG. 9·2 TENSILE CREEP STRAINS WITH TIME FOR 4 IN. DIA. SPECIMENS (CC6) UNDER CONSTANT APPLIED STRESS AT 70°F AND 50% REL. HUMIDITY

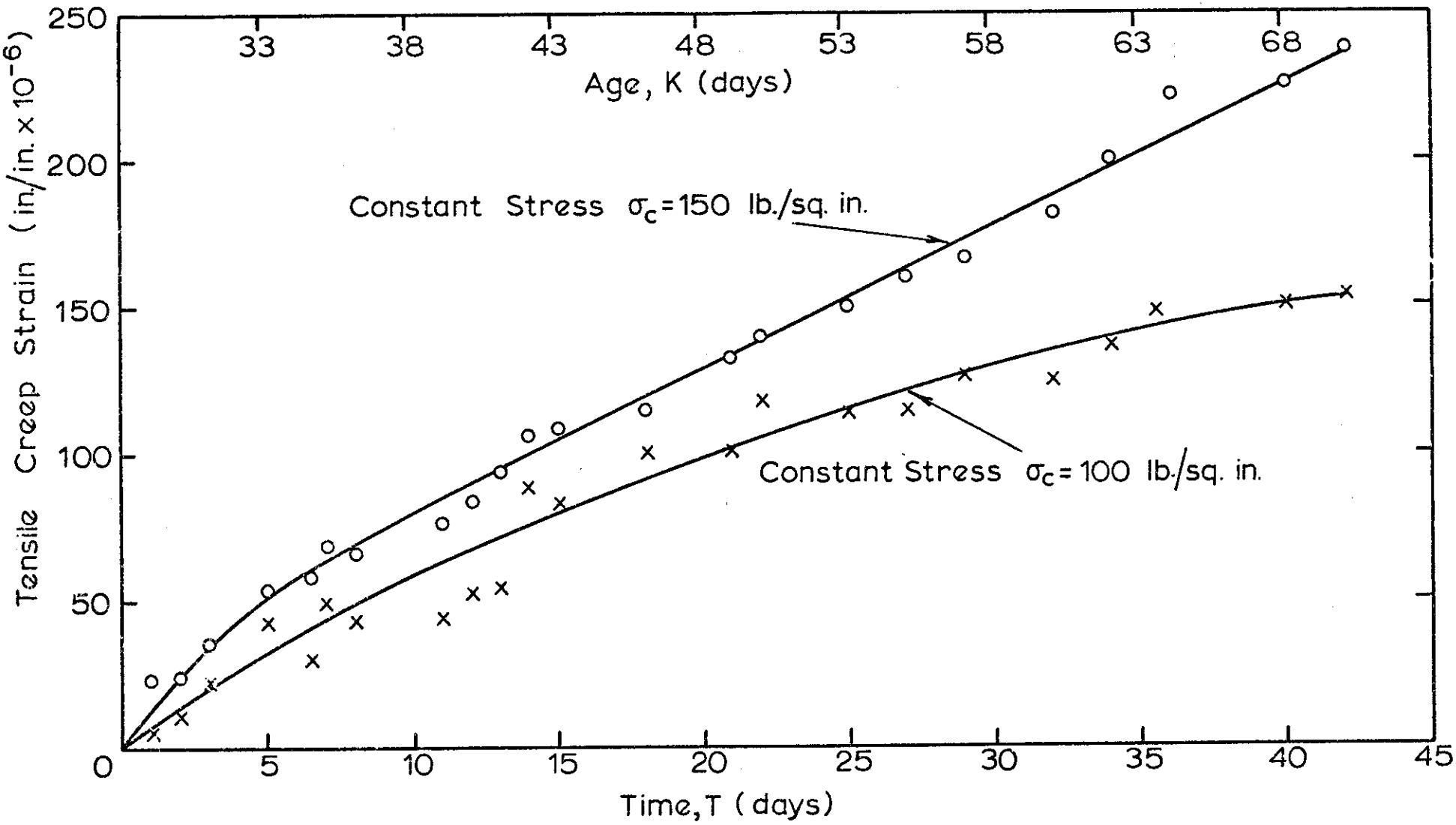

FIG. 9·3 TENSILE CREEP STRAINS WITH TIME FOR 4 in. DIA. SPECIMENS (CC12) UNDER CONSTANT APPLIED STRESS AT 70° F. AND 50% REL. HUMIDITY

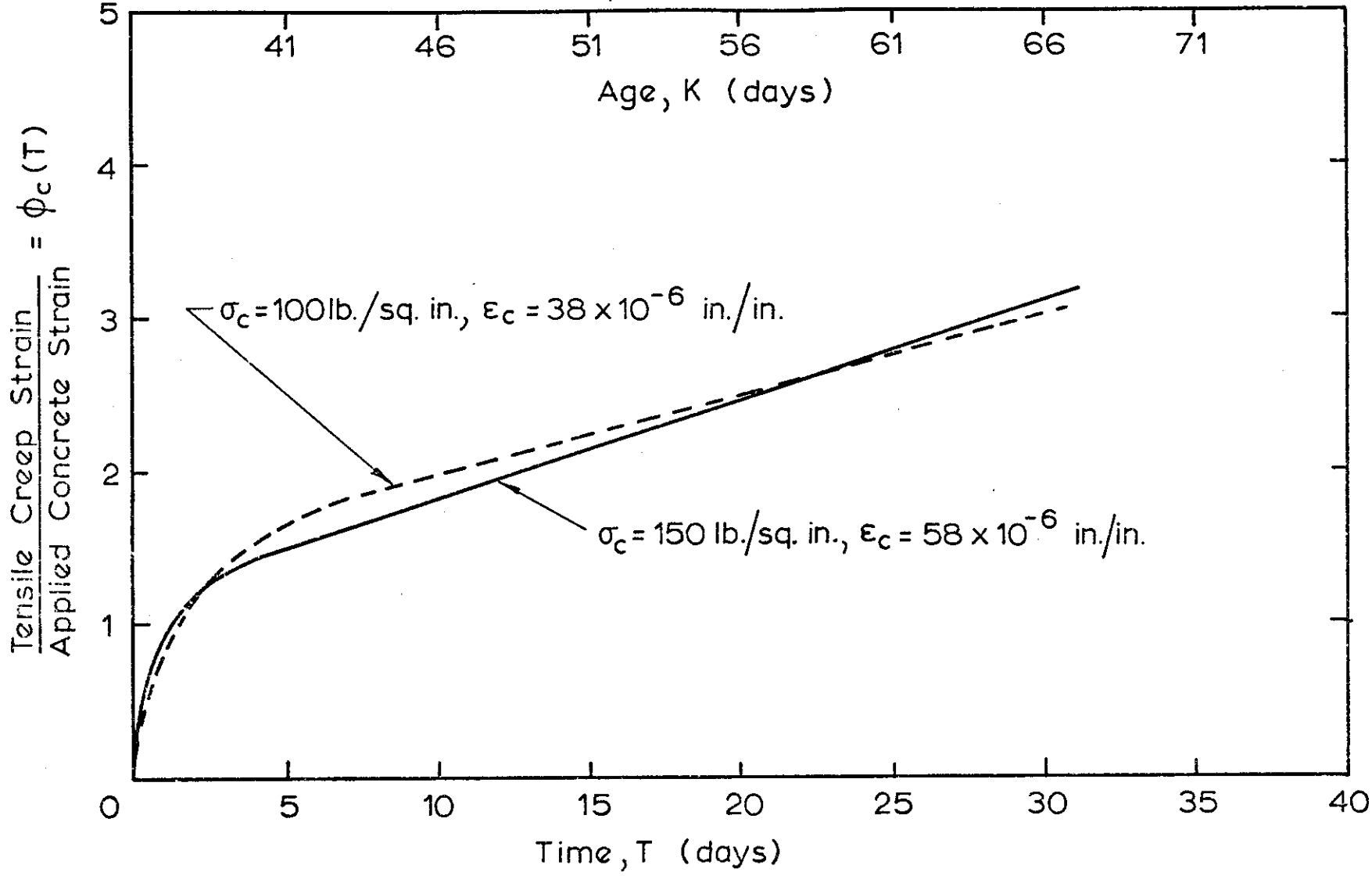

FIG. 9·4 CREEP COEFFICIENT WITH TIME FOR 4 IN. DIA. SPECIMENS (CC 6)

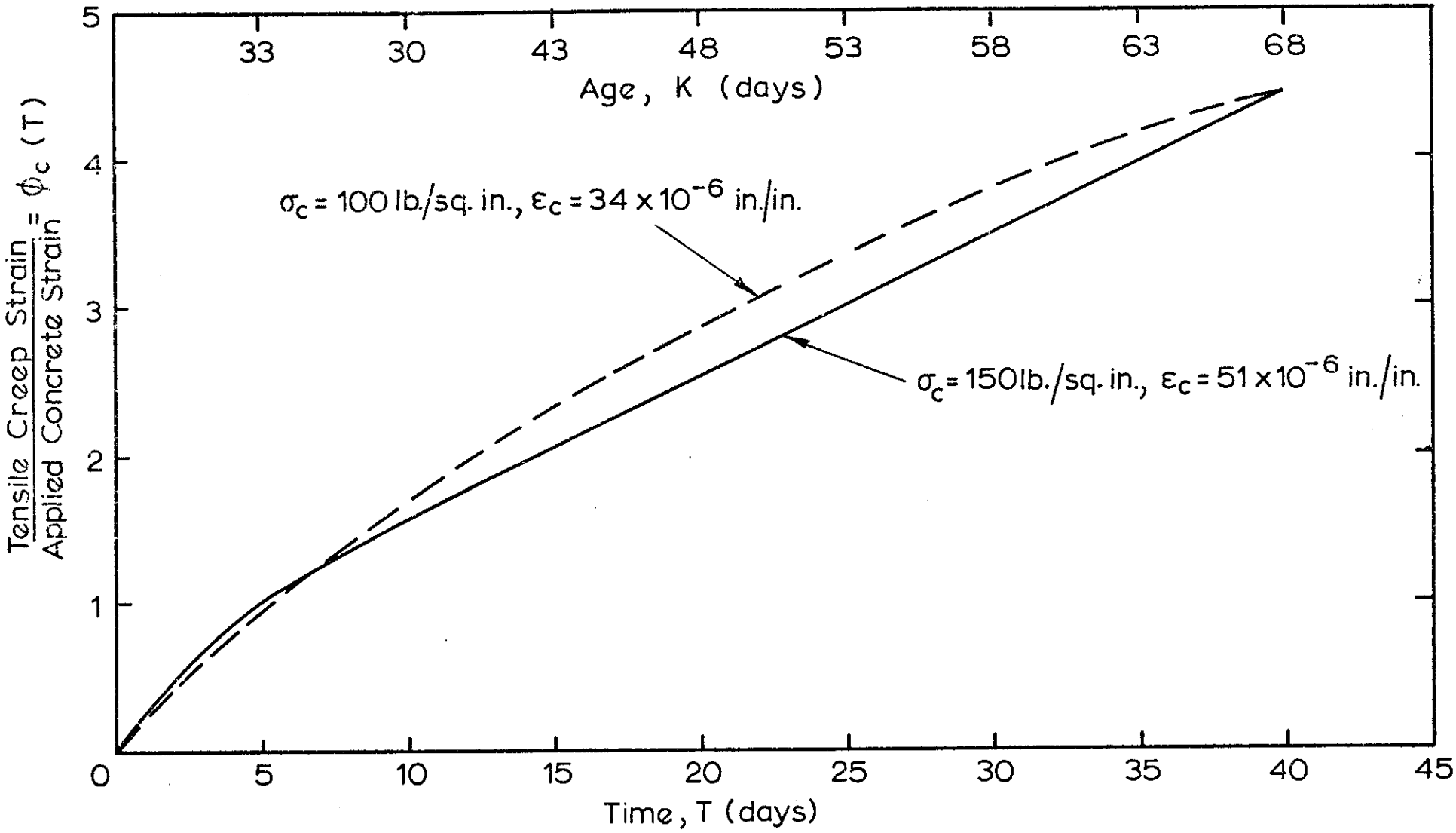

FIG. 9·5 CREEP COEFFICIENT WITH TIME FOR 4 IN. DIA. SPECIMENS (CC12).

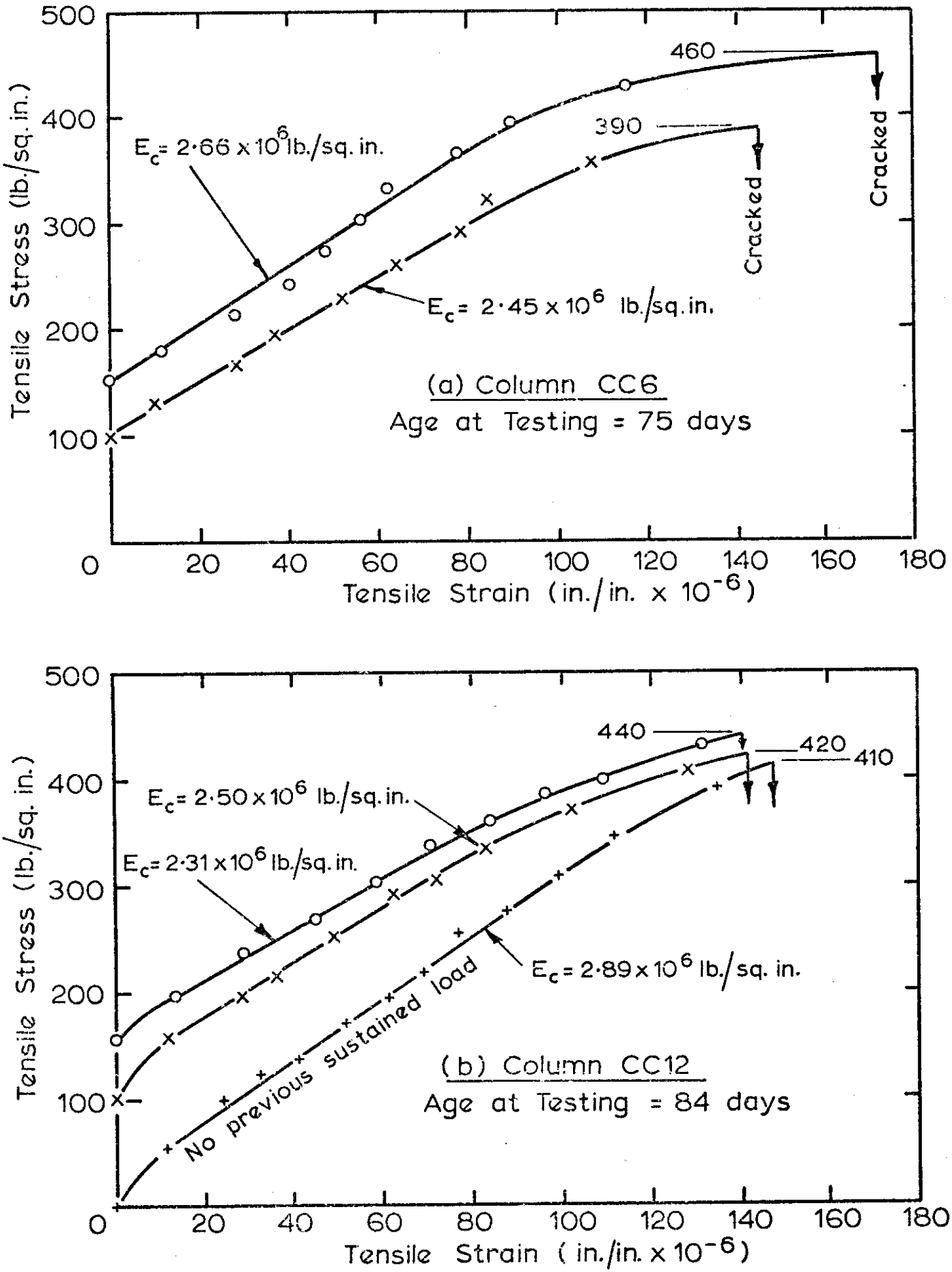

FIG 9·6 SHORT TERM DIRECT TENSION TESTS TO FAILURE ON 4 IN. DIA. CYLINDERS PREVIOUSLY UNDER CONSTANT SUSTAINED LOAD

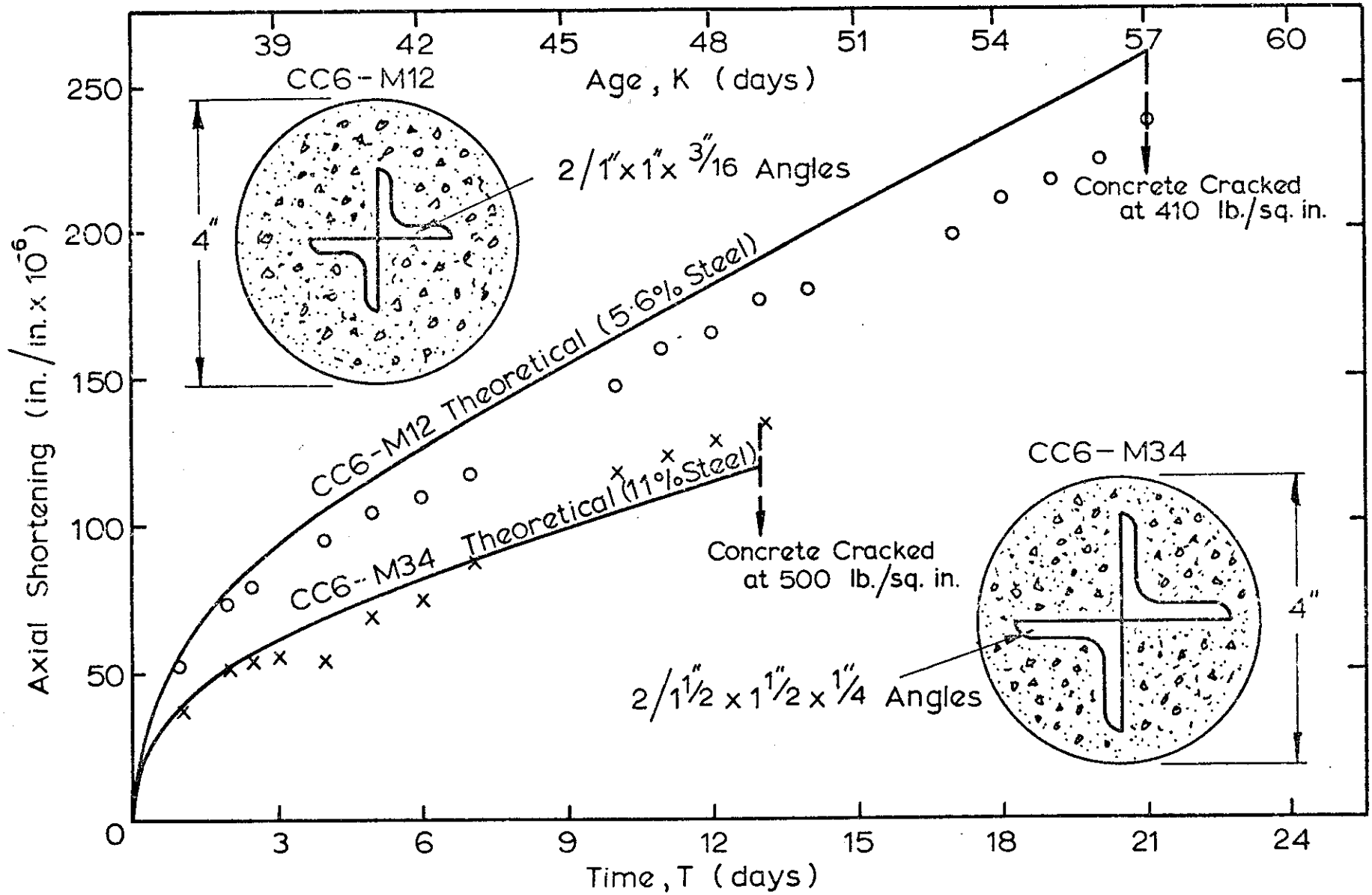

FIG. 9·7 AXIAL SHORTENING WITH TIME DUE TO CONCRETE SHRINKAGE FOR 4 IN. DIA. MODEL COLUMNS (CC6)

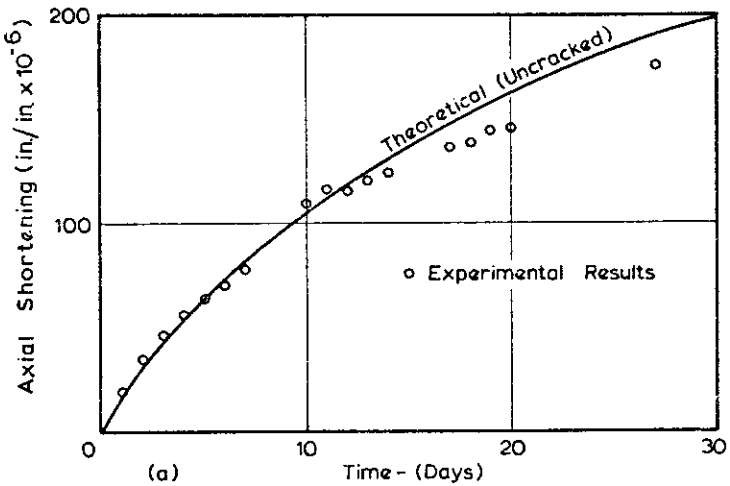

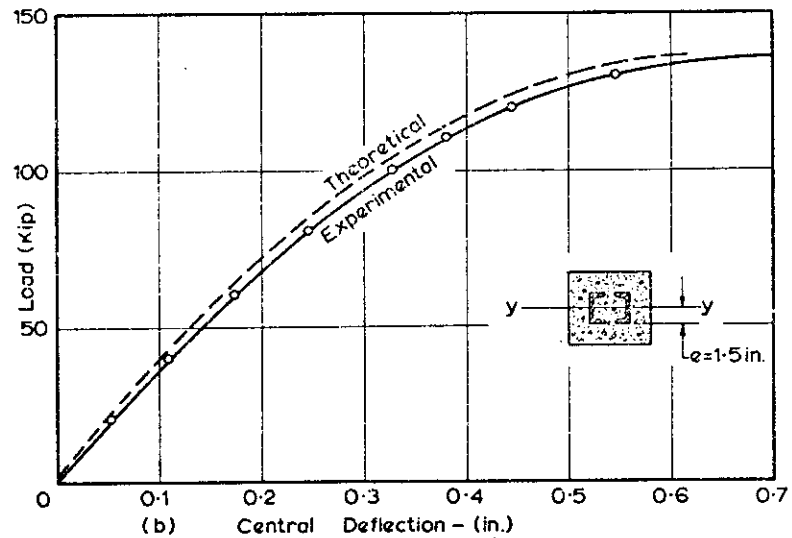

FIG. 9·8 STRAIN DATA AND LOAD - DEFLECTION CURVES FOR COLUMN CC6.

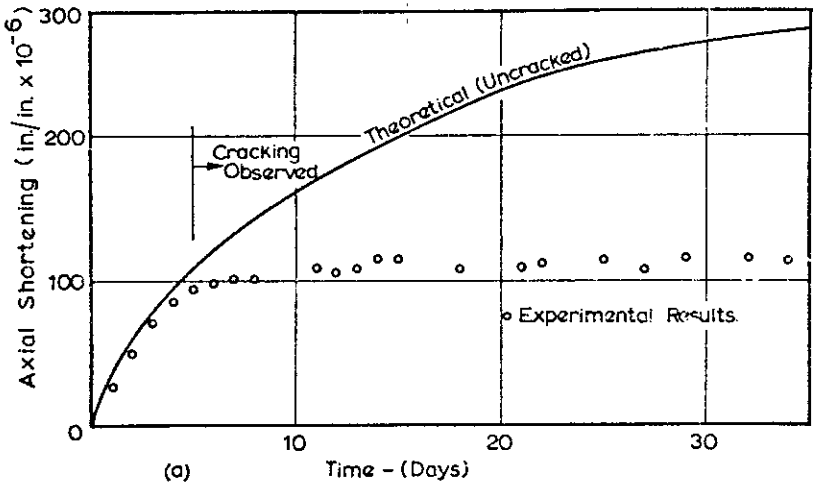

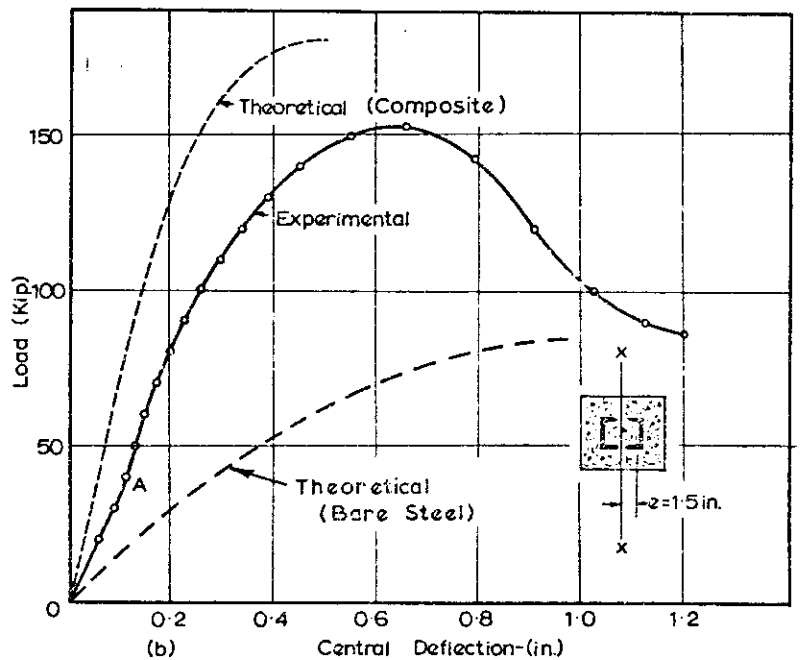

FIG 9·9 STRAIN DATA AND LOAD-DEFLECTION CURVES FOR COLUMN CC12.

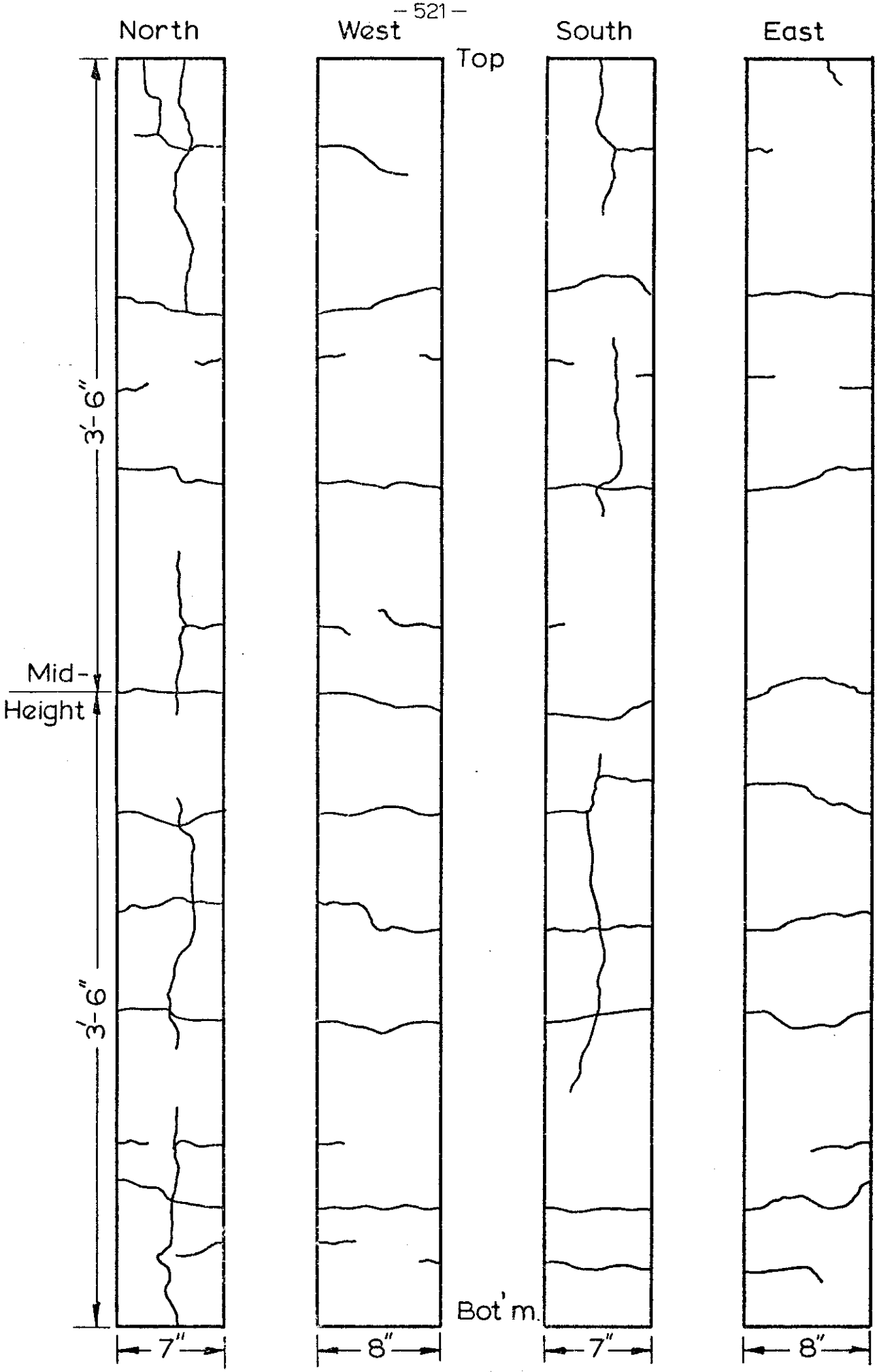

FIG. 9·10 SHRINKAGE CRACK PATTERN ON FACES OF COLUMN CC6

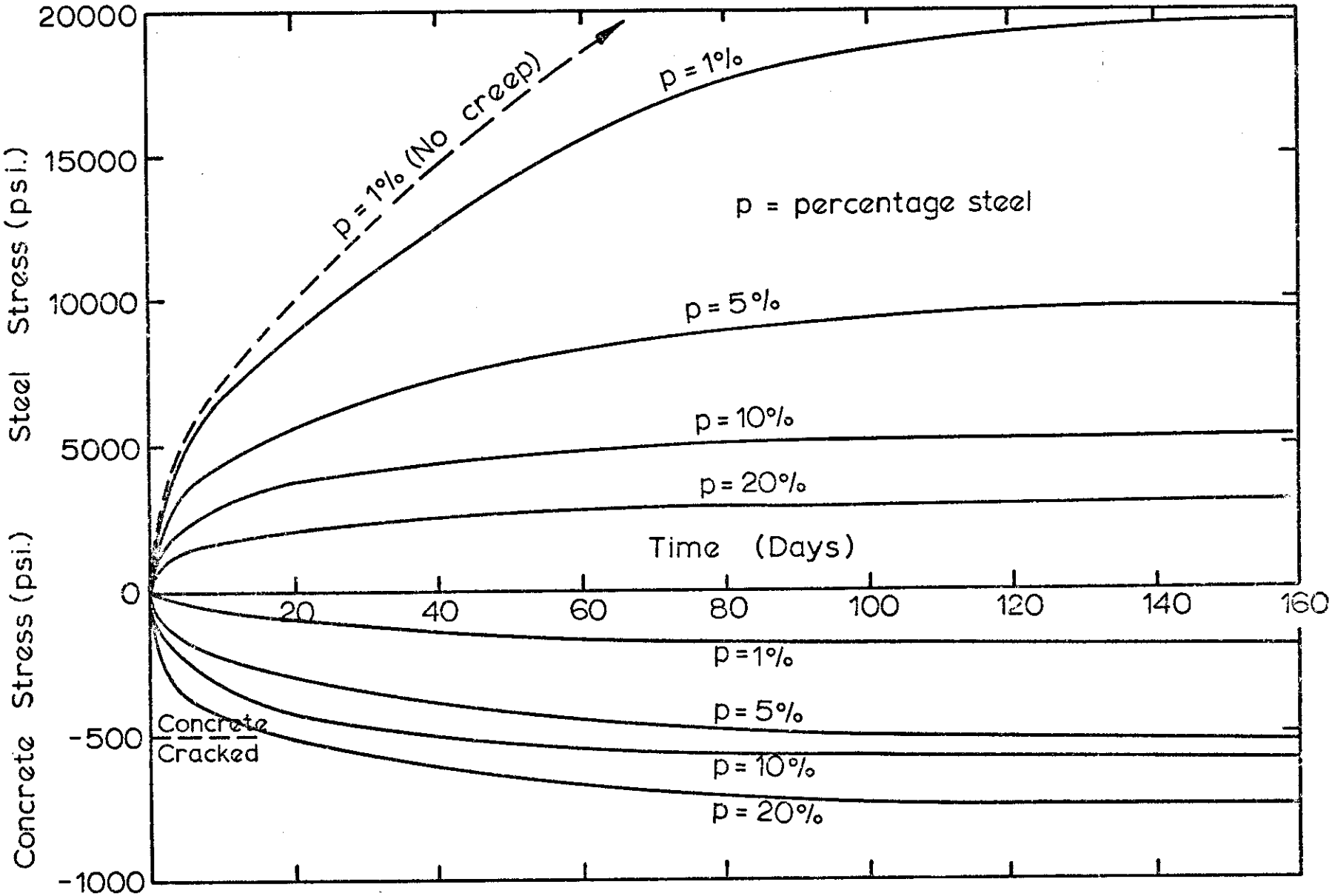

FIG. 9·11 STRESSES IN COMPOSITE COLUMNS DUE TO SHRINKAGE USING SHRINKAGE AND CREEP DATA IN FIG.9·1 AND FIG.9·4. (CC6)

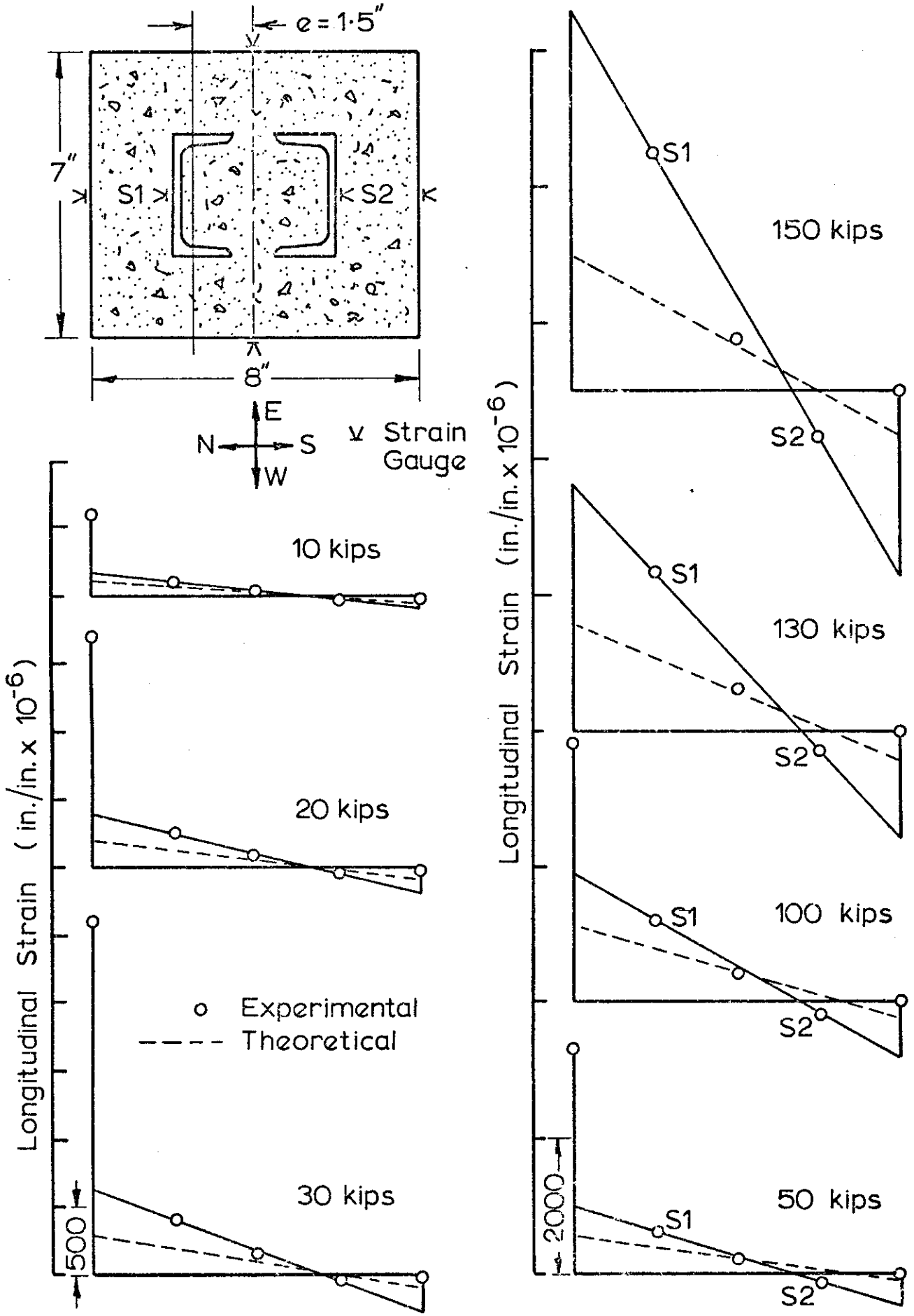

FIG. 9·12 STRAIN DISTRIBUTIONS FOR COLUMN CC6 CONTAINING SHRINKAGE CRACKS BEFORE LOADING.

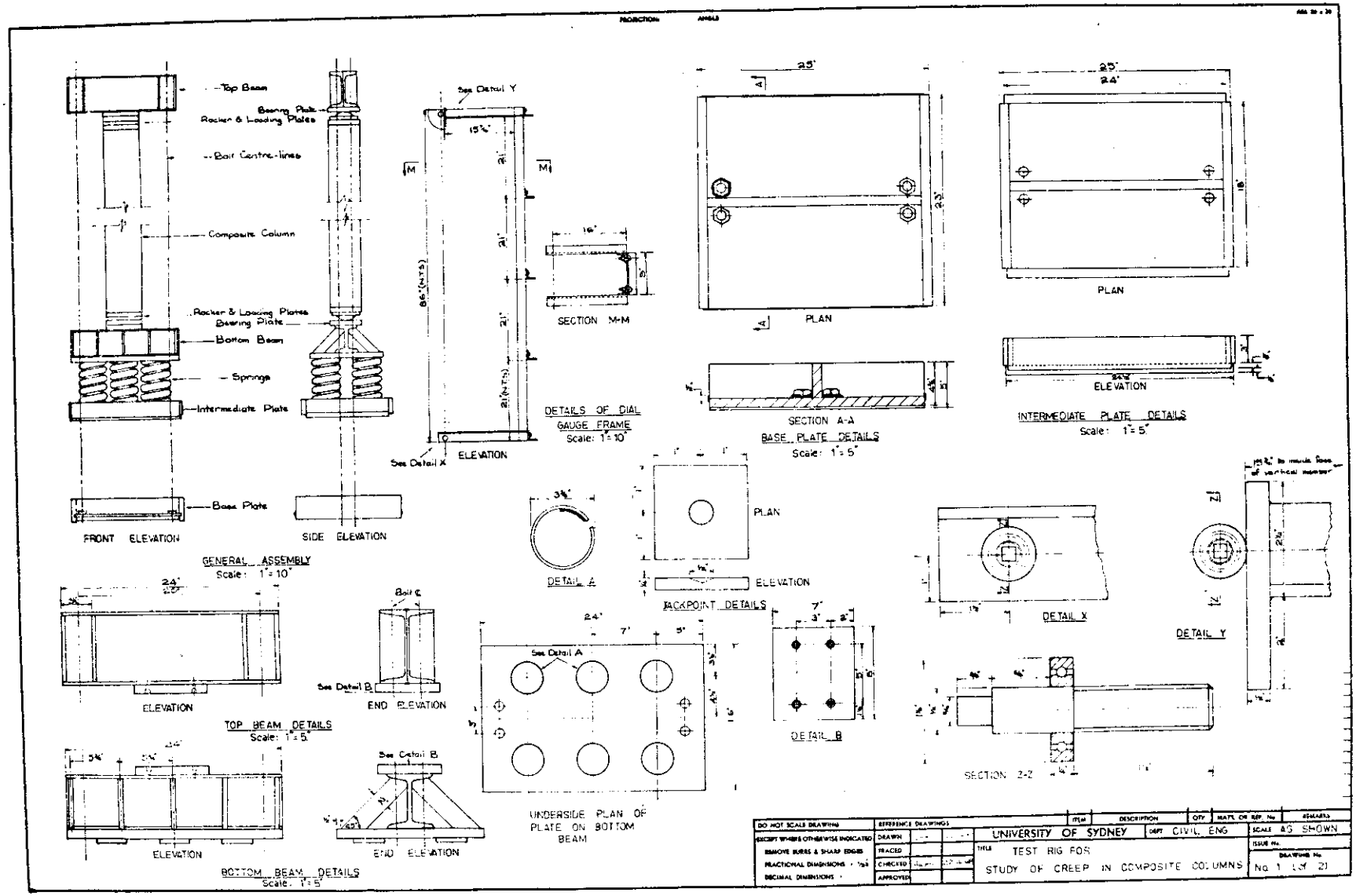

FIG. 10·1 DETAILS OF CREEP RIG FOR SUSTAINED LOADING

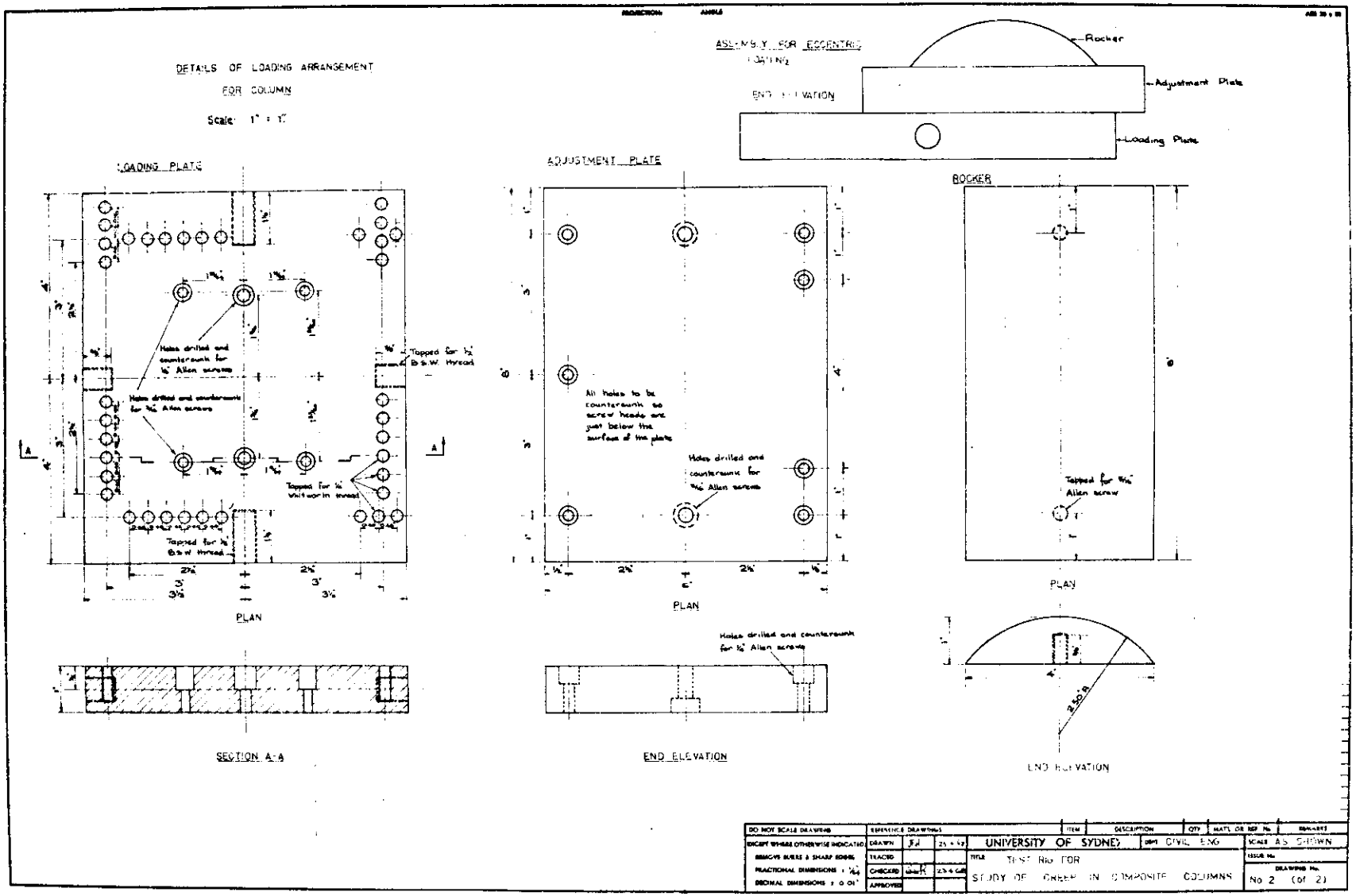

FIG. 10·2 END PLATES AND LOADING ROCKERS FOR CREEP COLUMNS

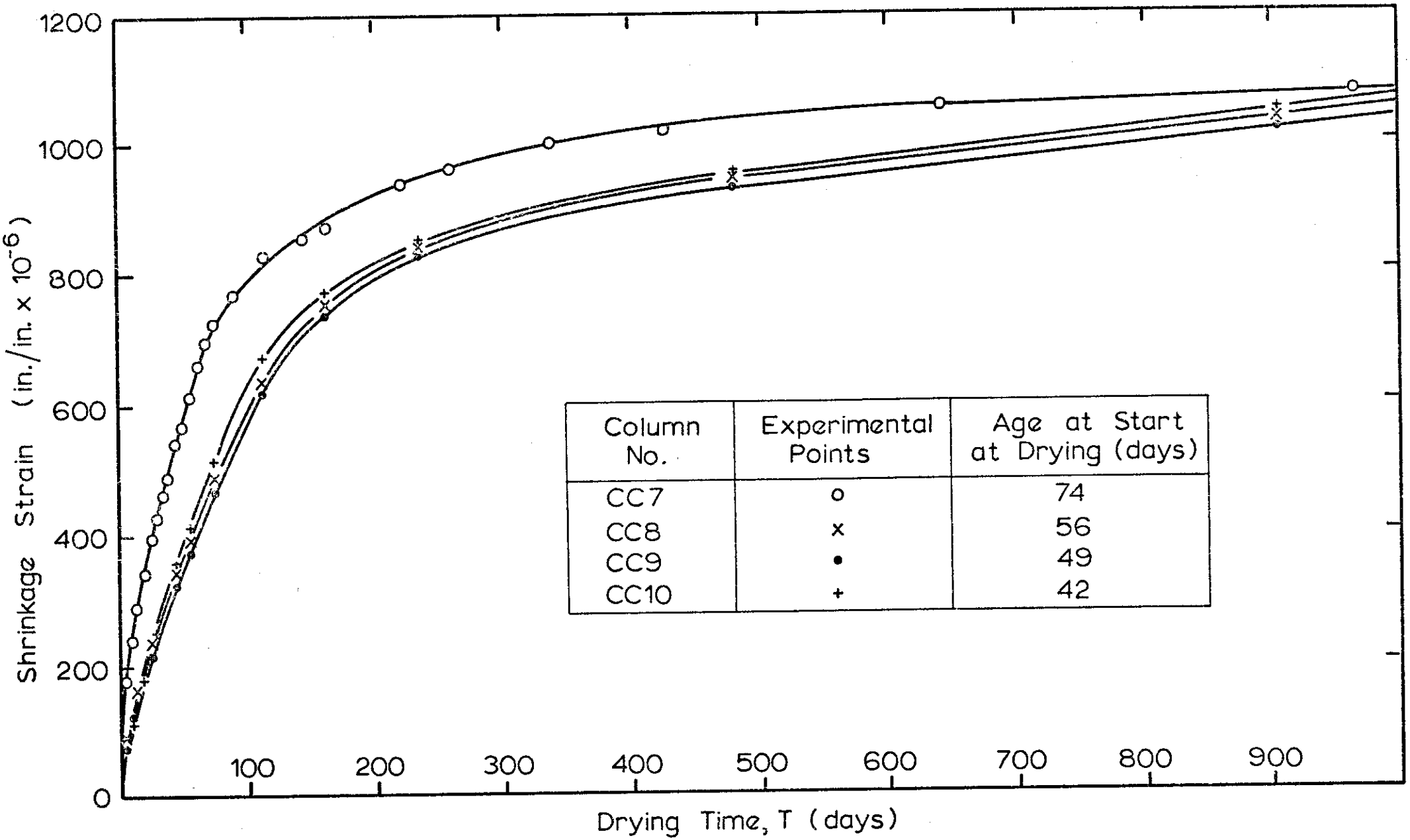

FIG. 10·3 FREE SHRINKAGE STRAINS FOR COLUMNS CC7, CC8, CC9 AND CC10

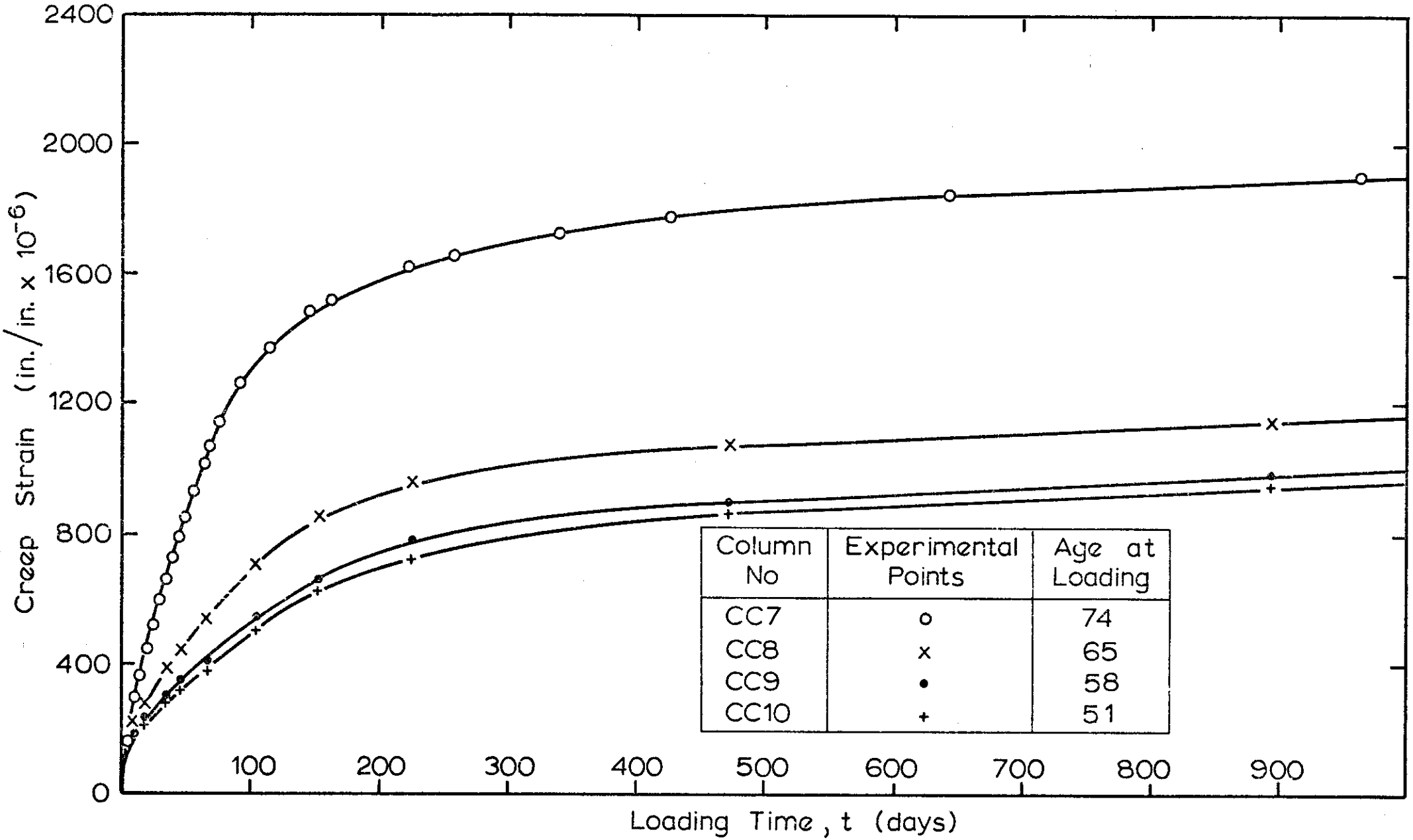

FIG. 10·4 CREEP STRAINS FOR 8 IN. x 7 IN. SPECIMENS AT CONSTANT STRESS OF 1140 LB./SQ. IN.

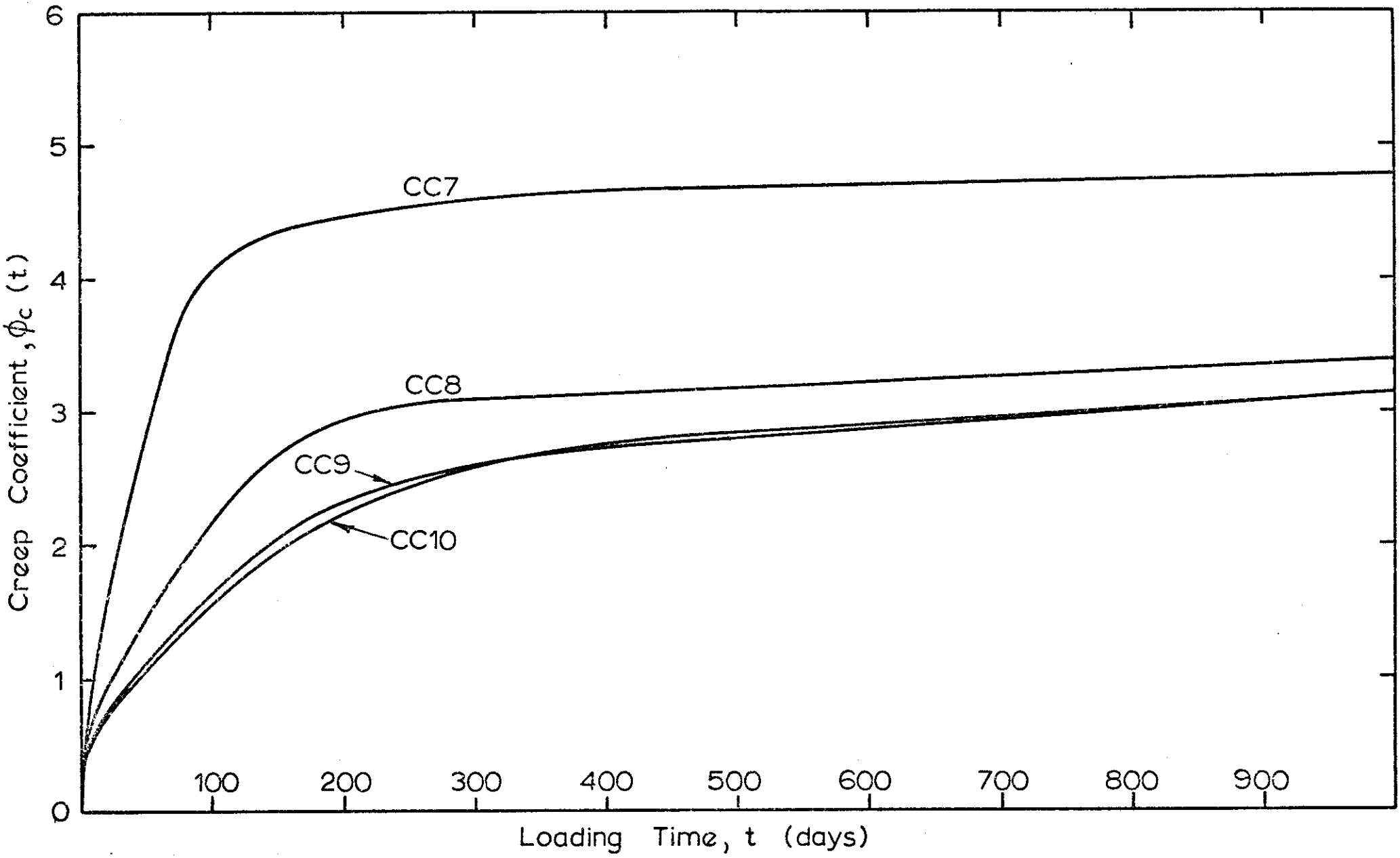

FIG. 10·5 VARIATION OF CREEP COEFFICIENT WITH TIME

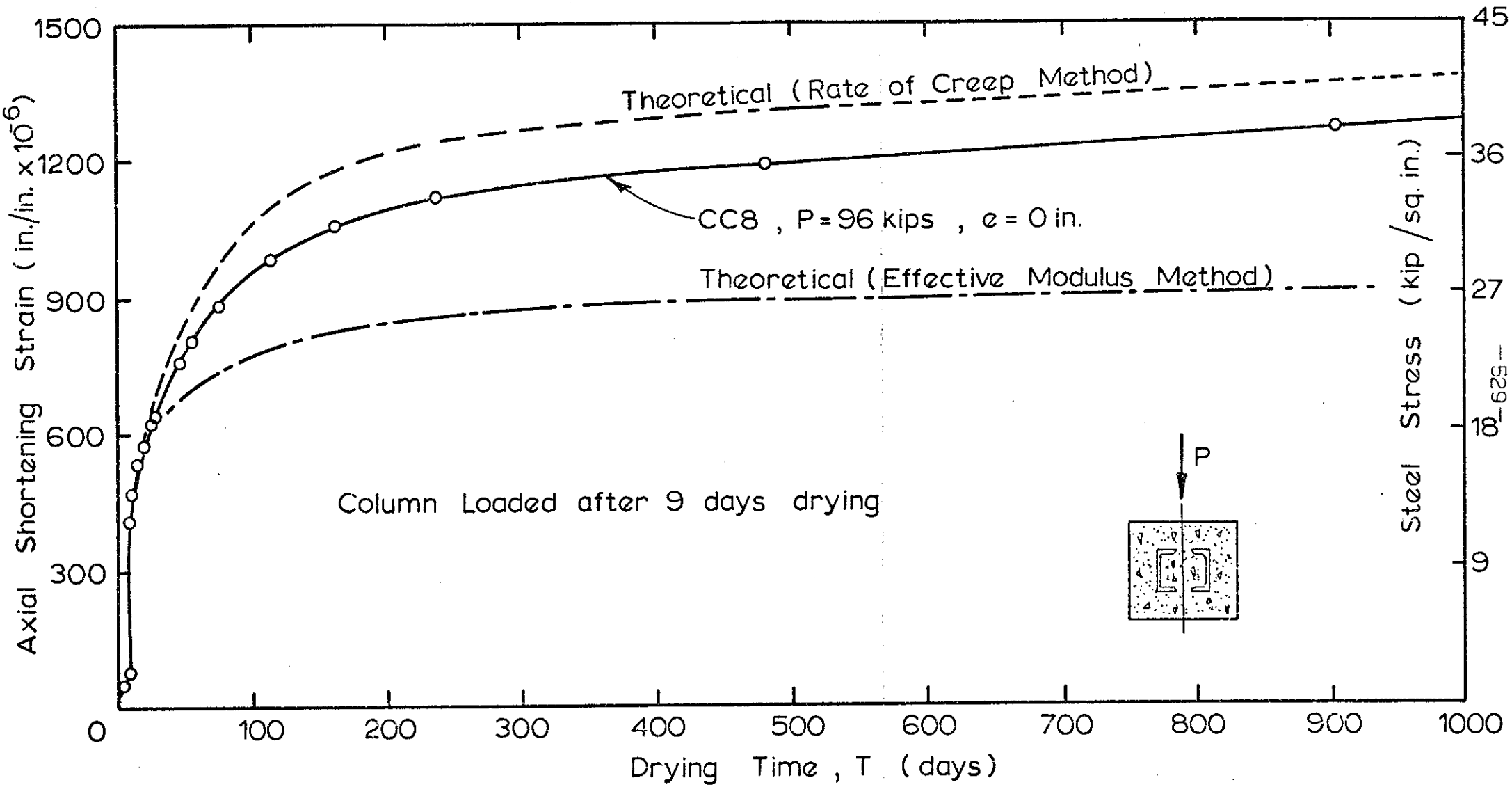

FIG. 10·6 AXIAL SHORTENING STRAIN FOR CONCENTRICALLY LOADED COLUMN CC8

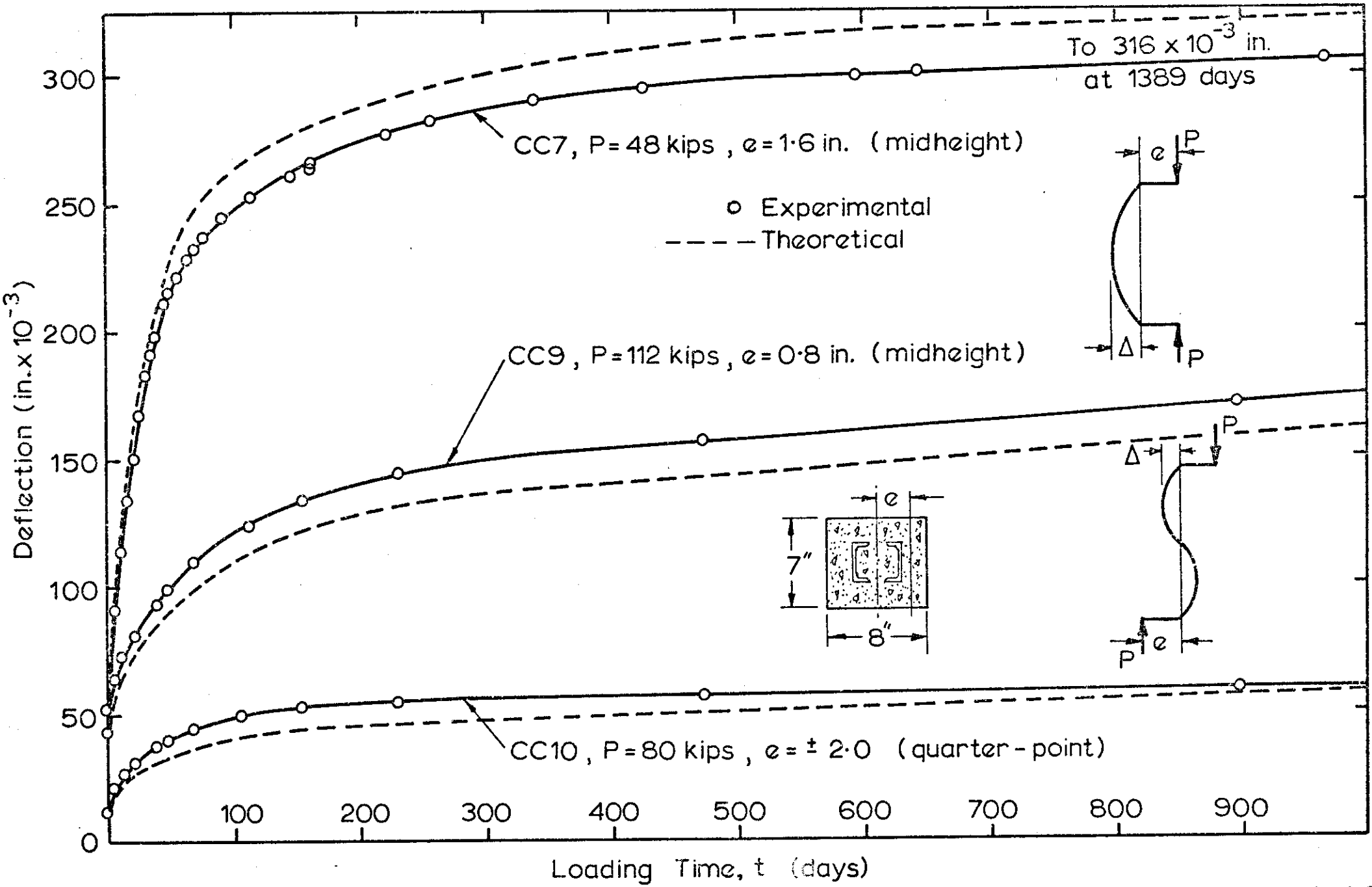

FIG. 10·7 VARIATION OF COLUMN DEFLECTION WITH TIME FOR CONSTANT APPLIED LOAD

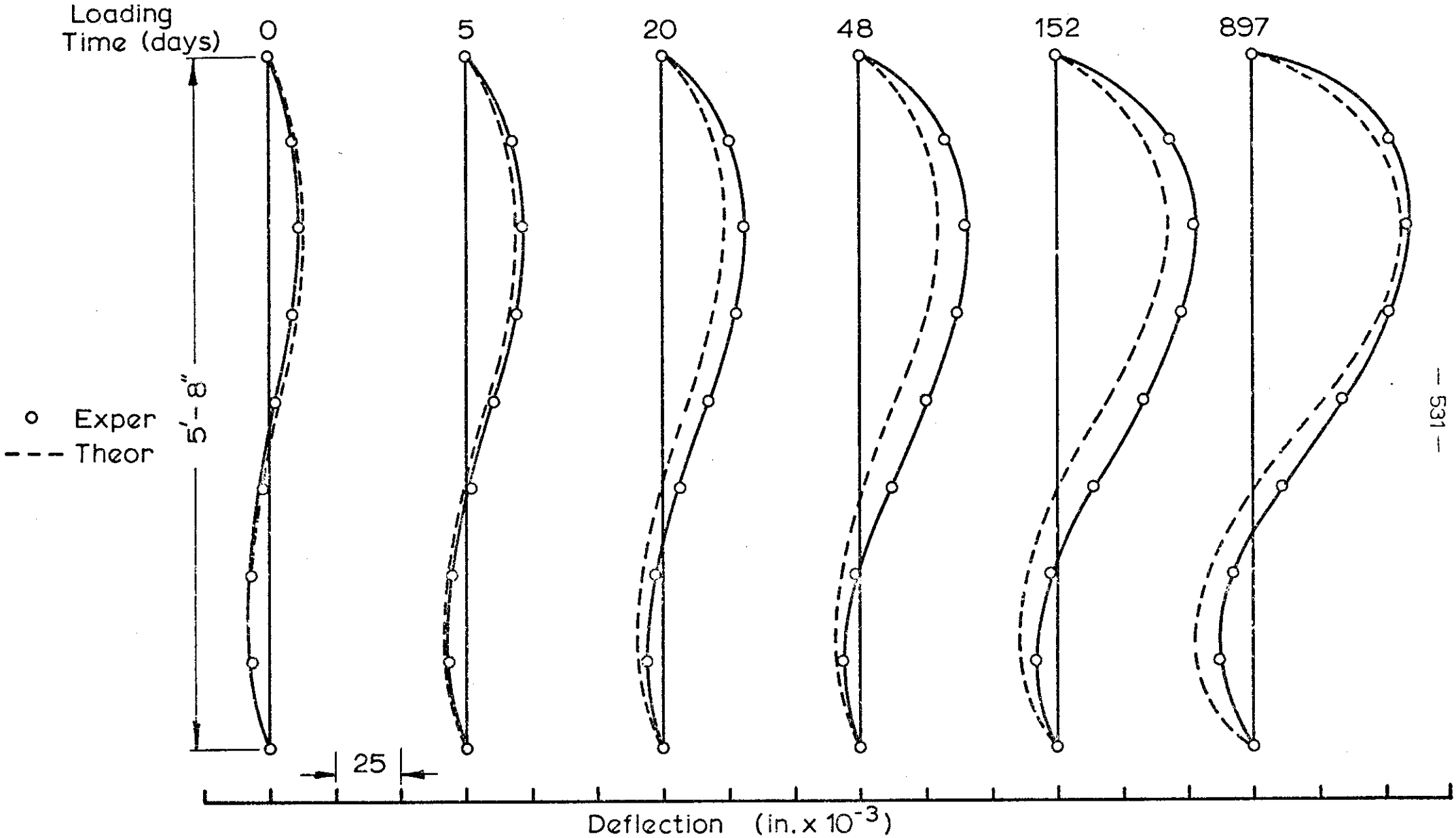

FIG. 10·8 DEFLECTION PROFILES FOR COLUMN CC10 BENT IN DOUBLE CURVATURE

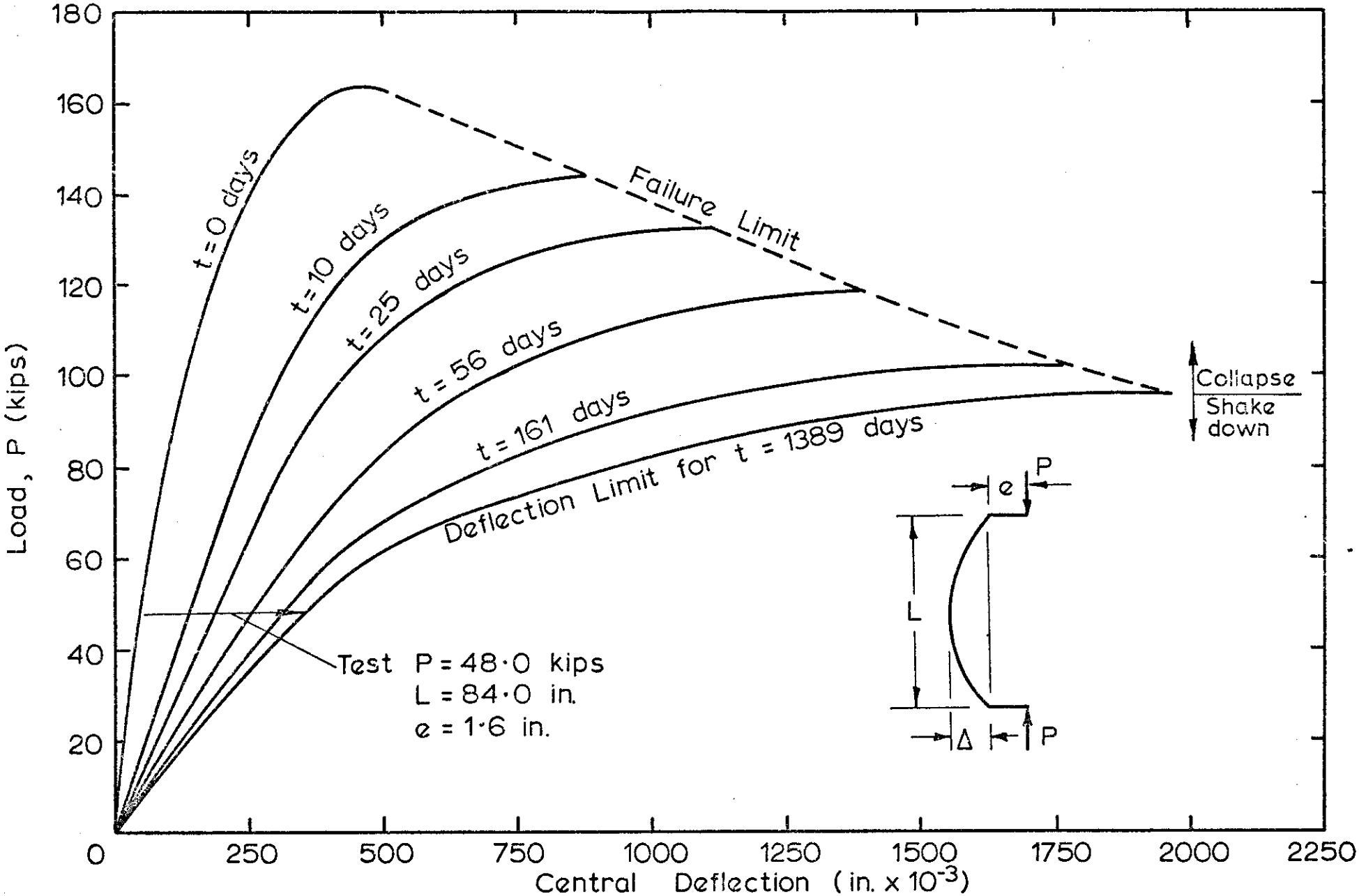

FIG. 10·9 THEORETICAL LOAD - DEFLECTION - TIME RELATIONSHIP FOR COLUMN CC7

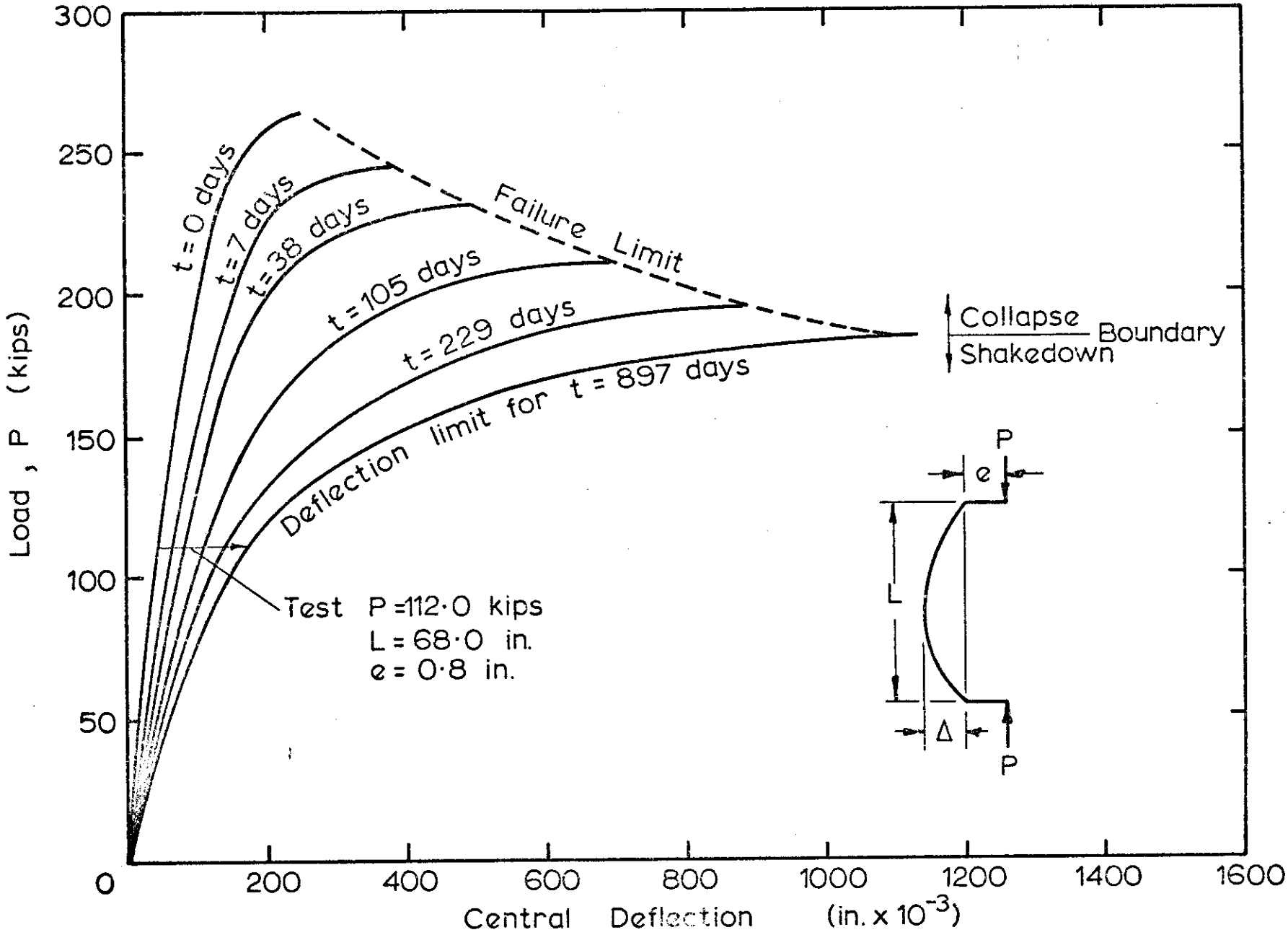

FIG. 10·10 THEORETICAL DEFLECTION – TIME RELATIONSHIP FOR COLUMN CC9

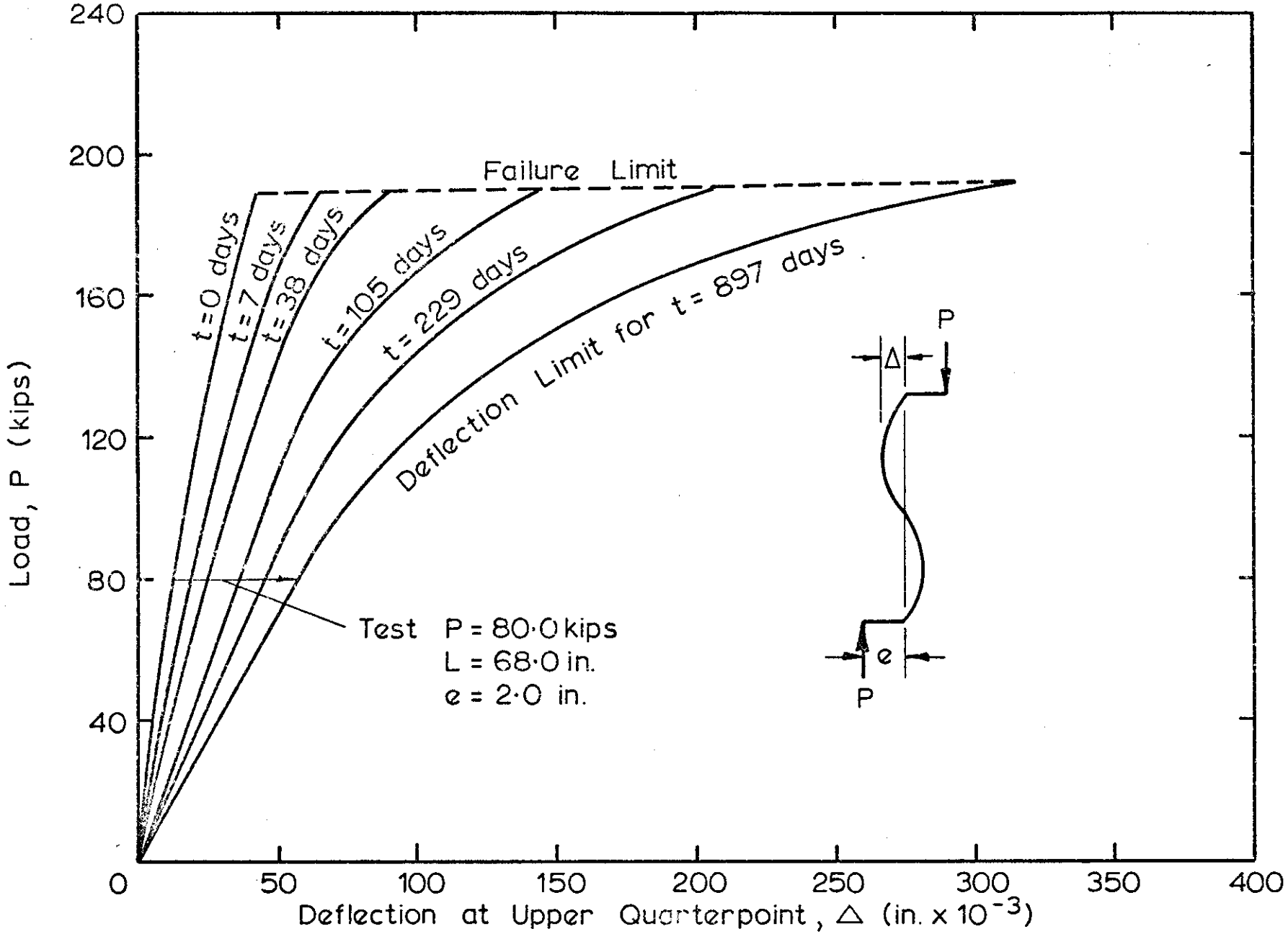

FIG. 10·11 THEORETICAL LOAD-DEFLECTION-TIME RELATIONSHIP FOR COLUMN CC10

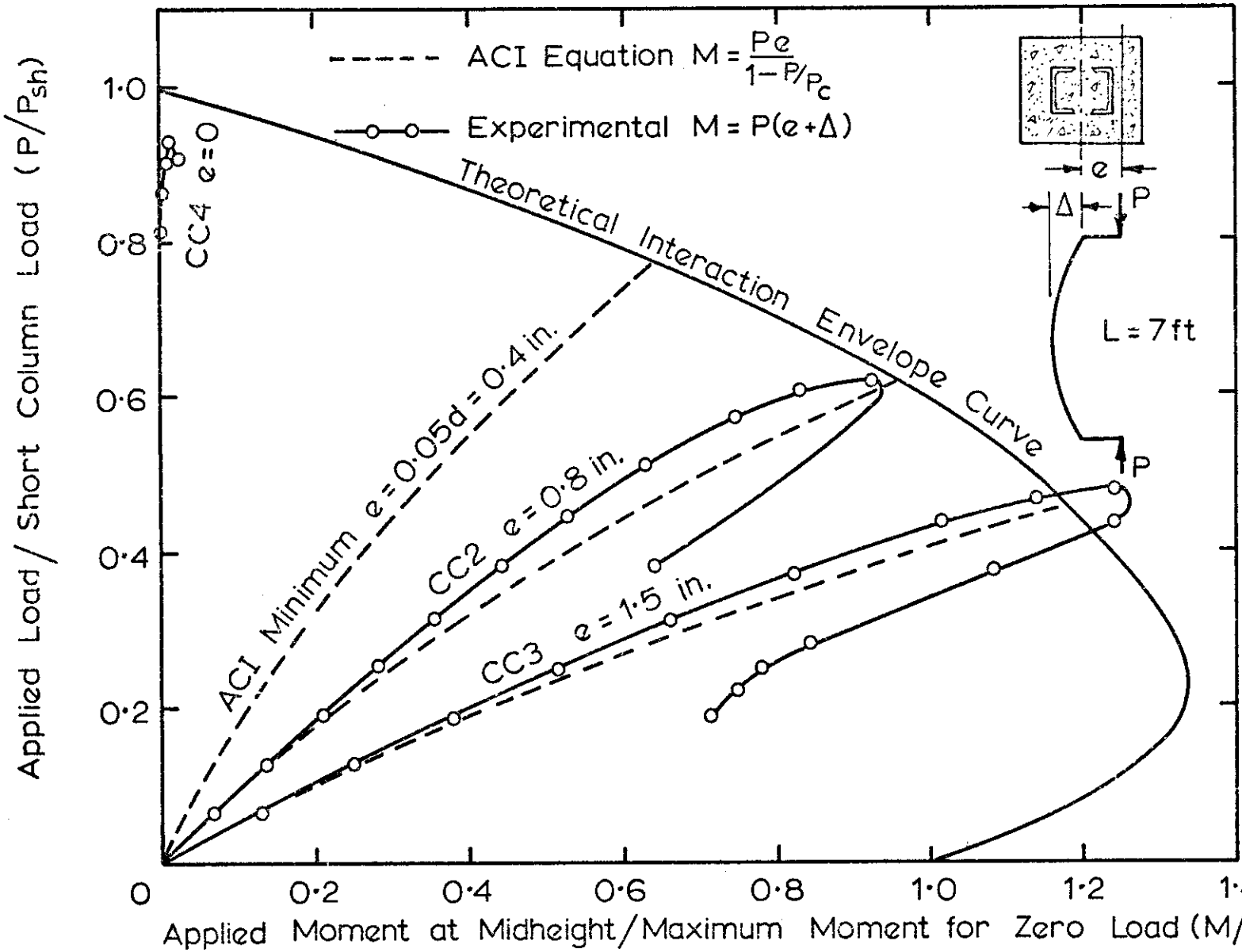

FIG. 11·1 LOAD - MOMENT BEHAVIOUR OF CC SERIES 7FT. COMPOSITE COLUMNS BENT ABOUT THE MAJOR AXIS

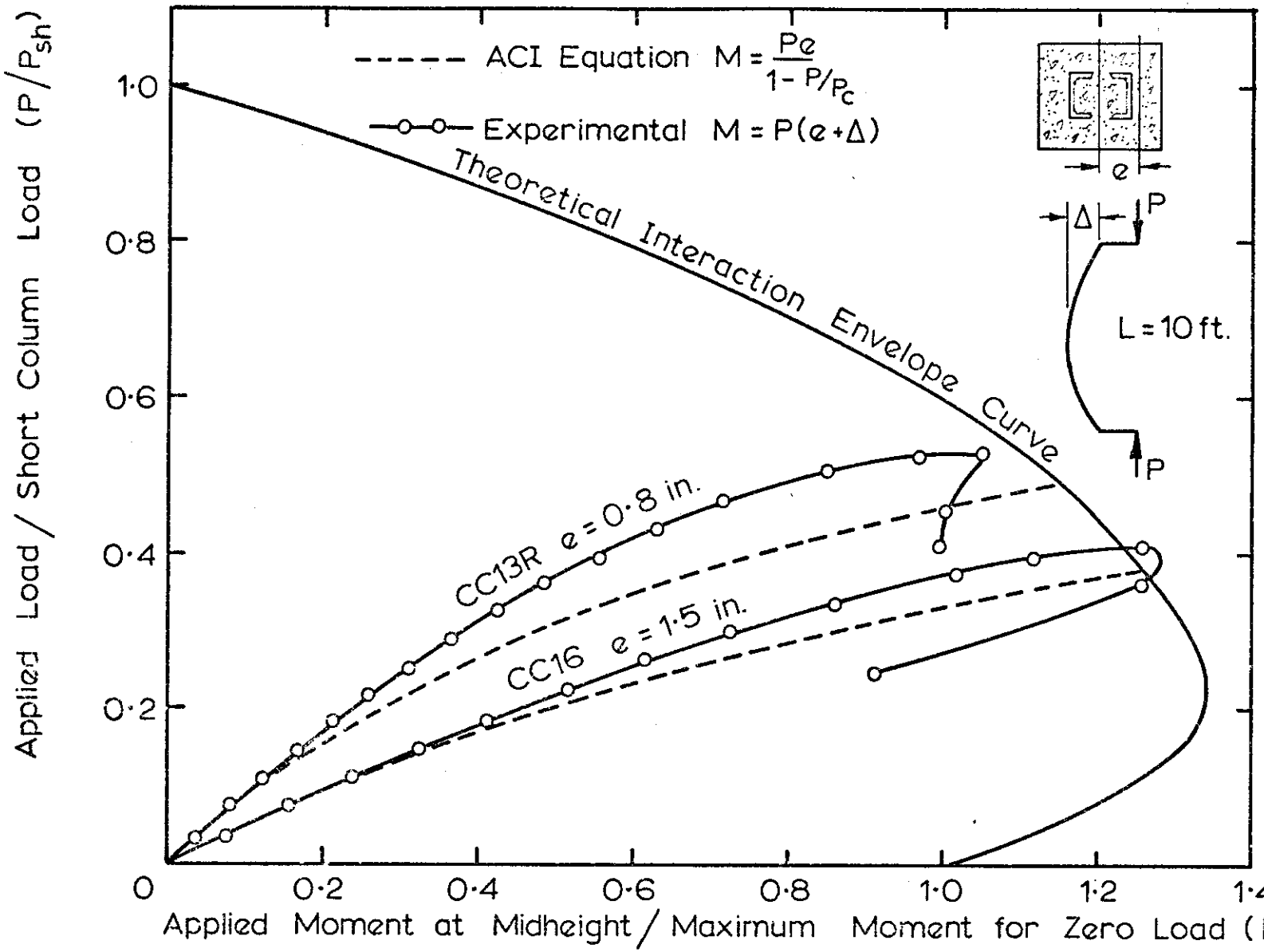

FIG. 11·2 LOAD - MOMENT BEHAVIOUR OF CC SERIES 10 FT. COMPOSITE COLUMNS BENT ABOUT THE MAJOR AXIS

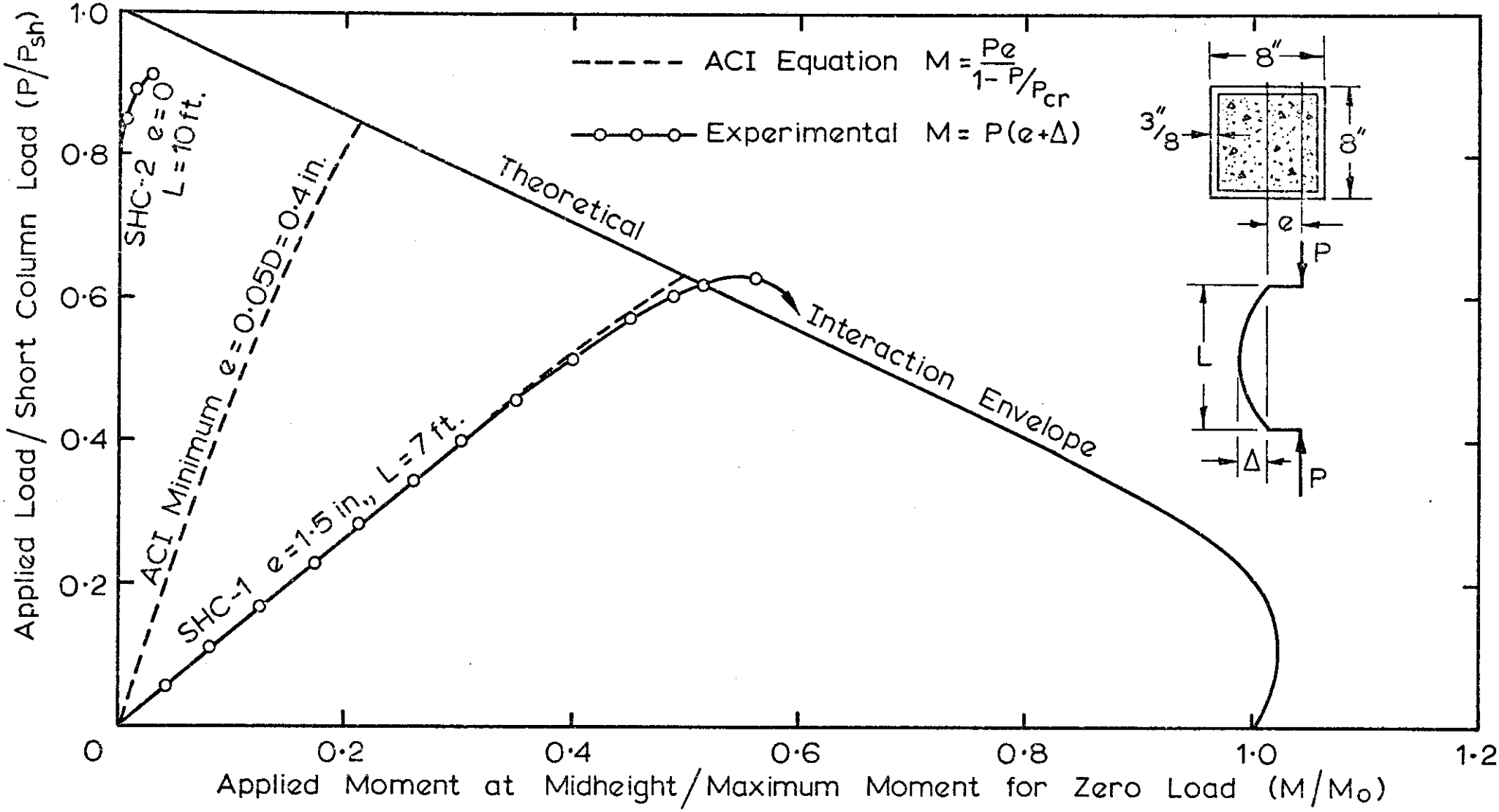

FIG. 11·3 LOAD MOMENT BEHAVIOUR FOR 8 IN. x 8 IN. x 3/8 IN. CONCRETE FILLED TUBES WITH 0° LOADING AXIS INCLINATION

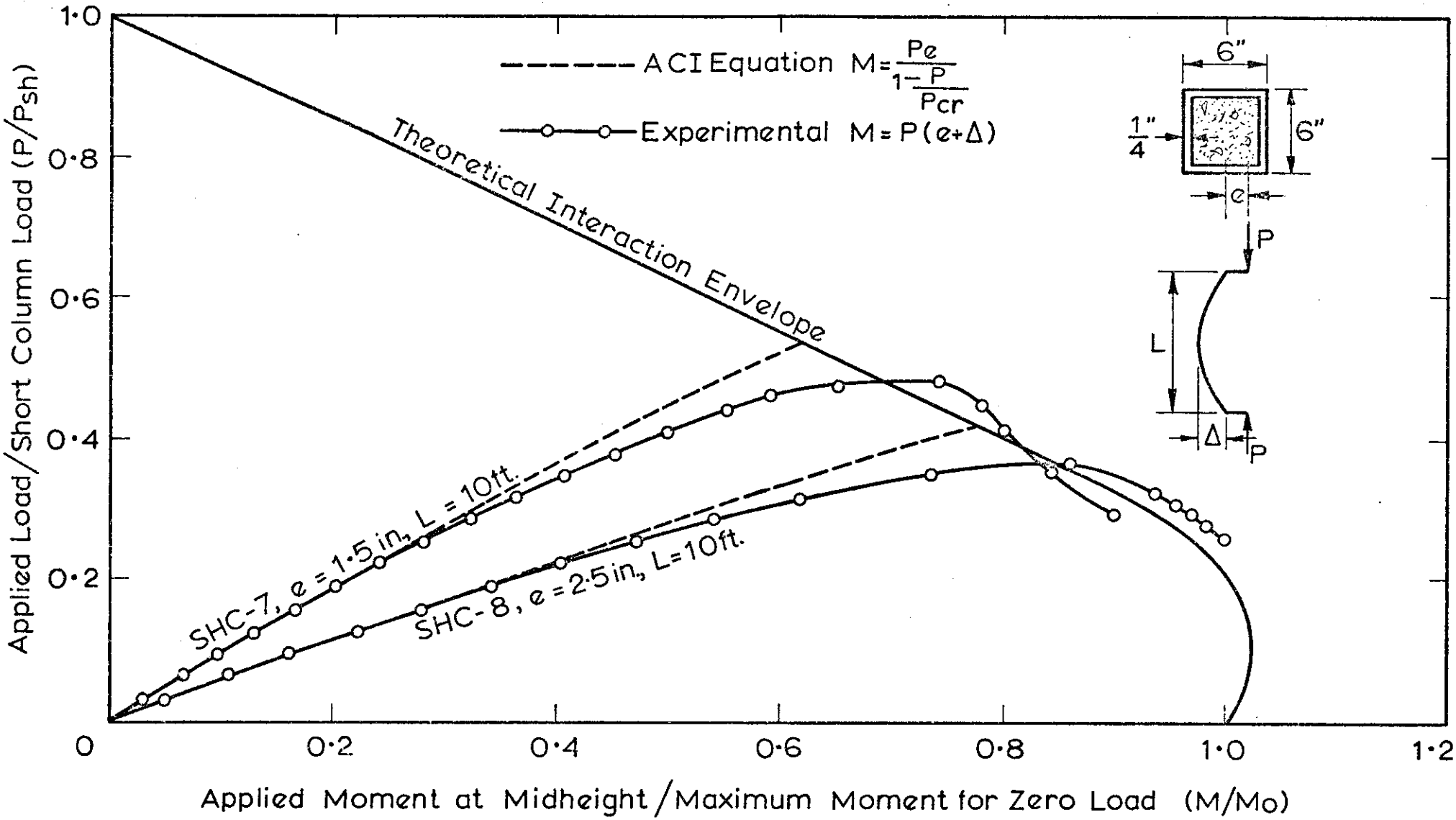

FIG. 11.4 LOAD MOMENT BEHAVIOUR FOR 6 IN x 6 IN x $\frac{1}{4}$ IN. CONCRETE FILLED TUBES WITH 0° LOADING AXIS INCLINATION

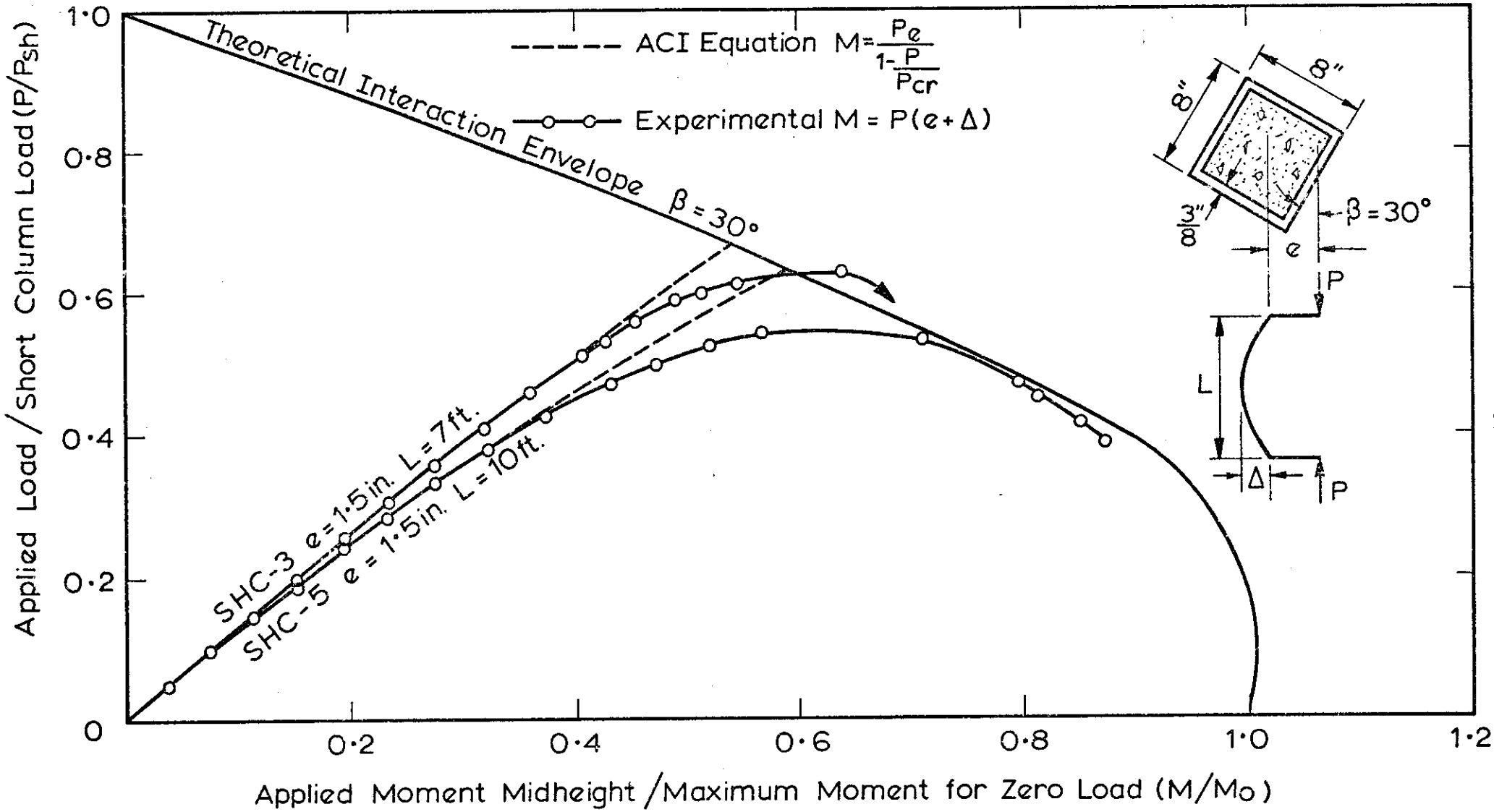

FIG. 11·5 LOAD MOMENT BEHAVIOUR FOR 8 IN. x 8 IN. x $\frac{3}{8}$ IN. CONCRETE FILLED TUBES WITH 30° LOADING AXIS INCLINATION

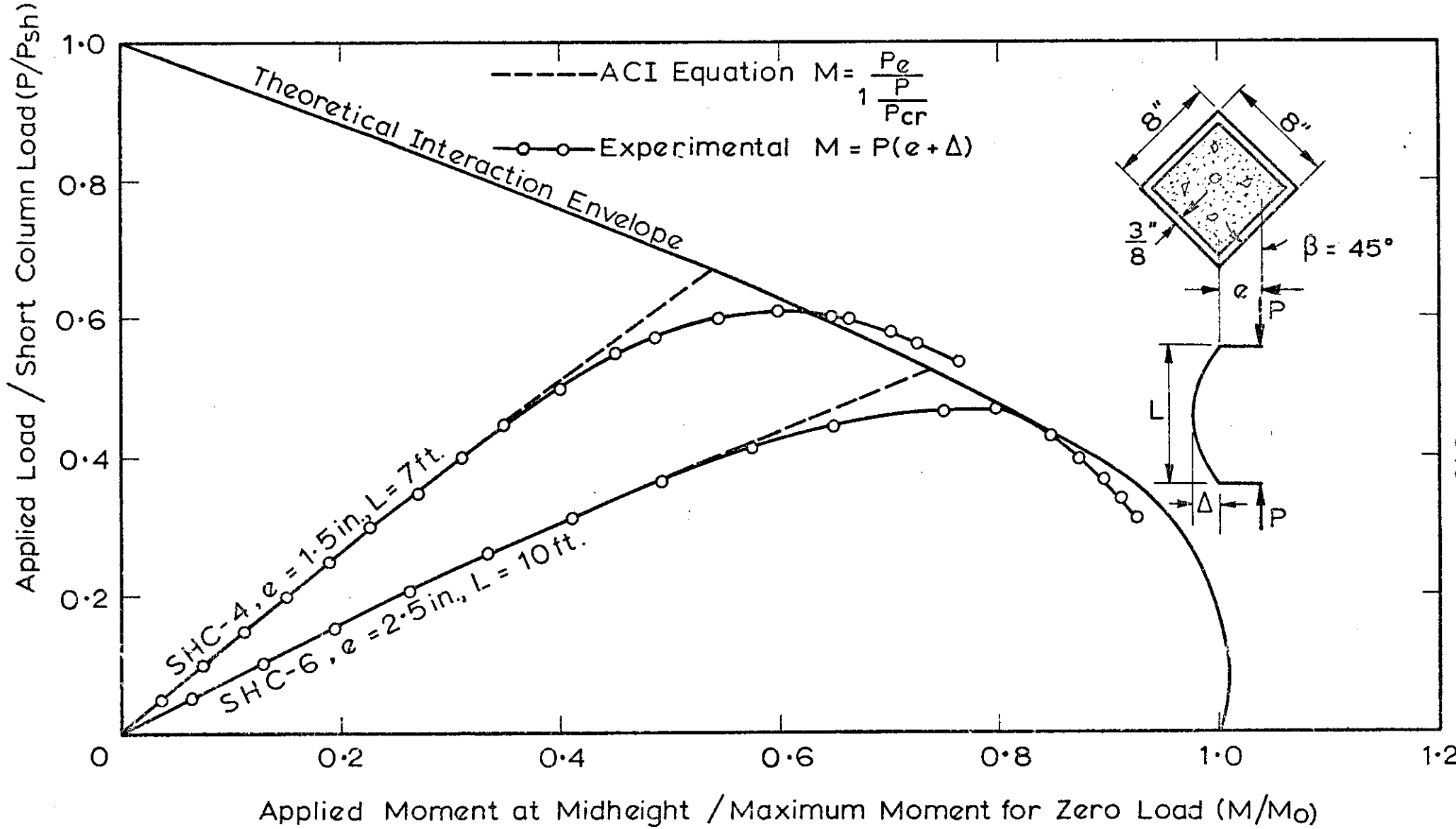

FIG. 11·6 LOAD MOMENT BEHAVIOUR FOR 8 IN. x 8 IN. x $\frac{3}{8}$ IN. CONCRETE FILLED TUBES WITH 45° LOADING AXIS INCLINATION.

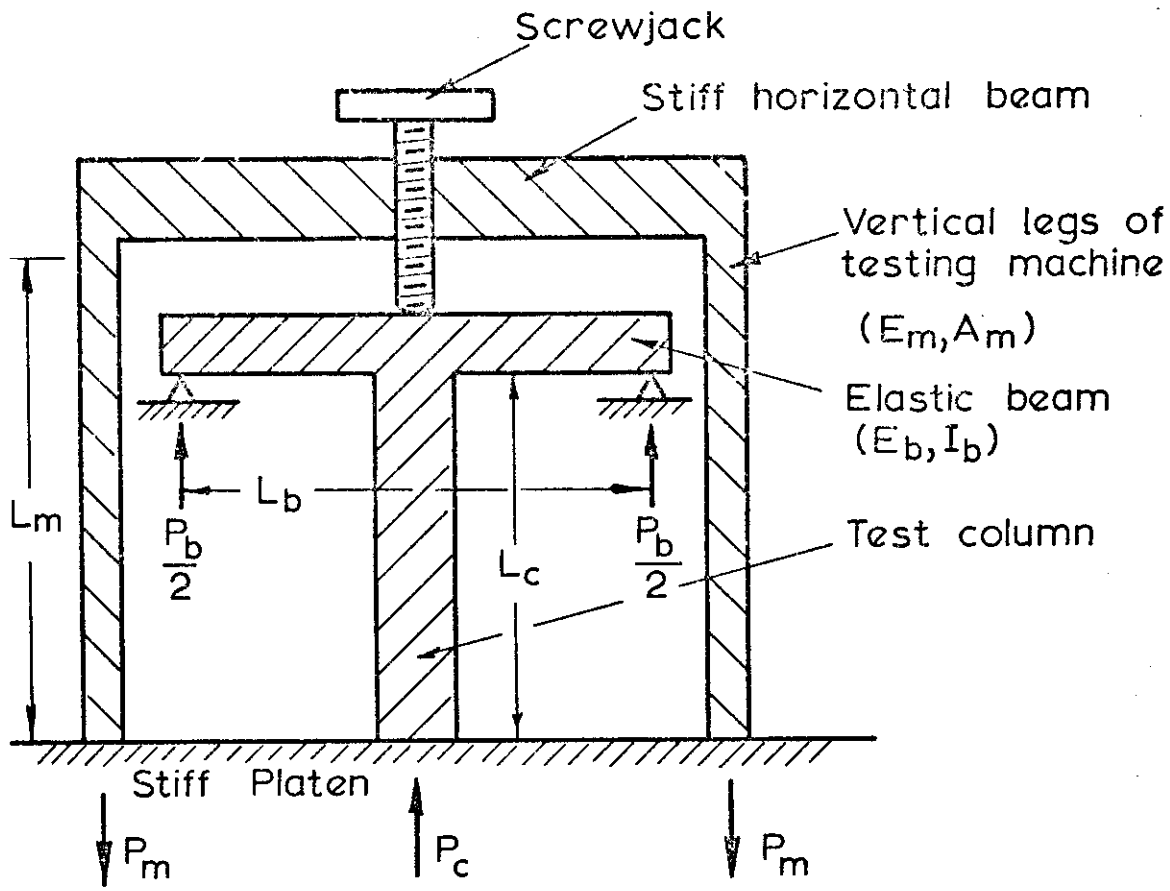

FIG. A·1 CONCENTRIC COMPRESSION TEST ON COLUMN IN SIMPLE REDUNDANT FRAME

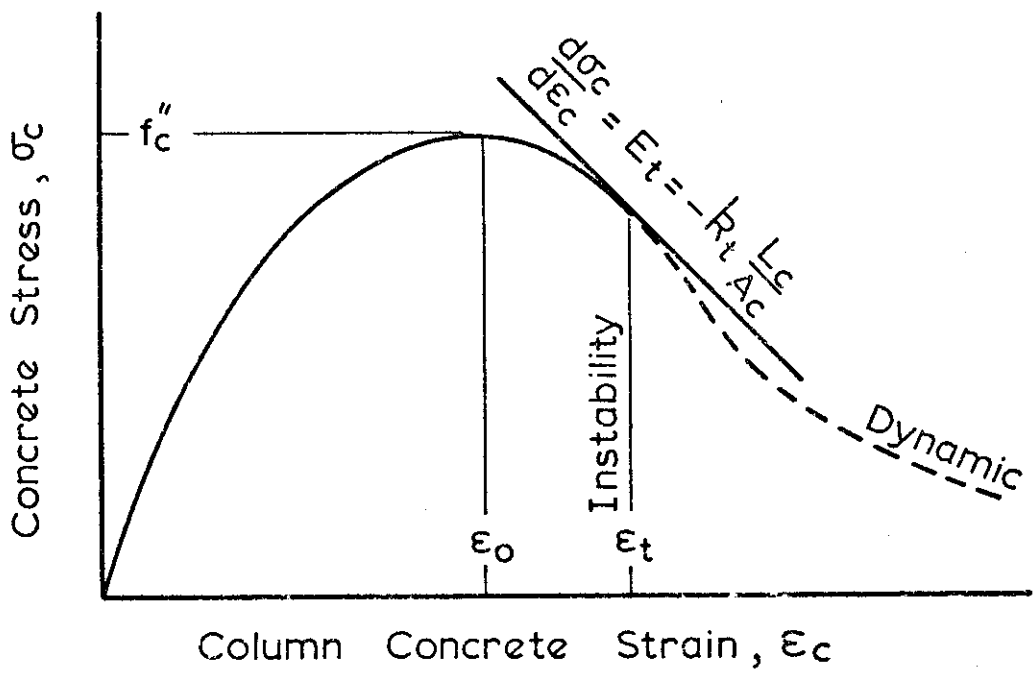

FIG. A·2 EFFECT OF TEST STIFFNESS ON THE INSTABILITY OF CONCENTRICALLY LOADED COLUMNS

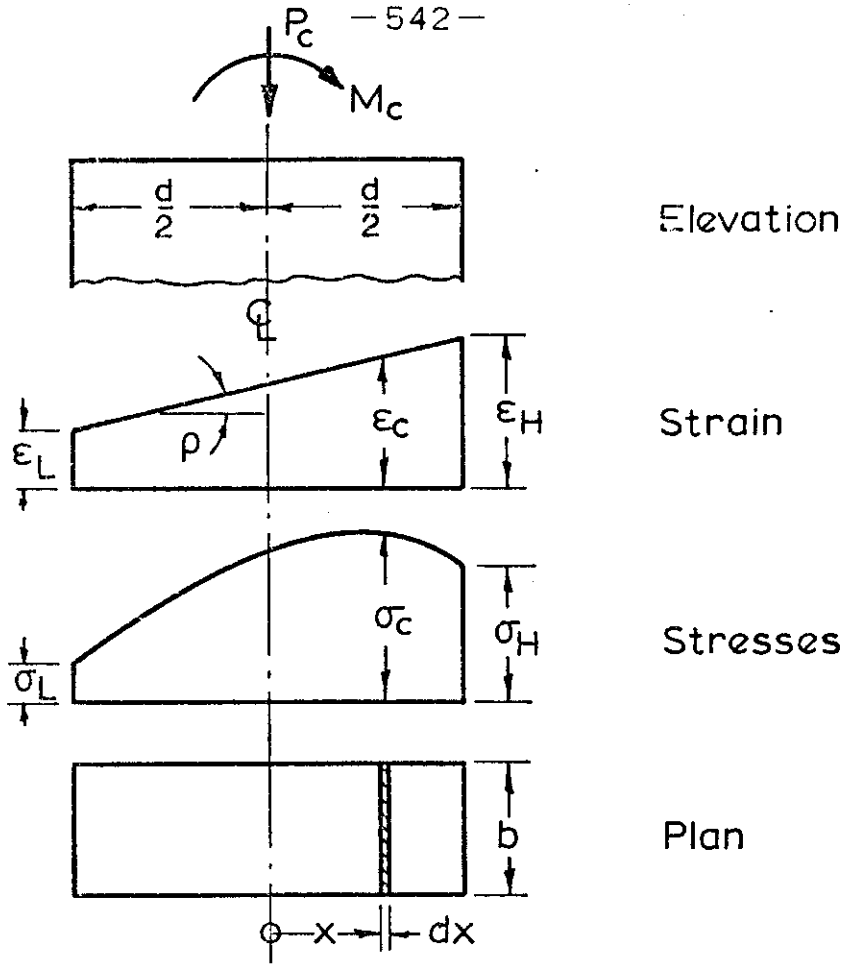

FIG. B·1 CONCRETE PRISM SUBJECTED TO AXIAL FORCE AND BENDING MOMENT

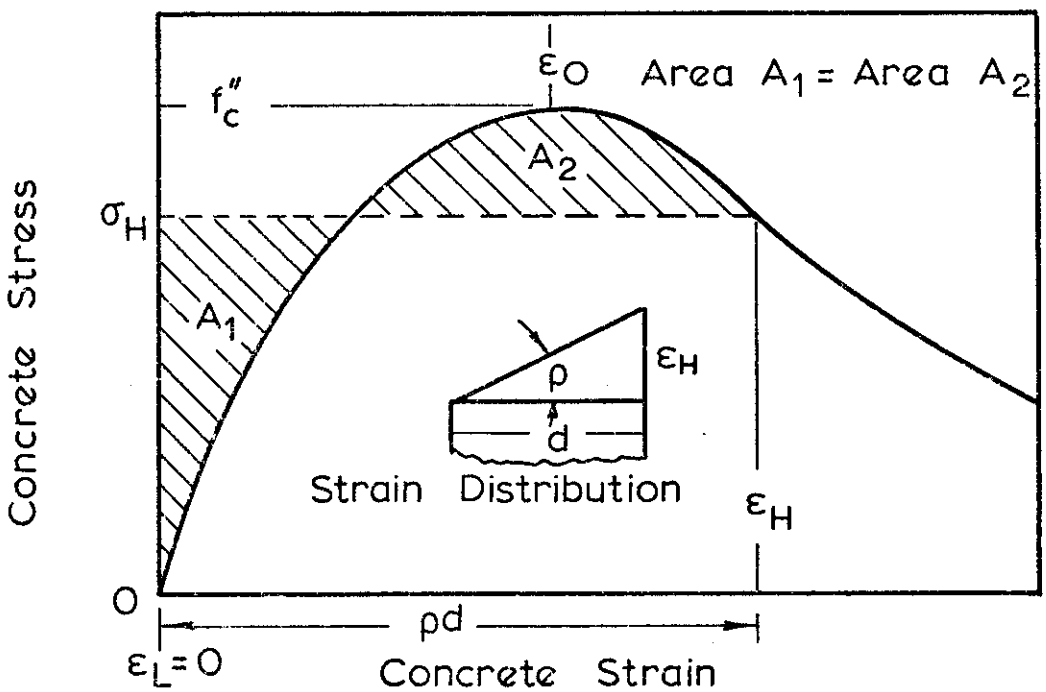

FIG. B·2 CONDITION FOR MAXIMUM LOAD FOR STRAIN DISTRIBUTION SHOWN

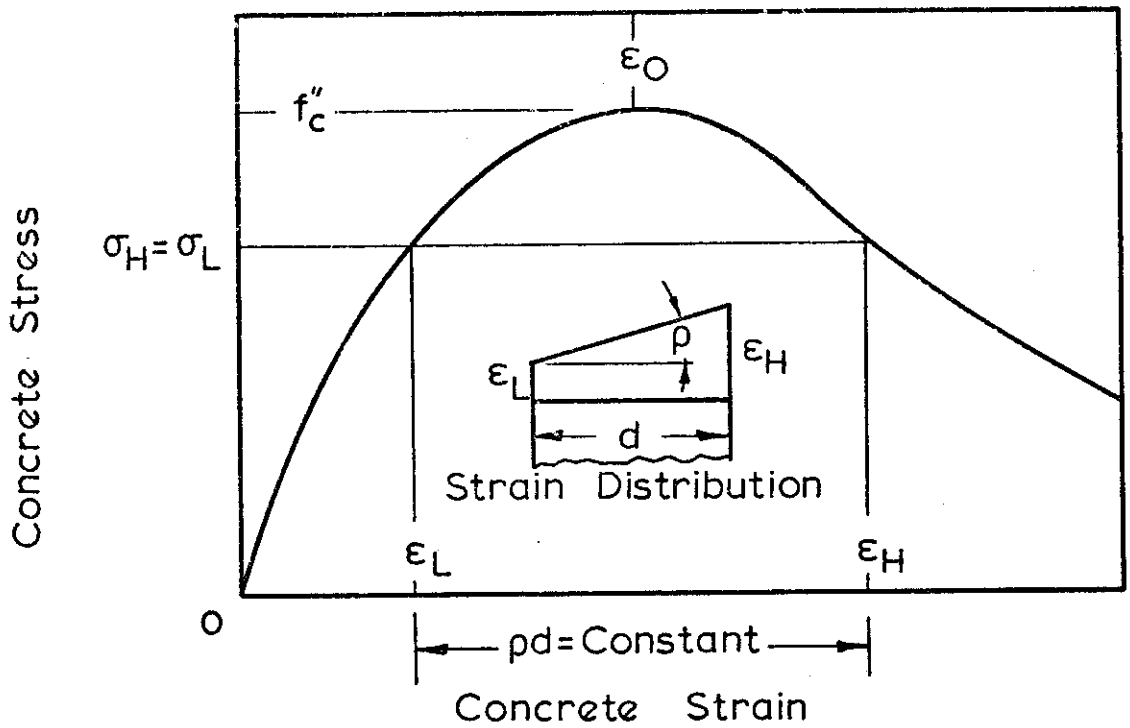

FIG. B·3 CONDITION FOR MAXIMUM LOAD FOR STRAIN DISTRIBUTION SHOWN

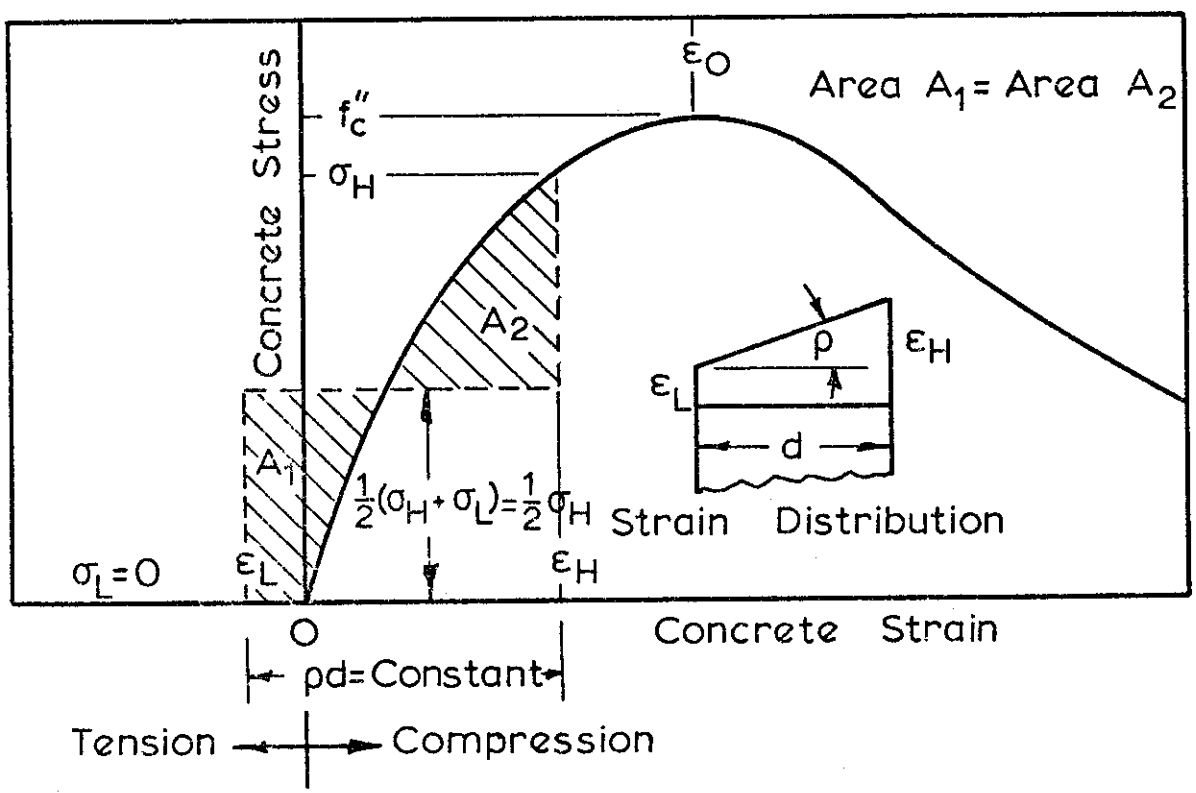

FIG. B·4 CONDITION FOR MAXIMUM MOMENT FOR STRAIN DISTRIBUTION SHOWN

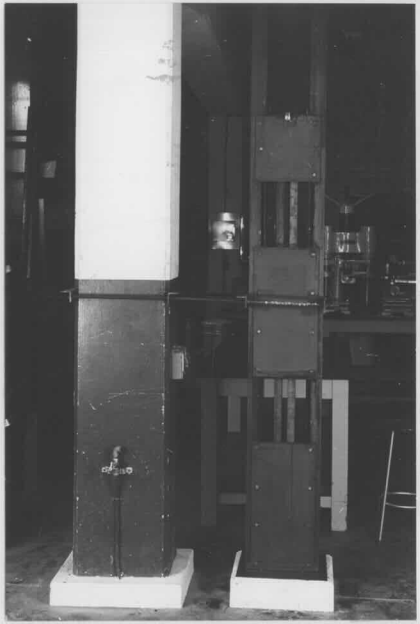

(a)

(b)

PLATE 1 COLUMN FORMWORK

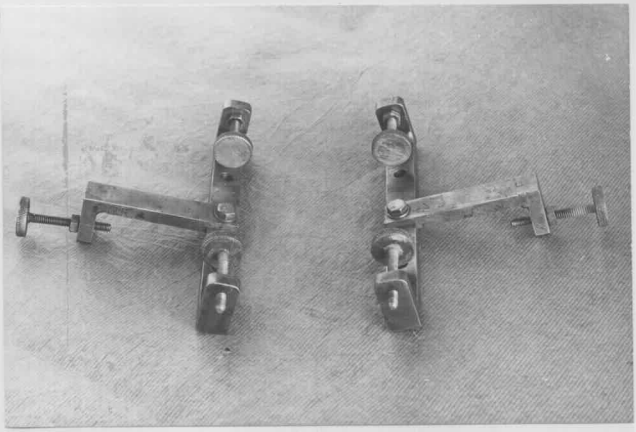

(a)

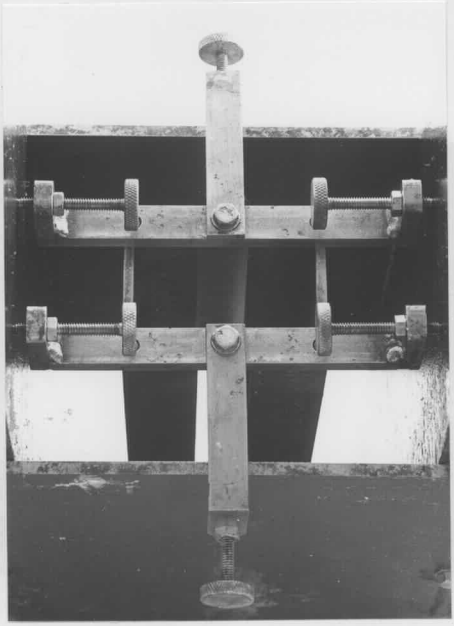

(b)

PLATE II ANCHORAGE OF CHANNELS AT TOP OF FORMWORK PRIOR TO CASTING

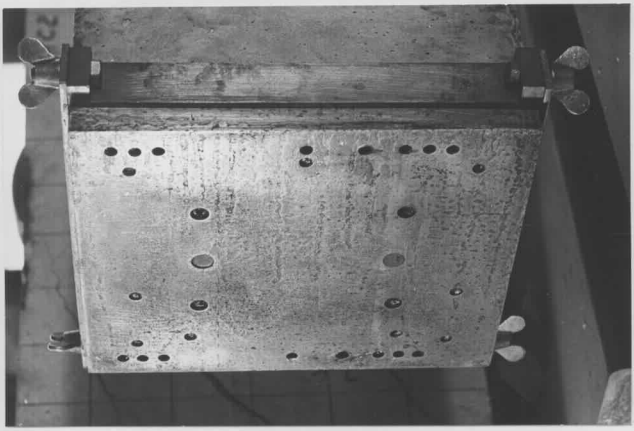

(a)

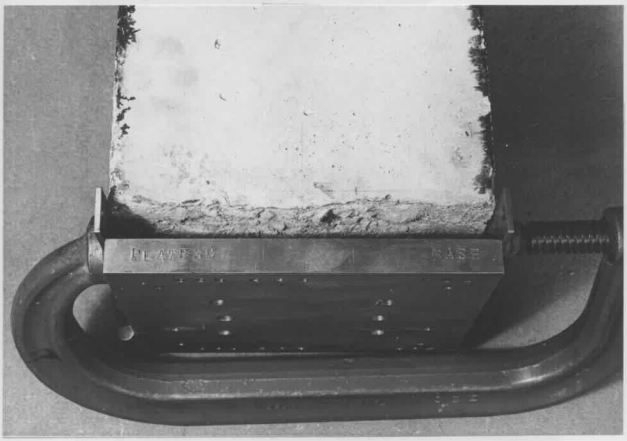

(b)

PLATE III USE OF COLLAR TO CAP END OF COLUMN

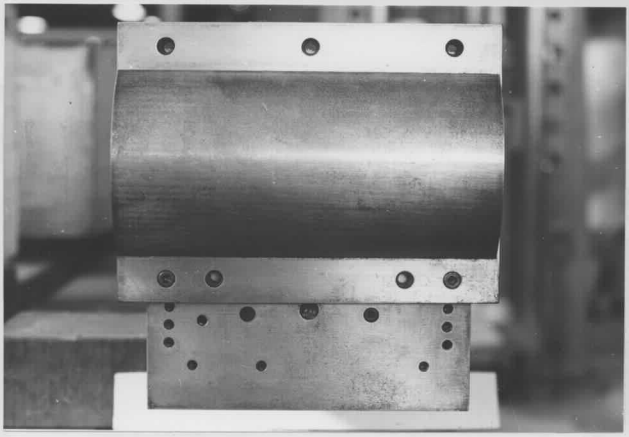

(a) Major Axis Bending

(b) Diagonal Axis Bending

PLATE IV ATTACHMENT OF LOADING ROCKERS

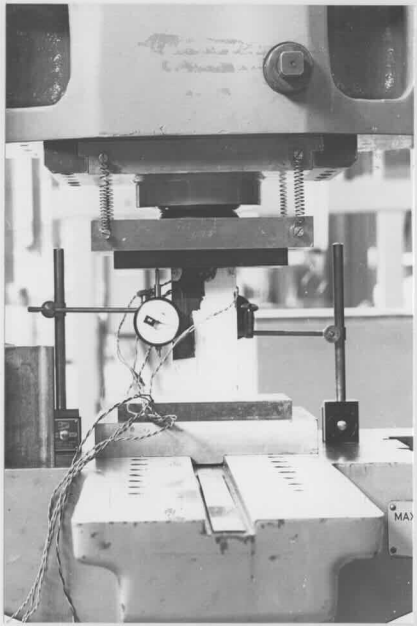

(a) Stub Column Test

(b) Coupon Tension Test

PLATE V STEEL CONTROL TESTS

PLATE VI TEST ARRANGEMENT FOR DETERMINATION OF STRESS-STRAIN RELATIONSHIP FROM CONCRETE CYLINDERS

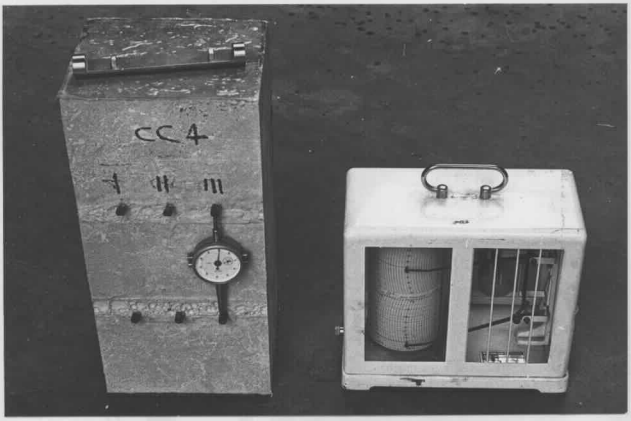

(a) Shrinkage Strain, Humidity and Temperature Measuring Equipment

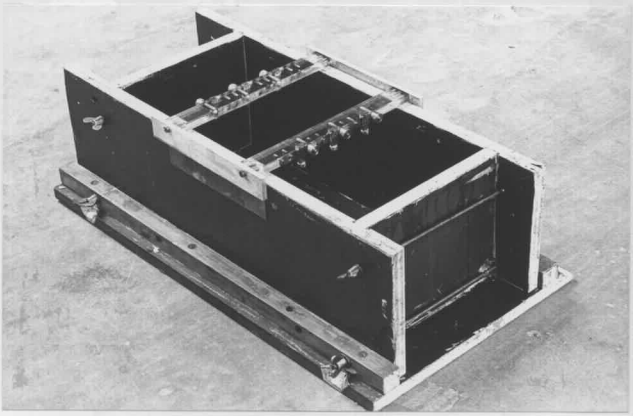

(b) Formwork for Shrinkage Specimens for Columns CC2, CC3, CC4 and CC5

PLATE VII APPARATUS FOR DETERMINATION OF SHRINKAGE STRAINS

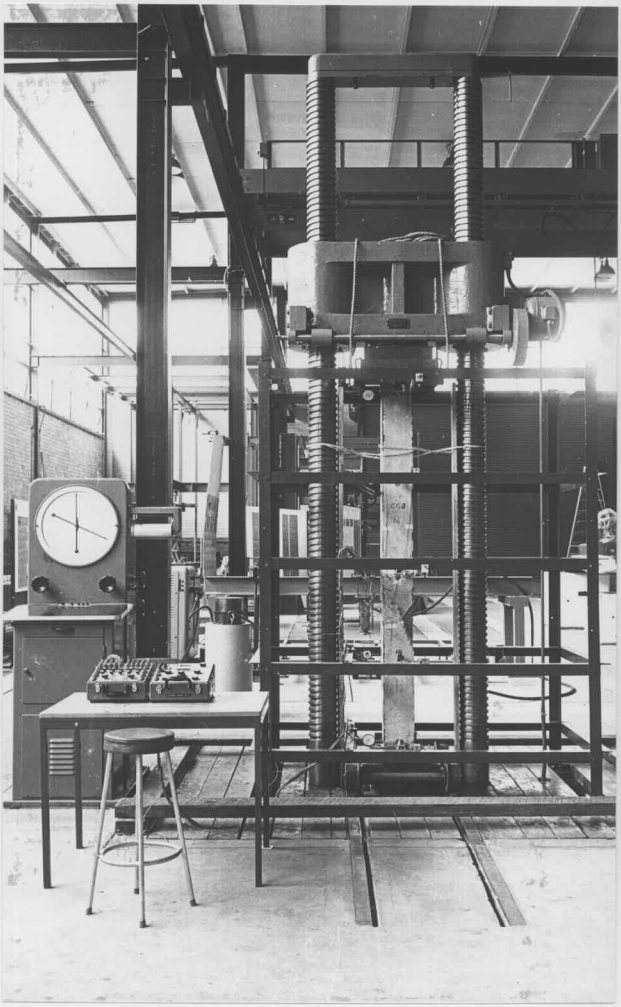

PLATE VIII TEST ARRANGEMENT FOR COLUMNS BENT ABOUT A PRINCIPAL AXIS

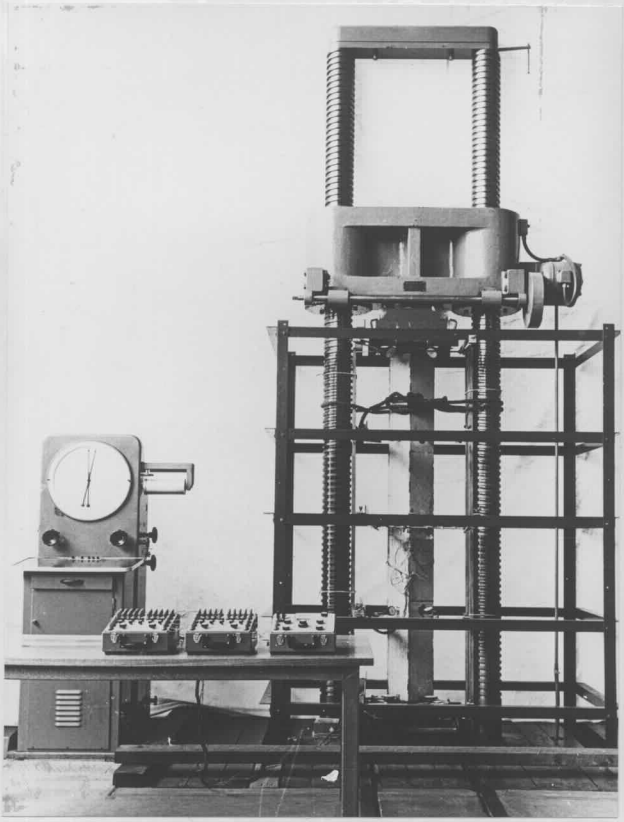

PLATE IX TEST ARRANGEMENT FOR COLUMNS BENT ABOUT A DIAGONAL AXIS

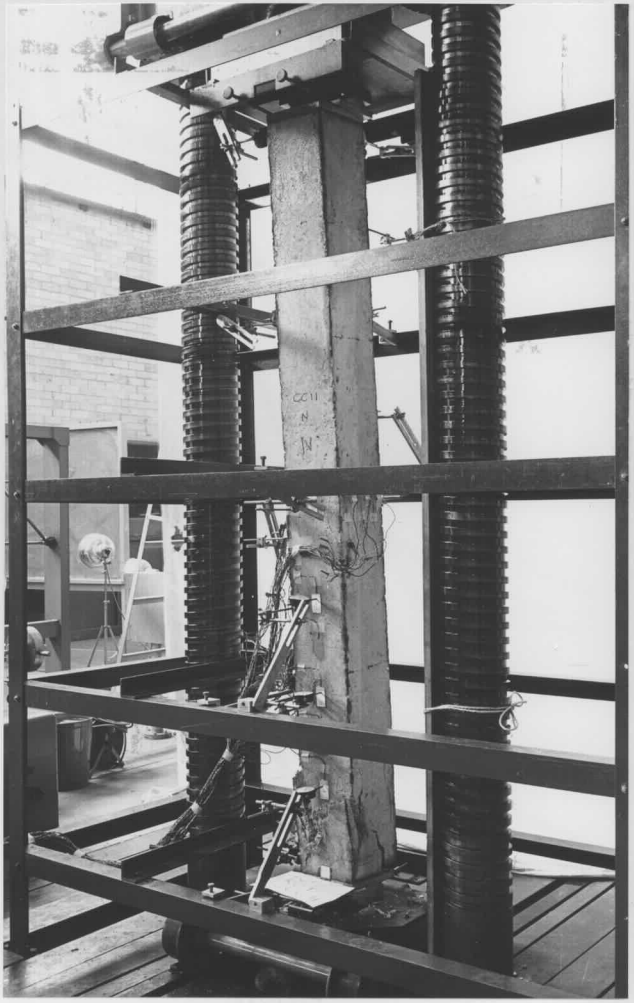

PLATE X TEST ARRANGEMENT FOR COLUMN CC11 BENT IN DOUBLE CURVATURE ABOUT THE MAJOR AXIS

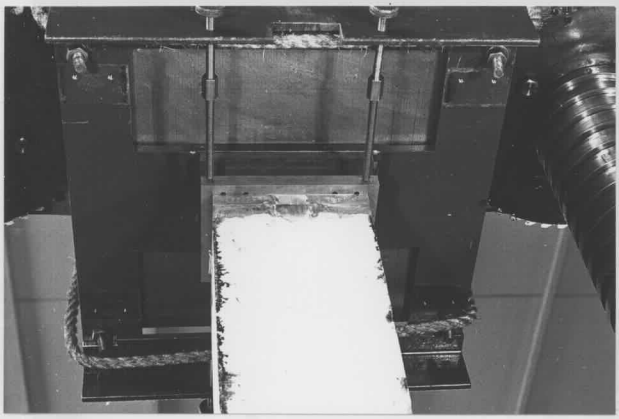

(a) Top End Fitting

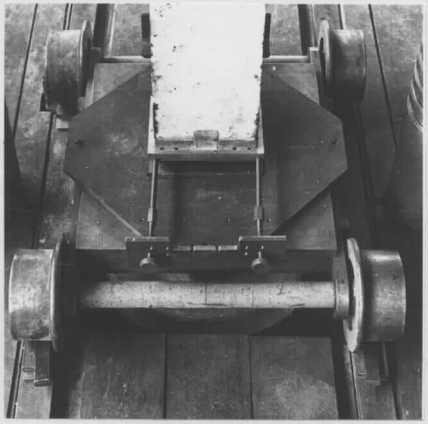

(b) Bottom End Fitting and Loading Trolley

PLATE XI END FITTING ATTACHED TO THE TESTING MACHINE

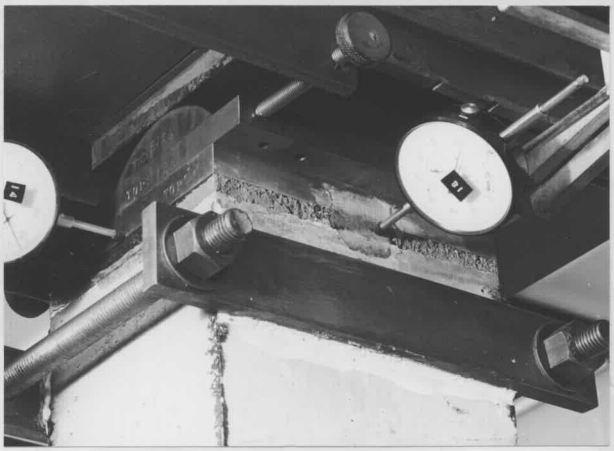

(a) Top End

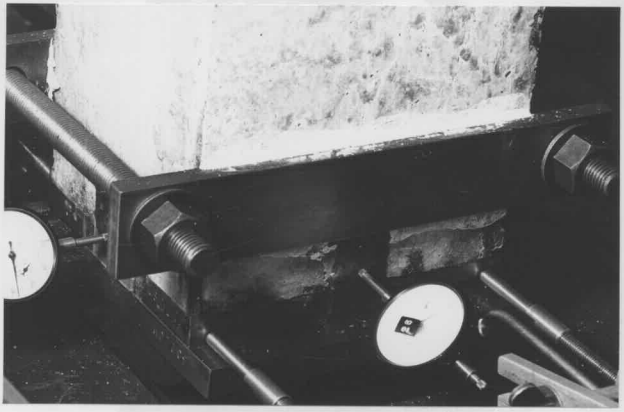

(b) Bottom End

PLATE XII POSITION OF COLUMN ENDS IN THE TESTING MACHINE

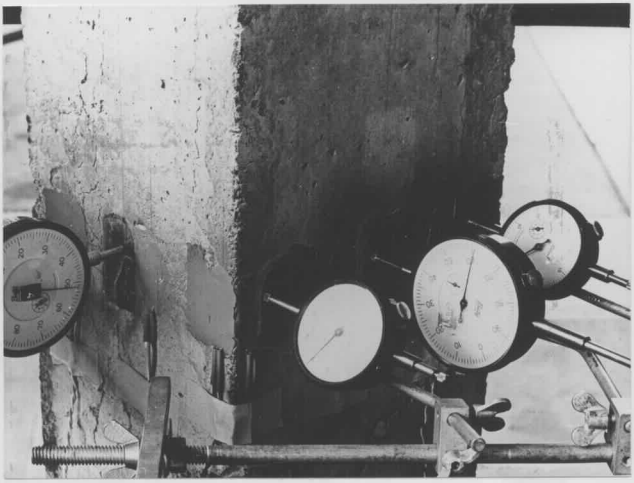

(a) Rotation Gauges at Central Section of Column CC5

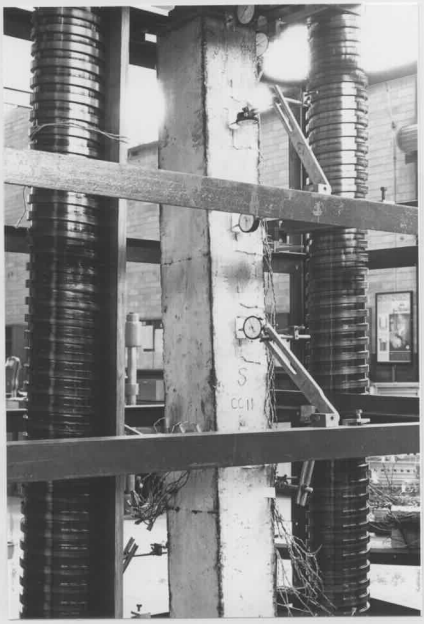

(b) Dial Gauges on South Face of Column CC11

PLATE XIII DIAL GAUGE ARRANGEMENTS

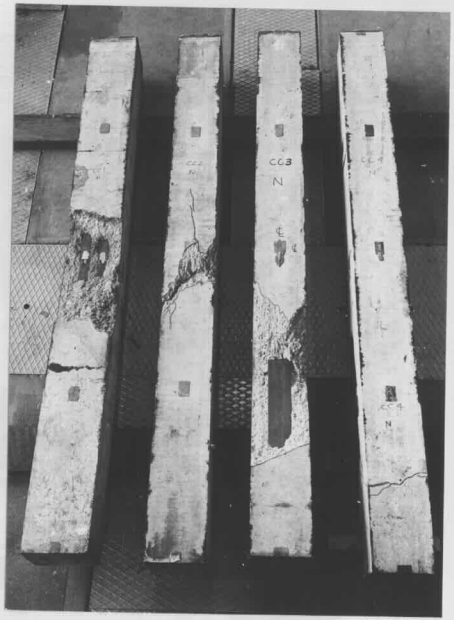

(a) North (Compression) Face

(b) South (Tension) Face

PLATE XIV FAILURE PATTERNS FOR 7FT. COLUMNS CC1, CC2, CC3 AND CC4

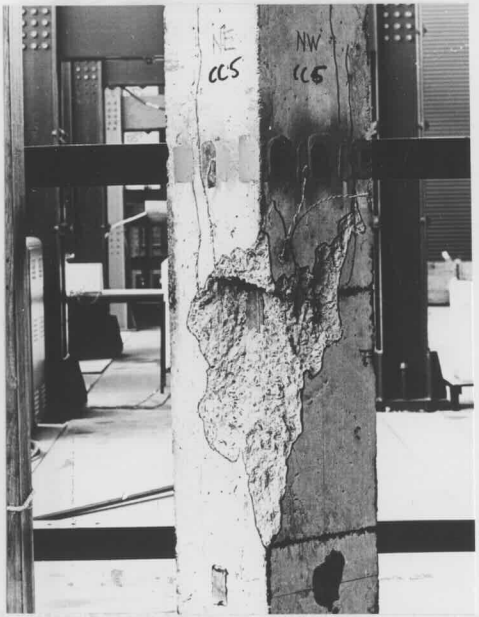

(a) North (Compression) Corner

(b) South (Tension) Corner

PLATE XV FAILURE PATTERN FOR 7FT. COLUMN CC5 BENT ABOUT A DIAGONAL AXIS (e = 0.8in.)

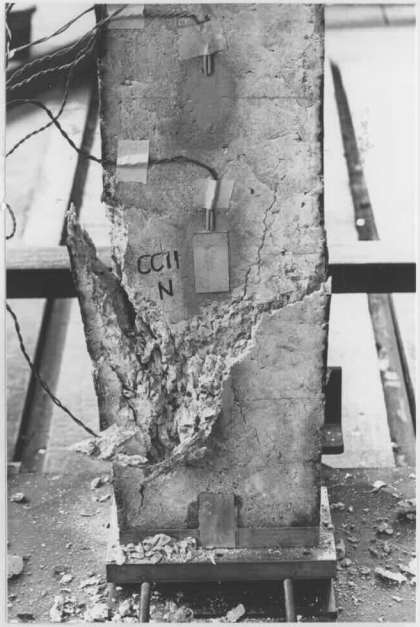

(a) Before Removal of Spalled Concrete

(b) After

PLATE XVI CRUSHING FAILURE AT END OF 7FT. COLUMN CC11 BENT ABOUT MAJOR AXIS IN DOUBLE CURVATURE (e = 2.0in.)

(a) Crushing on North Face

(b) Cracking on South Face

PLATE XVII FAILURE PATTERN FOR 10FT. COLUMN CC13R BENT ABOUT MAJOR AXIS (e = 0.8in.)

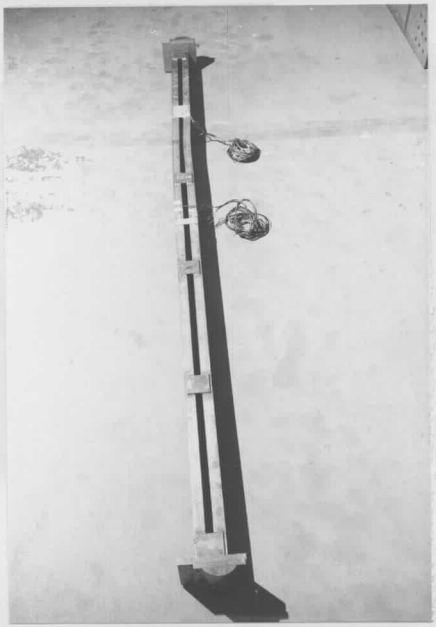

(a) Details of Column

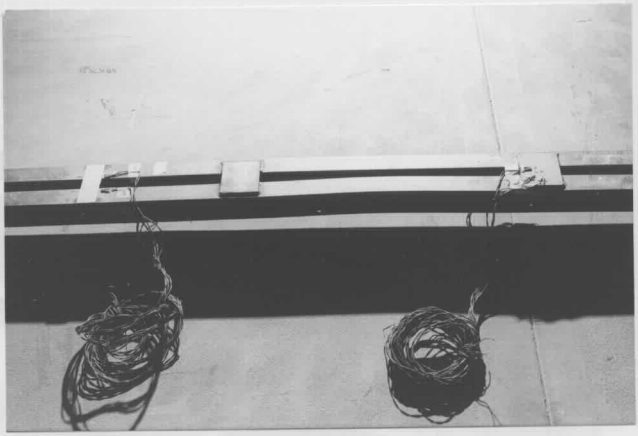

(b) Local Buckling in Second Panel from Top

PLATE XVIII FAILURE OF 10FT. BARE STEEL COLUMN CC14 BENT ABOUT THE MAJOR AXIS (e = 0.8in.)

(a) Crushing on North Face

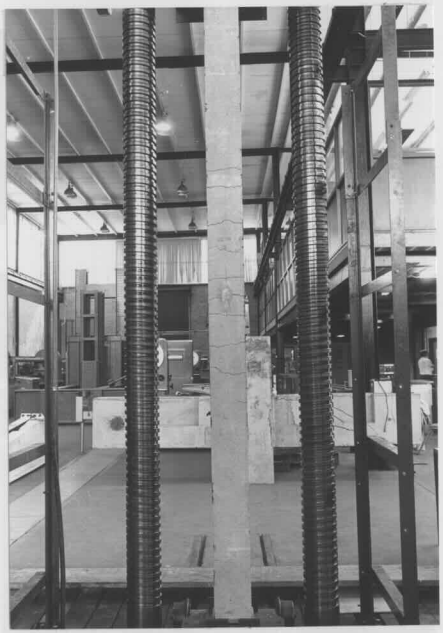

(b) Cracking on South Face

PLATE XIX FAILURE PATTERN FOR 10FT. COLUMN CC15 CONTAINING BATTENED CHANNELS AND BENT ABOUT THE MAJOR AXIS (e = 0.8in.)

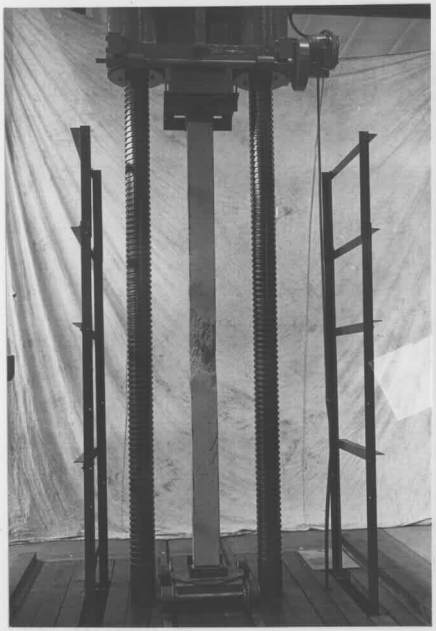

(a) Crushing on North Face

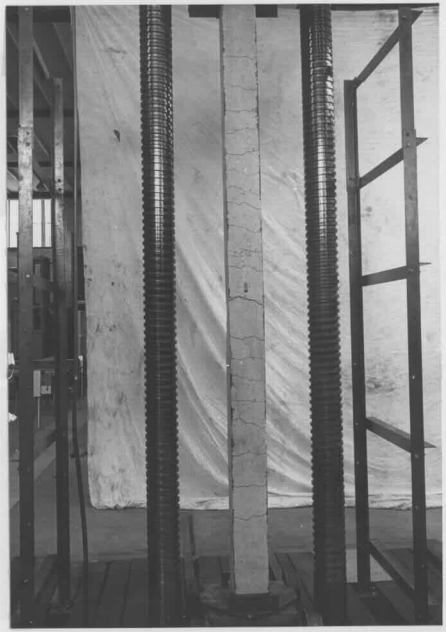

(b) Cracking on South Face

PLATE XX FAILURE PATTERN FOR 10FT. COLUMN CC16 BENT ABOUT THE MAJOR AXIS (e = 1.5in.)

PLATE XXI HOLLOW SQUARE STEEL TUBE IN POSITION FOR CASTING OF CONCRETE

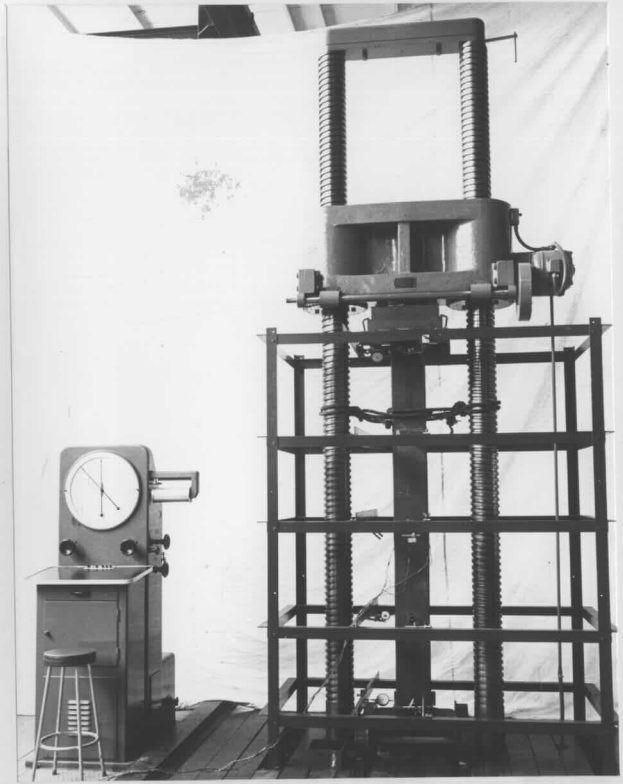

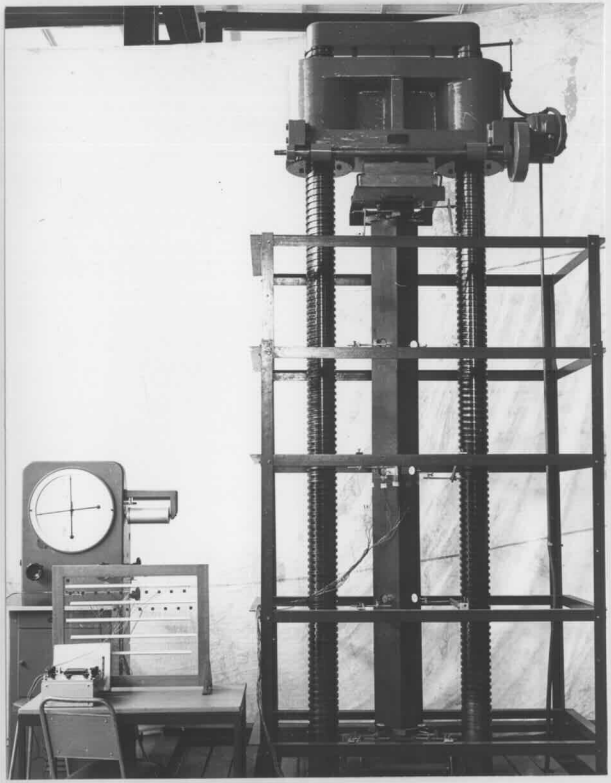

PLATE XXII TEST ARRANGEMENT FOR TUBES WITH 0° AND 45° LOADING AXIS INCLINATION

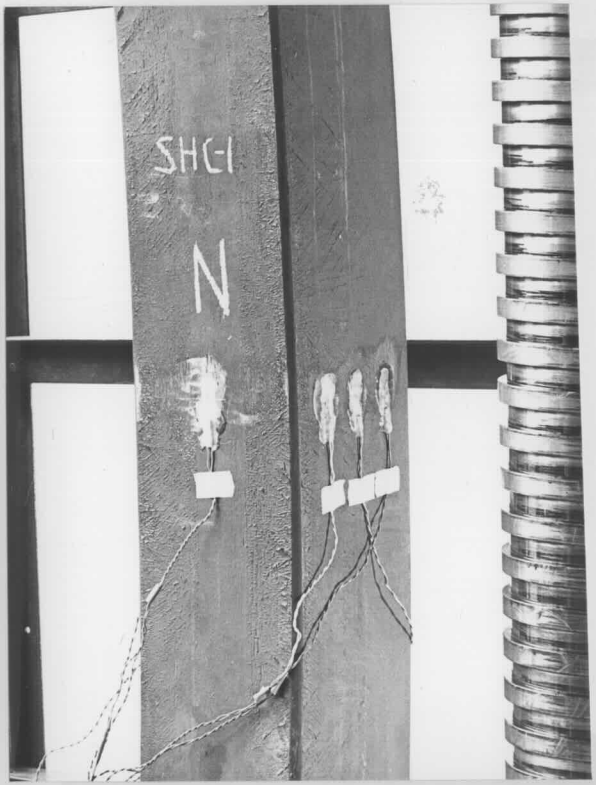

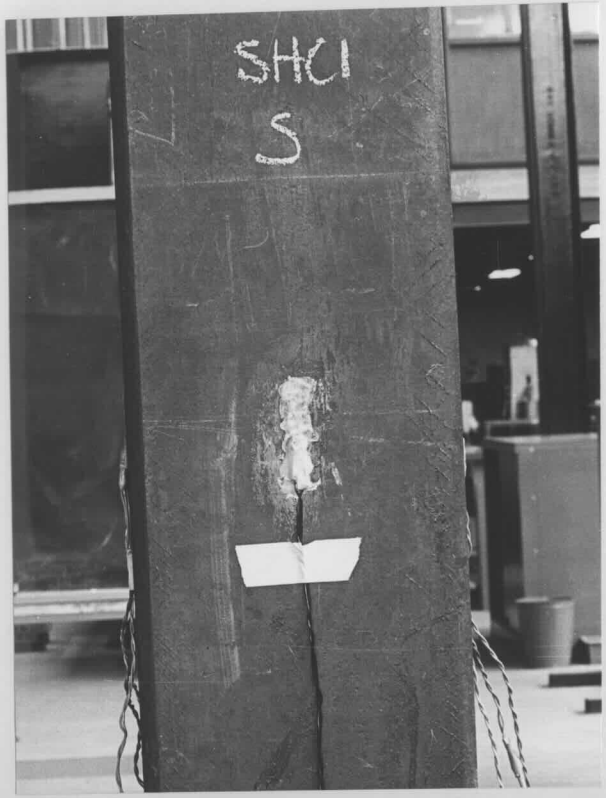

PLATE XXIII YIELDED CENTRAL REGION FOR COMPRESSION (N) AND TENSION (S) FACES OF COLUMN SHC-1

(e = 1.5IN., β = 0°)

PLATE XXIV LOCAL COMPRESSION FAILURE AT ENDS OF CONCENTRICALLY LOADED COLUMN SHC-2

(e = OIN., β = 0°)

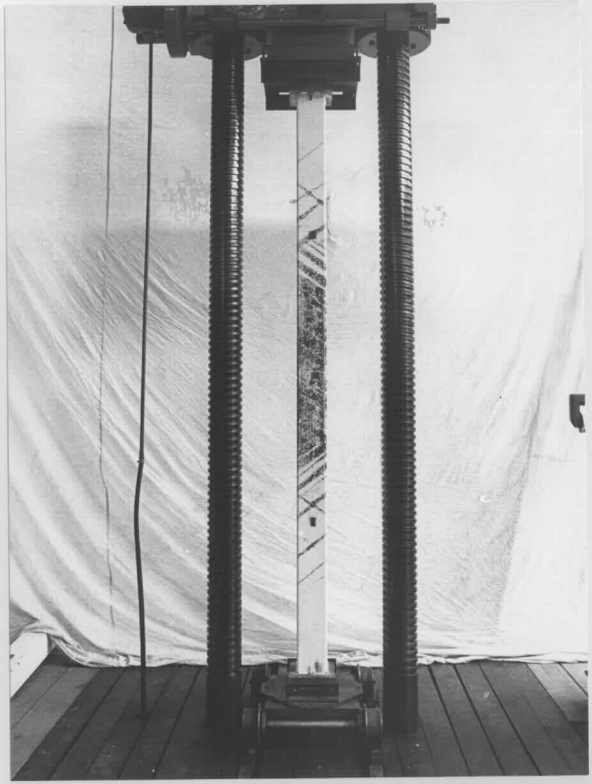

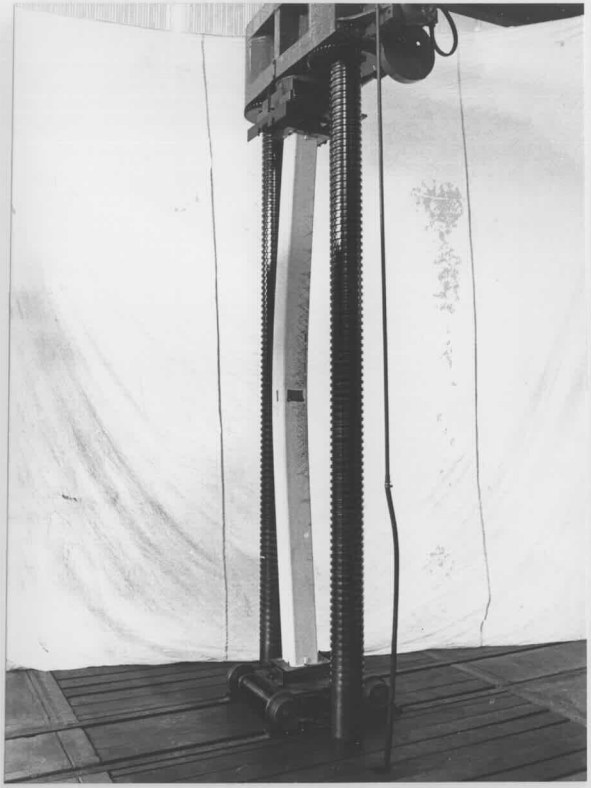

PLATE XXV YIELDED REGIONS AND DEFORMED SHAPE FOR 6IN. SQUARE COLUMN SHC-7 ($e = 1.5$IN., $\beta = 0°$)

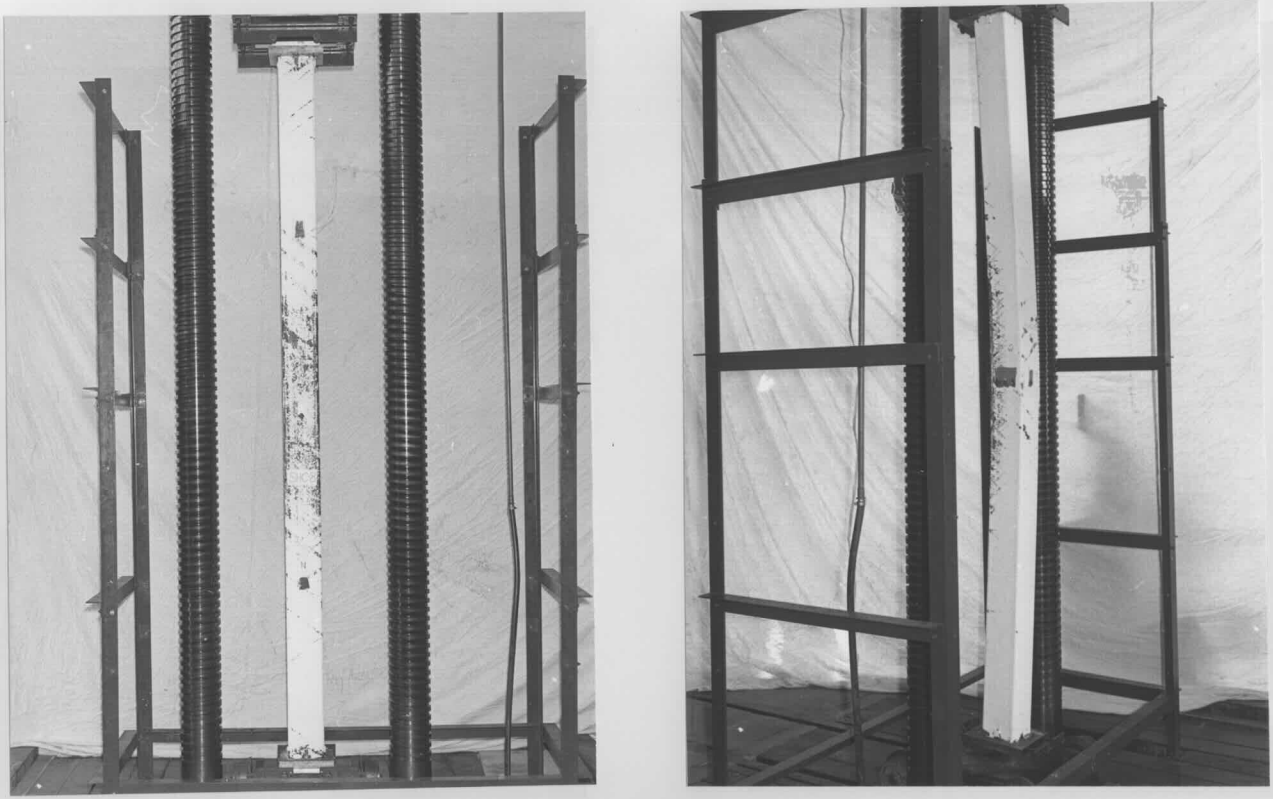

PLATE XXVI YIELDED REGIONS AND DEFORMED SHAPE FOR 6IN. SQUARE COLUMN SHC-8 (e = 2.5IN., β = 0°)

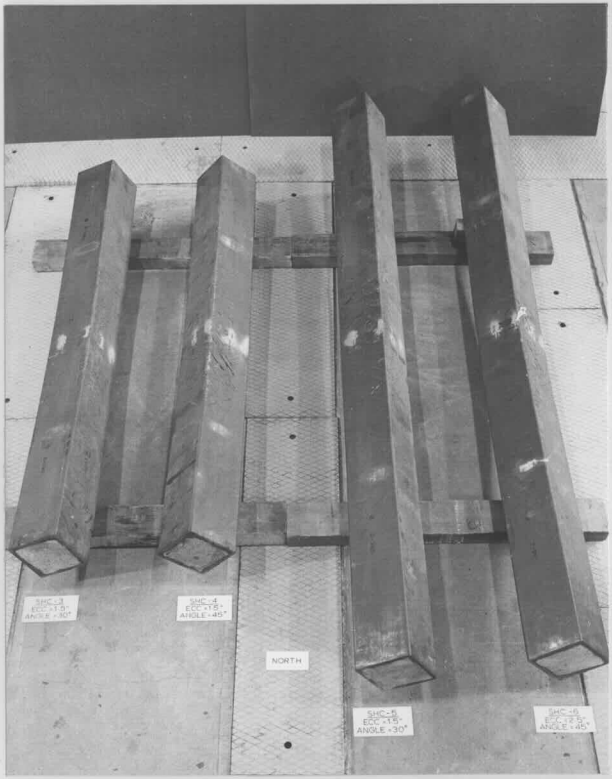

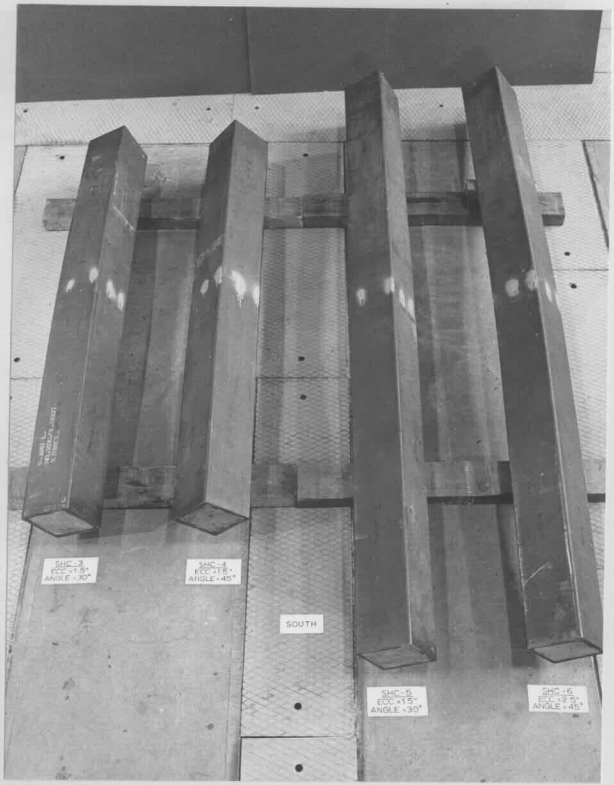

PLATE XXVII YIELDED REGIONS FOR COMPRESSION(N) AND TENSION(S) CORNERS OF COLUMNS SHC-3, SHC-4, SHC-5 AND SHC-6

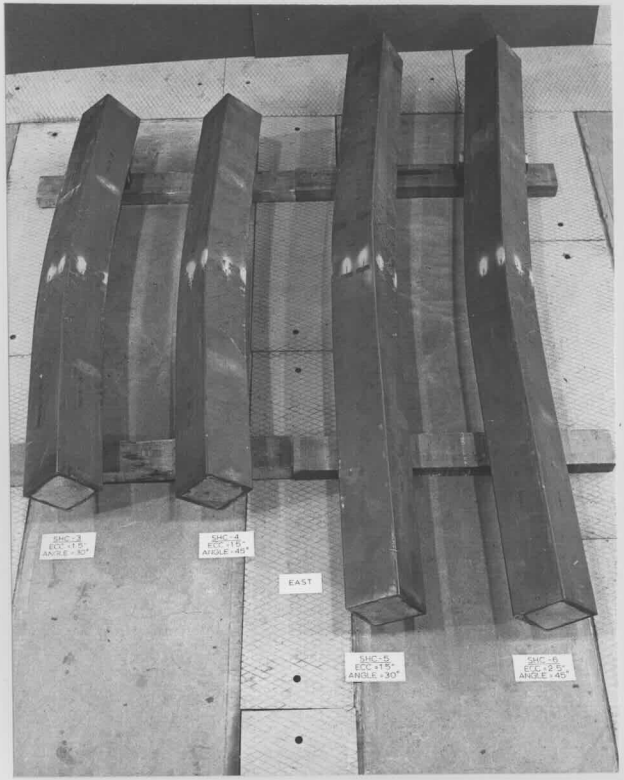

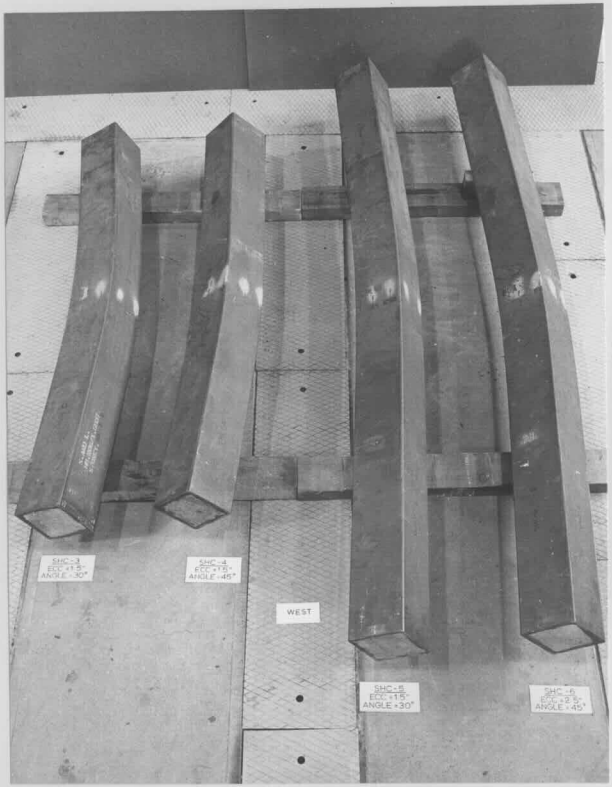

PLATE XXVIII YIELDED REGIONS AND DEFORMED SHAPES FOR COLUMNS SHC-3, SHC-4, SHC-5 AND SHC-6

PLATE XXIX MOULD FOR SHRINKAGE BLOCK WITH SAME CROSSECTION AS COLUMN

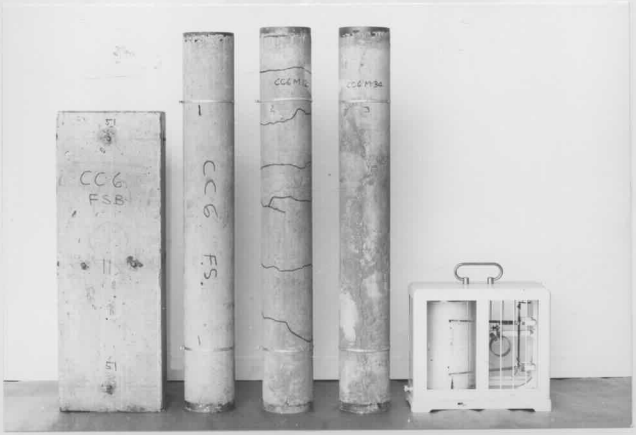

PLATE XXX 8IN. x 7IN. AND 4IN. DIA. SHRINKAGE SPECIMENS, 4IN. DIA. MODEL COLUMNS FOR COLUMN CC6

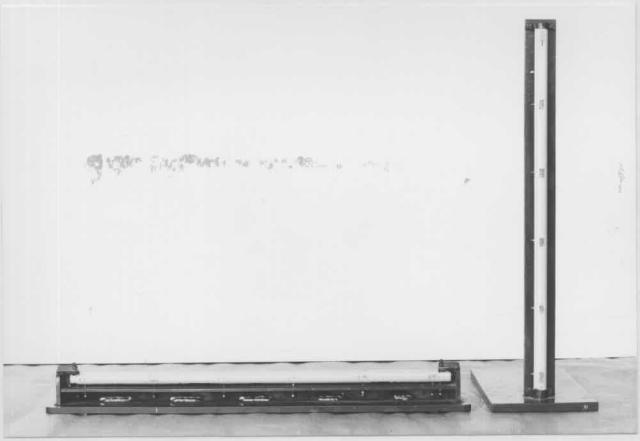

PLATE XXXI INVAR REFERENCE BARS FOR HUGGENBERGER TENSOMETER

PLATE XXXII HUGGENBERGER TENSOMETER MEASURING SHRINKAGE OVER 50cm. GAUGE LENGTH

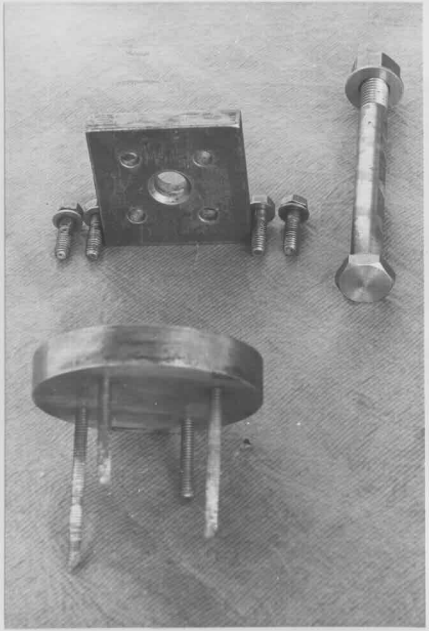

PLATE XXXIII END FITTINGS FOR APPLYING TENSILE STRESS TO 4IN. DIA. CYLINDERS

PLATE XXXIV TENSILE CREEP RIG

PLATE XXXV FAILURE OF 4IN. DIA. CYLINDERS IN DIRECT TENSION

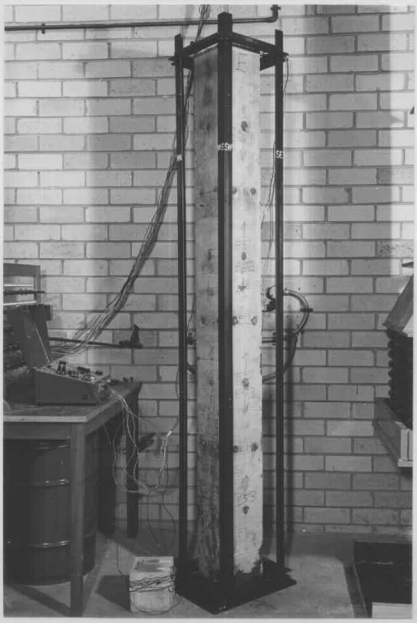

PLATE XXXVI COLUMN IN POSITION FOR MEASUREMENT OF AXIAL SHORTENING DURING DRYING PERIOD

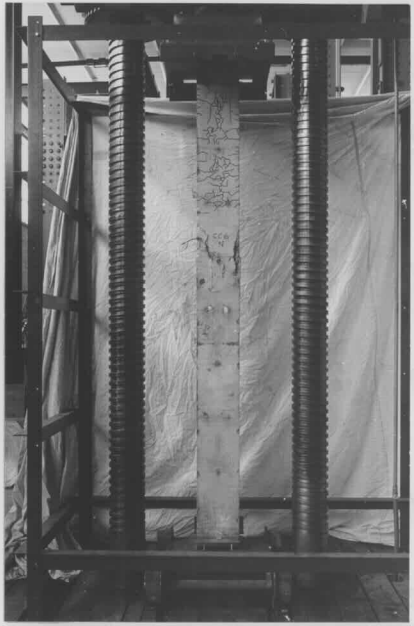

(a)

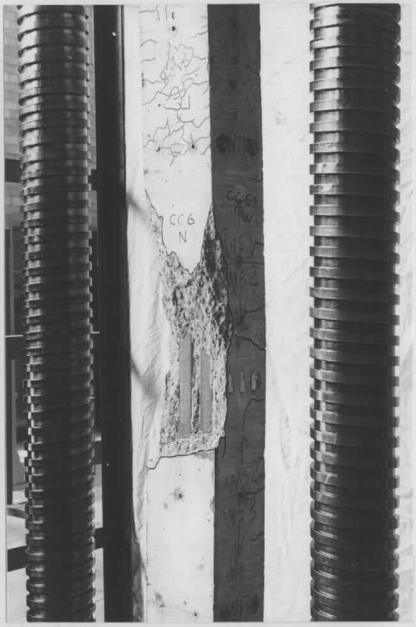

(b)

PLATE XXXVII FAILURE PATTERN OF COMPRESSION (NORTH) FACE OF COLUMN CC6 BENT ABOUT MINOR AXIS WITH 1.5IN. ECCENTRICITY

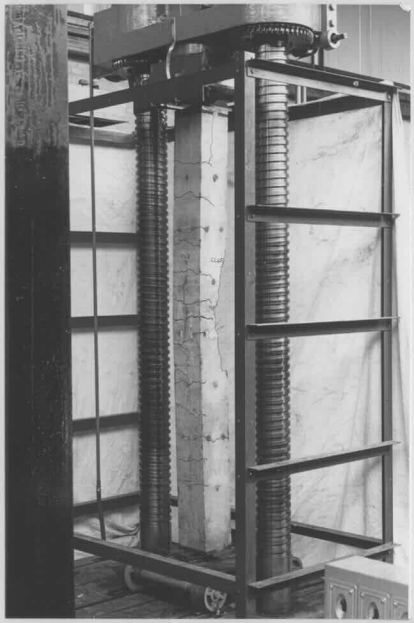

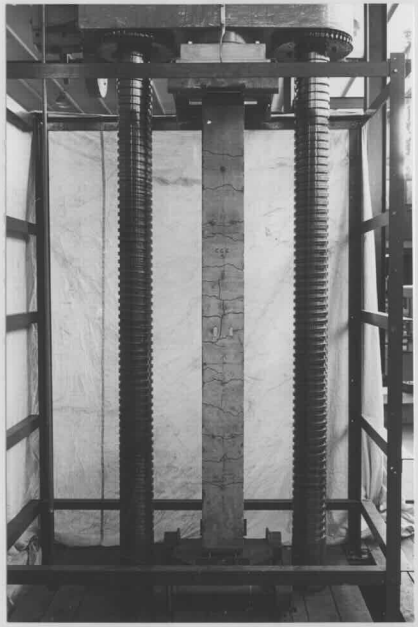

PLATE XXXVIII FAILURE PATTERN ON TENSION (SOUTH) FACE OF COLUMN CC6

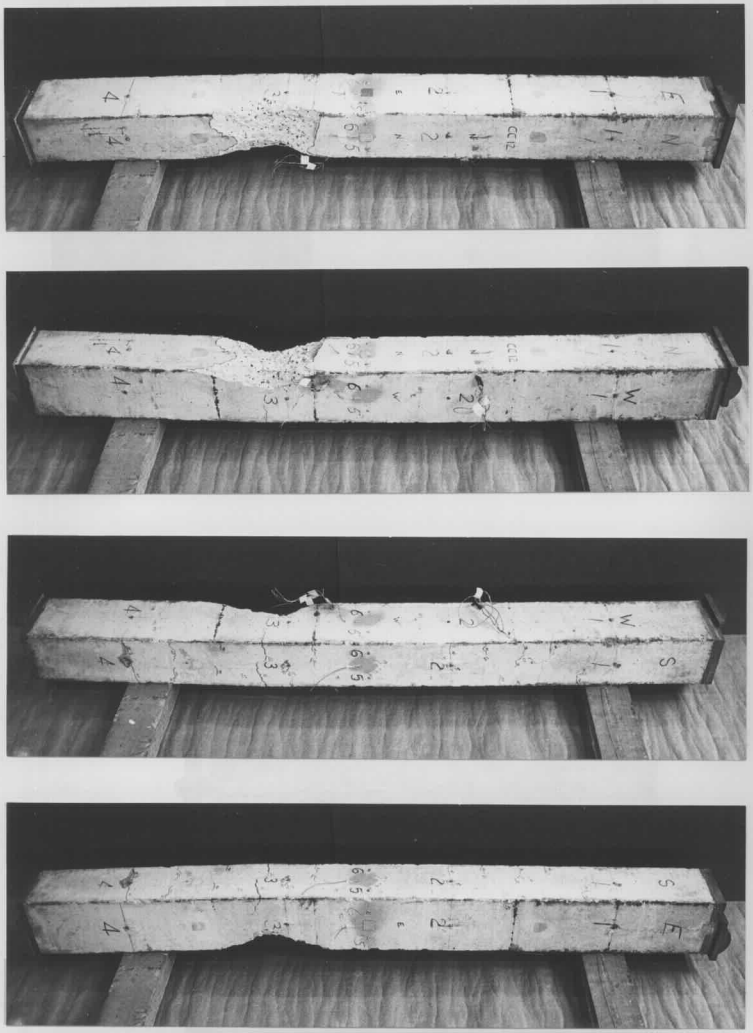

Bottom

Top

PLATE XXXIX FAILURE PATTERNS ON THE FOUR FACES OF COLUMN CC12 BENT ABOUT THE MAJOR AXIS WITH AN ECCENTRICITY OF 1.5IN.

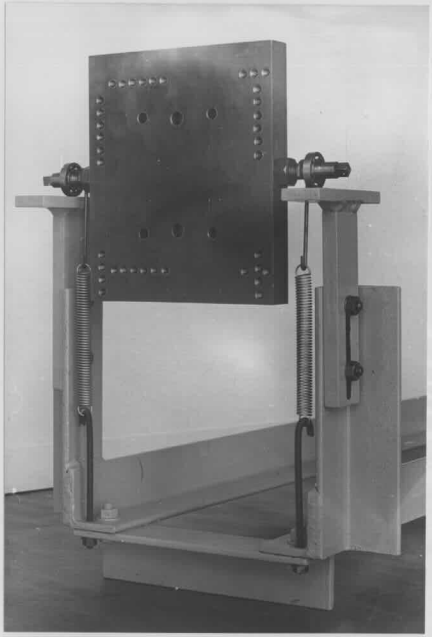

(a) Top

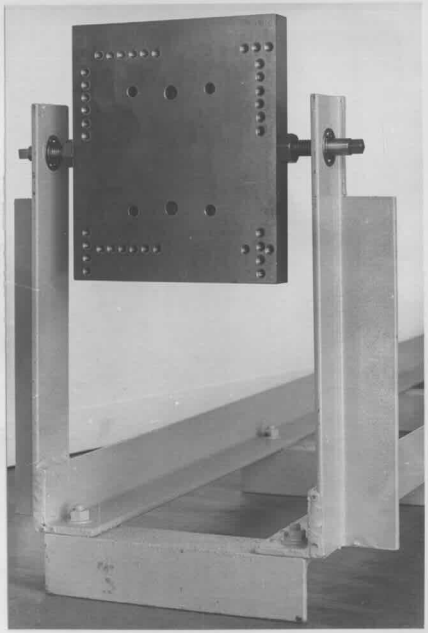

(b) Bottom

PLATE XL ATTACHMENT OF DIAL GAUGE FRAME TO COLUMN END PLATES

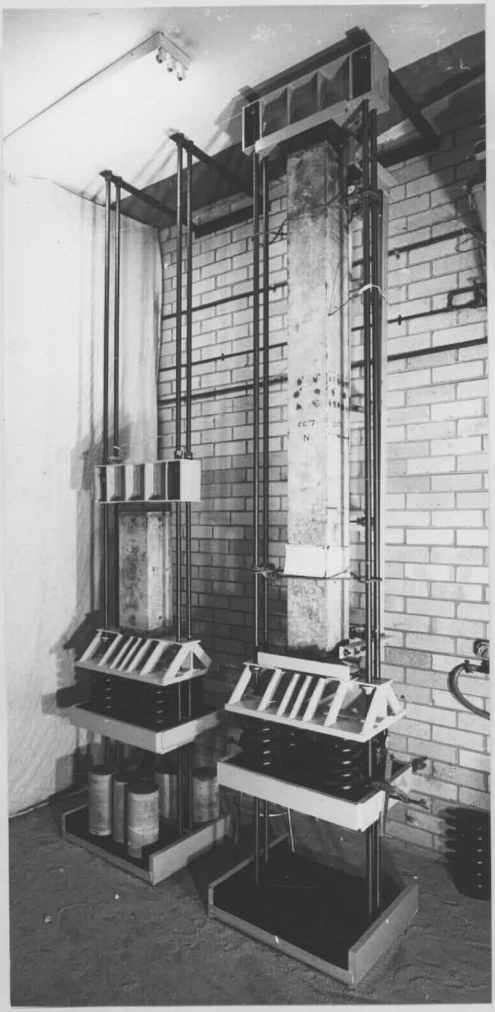

PLATE XLI COLUMN CC7 AND CREEP SPECIMEN UNDER SUSTAINED LOAD IN CREEP RIGS

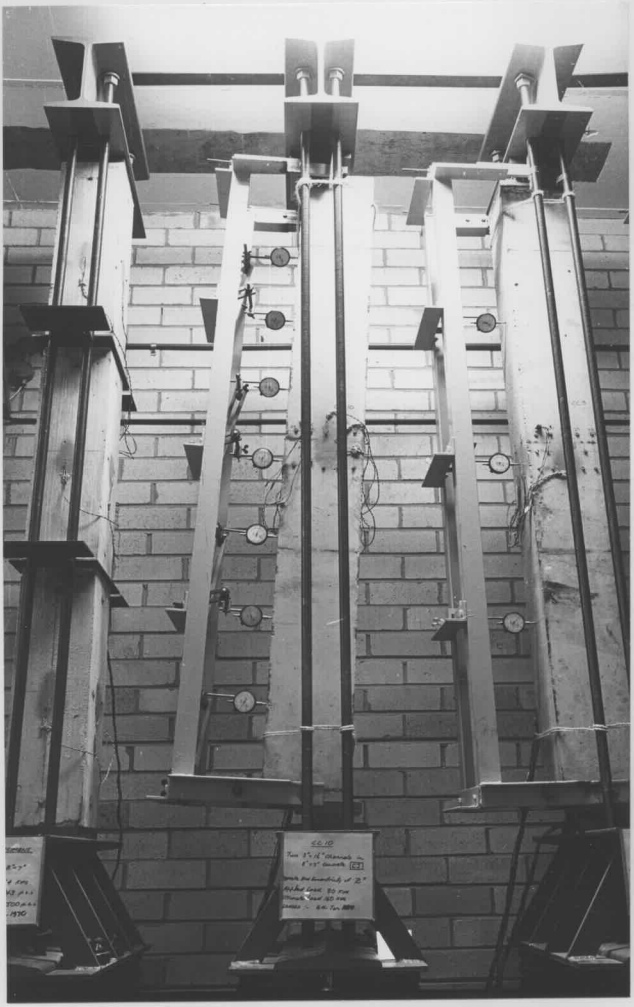

PLATE XLII COLUMNS CC8, CC9 AND CC10

AND CREEP SPECIMENS UNDER

SUSTAINED LOAD IN CREEP RIGS

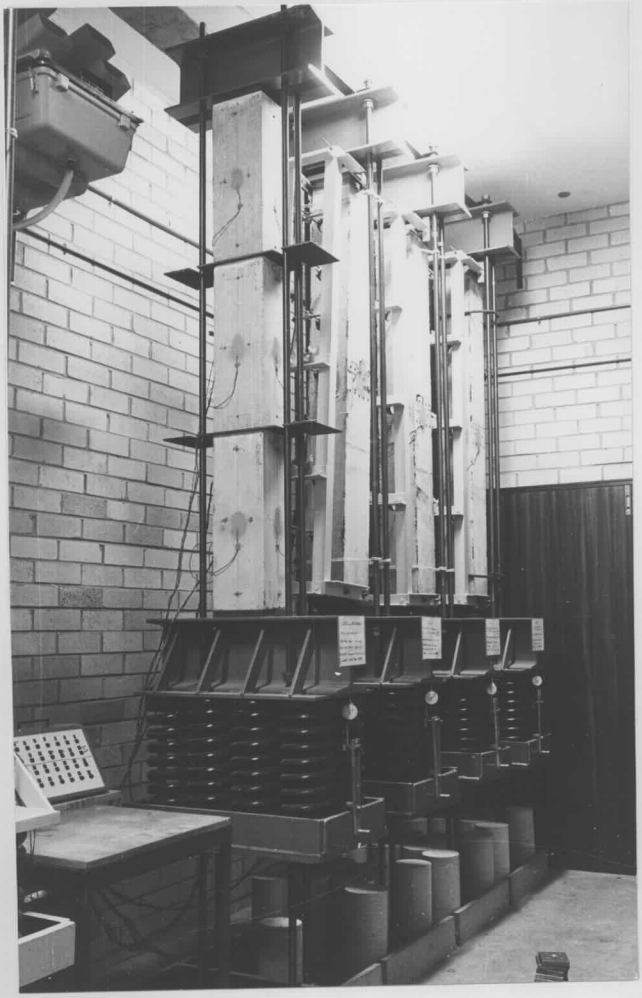

PLATE XLIII CREEP SPECIMENS FOR COLUMNS

CC8, CC9 AND CC10 IN CREEP RIGS